

**NOVEL MEMBRANE-BASED PROCESSES  
FOR NUTRIENTS, ENERGY AND WATER  
RECOVERY FROM SOURCE SEPARATED  
HUMAN URINE**

**by Federico Volpin**

Thesis submitted in fulfilment of the requirements for  
the degree of

**Doctor of Philosophy**

under the supervision of Prof. Ho Kyong Shon and Dr.  
Sherub Phuntsho

University of Technology Sydney  
Faculty of Engineering and Information Technology

June 2020



# STATEMENT OF ORIGINAL AUTHORSHIP

I, **Federico Volpin**, declare that this thesis, is submitted in fulfilment of the requirements for the award of **Doctor of Philosophy in the School of Civil and Environmental Engineering/Faculty of Engineering and IT** at the University of Technology Sydney.

This thesis is wholly my own work unless otherwise referenced or acknowledged. In addition, I certify that all information sources and literature used are indicated in the thesis.

This document has not been submitted for qualifications at any other academic institution.

This research is supported by the Australian Government Research Training Program.

Signature:                      Production Note:  
   Signature removed prior to publication.

Federico Volpin

Date:                      **30/06/2020**





I dedicate this Thesis to my parents

***Emanuela Lollo and Stefano Volpin***

And my sister

***Margherita Volpin***



# ACKNOWLEDGEMENTS

I owe many people my gratitude for the creation of this PhD Thesis. This work would not have been possible without the support and guidance of who supported me along the way. First, I would like to thank Prof. Ho Kyong Shon for providing me with all the resources, knowledge, and technical support to prove myself as a researcher. His advice, passion for research and never-ending strive for excellence allowed me to achieve the best possible outcome in my work. I would also like to express my gratitude Dr Sherub Phuntsho for always being supportive and caring.

I am also grateful to Prof. Hokyong Shon for providing me with a scholarship throughout my whole candidature tenure, and for supporting two fantastic overseas research experience in South Korea. In South Korea, I had the honour and pleasure to be hosted by two excellent researchers, Prof. Jaeweon Cho (UNIST) and Dr Yunchul Woo (KICT). I sincerely acknowledge Dr MD Johir and Dr Nirenkumar Pathak for their help in the laboratory and the administrative support from Maya, Trish and Van. I would also like to thank all my good friends and colleagues at UTS. All of you have always made me feel at home. I also want to send a special thanks to Seong Chul, Cristo and Ralph for the fantastic time spent together.

Last but not least, I would like to thank my family for their support throughout the whole duration of my PhD degree. They have always shown me just love and affection, in a truly selfless way. Finally, a special thanks to my girlfriend. Your joyful nature and company have been greatly valued, especially during these recent stressful and challenging times.

**FEDERICO VOLPIN**



### Journal Articles Published or Submitted (\*)

Part of the work performed during the PhD project resulted in peer-reviewed publications and presentations, which are listed hereafter in the order of acceptance and by category. They are directly or indirectly related to the main topics of this Thesis, and all of them have been accepted and published by the end of that project.

1. **F. Volpin**, L. Chekli, S. Phuntsho, J. Cho, N. Ghaffour, J.S. Vrouwenvelder, H. K. Shon, Simultaneous phosphorous and nitrogen recovery from source-separated urine: A novel application for fertiliser drawn forward osmosis, *Chemosphere*, 203 (2018) 482-489.
2. **F. Volpin**, E. Fons, L. Chekli, K. Jung Eun, J. Am, H. K. Shon, Hybrid forward osmosis-reverse osmosis for wastewater reuse and seawater desalination: Understanding the optimal feed solution to minimise fouling, *Process Safety & Environmental Protection: Transactions of the Institution of Chemical Engineers Part B*, 117 (2018) 523-532.
3. **F. Volpin**, L. Chekli, S. Lim, N. Pathak, S. Phuntsho, H. K. Shon, GreenPRO: A novel fertilizer driven osmotic power generation process for fertigation, *Desalination*, 447 (2018) 158-166.
4. **F. Volpin**, H. Heo, M. A. H. Johir, J. Cho, S. Phuntsho, H. K. Shon, Techno-economic feasibility of recovering phosphorus, nitrogen and water from dilute human urine via forward osmosis, *Water Research*, 150 (2019), 47-55.
5. **F. Volpin**, S. Phuntsho, N. Ghaffour, J.S. Vrouwenvelder, H. K. Shon, Optimisation of a forward osmosis and membrane distillation hybrid system for the treatment of source-separated urine, *Separation and Purification Technology*, 212 (2019), 368-375.

6. **F. Volpin**, H. Yu, J. Cho, C. Lee, S. Phuntsho, N. Ghaffour, J. S. Vrouwenvelder, H. K. Shon, Human urine as a forward osmosis draw solution for the application of microalgae dewatering, *Journal of Hazardous Materials*, 378 (2019).
7. **F. Volpin**, J. Jiang, I. E. Saliby, M. Preire, S. Lim, M.A.H. Johir, J. Cho, D. S. Han, S. Phuntsho, H. K. Shon, Sanitation and dewatering of human urine via membrane bioreactor and membrane distillation and its reuse for fertigation, *Journal of Cleaner Production*, p. 122390.
8. (\*) **F. Volpin**, Y. Woo, H. Kim, S. Freguia, N. Jeong, J. S. Choi, J. Cho, S. Phuntsho and H. K. Shon, Energy recovery through reverse electrodialysis: Harnessing the salinity gradient from the flushing of human urine, *Submitted for publication on Water Research*.
9. (\*) **F. Volpin**, U. Badeti, C. Wang, J. Jiang, J. Vogel, S. Freguia, D. Fam, J. Cho, S. Phuntsho and H. K. Shon, Urine treatment on the International Space Station: Current practice and novel approaches, *To be submitted for publication*.
10. M. M. Damtie, **F. Volpin**, M. Yao, L. D. Tijing, R. H. Hailemariam, T. Bao, K. Park, H. K. Shon, J. S. Choi, Ammonia recovery from human urine as liquid fertilizers in hollow fiber membrane contactor: Effects of permeate chemistry, *Environmental Engineering Research*, vol. 26, no. 1, pp. 190523-0.

## Conference Papers and Presentations

1. **F. Volpin**, L. Chekli, S. Phuntsho, J. Cho, H. K. Shon, "Simultaneous Nutrients Recovery and Osmotic Concentration of Source-Separated Urine via Fertilizer drawn Forward Osmosis", **Oral Presentation at the 10<sup>th</sup> International Desalination Workshop (IDW 2017)**, 22-25 November 2017, Busan, Republic of Korea.
2. **F. Volpin**, L. Chekli, S. Phuntsho, J. Cho, N. Ghaffour, J. S. Vrouwenvelde, H. K. Shon, "Simultaneous Phosphorous and Nitrogen Recovery from Source-Separated Urine: A novel application for Fertiliser Drawn Forward Osmosis", **Oral Presentation at the 4<sup>th</sup> IWA Specialised International Conference - Ecotechnologies for Wastewater Treatment (ecoSTP 2018)**, 25-28 June 2018, London, Canada.
3. **F. Volpin**, L. Chekli, S. Phuntsho, J. Cho, H. K. Shon, "Simultaneous Nutrients Recovery and Osmotic Concentration of Source-Separated Urine via Fertilizer drawn Forward Osmosis", **Oral Presentation at the 2018 School Research Showcase**, 27 April 2018, Sydney, Australia.
4. **F. Volpin**, H. Yu, J. Cho, C. Lee, S. Phuntsho, N. Ghaffour, J. S. Vrouwenvelder, H. K. Shon, "Human urine as a novel draw solution for forward osmosis processes and its application to dewater microalgae solution.", **Oral Presentation at The 11<sup>th</sup> Conference of the Aseanian Membrane Society (AMS 11)**, 3-6 July 2018, Brisbane, Australia.
5. **F. Volpin**, L. Chekli, S. Phuntsho, J. Cho, H. K. Shon, "Simultaneous Nutrients Recovery and Osmotic Concentration of Source-Separated Urine via Fertilizer drawn Forward Osmosis", **Oral Presentation at the Membrane Society of Australasia (MSA) Early Career Symposium (ECR)**, 30th of January to 2<sup>nd</sup> of February 2019, Melbourne, Australia.

6. **F. Volpin**, L. Chekli, S. Phuntsho, J. Cho, H. K. Shon, "Techno-economic feasibility of recovering phosphorous, nitrogen from urine via forward osmosis.", **at the Oral Presentation 9<sup>th</sup> International Water Association (IWA) Membrane Technology Conference and Exhibition for Water and Wastewater treatment and reuse**, 23-27 June 2019, Toulouse, France.

*Presentations made during the PhD candidature including proceedings, oral and poster presentations.*



# LIST OF ABBREVIATIONS

<b>AL-DS</b>	Active Layer facing Draw Solution
<b>AL-FS</b>	Active Layer facing Feed Solution
<b>AEMs</b>	Anion Exchange Membranes
<b>CAPEX</b>	Capital Costs
<b>COD</b>	Chemical Oxygen Demand
<b>CEMs</b>	Cation Exchange Membranes
<b>DCMD</b>	Direct Contact Membrane Distillation
<b>DI</b>	Deionised water
<b>DOC</b>	Dissolved Organic Carbon
<b>DS</b>	Draw Solution
<b>ED</b>	Electrodialysis
<b>EDX</b>	Energy Dispersive X-ray spectroscopy
<b>EPS</b>	Extracellular Polymeric Substances
<b>ES</b>	Electrolyte Solution
<b>FO</b>	Forward Osmosis
<b>FDFO</b>	Fertilizer Driven Forward Osmosis
<b>FS</b>	Feed Solution
<b>FU</b>	Fresh Urine (Nitrogen as urea)
<b>HC</b>	High Concentration
<b>HU</b>	Hydrolysed Urine (Nitrogen as ammonia)
<b>HRT</b>	Hydraulic Retention Time
<b>IEMs</b>	Ion Exchange Membranes
<b>ISS</b>	International Space Station
<b>LC</b>	Low Concentration
<b>LC-OCD</b>	Liquid Chromatography-Organic Carbon Detection
<b>LMW</b>	Low Molecular Weight
<b>MBR</b>	Membrane Bioreactor
<b>MD</b>	Membrane Distillation
<b>MLSS</b>	Mixed Liquor Suspended Solids
<b>NOB</b>	Nitrite Oxidizing Bacteria
<b>NF</b>	NanoFiltration
<b>OCV</b>	Open Circuit Voltage
<b>OPEX</b>	Operational Costs
<b>PD</b>	Power Density
<b>RED</b>	Reverse Electrodialysis
<b>RSF</b>	Reverse Salt Flux
<b>RO</b>	Reverse Osmosis
<b>SEM</b>	Scanning Electron Microscopy
<b>SRSF</b>	Specific Reverse Salt Flux
<b>TAN</b>	Total Ammoniacal Nitrogen

**TDS**

**TFC**

**UF**

**UPA**

**WWTP**

**Total Dissolved Solids**

**Thin-Film Composite**

**Ultrafiltration**

**Urine Processor Assembly**

**Wastewater Treatment Plant**

# ABSTRACT

Worldwide, the combined effect of urban intensification and ageing infrastructure is seriously challenging all utility providers. Wastewater treatment infrastructures are no different. The integration of novel decentralised solutions with the current centralised status quo is becoming an essential measure across the whole utility board, from energy production and storage to potable water harvesting, treatment, and supply and even to waste treatment. Decentralising the treatment of our wastes is especially of interest as it has the potential of transforming the water sector into a net producer of energy, water, and raw materials.

Urine source-separation is especially attractive due to urine low volume, high nitrogen (N) and phosphorus (P) concentrations (80% of N and 50% of P inputs into sewers), and the relative ease of collection and storage. As such, it has the potential of being a suitable raw material from the production of fertiliser, energy, and water.

While conventional technologies often struggle in dealing with urine alkalinity, high total ammoniacal nitrogen (TAN) and dissolved organic carbon (DOC) concentration (i.e. 3 to 5 g.L<sup>-1</sup>) and high salinity (i.e. 1 to 4%), the strong chemical resistance, small footprint, tuneable selectivity and versatility in the operation of membrane processes makes them suitable for extracting value from human urine. As such, this Thesis looked at novel stand-alone and membrane-based hybrid processes for the extraction of nutrients, energy, and clean water from source-separated human urine.

The Thesis begins by studying the use of moderate flux-opposing hydraulic pressure in forward osmosis (FO) and optimal membrane morphology in membrane distillation (MD), to minimise the leakage of nitrogen to the distilled water produced by the hybrid FO-MD process. Experimental results with both fresh and hydrolysed urine found that this novel approach can

decurtate the nitrogen flux in FO by up to 33%. Combining flux-opposing hydraulic pressure with optimum urine pH and draw solution (DS) salt concentration achieved FO water fluxes as high as  $28 \text{ L.m}^{-2}.\text{h}^{-1}$  while bringing the nitrogen leakage to a minimum of  $1.4 \text{ g.L}^{-1}$  (Starting from an initial nitrogen concentration of  $6.4 \text{ g/L}$ ).

While extracting water from urine is paramount on the International Space Station (ISS), producing sustainable and low-energy fertilisers from urine would help to alleviate the impacts of climate change by creating a more resilient food production network. This was addressed through the use of fertiliser driven-FO (which uses a concentrated fertiliser solution as DS) and a combination of membrane bioreactor (MBR) with MD. Each process was designed to cope with a specific “type” of urine: fresh or hydrolysed.

Firstly, it was shown that the combination of MBR and MD can produce an odourless concentrated liquid fertiliser with a concentration of nutrients similar to the commercial liquid products. The results showed that MBR was able to acidify the urine, removing  $> 95\%$  of its DOC and oxidising 50% of its ammonia to  $\text{NO}_3^-$ . By converting the volatile  $\text{NH}_3$  into ionic  $\text{NH}_4^+(\text{l})$  and  $\text{NO}_3^-(\text{l})$ , the MBR process enabled the MD dewatering step to achieve 95% water recovery without nitrogen losses. When tested for the growth of lettuce and Pak Choi, this fertiliser solution achieved plant biomass comparable to those from commercial fertilisers.

Alternatively, when treating diluted fresh urine, the Fertiliser Driven Forward Osmosis process (FDFO) proved to be an economical alternative to recover urine nutrients. In FDFO, a fertiliser DS is used to draw water from a less concentrated solution (in this case urine). One of the drawbacks of the FO process is the high reverse salt flux (RSF) or reverse diffusion of draw solutes but this was advantageously exploited to promote N and P recovery as liquid fertiliser and struvite, respectively. Using real urine as FS and a commercial fertiliser as DS, it was demonstrated that 50% urine concentration could be achieved, with 93% P recovery as struvite

and 50% N recovery as liquid urea. Operational and capital costs analysis showed that the benefit from the savings to the downstream wastewater treatment plant costs are of better value than any return from the sale of produced fertiliser.

Finally, the last two technical chapters of this Thesis looked at a novel use of FO and reverse electrodialysis (RED) processes to convert the urine salinity into osmotic driving force and electric energy, respectively. Where RED is a process that allows to convert an ionic flux into an electron flux thanks to the use of a stack of cation and anion exchange membranes.

For the first time, the use of a compact reverse electrodialysis (RED) system to convert the chemical potential energy of urine dilution into electric energy was explored. The results showed that 1 m<sup>3</sup> of real hydrolysed urine could produce 0.05 - 0.04 kWh of electrical energy. Also, when using urine as an electrolyte solution, it was demonstrated that the net chemical reactions occurring at the electrode compartments lead to TOC, TAN and urea removal of up to 13%, 6% and 4.4%. Overall, this process has the potential of providing off-grid urine treatment or energy production at a household or building level.

To conclude, in the last technical chapter it was proven that urine can be used as DS to dewater a microalgae solution. The combination of urine osmotic pressure (i.e. > 2000 kPa) and the high concentration of species with high self-diffusivity resulted in water flux as high as  $16.7 \pm 1.1$  L.m<sup>-2</sup>.h<sup>-1</sup> (with DI water was used as feed solution). Additionally, when dewatering a 0.2 g.L<sup>-1</sup> *Chlorella vulgaris* culture, urine DS achieved a fourfold increase in algal concentration with an average flux of 14.1 L.m<sup>-2</sup>.h<sup>-1</sup> and no support layer membrane fouling. The advantages of this process are that, once diluted during, urine could itself be used as growing media for microalgae cultivation.

Overall, this Thesis investigated the proof-of-concept of utilising multiple emerging technologies for the treatment of human urine. It was identified that, while processes like FO and RED so far seems to have a limited effectiveness in treating human urine, the combination of MBR with MD has showed to be a promising candidate in producing a fertiliser that is suitable for use in hydroponic cultivation.

**Keywords:** Human urine, urine treatment, membrane technology, membrane bioreactor, forward osmosis, membrane distillation, reverse electrodialysis, microalgae, International Space Station.



# TABLE OF CONTENTS

Statement of Original Authorship .....	iii
Acknowledgements .....	vii
List of Abbreviations.....	xiii
Abstract .....	2
Table of Contents .....	7
List of Figures .....	11
List of Tables.....	21
<b>Chapter 1: Introduction .....</b>	<b>23</b>
1.1 Research background .....	23
1.2 Objectives and scope of the research Aims.....	28
1.3 Thesis Outline .....	30
<b>Chapter 2: Literature Review .....</b>	<b>33</b>
2.1 Introduction.....	33
2.2 Human urine: composition and transformation under storage .....	34
2.3 Benefits of urine source-separation and reuse.....	45
2.4 Membrane-based processes for the treatment of human urine.....	60



2.5	Current and past implementation of urine source-separation.....	76
2.6	Conclusions.....	81

### **Chapter 3: Methodology..... 82**

3.1	Introduction.....	82
3.2	Experimental Materials.....	83
3.3	Analytical methods .....	86

### **Chapter 4: FO – MD optimisation to produce distilled water from human urine 90**

4.1	Summary.....	91
4.2	Introduction.....	92
4.3	Experimental investigation.....	95
4.4	Results and discussion .....	101
4.5	Conclusions.....	111

### **Chapter 5: Hybrid MBR - MD to produce concentrated fertiliser and distilled water 113**

5.1	Summary.....	114
5.2	Introduction.....	115
5.3	Experimental Investigation .....	118
5.4	Results and Discussion.....	127

5.5	Lettuce and Pak Choi plants growth .....	142
5.6	Conclusions.....	149

**Chapter 6: Nitrogen and phosphorus recovery from fresh urine via fertiliser driven forward osmosis..... 150**

6.1	Summary .....	151
6.2	Introduction.....	152
6.3	Experimental Investigation .....	155
6.4	Results and discussion .....	164
6.5	Conclusions.....	180

**Chapter 7: Energy recovery through reverse electrodialysis: Harnessing the salinity gradient from the flushing of human urine ..... 181**

7.1	Summary .....	182
7.2	Introduction.....	183
7.3	Experimental Investigations.....	185
7.4	Results and Discussion.....	194
7.5	Conclusions.....	211

**Chapter 8: Human urine as a forward osmosis draw solution for the application of microalgae dewatering ..... 213**

8.1	Summary .....	214
-----	---------------	-----

8.2	Introduction.....	215
8.3	Experimental Investigation .....	217
8.4	Results and discussion .....	221
8.5	Conclusions.....	233
<b>Chapter 9:</b>	<b>Conclusions and Recommendations.....</b>	<b>235</b>
9.1	Distilled water production from urine through FO – MD .....	235
9.2	Hybrid MBR - MD to produce fertiliser and distilled water.....	236
9.3	N and P recovery from fresh urine via FDFO.....	237
9.4	Energy recovery from urine dilution through RED .....	238
9.5	Urine as a FO draw solution to dewater microalgae .....	238
9.6	Recommendation for future work .....	240
9.7	Concluding remarks .....	242
	<b>Bibliography .....</b>	<b>245</b>

# LIST OF FIGURES

Figure 1-1 Classification of the separate waste streams from a household. (Adapted from (Larsen et al. 2016)).	24
Figure 1-2 Urine source-separation and re-use in the context of a circular approach to urban and space water management.	26
Figure 1-3 Schematic diagram of the five technical chapters and the different goals of each technical chapter.	29
Figure 2-1 shows the change in pH, EC and osmotic pressure during urea hydrolysis in the urine. * The OLI Studio Analyser software was used to estimate the osmotic pressure based on the chemical analysis of the urine solution. The van't Hoff equation $\pi = vRTc$ is used for the calculation (where c is the concentration, T the temperature and R the universal gas constant). Adapted from Volpin, Yu, et al. (2019).	42
Figure 2-2 Urine in relationship with combined domestic wastewater.	49
Figure 2-3 World nutrient balance of ammonia, phosphate $P_2O_5$ , potash $K_2O$ in 2020 (million tonnes) (FAO 2017b).	50
Figure 2-4 Schematic diagram of the potential benefits of shortcutting the nitrogen and phosphorus cycles for fertiliser production.	53
Figure 2-5 Schematic of the water recovery and management architecture for the ISS US segment. Adopted and modified from (Layne et al. 2015; Pruitt et al. 2015).	57
Figure 2-6 Schematic of the Urine Processor Assembly (A) and the Water Processor Assembly (B) installed at the ISS. Adopted and modified from (Layne et al. 2018; Pruitt et al. 2015).	59

Figure 2-7 On the left: Principles of FO and RO. Adapted from (Wicaksana et al. 2011). On the right: Relationship between pressure difference and molecular size cut-off in the different pressure-driven processes. Taken from (Fritzmann et al. 2007). .....	63
Figure 2-8 Principles of electrically driven processes and how they correlate with pressure-driven processes. Modified from (Mei & Tang 2018). .....	68
Figure 2-9 Initial concept of Water Wall system architecture. Credit to (Cohen et al. 2014). Permission granted by the copyright holder (Marc M. Cohen). .....	76
Figure 2-10 Graphic renderings of Aurin fertiliser production (A) and Vuna ltd. ( <a href="http://vuna.ch/index_en.html">http://vuna.ch/index_en.html</a> ) urine express vehicle (B). Permission granted by the copyright holder (Bastian Etter). .....	78
Figure 3-1 Flow diagram of the step-wise process adopted for each investigation.....	83
Figure 3-2 Urine storage tanks and urine piping system in the UTS Faculty of Engineering and IT building. ....	86
Figure 4-1 Schematic of the source-separated urine treatment system proposed. Water is extracted from the urine solution to the draw solution, through forward osmosis, while the MD system is used to reconcentrate the draw solution and produce distilled water. ....	95
Figure 4-2 Forward osmosis water flux using fresh or stored urine as feed, and NaCl at different concentrations as draw solution. ....	103
Figure 4-3 Nitrogen rejection (right axis) and transport from feed to draw per volume of treated water (left axis). For every draw concentration, the stacked column on the left refers to the fresh urine while the column on the right to the hydrolysed urine. ....	104
Figure 4-4 Water and urea flux as a function of transmembrane pressure exerted on the draw side. The operating conditions are also detailed in the picture. ....	105

Figure 4-5 Impact of feed acidification in the transport of nitrogen (A) and water (B) across the TFC-FO membrane. Figure (B) also displayed the calculated feed osmotic pressure as a function of the pH. The osmotic pressure of the solution was calculated using ROSA software (Version 9.1, Dow Filmtech, USA).....	107
Figure 4-6 Water flux of PVDF and PTFE MD membranes using 1.5M NaCl as DS and feed temperature of 40, 50 or 60 °C. Permeate temperature was kept at 20 °C.....	108
Figure 4-7 Specific nitrogen flux from the urine solution (T= 60 °C, pH = 8.87) to the de-ionised water permeate (T= 20 °C) using PVDF or PTFE MD membranes. The feed solution consists of stored urine with a dilution factor of 1:1, 1:10 and 1:100.....	110
Figure 5-1 Schematic diagram showing the collection, nitrification via MBR, dewatering via DCMD and testing of urine fertiliser on a vertical garden.....	119
Figure 5-2 Picture of the membrane bioreactor unit used to nitrify real human urine. ....	120
Figure 5-3 potting mix used for the hydroponic experiments. PM1 is a cylindrical media made of special mix material mainly composed of Peatmoss, PM2 is a cubic media made of Cocopeat and PM3 is a vermiculite fine grade/Perlite P400/Orchiata Pine bark 6-9 mm (ratio 1/1/1) filled in a 105 mm MIDI pot.....	125
Figure 5-4 Performance of the MBR when using raw undiluted urine as feed. The top graph (A) shows the removal of DOC while the bottom (B) the conversion of $\text{NH}_3$ to $\text{NO}_2^-$ and $\text{NO}_3^-$ . The operating pH was $6.2 \pm 0.2$ . ....	129
Figure 5-5 OCD signals obtained by analysing urine before and after the MBR as well as the MD concentration and permeate. ....	132
Figure 5-6 Above: Permeate flux and electric conductivity of synthetic and real nitrified urine as a function of urine concentration factor ( $T_f = 55^\circ\text{C}$ , $T_p = 20^\circ\text{C}$ , $V_{f,p} = 0.06\text{ m.s}^{-1}$ ).	

Below: Anions, cations and organics concentration in the urine and the final MD permeate using synthetic urine (Fig. B) and real urine (Fig. C). Relative rejection is plotted in red. .... 136

Figure 5-7 (A) Amount of ammoniacal nitrogen and DOC transported to the permeate side from real and synthetic urine using membrane distillation. (B) Theoretical fractionation of ammoniacal nitrogen into  $\text{NH}_3$  and  $\text{NH}_4^+$  based on the pH and temperature. The pKa coefficient at different temperature was obtained using OLI Studio Analyser (Version 9.5, Oli Systems Inc., USA) and from the literature (Bates & Pinching 1950). ... 138

Figure 5-8 Pictures A and B show the MD membrane (B) and spacers (C) after reaching 95% real urine concentration. Picture C shows the membrane after cleaning with DI water, citric acid and sodium hydroxide. .... 140

Figure 5-9 Above: MD permeate flux, feed and permeate conductivity for two repeated cycles (A and B) of real urine concentration, with 0.1 M NaOH cleaning procedure. Below: SEM images of the MD used for real urine concentration, after DI-water flushing (C) and after alkaline with 0.1 M of NaOH (D). .... 141

Figure 5-10 Picture of the pristine membrane and the fouled membrane before and after NaOH and Citric Acid cleaning. .... 142

Figure 5-11 Electrical conductivity and pH of the fertiliser solutions during part of the growing experiment. .... 144

Figure 5-12 Picture of the GSky Versa Wall set up with the different growing media. The first three rows (A) were fertilised with Half-strength Hoagland's solution (Hs), the second three (B) with urine (Us) and the bottom three (C) with the commercial nutrients solution (Cs). .... 146

Figure 5-13 Fresh and dry weight of aerial parts and roots for lettuce (green) and Pak Choi (brown) grown in PM1. Roots to shoots ratio are also displayed in the column on the right. A picture of the separation between leaves (aerial parts) and roots of lettuce is shown at the top. ....	147
Figure 5-14 Fresh and dry weight of shoots and roots for lettuce (green) and Pak Choi (brown). Roots to shoots ratio are also displayed in the last row. ....	148
Figure 6-1 Schematic representation of the process.....	156
Figure 6-2 Water flux using 0.5 M $\text{Mg}(\text{NO}_3)_2 \cdot 6\text{H}_2\text{O}$ as DS and real urine as feed. The pH of the urine was adjusted to 6, 6.5, 6.75, 7, and 7.5 to understand its influence on membrane scaling. On the right side, an SEM picture of the fouled membrane is also displayed. ....	165
Figure 6-3 Phosphorus removal via struvite precipitation with different urine dilution factors. ....	166
Figure 6-4 Picture of the membrane coupon before and after the alkaline cleaning. The feed solution was real urine while the draw was commercial fertiliser. The experimental run time was 11 days.....	168
Figure 6-5 On the left (Fig. A), forward osmosis water flux having as FS urine with different dilution factors (i.e., 1, 2 and 5 times) and 0.5 M $\text{Mg}(\text{NO}_3)_2 \cdot 6\text{H}_2\text{O}$ as DS. The time necessary to reach the urine concentration factor was displayed at the end of the plot. On the right (Fig. B) it is shown the water flux before and after the urine tests, and subsequent membrane cleaning, using 0.5 M NaCl as DS and DI-water as feed. ....	169
Figure 6-6 Statistical correlation between the total nitrogen (TN) recovery from the urine and the urine concentration during the FO process. ....	171



Figure 6-7 (A) Nitrogen and magnesium flux. The blue columns represent the average specific nitrogen flux, in the form of urea and TAN, from the urine to the fertiliser solution. The red dots represent the specific reverse magnesium flux from the fertiliser (i.e.,  $\text{Mg}(\text{NO}_3)_2 \cdot 6\text{H}_2\text{O}$ ) to the urine. (B) Measured recovery of phosphorus ( $\text{PO}_4^{3-}$ ), total nitrogen (TN) and urea + ammonia at the end of each experiment. .... 171

Figure 6-8 XRD spectrum of the precipitates obtained from the concentrated FS after FO filtration. .... 172

Figure 6-9 SEM picture and EDX spectrum of the precipitates obtained after filtration of the concentrated urine. .... 173

Figure 6-10 (A) Theoretical and experimental water flux and fertiliser dilution as a function of the urine concentration factor. Clean in place (CIP) with 0.1 M NaOH was performed after about 33% urine concentration. (B) Total nitrogen and phosphorus in the urine. .... 175

Figure 6-11 (A) shows the comparison of the estimated costs and revenues of this process. (B) shows the economic analysis of using FDFO, assuming that the construction of the plant is finalised in 1 year. For both analyses, the costs consist of the sum of OPEX and CAPEX while the revenues as the sum of produced fertiliser (urea + struvite) and downstream WW treatment savings. .... 178

Figure 6-12 Breakdown of the operational costs (A) and capital costs (B)..... 179

Figure 6-13 Breakdown of fertiliser revenue (A) and downstream nitrogen and phosphorous removal savings (B). .... 179

Figure 7-1 (A) Schematic drawing of the single-pass RED experiments using fresh and hydrolysed urine. (B) Schematics of the two different configurations used for the experiments. In the first configuration, (System A)  $\text{K}_4\text{Fe}(\text{CN})_6/\text{K}_3\text{Fe}(\text{CN})_6$  are used as ES and

recirculated in the anode and cathode chamber. In the second configuration (System B), real fresh or hydrolysed urine is used as ES. ....	186
Figure 7-2 Picture of the RED setup used for the experiments. ....	187
Figure 7-3 Baseline performances of the RED stack operated with an 0.6M NaCl solution as HC solution and $K_3Fe(CN)_6$ / $K_4Fe(CN)_6$ as ES. HC and LC solutions were flowed inside the stack in single-pass and with flow rates of 5, 10, 15, 25 and 35 mL.min <sup>-1</sup> . ....	195
Figure 7-4 Performances of the RED stack operated with an 0.6M NaCl solution, Synthetic FU and HU and real FU and HU. The solutions were flowed inside the stack in single-pass and with flow rates of 5, 10, 15, 25 and 35 mL.min <sup>-1</sup> and $K_3Fe(CN)_6$ / $K_4Fe(CN)_6$ was used as ES. ....	197
Figure 7-5 (A) shows the net power densities achieved ( $PD_{Net}$ ), Figure (D) displays the energy recovered $E_{Net}$ and energy efficiency $\eta$ are displayed. HC and LC solutions were flowed inside the stack in single-pass and with flow rates of 5, 10, 15, 25 and 35 mL.min <sup>-1</sup> and $K_3Fe(CN)_6$ / $K_4Fe(CN)_6$ was used as ES. ....	199
Figure 7-6 Single ion species transport from HC to LC at different flow velocities. In Figure (A) synthetic FU was used while synthetic HU was used in Figure (B). ....	201
Figure 7-7 (A) shows the overall ions transport, based on electric conductivity measurements, from the HC to the LC solution at increasing urine flow rate. The overall nutrients recovery, measured as the transport of nitrogen/phosphorus/potassium from urine to the Lc solution, is displayed in Figure (B). ....	201
Figure 7-8 Performances of the RED stack operated with a Synthetic FU and HU and real FU and HU as both HC and ES solution. HC and LC solutions were flowed inside the stack in single-pass and with flow rates of 5, 10, 15, 25 and 35 mL.min <sup>-1</sup> while the ES solution flowed at 5 mL.min <sup>-1</sup> . ....	203

Figure 7-9 Baseline performances of the RED stack tested with synthetic and real FU and HU solutions both as HC and ES solutions. HC and LC solutions were flowed inside the stack in single-pass and with flow rates of 5, 10, 15, 25 and 35 mL.min <sup>-1</sup> while ES was pumped with a flow rater of 5 mL.min <sup>-1</sup> .....	204
Figure 7-10 (A) shows the overall ions transport, based on electric conductivity measurements, from the HC to the LC solution at increasing urine flow rate. The overall nutrients recovery, measured as the transport of nitrogen/phosphorus/potassium from urine to the LC solution, is displayed in Figure (B).....	205
Figure 7-11 Mass balance of the Cl <sup>-</sup> , TOC, NH <sub>4</sub> <sup>+</sup> and urea in the urine used as electrolyte solution at different stack's voltage and current. The mass balance was calculated as per section 2.3.3, and the ES was pumped with a flow rate of 5 mL/min. Figure A shows the results for real FU while real HU is shown in Figure B.....	206
Figure 7-12 Characterisation of the AEMs (top) and CEMs (bottom) before and after the tests with real fresh and hydrolysed urine. Each picture shows the pristine membrane at the bottom, the membrane fouled with HU at the top, and the membrane fouled with FU in the middle. Energy dispersive X-Ray spectra are displayed on the left-hand side while Fourier-transform infrared spectra are shown on the right-hand side.....	210
Figure 8-1. Conceptual design of the process where urine is used as DS to concentrate a microalgae solution.....	219
Figure 8-2. Measured urea and ammonia (A), pH and conductivity (B) during urine storage. * The osmotic pressure of the urine was calculated using OLI Stream Analyser 3.1 software based on the chemical analysis of the urine during storage (OLI Systems Inc., Morris Plains, NJ, USA).....	223

Figure 8-3 Histograms representing the water flux and EC of several samples of fresh (A) and hydrolysed (B) urine. The red triangles indicate the EC of the samples tested. These experiments were run for one hour, using 500 mL of DS (urine) and 500 mL of FS (DI-water). .....	225
Figure 8-4 Summary of the experiments conducted with real, synthetic, fresh and hydrolysed urine using DI-water as FS. The water flux is presented in (A), while the SRSF of TN and TOC are displayed in (B).....	225
Figure 8-5. Experiments with real hydrolysed urine as draw solution and deionised water as feed. The tests were performed until > 70 % DS dilution (A). The membrane was tested with standard 0.5 M NaCl as DS and DI – water as FS before and after the experiments. The differences in flux before and after the urine tests are displayed in Figure 8-5 (B).	227
Figure 8-6. (A) Picture of the support layer after using real hydrolysed urine as DS and DI-water as FS. SEM image of the pristine membrane support layer (B) and SEM image of the support layer after FO experiments with hydrolysed urine as DS and DI-water as FS (C). .....	228
Figure 8-7. Long-term testing (>20 hours) of real and synthetic urine in dewatering a 0.2 g/L solution of <i>Chlorella vulgaris</i> . The experiments were carried out using 2 L of draw solution and 500 mL of feed until the FS was concentrated four times. Synthetic seawater (0.6 M NaCl) was also tested as a benchmark for the results. ....	230
Figure 8-8. Photo (A) and SEM picture (B) of the active layer of the FO membrane after microalgae filtration.....	230
Figure 8-9. Extracellular carbohydrate content (histograms) and total nitrogen (red squares) in the solution before dewatering and after the FO concentration, using different draw solutions. ....	232

Figure 9-1 Schematic diagram of the main benefits (green) and limitation (red) of the processes presented in the five technical chapters. ....	239
Figure 9-2 Proposed roadmap for the implementation of urine-derived fertilisers. ....	241

# LIST OF TABLES

Table 2-1 Organic and inorganic chemical composition of human urine from the literature. The results from the first two rows are from the analysis conducted at the University of Technology Sydney (UTS), urine source separation system. The main difference between waterless urinals and urine-diverting toilets is that, in the latter, urine gets diluted 2 to 4 times with tap water.....	37
Table 2-2 Pharmaceuticals and hormones concentrations in human urine from the literature. The results from the first two rows are from the analysis conducted at the University of Technology Sydney. The main difference between waterless urinals and urine-diverting toilets is that, in the latter, urine gets diluted 2 to 4 times with tap water. The frequency of occurrence row indicates how frequently the compound was detected in the samples. ....	38
Table 3-1 Composition and characteristics of the synthetic fresh and hydrolysed urine feed solutions (Putnam 1971a; Udert, Larsen & Gujer 2006; Zhang, She, et al. 2014b).85	
Table 4-1 Pure water permeability (A) and solute permeability (B) of the membrane used for the experiments. The B value for urea, ammonium and ammonia in both FU and SU, were determined in RO mode at 10 bar pressure.....	97
Table 4-2 Proprieties of the MD membranes employed. * The contact angle was based on a recent study with the same membranes (Silva et al. 2018).....	98
Table 5-1 Characteristics and composition of urine before and after MBR and MD.....	130
Table 5-2 LC-OCD data of raw urine, MBR permeate (during stable operation), and MD permeate. Samples from MD permeate and concentrate were collected at 95% urine concentration factor. ....	133

Table 5-3 Concentration of the elements in the nutrient solutions before and after dilution.	143
Table 6-1 Ionic composition, osmotic pressure, pH and EC of fresh urine and the commercial liquid fertiliser used in this study.	158
Table 6-2 Input parameters used for the modelling of water flux. Osmotic pressure and diffusivity were estimated using OLI Studio Analyser (Version 9.5, Oli Systems Inc., USA) while rejection, A and S are based on experimental data. The A value was measured by applying 10 bar of hydraulic pressure and recording the transmembrane flux. To calculate the B value of the commercial fertiliser, the membrane rejection of a 500 mg/L fertiliser solution was measured under 10 bar operating pressure.	161
Table 6-3 Summary of the main assumptions used to calculate the OPEX/CAPEX cost of operating an FDFO plant (Valladares Linares et al. 2016). Australian Energy Market Commission data were used for the New South Wales energy prices (AEMC 2013).	163
Table 6-4 Summary of the main assumptions used to calculate the revenue and savings of operating an FDFO plant to recover N and P from human urine.	164
Table 7-1 Characteristic and proprieties of Fujifilm Type I membranes.	190
Table 8-1. Ionic composition, pH and conductivity of fresh and hydrolysed urine.	222

# Chapter 1: Introduction

---

## 1.1 Research background

With rising resource prices and climate change, moving from a linear economic model of "take-make-dispose", to a circular model of "take-make-revalorise-reuse" is gaining traction as an emerging sustainable policy goal (Gregson et al. 2015). In the field of urban water management, this also means investing in flexible and decentralised sewage treatment solutions that would allow for the recovery and re-use of the water, energy and nutrients in our wastes. However, the heterogeneous and "dilute" nature of typical wastewater streams steeply increases the complexity and cost of downstream value recovery.

In this context, source-separation of urine, faeces and greywater source has been proposed as a way to achieve more resilient and energy-efficient sanitation (Figure 1-1) (Larsen & Gujer 1996; Larsen & Gujer 1997). This would help to safeguard our cities' ability to deal with an increasingly dense urban population as well as allowing for the potential of producing "recycled" fertilisers helping to cope with the increasing demand for nitrogen, phosphorus and potassium (N-P-K) fertilisers (FAO 2017a).



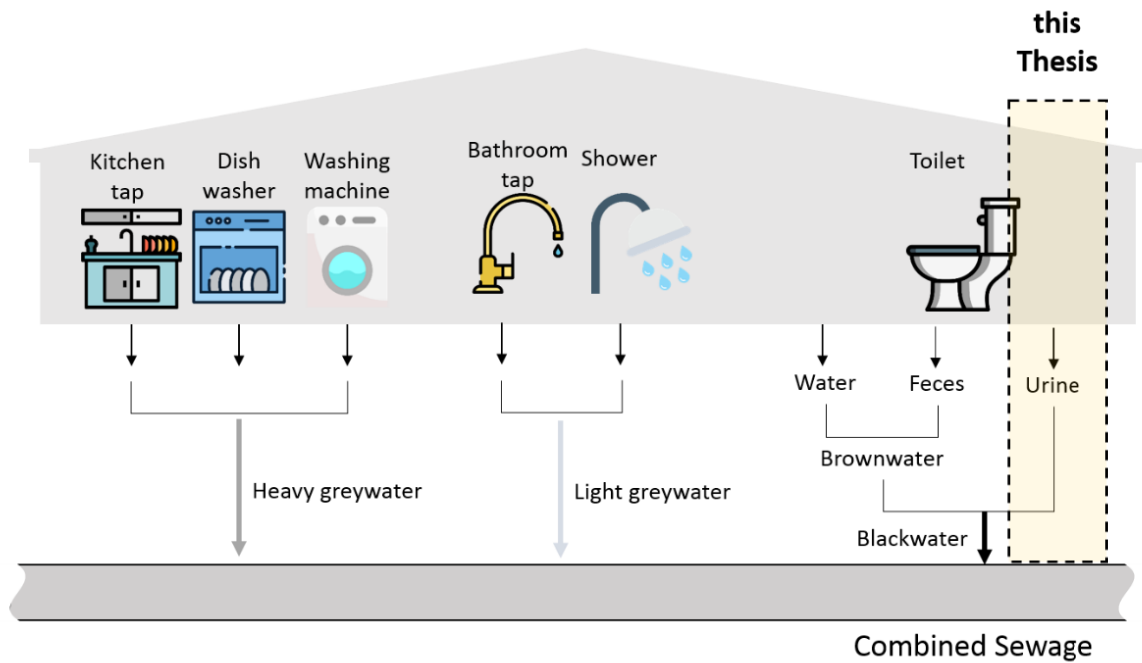


Figure 1-1 Classification of the separate waste streams from a household. (Adapted from (Larsen et al. 2016)).

Separate collection and treatment of urine is especially attractive due to its low volume (< 1% of the sewers flow) and high N and P concentrations (80% of N and 50% of P inputs into sewers) (Maurer, Pronk & Larsen 2006; Randall & Naidoo 2018). Besides its composition, the relative ease of collection of urine and its storage makes it an excellent raw material for fertiliser and energy production (Ledezma et al. 2015; Udert & Wächter 2012).

The side effect of urine's dense nutrients composition is that, when mixed with combined wastewater, it increases the cost and complexity of the treatment significantly. In Chapter 2 section 2.3.1.1, it is shown how the residents of the Greater Sydney area are spending up to 35 million dollars per year just to remove the TAN and  $\text{PO}_4^{3-}$  coming from urine. On top of that, the high concentration of pharmaceuticals in urine (i.e., 2-3 orders of magnitudes higher than average sewage water) further complicates the downstream treatment of domestic wastewater (Zhang et al. 2015).

Both the cost and complexity of the treatment are significantly reduced when urine is processed separately. That is because of its low volume and relatively consistent composition (Larsen et al. 2009).

The high water content of urine is also a precious resource in the context of Bioregenerative life-support in space (NASA 2015). Onboard the International Space Station any source of wastewater has to be reclaimed to minimise resupply costs. That is why space agencies such as NASA were the first to promote research to provide detailed chemical and physical properties of human urine to understand how to extract water from it (Putnam 1971a; Putnam & Thomas 1969). Additionally, in the context of biological life support systems, being able to re-use the nutrients in astronaut's urine to support food production on the ISS will be necessary when targeting long-term space exploration missions.

Based on the above, Figure 1-2 shows a conceptual diagram to support the hypothesis that urine source-separation and re-use can foster circular nutrient economy while improving the efficiency and effectiveness of our wastewater treatment infrastructure.

This Thesis will focus specifically on the technologies that would enable water, nutrients and energy recovery.

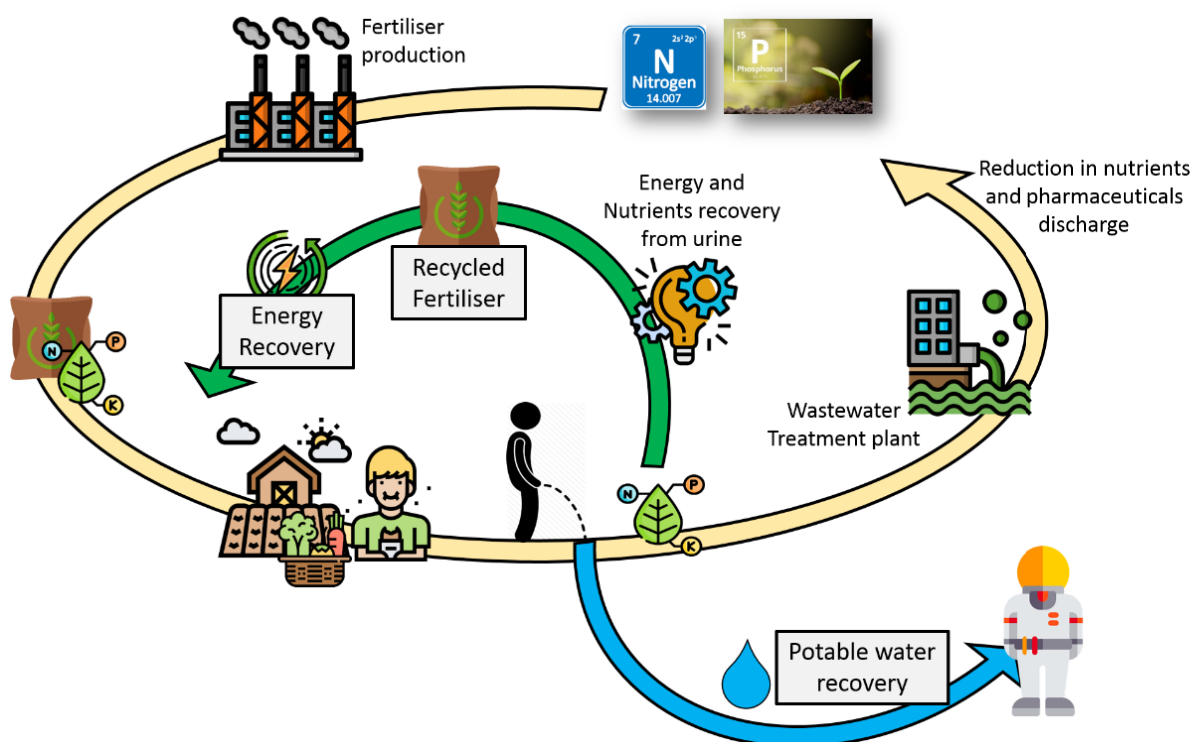


Figure 1-2 Urine source-separation and re-use in the context of a circular approach to urban and space water management.

In recent years, the effectiveness of different technologies on the treatment and re-use of human urine has been investigated, with most of the research focusing on urine as a source of energy and nutrients in an urban context and urine as a source of water in the ISS context. However, conventional technologies are often not capable of dealing with urine's complex matrix, high salinity, pH and free ammonia concentration, as well as its contamination with hormones and pharmaceuticals (Clauwaert et al. 2017; Maurer, Pronk & Larsen 2006).

As membrane technologies have specifically been designed to separate water or other compounds from the bulk solution, they have recently been proposed as suitable stand-alone or combined processes for urine treatment. The small footprint, tuneable selectivity, strong chemical resistance and versatility in the operation are all desirable proprieties to have when treating human urine. However, conventional pressure-driven processes like RO and NF have

shown to suffer from severe membrane fouling and scaling, low rejection of urea/ammonia and high operating pressures to overcome urine salinity (Maurer, Pronk & Larsen 2006; Pronk et al. 2006). Therefore, they are rarely adopted as a stand-alone process for the filtration of real human urine.

On the other hand, the effectiveness of recently emerged membrane technologies on human urine, and their hybridisation with other conventional processes have still not yet been adequately studied and understood. It was hypothesised that the unique transport proprieties of processes like forward osmosis, membrane distillation and reverse electrodialysis could be used to exploit the following proprieties of human urine:

- **High salinity:** It was used, for the first time:
  - To extract water from a more dilute solution via FO process.
  - To produce electric energy and redox reactions via RED process.
- **High urea and  $\text{PO}_4^{3-}$  concentration in fresh urine:** It was taken advantage of using FDFO process to enrich the fertilizer DS with additional nitrogen and promote struvite recovery thanks to the RSF of the magnesium in the DS.
- **High ammonia concentration when hydrolyzed:** The nitrogen losses during dewatering via MD or FO were minimized by:
  - Biological urine pre-treatment to convert volatile ammonia into  $\text{NH}_4^+$  and  $\text{NO}_3^-$  to avoid N losses during MD.
  - FO-MD process optimization through the application of back-pressure in the FO step.

## 1.2 Objectives and scope of the research Aims

This Thesis is aimed to propose novel configurations using recently emerged membrane technologies such as forward osmosis, membrane distillation and reverse electrodialysis to maximise their effectiveness in recovering water, nutrients or energy from real human urine.

The specific objectives of this Thesis are graphically shown in different segments in Figure 1-3 and below summarised:

- Evaluate the effectiveness of hybrid FO-MD in recovering freshwater from fresh human urine, and optimise its performances.
- Demonstrate that urine can be used as raw material to produce two types of fertiliser:
  - ✓ A concentrated liquid fertiliser via a novel MBR-MD process
  - ✓ A solid slow-release fertiliser together with a dilute liquid fertiliser through fertiliser driven FO
- Demonstrate that the chemical energy in typical urine can be exploited by using:
  - ✓ FO process, when the target is to dewater a high-value mixture such as microalgae culture
  - ✓ RED, when the objective is to convert the potential energy of mixing urine with tap water into electric energy.

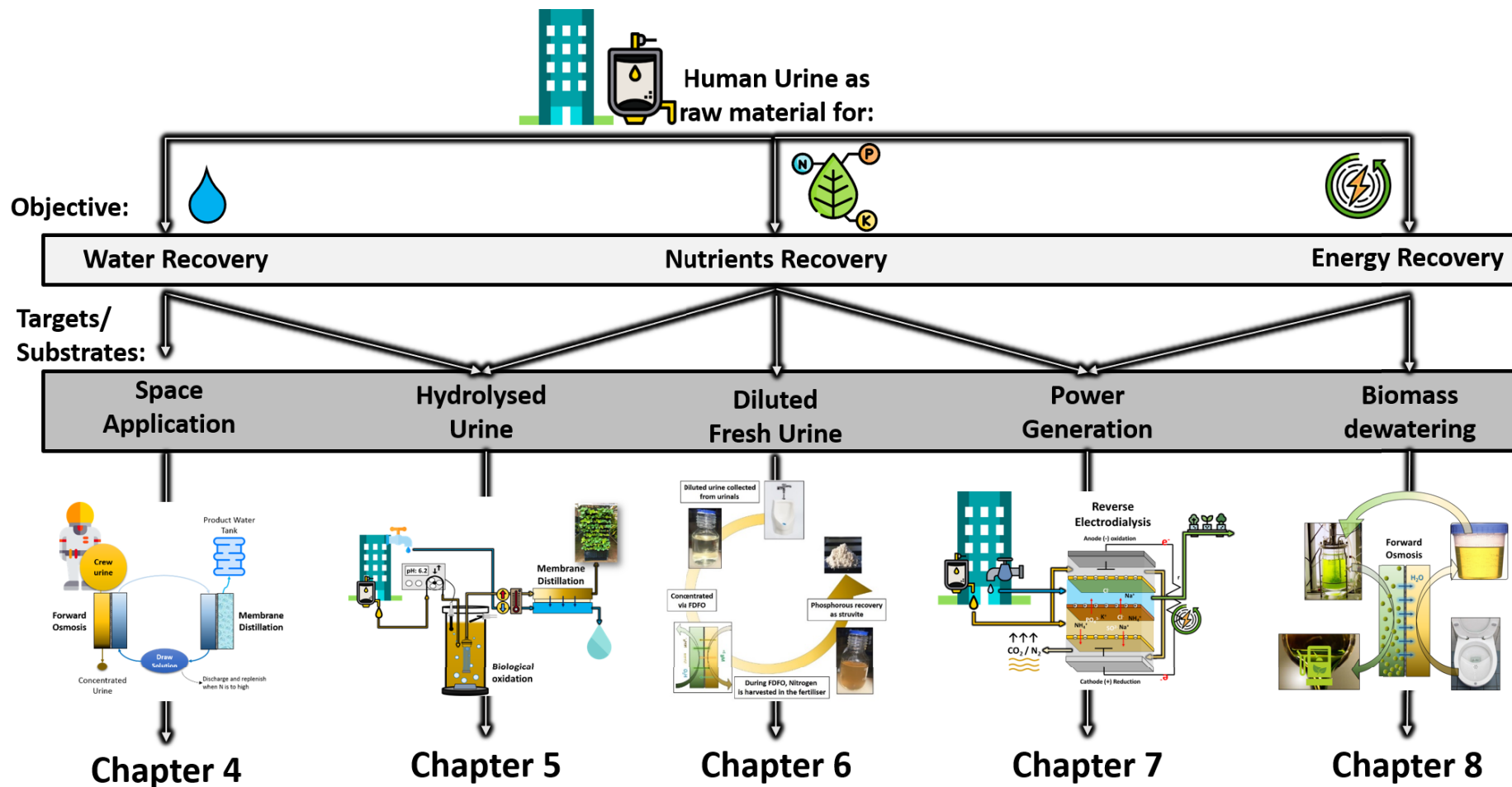


Figure 1-3 Schematic diagram of the five technical chapters and the different goals of each technical chapter.

### 1.3 Thesis Outline

This Thesis is organised into eight main chapters, as follows:

- Chapter 1 introduces the research background, objectives and scope of the research.
- Chapter 2 provides background information by way of a literature review to highlight the research motivation and gaps in the literature. It starts by describing the social and economic costs of conventional urine treatment and the benefits associated with urine source-separation and recovery. Following that, it argues the benefits of adopting membrane-based processes for urine treatment. Then it describes how novel processes such as FO, MD and RED could be used to valorise human urine. Finally, it presents some real pilot and large-scale implementation of urine source-separation.
- Chapter 3 describes the methodology used for the collection/preparation and characterisation of urine.
- Chapter 4 focuses on the optimisation of hybrid FO-MD to minimise the leakage of nitrogen to the produced water.
- Chapter 5 presents a comprehensive study on how to produce distilled water and safe and odourless concentrated liquid fertiliser from real human urine. Hybrid nitrification MBR and MD were used in this chapter. The performance of the fertiliser in growing leafy vegetables hydroponically was also tested.
- Chapter 6 is on a novel FDFO process to achieve simultaneous P and N recovery from fresh urine. The novelty of the process was to utilise a

magnesium-based draw solution to use the RSF phenomenon to trigger the recovery of P as struvite in the concentrated urine.

- Chapter 7 proposed a novel use of RED to recover the chemical energy of mixing urine with tap water. Through RED this chemical energy was converted into electric energy.
- Chapter 8, similarly to Chapter 7, proposed a novel way to exploit the high chemical energy in human urine. This time, through FO. This chapter shows how urine can be used as a novel FO draw solution for the dewatering of complex mixtures such as microalgae.

Finally, Chapter 9 concludes the Thesis and provides recommendations for future research.





# Chapter 2: Literature Review

---

## 2.1 Introduction

This chapter begins with a detailed description of the chemical-physical proprieties of human urine and its adequate disinfection and storage (Section 2.1). Following that, it reviews the literature on the following topics: Topic 1: Benefits of source-separation and reuse of human urine (section 2.3). Here the opportunities that urine source-separation can provide in achieving (i) cheaper and cleaner WWTPs, (ii) closing the nutrients loop and (iii) allowing for water reuse on the International Space Station (ISS) are presented. Topic 2: Membrane-based technologies for urine treatment (section 2.4). Here the role that membrane technologies have in enhancing urine treatment efficiency are outlined. Topic 3: Current and past implementations of urine recovery and re-use (Section 2.5). Here examples of urine recovery and reuse all around the world are presented and analysed. Finally, the last section concludes the review of the literature and highlight its implications to develops a conceptual framework for the study.

## **2.2 Human urine: composition and transformation under storage**

### **2.2.1 Chemical composition of urine**

#### **2.2.1.1 Urine production and general composition**

In a well-functioning renal system, the kidneys would retain larger molecules such as proteins and serum aluminium (MW: 67,000 Da) while allowing for the passage of compounds like urea, creatinine and uric acid (Yang, Chung & Santoso 2007). That is why normal urine contains mostly electrolytes, nitrogenous compounds, vitamins, hormones, organic compounds (acids and non-acids). These constituents can add up to a concentration of 35000 mg.L<sup>-1</sup> in normal urine (Putnam 1971a). Although the actual concentration of the above varies depending on the diet, environmental conditions and physical exertion, it shows that 1-4% of urine mass consists of ions and soluble organic compounds. As, on average, we excrete about 1270 g<sub>urine</sub>.p<sup>-1</sup>.d<sup>-1</sup>, a substantial amount of solids could be retrieved from each individual (Randall & Naidoo 2018; Rose et al. 2015). Rose et al. (2015) calculated that up to 22 ± 1.3 kg.cap<sup>-1</sup>.yr<sup>-1</sup> of total solids are produced by an adult.

Overall, despite the variation in urine composition dictated by the various collection methods, this Thesis will focus on two different broad categories: Macro and micronutrients and trace organics.

#### **2.2.1.1 Macro and micronutrients in urine**

Among the different constituents, nitrogen makes up 14-18% of the solids in dry urine, carbon 13% and phosphorus and potassium 3.7% (Strauss 1986). Overall, Figure 2-1 shows that urea (or ammonia after ureolysis) is by far the dominant compound, with concentrations averaging around 6-8 g.L<sup>-1</sup>, followed by K<sup>+</sup> and Na<sup>+</sup> (both with a

concentration between 1-2 g/L) (Kirchmann & Pettersson 1994; Putnam 1971a). Urea and ammonia only account for 75-90% of the N excreted, the remaining being creatinine (up to 2 g.L<sup>-1</sup>).

Essential trace elements and heavy metals such as B, Cu, Zn, Mo, Fe, Co and Mn are also detected in human urine at concentrations suitable for fertiliser production (Table 2-2) (Maurer, Pronk & Larsen 2006; McBride & Spiers 2001).

#### 2.2.1.1 Trace organics (TrOCs) in urine

A meta-analysis of 212 pharmaceuticals performed by Lienert, Bürki & Escher (2007) showed that an average of 64% of the TrOCs mass consumed is excreted through urine. That is because they generally are hydrophilic and able to pass through the kidneys. It has been estimated that between 50-90% of the antibiotics that we take are excreted via urine as a mixture of metabolites and parent compounds (Kümmerer 2009; Landry & Boyer 2013; Tran, Reinhard & Gin 2018). For example, when studying the toxicity of 42 pharmaceuticals in human urine, Lienert, Güdel & Escher (2007) showed that nearly 67% of them retained at least half of their toxicity. Among the tested pharmaceuticals ibuprofen, acetylsalicylic acid, bezafibrate, carbamazepine, diclofenac, fenofibrate, and paracetamol were found to, possibly, pose an ecotoxicological risk (Lienert, Güdel & Escher 2007).

In Table 2-2 the concentration of pharmaceuticals in the urine collected from the UTS urine-diverting toilets is displayed, together with values from the literature (Abey Suriya, Fam & Mitchell 2013; Bischel, Özel Duygan, et al. 2015). The results show that compounds like caffeine and 4-acetaminophen, which are widely consumed

in office buildings, can reach concentration levels 100 times higher than in the combined wastewater).

Table 2-1 Organic and inorganic chemical composition of human urine from the literature. The results from the first two rows are from the analysis conducted at the University of Technology Sydney (UTS), urine source separation system. The main difference between waterless urinals and urine-diverting toilets is that, in the latter, urine gets diluted 2 to 4 times with tap water.

	EC	COD	NH <sub>3</sub> -N	Urea	Creatinine	PO <sub>4</sub> <sup>3-</sup> -P	K <sup>+</sup>	Mg <sup>2+</sup>	Na <sup>+</sup>	Ca <sup>2+</sup>	B	Mn	Fe	Cu	Zn
	[mS/m]	[mg/L]				[mg/L]									
UTS Waterless Urinal (Hydrolysed urine) <sup>1</sup>	40.5 ± 0.7	6170 ± 621	6820 ± 145	n.d.	-	178 ± 15	1600 ± 112	13 ± 21	1970 ± 129	5 ± 31	883 ± 101	<1	19 ± 8	6.7 ± 1.1	200 ± 34
UTS Urine Diverting Toilet (Hydrolysed urine) <sup>1</sup>	25.9 ± 0.4	4870 ± 728	3850 ± 121	n.d.	-	85 ± 5	1387 ± 97	36 ± 25	1200 ± 83	7 ± 20	1170 ± 50	<1	23 ± 11	18 ± 3	137 ± 31
Fresh Urine <sup>2</sup>	15.5 – 19.6	-	200 - 730	9300 - 23300	670 - 2150	470 - 1070	750 - 2610	102 - 205	1170 - 4390	30 - 390	435 - 440	0.0 - 62	165 - 205	13 - 10.8	19 - 665

<sup>1</sup>(Abey Suriya, Fam & Mitchell 2013; Mitchell, Fam & Abey Suriya 2013b), <sup>2</sup>(Heitland & Köster 2004; Kirchmann & Pettersson 1994; Putnam 1971a).

Table 2-2 Pharmaceuticals and hormones concentrations in human urine from the literature. The results from the first two rows are from the analysis conducted at the University of Technology Sydney. The main difference between waterless urinals and urine-diverting toilets is that, in the latter, urine gets diluted 2 to 4 times with tap water. The frequency of occurrence row indicates how frequently the compound was detected in the samples.

	Caffeine	Carbamazepine	Ibuprofen	Naproxen	Estrone	Estriol	Fluoxetine	4-acetamidophenol	Triclosan	Diclofenac
UTS Waterless Urinals <sup>1</sup> [µg/L]	1480 ± 35	37 ± 3	497 ± 41	<10	<10	6 ± 4	12 ± 2	477 ± 278	48 ± 9	<10
UTS Urine Diverting Toilet <sup>1</sup> [µg/L]	2170 ± 145	<5	<10	197 ± 195	<10	9 ± 7	<5	2700 ± 1560	25 ± 4	<10
	Diclofenac	Sulfamethoxazole	N4 Acetyl-SMX	Trimethoprim	Hydrochlorothiazide	Atenolol acid	Ritonavir	Atenolol	Emtricitabine	Clarithromycin
Concentration Range <sup>2</sup> [µg/L]	3.2 - 72	<2 - 6800	<1 - 3500	<2 - 1300	<3 - 134	<4 - 1100	<1 - 4.6	<1 - 300	<6 - 920	<1
Frequency of occurrence <sup>2</sup>	100%	95%	90%	85%	80%	75%	70%	55%	40%	20%

2.2.1.1 <sup>1</sup>(Abey Suriya, Fam & Mitchell 2013; Mitchell, Fam & Abey Suriya 2013b), <sup>2</sup>(Bischel, Özel Duygan, et al. 2015).

#### 2.2.1.2 Urine composition in microgravity

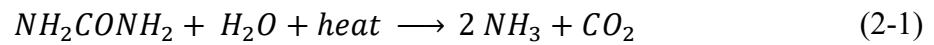
The urine collected in space from crew members generally contains higher calcium concentrations compared to the same urine if collected on Earth. This is because of the renal adaptation and compensation induced by the change in bone stress during microgravity (Pietrzyk et al. 2007; Schneider et al. 1995; Smith et al. 2005). In microgravity, the combined effect of reduced fluid intake, hypercalciuria and the presence of nanobacteria all contribute to increased kidney stone formation (Liakopoulos et al. 2012). As a result, during long-term microgravity exposure (>1000 days) the calcium metabolism is altered with decreased intestinal calcium absorption and increased urinal calcium excretion (Heer et al. 1999; Smith et al. 2005). In addition, the reduced urine output observed during space missions is likely to magnify the saturation of solutes like uric acids, cystine, struvite, calcium oxalate and calcium phosphate (Liakopoulos et al. 2012). This causes both a physiological issue (as it can cause diseases like kidney stones) and technical problem as high calcium levels can cause  $\text{CaCO}_3$ ,  $\text{Ca}_3(\text{PO}_4)_2$  and  $\text{CaC}_2\text{O}_4$  scaling on pipes or appliances used on the ISS. After studying the urine biochemistry of 332 astronauts, pre- and post-flight, after landing an 18% and 9.8% increase in hypercalciuria and hypomagnesuria and lower urinary pH were measured (Liakopoulos et al. 2012). To reduce the bone mass loss problem, during space flights dietary calcium intake of 800 mg/day was also recommended. Overall, the change in the concentration and ratio of monovalent and multivalent cations in the presence of microgravity poses significant problems to the onsite treatment of urine as it promotes scaling and clogging of the equipment.

#### 2.2.2 Ureolysis in urine, and the change in its proprieties

Understanding the change in the chemical and biological composition of urine is crucial to selecting the most appropriate urine treatment technology. Figure 2-1 shows how the storage



of urine in non-sterile conditions or at elevated temperatures ( $> 40^{\circ}\text{C}$ ) causes the urea to hydrolyse into  $\text{NH}_3/\text{NH}_4^+$  and  $\text{CO}_2$  leading to an increase in the pH, conductivity and osmotic pressure (Randall et al. 2016; Udert, Larsen, et al. 2003; Udert, Larsen & Gujer 2003). This graph was obtained by continuously measuring the pH, electric conductivity, anions, cations, ammonia and urea concentration of a urine sample exposed to environmental conditions for 12 days (Volpin, Yu, et al. 2019). This led to the distinction between urine pre and post urea hydrolysis. The former is generally referred to as “fresh urine” while the latter as “hydrolysed urine”. During the enzymatic hydrolysis of one mole of urea, two moles of ammonia plus one mole of  $\text{CO}_2$  are produced (reaction (2-1)). As the osmotic pressure is a colligative propriety of any solution, the increase in the net amount of dissolved species leads to an increase in the osmotic pressure of the urine. This process is inevitable if the urine is stored in non-sterile conditions.



With ureolysis, pH rises to 9-9.5 triggering the precipitation of  $\text{Mg}^{2+}$  and  $\text{Ca}^{2+}$  in the form of carbonates and phosphates (Maurer, Pronk & Larsen 2006; Randall et al. 2016). Besides the possible clogging and scaling of pipes, the precipitation of calcium phosphate and struvite would sequester part of the available orthophosphate. The amount depends on the initial stoichiometric amount of magnesium and calcium.

After hydrolysis, the increase in the pH would also shift the equilibrium reaction (2-2) toward ammonia, which is volatile. The results would be nitrogen losses as well as possible environmental pollution as ammonia is considered hazardous at high concentrations.



Finally, the high concentration of LMW organic acids, such as oxalic, uric, citric, hippuric, lactic and acetic acid in urine can be used as electron donors by anaerobic microorganisms to grow (Udert, Larsen & Gujer 2006). The high concentration of organic compounds in urine, together with the microbial reduction of sulphate to hydrogen sulphide is the cause of the malodour of stored hydrolysed urine (Troccaz et al. 2013).

For these reasons, urine stabilisation and disinfection are often required to avoid ureolysis (Randall et al. 2016). Ammonia volatilisation, in particular, should be minimised as it constitutes both an environmental threat and a loss of valuable fertiliser. Onboard of the ISS urine stabilisation is crucial to ensure safe water production and avoid precipitation of carbonates and phosphates on equalisation tanks, pipes and other treatment apparatus.

Different approaches have been proposed, including acidification/alkalinisation, salinization, electrochemical sanitation, freeze-thaw, biological nitrification and lactic acid fermentation. Details about these approaches are summarised as follows.

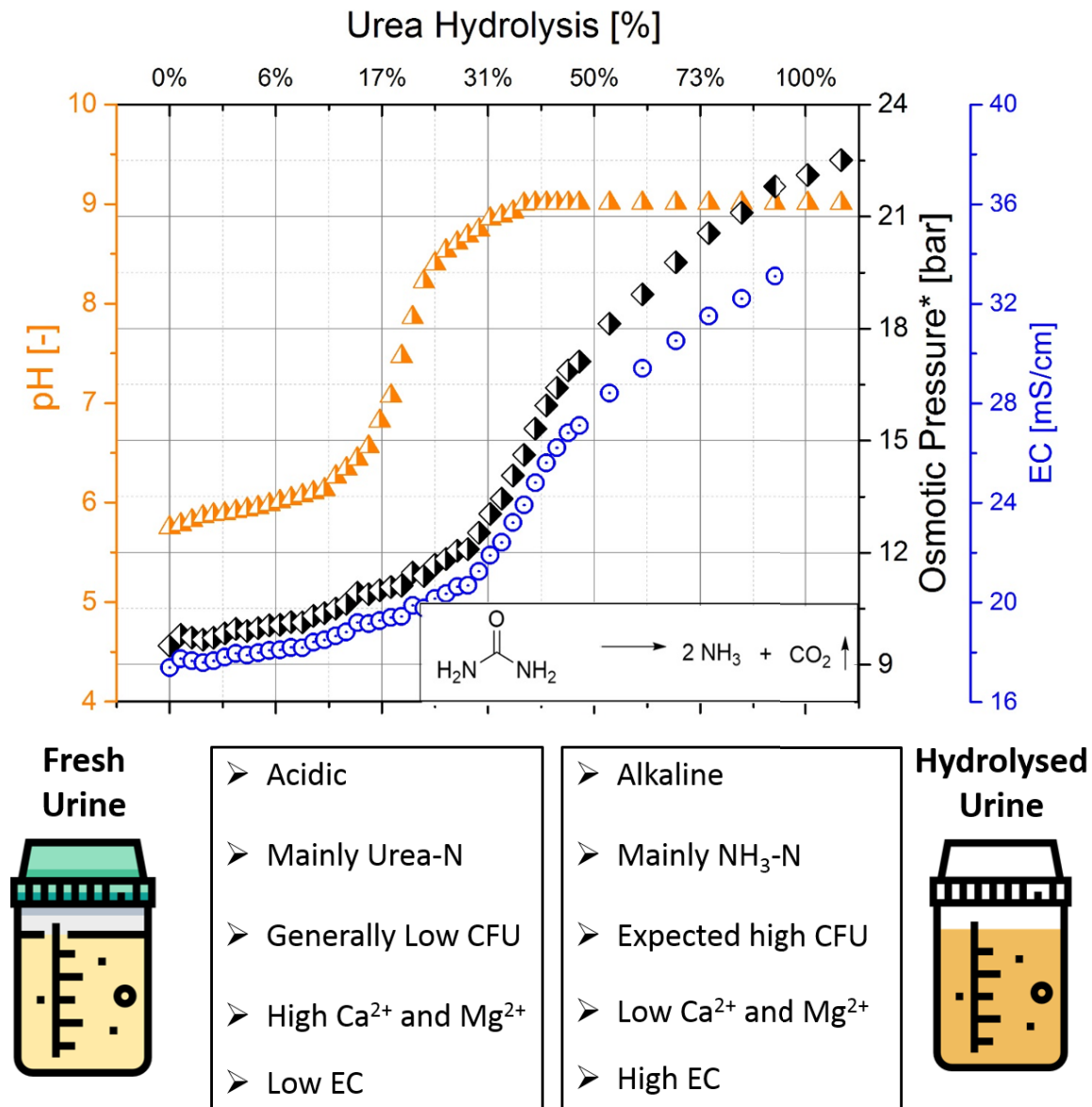


Figure 2-1 shows the change in pH, EC and osmotic pressure during urea hydrolysis in the urine. \* The OLI Studio Analyser software was used to estimate the osmotic pressure based on the chemical analysis of the urine solution. The van't Hoff equation  $\pi = vRTc$  is used for the calculation (where  $c$  is the concentration,  $T$  the temperature and  $R$  the universal gas constant). Adapted from Volpin, Yu, et al. (2019).

#### 2.2.2.1 Acidification

One of the first approaches investigated to slow down urease' activity, was through acidification (either chemical or biological) or alkalinisation.

On the ISS, urine is mixed with flushing water and stabilised using a pre-treatment formula containing chromium trioxide and sulphuric acid to control microbial growth and urea hydrolysis (Jackson et al. 2017; Layne et al. 2015; Pruitt et al. 2015). However, this pre-treatment is inherently hazardous, it needs to be resupplied, and it limits the recovery by distillation to <75% (Jackson et al. 2014). One of the "Green Pre-Treat" solutions proposed to mitigate the side effects of toxic chemicals is to substitute mineral acids (i.e.,  $\text{H}_3\text{PO}_4$ ,  $\text{H}_2\text{SO}_4$ ) with organic acids (i.e., citric, benzoic) and replace  $\text{Cr}^{6+}$  with other inhibitory compounds such as quaternary amines (Jackson et al. 2014; NASA 2015). However, Daniel Hellstrom (1999) showed that inorganic acids were more effective than organic acids in preventing ureolysis.

An alternative way to reducing the pH of urine and convert urea into stable  $\text{NH}_4^+$  and  $\text{NO}_3^-$  is by biological ammonification and nitrification (Clauwaert et al. 2017; Deng, Xie & Liu 2016; Udert & Wächter 2012). The advantages of biological oxidation of urine wastewater are the prevention of the ammonia (g) loss during distillation, reduction of volatile organic carbon (VOC) load to adsorptive beds with finite capacity and reduction in downstream growth potential (Fumasoli et al. 2016; Jackson et al. 2017; Udert & Wächter 2012). Jackson et al. (2017) showed oxidising urine biologically, with the addition of organic acids (i.e., 1 g/L benzoic acid or 5 g/L citric acid), could be an alternative to the current storage method.

Acid fermentation was also tested to achieve the same goal. Andreev et al. (2017) investigated the use of lactic acid fermentation to stabilise the fresh urine. In this study, fresh urine was lacto-fermented in a closed glass jar for 36 days and compared with the stored untreated urine.

The lactic acid bacterial was inoculated from sauerkraut juice. During fermentation the pH was reduced to 3.8 - 4.7 and the  $\text{NH}_4^+$  content maintained to about 22-30% of the total nitrogen (i.e., the remaining was in the form of urea).

#### 2.2.2.1 Alkalinisation

On the other side of the pH spectrum, Randall et al. (2016) showed that ureolysis would not occur when the pH is between 11 and 13 and the temperature below 40 °C. The authors proposed the urease inhibition by addition of three common calcium compounds: calcium carbonate, calcium oxide and calcium hydroxide. The results revealed that calcium hydroxide was the best choice as it quickly raises the pH to 12.5. In addition to inhibiting urea hydrolysis, calcium hydroxide was also found effective in killing bacteria and viruses and precipitating the P as calcium phosphate. The optimal recommended dosage was 10 g calcium hydroxide per litre of fresh urine, and the optimal temperature range from 14 to 40 °C.

#### 2.2.2.2 Urine salinization

Hotta & Funamizu (2008) investigated the effect of urine salinity in the inhibition of ureolysis. Sodium chloride was added to urine with concentrations ranging from 0 to 200 g/L. As anticipated, the test with no NaCl addition showed the fastest ammonification rate, while the addition of 150-200 g<sub>NaCl</sub>/L showed a 50% reduction of ammonification potential. Pahore et al. (2012) also showed that using a mixture of salts, urea and creatinine could inhibit urea hydrolysis in urine contaminated with faecal biomass. However, urease activity was inhibited only when the salinity of the solution was higher than 227 g/L.

### 2.2.2.3 Oxidation and electro-oxidation

Ikematsu et al. (2007) proposed using electrochemical methods to prevent ureolysis during storage. It was found that the reactivity of urease is suppressed with a redox potential of 240 mV or above. The electrochemical treatment was operated continuously for 64 cycles without any ureolysis and total energy consumption of approximately 15 kWh. New advanced oxidation processes have also been proposed for the treatment of human urine in space. Non-thermal plasma is one example (Peerapong 2018). Non-thermal plasma uses electric discharge at the water-gas interface to generate multiple reactive species, such as  $\text{OH}^\bullet$ ,  $\text{O}_3$ ,  $\text{H}_2\text{O}_2$ , which are able to mineralise the residue VOCs (Reddy & Subrahmanyam 2012). As such, it has been used to degrade refractory or challenging compounds such as phenol, crystal violet, methylene blue, acid red 88, pentoxifylline (Magureanu et al. 2010; Magureanu et al. 2008; Reddy & Subrahmanyam 2012; Tang et al. 2009). It was also found to be effective in inactivating coliform and *E. coli* (Nguyen et al. 2019; Patange et al. 2018). At present, though, only one article has been published on the use of non-thermal plasma on human urine for space application (Peerapong 2018).

## 2.3 Benefits of urine source-separation and reuse

### 2.3.1 Urine separation for cheaper and cleaner WWTPs

Cities around the world are changing at an unprecedented rate due to the combined effect of increasing population density, water usage and increasing impacts of climate change. The combination of the above along with widespread ageing of wastewater infrastructure and urban intensification is causing the need for significant investments in infrastructure replacement and upgrade. To safeguard the future of our utilities investing in both conventional centralised wastewater infrastructure and novel decentralised solutions is paramount.

Separate urine recovery is gaining traction as an alternative pathway for achieving a more flexible and resilient urban wastewater network. Despite being less than 1% of the overall wastewater volume, urine composition is a heavy burden for conventional biological sanitation, and the reason is twofold: (i) high nutrient density and (ii) high pharmaceuticals and hormones concentration.

#### 2.3.1.1 Economic and social cost of nutrients removal from human urine

Urine contributes to about 70-80% of the N, 50% of the P and 75% of the S in municipal WW (Larsen & Gujer 1996). If released untreated in the environment, the high TAN content in urine can lead to the eutrophication of recipient water bodies threatening the aquatic life in it (Kir et al. 2016; Wang & Leung 2015). As such, it is paramount to remove it before its discharge.

However, the high energy required for the removal of ammonia through biological oxidation/reduction means that urine accounts for a large portion of the energy consumed by a WWTP. For example, in a catchment area like Greater Sydney, with a population of about 4.82 million residents, urine treatment accounts for the yearly energy consumption of 50 - 350 GWh.  $y^{-1}$  (see below for more details on the assumptions). When assuming a conservative wholesale industrial energy price of 70-100 \$AUD per  $MWh^{-1}$ , this value translates into a cost of 3 to 35 million \$AUD.  $y^{-1}$  (AEMC 2013; Maurer, Schwegler & Larsen 2003a). Equation (2-3) and (2-4) show the calculations for these values.

$$\begin{aligned} \textbf{Minimum: } & 4.8 \cdot 10^6 p \cdot 0.464 \frac{m^3}{p \cdot y} \cdot 0.024 \frac{MWh}{m^3} \cdot 70 \frac{AUD}{MWh} & (2-3) \\ & = 3.8 \cdot 10^6 AUD \cdot y^{-1} \end{aligned}$$

$$\begin{aligned} \text{Maximum: } & 4.8 \cdot 10^6 p \cdot 0.464 \frac{m^3}{p \cdot y} \cdot 0.157 \frac{MWh}{m^3} \cdot 100 \frac{AUD}{MWh} & (2-4) \\ & = 35 \cdot 10^6 AUD \cdot y^{-1} \end{aligned}$$

The aeration necessary for the biological nitrification is the main driver for such high costs as it accounts for approximately 50% of the overall energy consumption (Foley et al. 2010). Maurer, Schwegler & Larsen (2003a) calculated that 16 to 109 MJ of primary energy are required for every kg of ammoniacal nitrogen. Where 16 MJ.kg<sub>N</sub><sup>-1</sup> is assuming nitrification/autotrophic denitrification (Sharon/Anammox) and 109 MJ.kg<sub>N</sub><sup>-1</sup> is assuming nitrification/heterotrophic denitrification with additional carbon source substrate (Henze et al. 2002; Maurer, Schwegler & Larsen 2003a). Practically, this means that for every m<sup>3</sup> of urine, about 20 - 150 kWh of electric energy is consumed just for N removal (assuming an average N concentration of 5 kg<sub>N</sub>.m<sup>-3</sup> of urine) (Batstone et al. 2015; Maurer, Schwegler & Larsen 2003a). Besides the CO<sub>2</sub> emissions associated with the consumption of electric energy necessary to operate the air blowers, the biological removal of the TAN in the urine also seems to be responsible for a large share of the N<sub>2</sub>O emission from a WWTP (Peter-Fröhlich et al. 2007). N<sub>2</sub>O is a potent greenhouse gas, with a 300-fold stronger effect than CO<sub>2</sub>. It was shown that N<sub>2</sub>O is mainly emitted in the aerated zone of the biological process and that two of the three main cause of its emission are low COD/N ratio in the denitrification stage and increased NO<sub>2</sub><sup>-</sup> accumulation in both nitrification and denitrification stage (Kampschreur et al. 2009). As urine is the primary source of nitrogen in WW, and the main source of nitrogen in WW, its upstream separation is expected to increase the COD/N ratio in municipal WW (Jacquin et al. 2018).

Phosphorus, on the other hand, is generally removed by chemical precipitation, generally though iron (II) sulphate, or incorporation in the activated sludge via enhanced biological P removal (EBPR). It was estimated that 28 - 49 MJ.kgP<sup>-1</sup> are required for its removal (Maurer,



Schwegler & Larsen 2003a). This means that 4 - 7 kWh.m<sup>-3</sup> of electric energy is consumed for each m<sup>3</sup> of human urine (assuming 0.5 kgp.m<sup>-3</sup> of urine) (Bashar et al. 2018).

Because of the combined high cost of N and P removal Wilsenach & Loosdrecht (2006) demonstrated that, if 50% or more urine is treated separately, conventional WWTPs can achieve higher effluent quality and even become a source of net-energy production. On top of that, the diversion of urine may also have direct effects on sewer odour and corrosion due to the reduction of sulphate to H<sub>2</sub>S by sulphur-reducing bacteria (Troccaz et al. 2013).

#### 2.3.1.2 The burden of pharmaceuticals in human urine

Human urine contains pharmaceutical and hormone concentrations 2-3 orders of magnitude higher than average sewage WW (Zhang et al. 2015). While most of the xenobiotics in WW are in ppb level concentrations, in urine they often are in ppm levels. Unless equipped with tertiary effluent polishing processes, which can cause up to 40 - 55% surge in OPEX of a WWTP, most pharmaceuticals and metabolites can make their way out through the treatment to the final catchment (Calero-Cáceres et al. 2014; Kim, Kuntz, et al. 2019; Zhang et al. 2015). As most of the WWTPs still rely on just primary and secondary sewage treatment, the presence of xenobiotics in catchments and waterways is now a significant concern worldwide (Escher et al. 2006; Tran, Reinhard & Gin 2018; Verlicchi, Al Aukidy & Zambello 2012; Verlicchi & Zambello 2015). Based on the above and given the low volume of urine compared to the volume of wastewater, the removal of xenobiotic from source-separated urine could be a more feasible and cost-effective way of reducing the discharge toxic compounds in the environment.

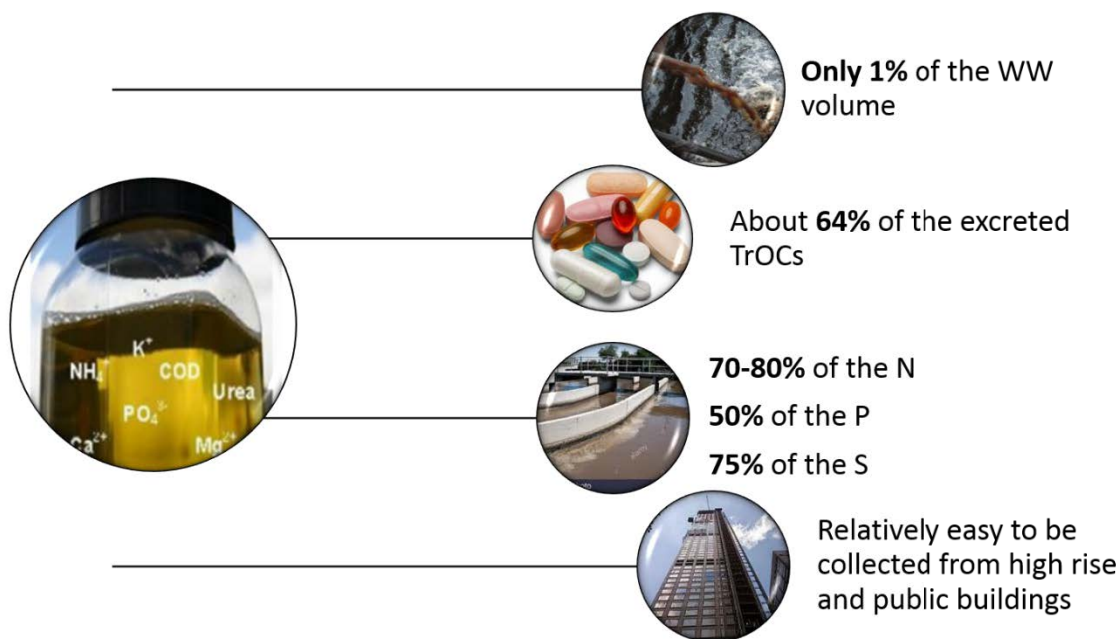


Figure 2-2 Urine in relationship with combined domestic wastewater.

To conclude this section, Figure 2-2 shows a schematic of the composition of urine relative to combined WW and the potential benefits of its upstream separation and treatment. The data summarised in Figure 2-2 lead to the hypothesis that treating or reusing urine before it gets combined with other domestic WWs would result in cheaper and cleaner WWTPs.

#### 2.3.1.3 Urine separation to close the nutrients cycle

The combination of an ever-growing world population combined with an increase in urban population density is expected to increase the needs for fertiliser imports and manufacturing. Although developed countries decreased their fertiliser consumption due to stricter environmental regulations and optimal levels of P in the soil, developing countries are seeing the opposite trend (Cordell & White 2014).

The Food and Agriculture Organization of the United Nations (FAO) reported that the global fertilizer demand of the three primary plant nutrients - ammonia ( $\text{NH}_3$ ) as N, phosphate ( $\text{P}_2\text{O}_5$ ) as P, potash ( $\text{K}_2\text{O}$ ) as K— is estimated to reach 201.66 million tonnes by 2020/21 (FAO 2017b).

With a world population expected to reach 11.2 billion people by 2100, the increase in the demand for nutrients is expected to keep rising (Bicer et al. 2017; United Nations 2017).

From 2015 to the end of 2020, the demand for N, P and K is predicted to grow at an annual rate of 1.5%, 2.2% and 2.4% respectively. Although the world total nutrient capacity of fertilizers is expected to increase further to 273.38 million tonnes by 2020, regions such as Latin America & Caribbean, South Asia, West Europe and Oceania would solely rely on fertilizer import (Figure 2-3) (FAO 2017a). Therefore, the recovery and reuse of the nutrients in urine could be an alternative pathway to ease the reliance on energy-intensive ammonia production (which consumes about 1-2% of global energy) as well as the dependency on fertiliser importation (Kavvada et al. 2017).

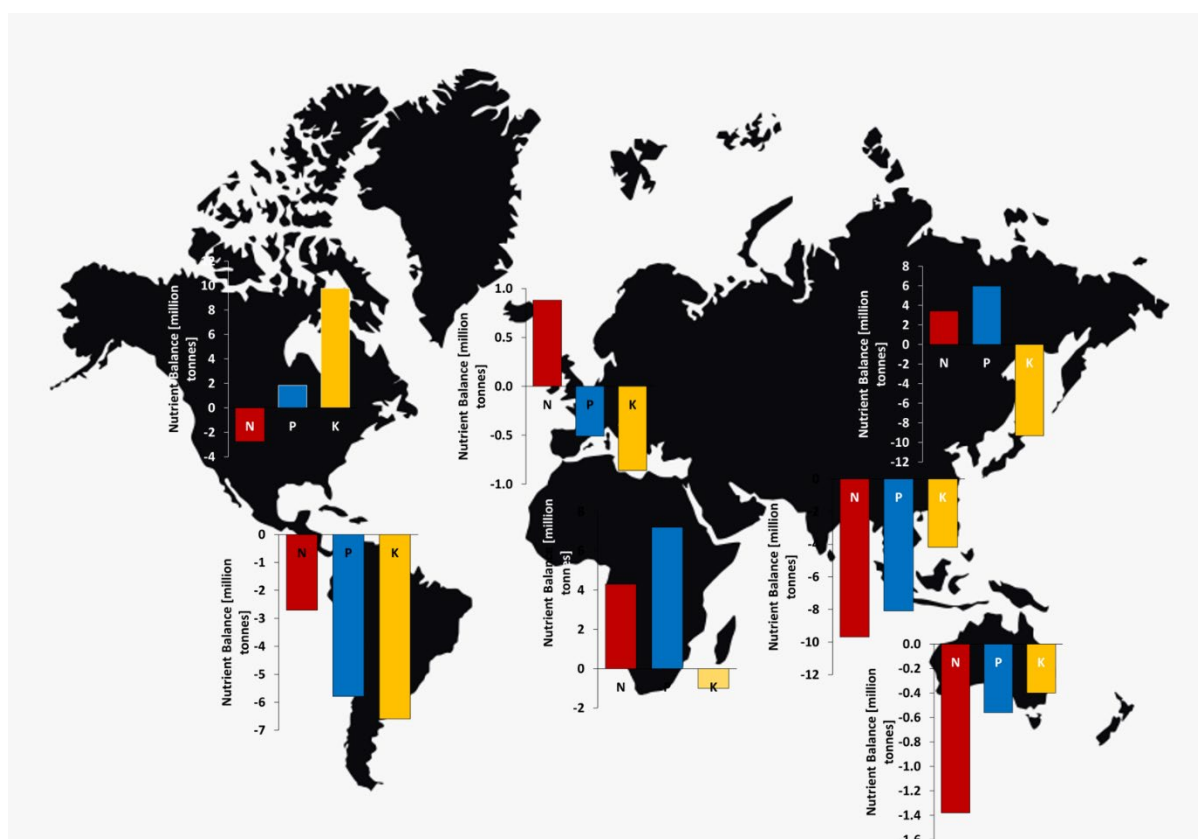


Figure 2-3 World nutrient balance of ammonia, phosphate  $P_2O_5$ , potash  $K_2O$  in 2020 (million tonnes) (FAO 2017b).

#### 2.3.1.4 Phosphorus: A Finite Element

Phosphorus is an essential element to all life - plants, animals and bacteria. At the molecular level, it is necessary for the structure of DNA, RNA and ATP (primary carrier of chemical energy in cells). In the agribusiness, P deficiency limits crops quality and growth rate. Consequently, its annual demand is rising nearly twice as fast as the population growth rate. However, much like carbon, P can only be mined from the soil, and its reserves are limited and localised mainly in North Africa and China. The top five phosphate rocks holders – Morocco and Western Sahara, China, Algeria, Syria, and Brazil – account for 84% of the world reserves (National Minerals Information Center 2019). Australia holds just 1.6%. The uncertainties around our future P supplies means that the importance of recovering and re-using nutrients in our wastes cannot be understated.

As human urine is the single largest source of P from urban areas, mining P from it will be increasingly necessary to fulfil the world fertiliser demand (Ashley, Cordell & Mavinic 2011). In fact, by reviewing the available P in urine and faeces over two population scenarios between 2009 and 2050, Mihelcic, Fry & Shaw (2011) showed that the P available from urine would increase from 1.68 million metric ton (2009) to 2.16 million metric ton in 2050. This could account for 11% of the total global P demand. This is particularly attractive for regions that often lack adequate sanitation infrastructure, such as Latin America & Caribbean and South East Asia, which have the opportunity of recovering the P from their source-separated streams to offset their negative P balance (Figure 2-3).

Ishii & Boyer (2015) also performed a life cycle assessment (LCA) to compare existing centralised WWTPs with a decentralised phosphorus recovery process. Specifically, they investigated the source-separation of urine to achieve phosphorus recovery as struvite, aided by the addition of MgO. Using the Tool for the Reduction and Assessment of Chemical and

Other Environmental Impacts (TRACI) the researchers proved that urine P recovery as struvite has the smallest environmental cost (Ishii & Boyer 2015).

#### 2.3.1.5 Nitrogen: The socio/economic cost of producing ammonia fertiliser

Nitrogen is also an essential element as it is necessary for DNA formation as well as for the structure of amino acids (proteins building blocks). Despite constituting 78% of the Earth's atmosphere, the nitrogen in the atmosphere is found only in the form of unreactive  $N_2$  gas. To be made energetically available for plants,  $N_2$  has to be fixed into a reactive nitrogen form (e.g., ammonia,  $NO_3^-$  or urea). While  $N_2$  fixation naturally occurs in nature, its rate of production is too slow to keep up with the current demand which is estimated to be 118.76 million tonnes in 2020 (Dang & Chen 2017; FAO 2017b).

Thanks to the invention of the Haber-Bosch process ammonia and urea can be economically produced using high pressure and an iron-based catalyst (Cherkasov, Ibadon & Fitzpatrick 2015). This process was so revolutionary in the field of agriculture that allowed for a tenfold increase in agricultural production between 1961 and 2014 (Max & Hannah 2020). This was the so-called “green-revolution”. The Haber-Bosch process, however, is very energy-intensive. Over 1% of the energy produced worldwide is used for the Haber-Bosch process (Kavvada et al. 2017). This, in turns, has tremendous impacts on the global GHGs emissions. In fact, at present 2-3 tons of  $CO_2$  are produced for each ton of ammonia. Given the 118.76 million tonnes of ammonia that are produced yearly, just reactive nitrogen synthesis subsidised about 0.93% of the world GHGs emissions (Bicer et al. 2017; Canfield, Glazer & Falkowski 2010).

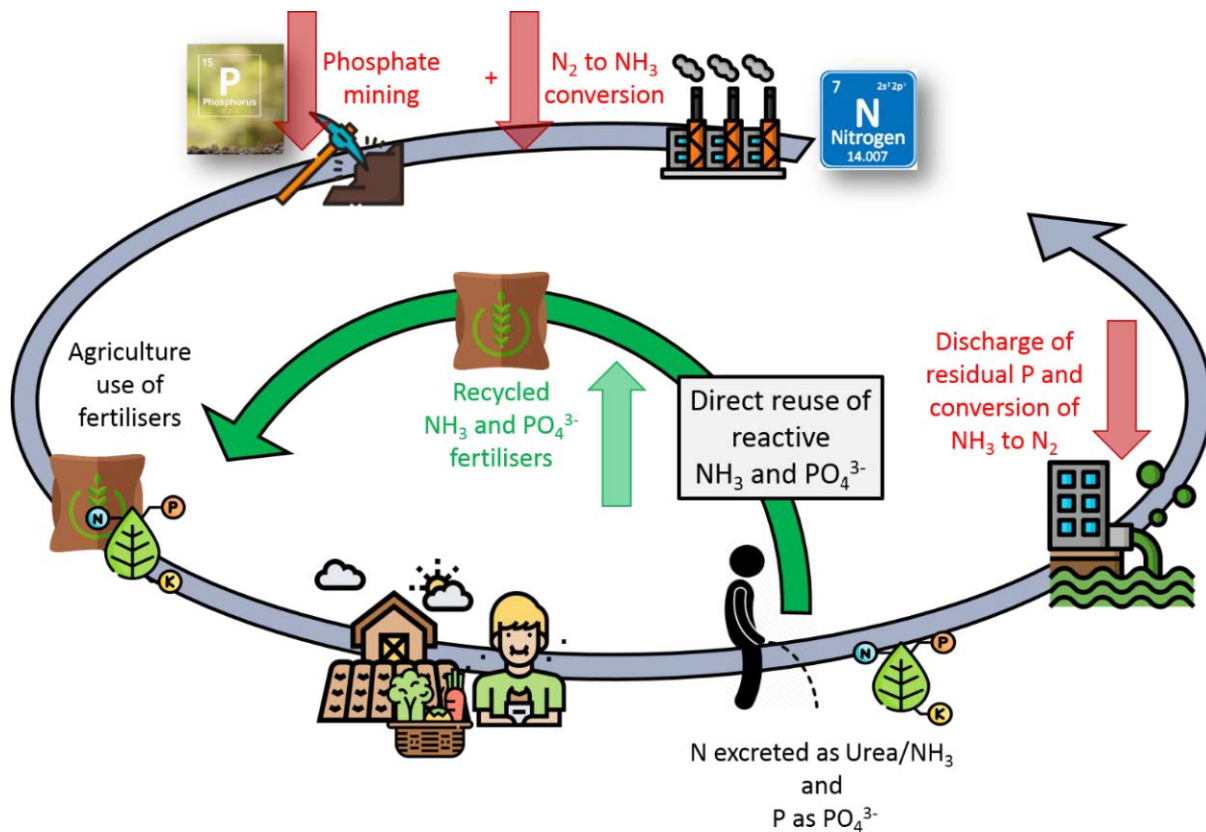


Figure 2-4 Schematic diagram of the potential benefits of shortcutting the nitrogen and phosphorus cycles for fertiliser production.

As the nitrogen concentration in urine is over 100 times higher than in the combined sewage, its recovery from urine has been widely investigated as an alternative source of reactive nitrogen. In 2017 Kavvada et al. (2017) performed a detailed system scale evaluation and LCA of recovering nitrogen from the San Francisco bay area using ion-exchange resins. The results show that, if fertiliser production is accounted for, the decentralised approach has a lower cost, unit energy and GHGs emissions compared to the traditional nitrogen removal via a centralised nitrification-denitrification process.

To conclude, the benefits of urine source-separation for nutrients recovery are highlighted in Figure 2-4, which shows how the integration of decentralised WWTPs could significantly

reduce the costs associated with WW treatment and ammonia synthesis, as well as the environmental impact of phosphate rocks mining.

### 2.3.2 Urine separation for a bio-regenerative life support in space

While separate collection, treatment and re-use of human urine is increasingly adopted here on Earth, on the ISS it has always been a priority. That is because, despite the current technological advances in space transportation, the cost of shipment in space remains over \$10000 per kg (Harper et al. 2016; Sherwin Gormly, Michael Flynn & Howe 2012). This is a strong incentive to reduce the payload mass which, on a best-case scenario, amounts to 15 kg/day (and just considering life support consumables such as air, food and water) (Harper et al. 2016). However, recycling the water and wastes produced on the ISS can bring down this value to less than 1 kg/day (Clauwaert et al. 2017). As such, urine recovery and reuse is a top priority in space as it is currently performed to produce fresh drinking water for the crew as well as for hygiene and oxygen generation (Pruitt et al. 2015). Exploration Life Support (ELS) or Bioregenerative Life Support Systems (BLSS) are increasingly investigated as a mean to the in-situ regeneration of water, oxygen and nutrients from urine (Clauwaert et al. 2017; Deng, Xie & Liu 2016; Gòdia et al. 2002; Sherwin Gormly & Flynn). The ideal life support systems in space must provide the highest possible percentage of water recovery with the lowest energy, operation and maintenance costs (Sherwin Gormly & Flynn). System reliability and the need for virtually no supply or maintenance is especially required. This is particularly necessary for future permanent habitation in life support systems. On the other hand, the initial CAPEX requirements, necessary for an ESL/BLSS to perform reliable high water recovery and high permeate quality, are more relaxed (Hanford & Ewert 2006; Sherwin Gormly & Flynn).

#### 2.3.2.1 Current practice on the International Space Station

The Water Recovery and Management (WRM) system implemented on the ISS ensures availability of potable water for crew drinking and hygiene, oxygen production and urinal flush water (Layne et al. 2015; NASA 2015; Pruitt et al. 2015). The primary sources of wastewater that can be reclaimed and reused in long-term space missions are hygiene, urine and crew latent wastewater, where the last one is the condensed water vapor from crew perspiration and respiration (Cath et al. 2005). Figure 2-5 shows the schematic diagram of WRM currently implemented on the ISS (Layne et al. 2015; Pruitt et al. 2015). Besides the wastewater produced by the crew, the WRM receives the water produced from the carbon dioxide reduction system which uses the Sabatier technology to produce water from CO<sub>2</sub> and H<sub>2</sub> (Layne et al. 2015; Pruitt et al. 2015). The WRM processes the received wastewaters (i.e., crew urine, humidity condensate and Sabatier product water) to potable standards (Layne et al. 2015). The water recovery systems can be subdivided into two sections:

1. Urine Processor Assembly (UPA) and,
2. Water Processor Assembly (WPA).

UPA only treats urine, while WPA treats the humidity condensate, hygiene wastewater, Sabatier product water and the water treated by the UPA. The details of the UPA and WPA are discussed below.

#### 2.3.2.2 Urine Processor Assembly (UPA)

Between 2008 (initial UPA operation) and 2017, the total UPA distilled water production was over 11.2 m<sup>3</sup> (Pruitt et al. 2015). This produced water is then sent through the WPA unit and then used for potable purposes and oxygen generation (see Figure 2-6). Initially, to ensure microbial growth control and chemical stability, urine is stabilised using a mixture of H<sub>3</sub>PO<sub>4</sub>



and  $\text{Cr}^{6+}$  and stored in the Wastewater Storage Tank Assembly (WSTA) until reaching a sufficient quantity for the treatment unit to start (NASA 2015). Afterwards, the urine is pumped to the distillation assembly (DA) (Figure 2-6). The distillate stream then goes through a gas separation unit, which separates the water from the purge gas, and back to the DA before it can go to the WPA. The DA unit, in particular, uses a low-pressure rotating vapour-compression evaporation system to promote the urine distillation process (Layne et al. 2015; Pruitt et al. 2015). Finally, a firmware controller assembly provides the online monitoring, command control and data downlink for UPA sensors and effectors (Layne et al. 2015). The UPA was designed for a nominal load of 9 kg/day and water recovery of 85%. However, up until 2016, it operated at water recoveries of 70-75% due to  $\text{CaSO}_4$  precipitations which caused severe hardware scaling (Layne et al. 2015). To cope with the higher  $\text{Ca}^{2+}$  concentration in the crew's urine a new type of pre-treatment, using  $\text{H}_3\text{PO}_4$  instead of  $\text{H}_2\text{SO}_4$ , was adopted which allowed the UPA to return to 85% recovery on ISS (Layne et al. 2018).

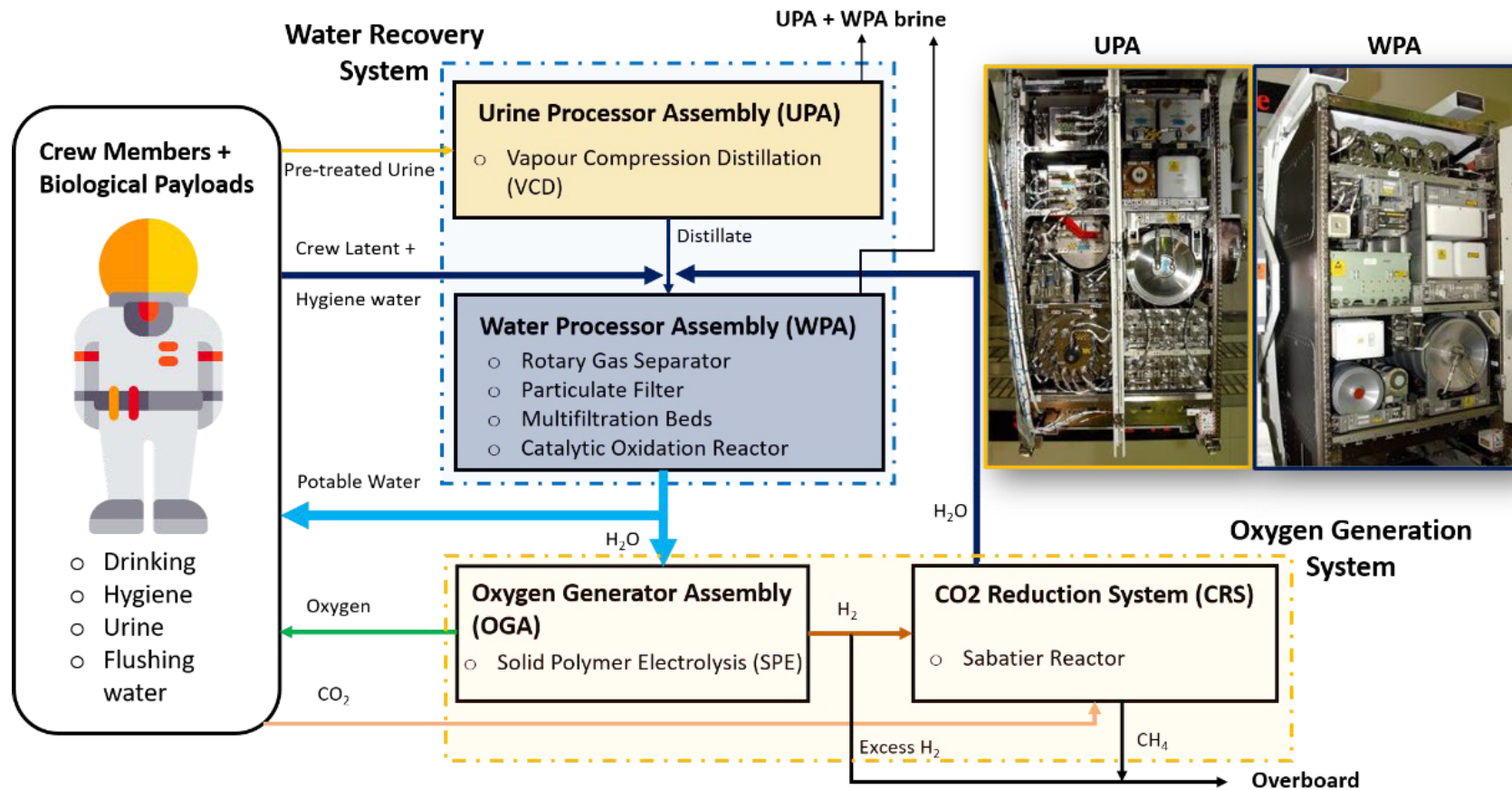


Figure 2-5 Schematic of the water recovery and management architecture for the ISS US segment. Adopted and modified from (Layne et al. 2015; Pruitt et al. 2015).

### 2.3.2.3 Water Processor Assembly (WPA)

The distilled water produced with the UPA is then sent to the WPA unit (Figure 2-6). Here it is combined with the condensate from the temperature and humidity control system and the Sabatier product water, degassed and sent through a particulate filter followed by multifiltration beds where inorganic and non-volatile organic compounds are removed (Layne et al. 2015; Pruitt et al. 2015; Sherwin Gormly & Flynn). Following the multifiltration beds, the low molecular weight organics in the wastewater are oxidised in the catalytic reactor that, in the presence of gaseous oxygen feed and 130 °C has a conversion efficiency of over 95% (Ping & Tim 2016). After purging the remaining oxygen and gaseous by-products via liquid-gas separation, the carbonate and bicarbonate ions produced during the oxidation are removed via an ion-exchange bed (Ping & Tim 2016). The ion-exchange bed also provides iodine (or silver) for residual microbial control (Layne et al. 2018). Finally, regenerative heat exchanges recover the heat from the catalytic oxidation. The total organic carbon (TOC) concentration of the product water can be evaluated on board of the ISS to check if the filters need replacement (Layne et al. 2018; Straub et al. 2018). So far, there have been six instances where the TOC analyser on board of the ISS detected a spike in the TOC concentration. In such cases, if the concentration exceeded the potable specification of 3000 µg/L, both multifiltration beds are replaced. Additional analysis of water samples is conducted on the ground.

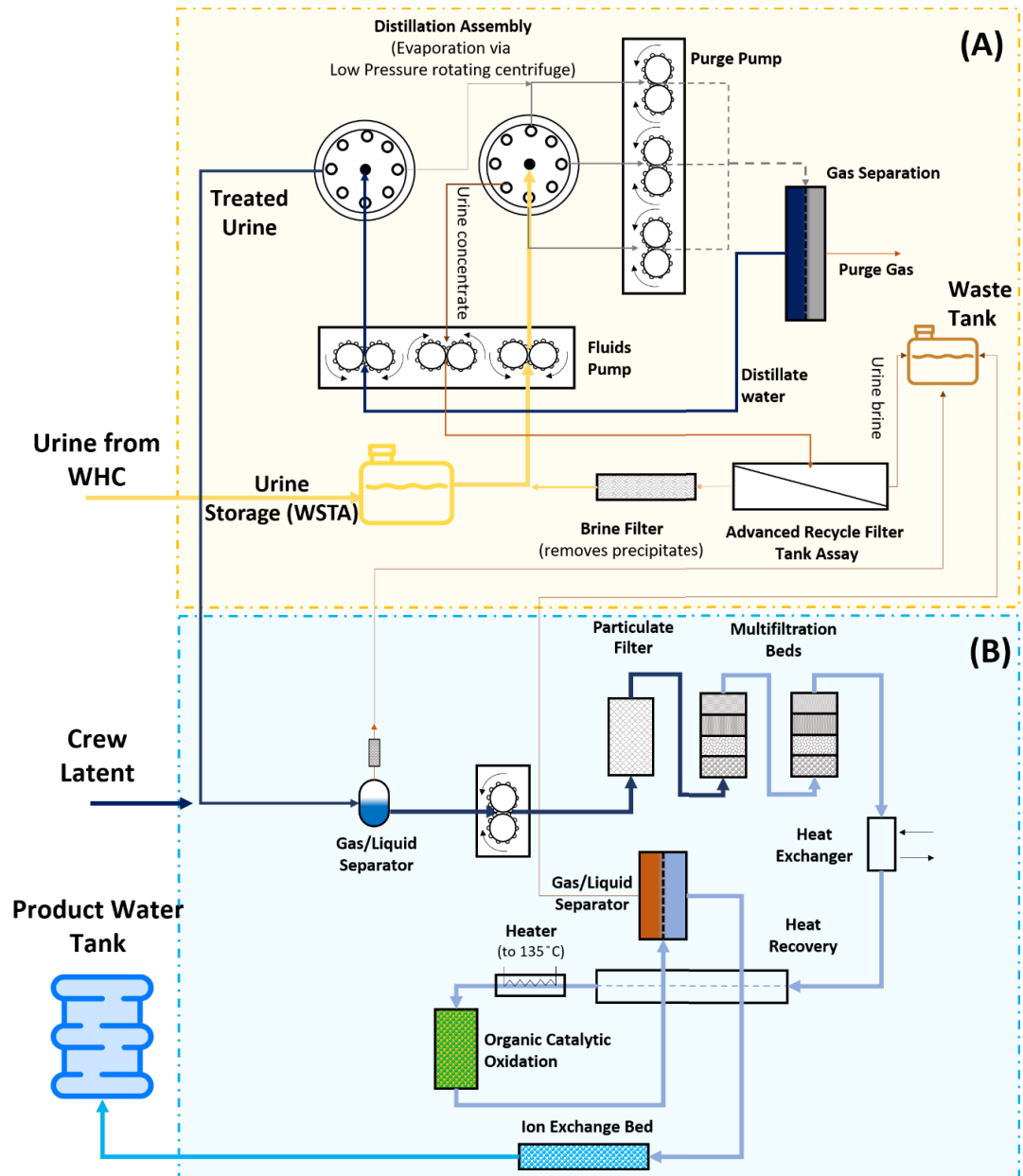


Figure 2-6 Schematic of the Urine Processor Assembly (A) and the Water Processor Assembly (B) installed at the ISS. Adopted and modified from (Layne et al. 2018; Pruitt et al. 2015).

## **2.4 Membrane-based processes for the treatment of human urine**

Urine nutrients imbalance (i.e., mainly N), low concentration compared to commercial fertilisers (i.e., N: 0.9%, P: 0.06%, K: 0.3%), pungent smell, high pH, and possible contamination of pathogens and pharmaceuticals contribute to a generally poor public acceptance toward its use for fertigation. However, recent surveys have shown that the opinion of the public can be changed if urine is adequately treated. For example, a recent survey of a university community in South India by Simha et al. (2018) showed that 80% of interviewees believed that urine could be treated to prevent any health risk from its use. Similar results were found from seven European countries, where 93% of those surveyed that the use of a urine-derived fertiliser was a good idea. As a result, the scientific community have embarked in the challenge of developing, testing and optimising a wide range of technologies to produce safe fertilisers from urine.

Several technologies for the treatment and re-use of human urine have been investigated. However, urine's complex matrix, high salinity, high pH, ammonia and trace organics concentration made membrane technologies to stand out for this task. That is because commercial water-filtration membranes generally have a strong chemical resistance, small footprint, tuneable selectivity and versatility in the operation are all desirable proprieties to have when treating human urine.

In this section, stand-alone and hybrid membrane-based processes were reviewed based on their ability to achieve selective recovery of water, N, P or K from urine as well as to achieve pathogens and micropollutants removal, volume reduction or nutrients removal.

The different separation techniques were grouped as follows:

- I. Osmotic and hydraulic-driven processes (Section 2.4.2)
- II. Thermal and partial vapour pressure-driven processes (Section 2.4.3)
- III. Electric potential driven processes (Section 2.4.4)

Finally, the last subsection (Section 2.4.5) analyses novel membrane-based processes that are investigated to overcome the current issues with the water and urine processing units on board of the ISS.

#### 2.4.1 Precipitation and crystallisation

A straightforward way to recover the P in urine is through precipitation as  $\text{MgNH}_4\text{PO}_4 \cdot 6 \text{H}_2\text{O}$ , i.e. struvite or through  $\text{KMgPO}_4 \cdot 6 \text{H}_2\text{O}$ , i.e. K-struvite (Etter et al. 2011). Both Struvite and K-struvite are widely used as slow-release fertilisers. Struvite precipitation spontaneously occurs when the required stoichiometric amount of magnesium is added to hydrolysed urine.  $\text{Mg}^{2+}$  addition is necessary as the molar concentration of  $\text{Mg}^{2+}$  is lower compared that of  $\text{PO}_4^{3-}$ .  $\text{MgO}$ ,  $\text{MgOH}$ ,  $\text{MgCl}$  or bittern were found to be suitable for this process (Etter et al. 2011). Even though struvite crystallisation starts at pH as low as 7.5, the optimal pH for the process was found to be around 9 (Kim, Min, et al. 2017). When the ammonium is oxidized or removed, K-struvite was found to precipitate instead. Also, since the molar ratio of  $\text{NH}_4^+ : \text{K}^+ : \text{PO}_4^{3-} : \text{Mg}^{2+}$  in urine is generally 260: 13: 6: 1, even with the addition of an external  $\text{Mg}^{2+}$  source, only about 2.5% of the  $\text{NH}_4^+$  and 5% of  $\text{K}^+$  in the urine can be removed with this method (unless additional phosphate and base is added) (Ishii & Boyer 2015). Additionally, urine dilution due to toilet flushing was found to decrease the amount of  $\text{PO}_4^{3-}$  recoverable through this process (Volpin, Heo, et al. 2019).

As such, the main disadvantages of the process are the minimal N recovery, the requirement for cheap  $\text{Mg}^{2+}$  source to keep the process economically feasible as well as the need for undiluted (or concentrated) urine to achieve high P recoveries. The combination of struvite precipitation with forward osmosis was then investigated in this Thesis and the results are presented in Chapter 6:.

#### 2.4.2 Hydraulic and osmotic-driven processes

Hydraulic and osmotically driven membrane processes are technologies whose applications range from water treatment and desalination, power generation, and dewatering of solutions.

High-rejection pressure-driven (osmotic or hydraulic) membrane processes such as NF, RO and FO have proven to be very useful in the dewatering of water and wastewater solutions. As such, they have been investigated as a mean to achieve urine up-concentration for more efficient struvite precipitation or concentrated fertiliser production. That is because of urine's low nutrients concentration compared to commercial liquid fertiliser (i.e., 10-1000 times lower depending on the dilution factor) which would significantly increase its transportation costs (Maurer, Pronk & Larsen 2006). Alternatively, the effectiveness of more loose NF membrane was also tested to produce a pharmaceuticals-free fertiliser solution (Pronk et al. 2006).

##### 2.4.2.1 Theory of pressure driven and osmotic driven processes

In pressure-driven membrane processes separation is achieved via exertion of hydraulic pressure which, in the case of non-porous RO and NF membranes, has to be higher than the osmotic pressure of the solute to be separated (Figure 2-7). Based on the size of the membranes' pores, different separation techniques are identified (i.e.,

MF, UF, NF and RO/FO) (Figure 2-7). The pore size and charge of the membrane then defines the performances of the system in terms of rejection and water transport (Fritzmann et al. 2007).

In contrast, osmotically driven processes rely on the osmotic pressure difference between a diluted feed solution and a concentrated draw solution to induce a trans-membrane mass transport from the feed to the draw (Cath et al., 2013) (Figure 2-7). Osmosis is a physical phenomenon that allows the transport of water across a selectively semipermeable membrane from a region of lower chemical potential to a region of higher chemical potential. Water is driven by the osmotic pressure gradient across a tight membrane. The dissolved ions are rejected depending on the morphology and charge of the membrane as well as the size and charge of the solute (Cath et al., 2006; Xie et al., 2016).

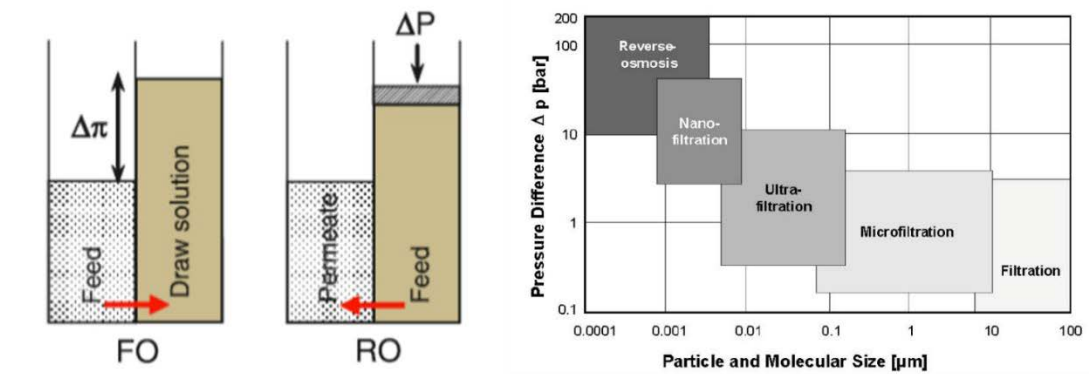


Figure 2-7 On the left: Principles of FO and RO. Adapted from (Wicaksana et al. 2011). On the right: Relationship between pressure difference and molecular size cut-off in the different pressure-driven processes. Taken from (Fritzmann et al. 2007).



#### 2.4.2.2 Nanofiltration and reverse osmosis for urine treatment

While RO and NF showed promising results in the rejection of micropollutants and urine volume reduction, they fail to reject small uncharged compounds like urea, ammonia and LMW compounds adequately (Jacquin et al. 2018; Maurer, Pronk & Larsen 2006; Pronk et al. 2006). Though, in RO the rejection of ammonia can be enhanced through urine acidification which shifts uncharged ammonia into charged  $\text{NH}_4^+$ , which is easier to be rejected by electrostatic repulsion (Maurer, Pronk & Larsen 2006). However, both NF and RO were found to severely suffer from fouling or scaling when tested on real human urine (Maurer, Pronk & Larsen 2006; Pronk et al. 2006). Additionally, as the initial urine osmotic pressure is in the range of 10-22 bar, RO can concentrate it up to maximum 3-7 times (which is much lower than the concentration of commercial fertilisers) (Putnam 1971a).

The combination of a low rejection of urea/ ammonia, high operating pressures and severe membrane fouling means that pressure-driven NF and RO are rarely adopted in the treatment of real human urine.

#### 2.4.2.3 Forward osmosis for urine treatment

The absence of hydraulic pressure in FO has shown to make the process more resilient toward flux decline when fouling occurs, making this process more suitable for complicated waste streams such as urine (Siddiqui et al. 2018). However, the reverse salt diffusion from the DS to the feed, inevitable in FO, has often been identified as one of the major hindrances of the process' feasibility.

Zhang, She, et al. (2014a) were the first to use FO for the up-concentration of source-separated urine. The results showed relatively low rejection of urea (< 50%). In

contrast, high rejection of  $\text{NH}_4^+$ ,  $\text{PO}_4^{3-}$  and  $\text{K}^+$  were achieved (i.e., 31 - 91%, 97 - 99% and 79 - 97% respectively). Nonetheless, as the authors only tested synthetic urine, and they chose NaCl as DS, this would mean that this system would only be feasible if located next into a sea. Additionally, the low urea rejection would impede a safe discharge of the diluted RO brine in the environment.

Finally, the concept of fertiliser driven forward osmosis has also been shown to be a viable FO application to reclaim and reuse wastewater and impaired waters for agriculture application (Chekli et al. 2017; Valladares Linares et al. 2016; Van Der Bruggen & Luis 2015). In this process, a fertiliser solution is used as DS to achieve simultaneous FS dewatering and fertiliser dilution (which could then be used as fertigation solution). However, the primary inherent drawback of this process was identified as the reverse draw solute diffusion. The RSF of the fertiliser draw solution to the feed can compromise the final quality of the brine (i.e., by exceeding the nutrients concentration standards for direct brine discharge) but also can cause an economic loss of valuable fertiliser.

#### 2.4.3 Thermal driven processes

Thermal processes such as distillation and MD have been widely investigated as a mean to dewater human urine. If urine is adequately pre-treated, these processes have the advantages of producing high quality distilled water, useful especially for space application, and achieving high urine concentration factors (Maurer, Pronk & Larsen 2006). However, urine evaporation presents the challenge of (i) having high concentrations of volatile ammonia as well as (ii) requiring a large amount of thermal or electric energy (up to  $400 \text{ MJ.m}^{-3}$  for a vapour compression distillation plant with 85% energy recovery) (Wood 1982).

Nitrogen losses can be reduced by pre-treating urine through acidification or nitrification (Daniel Hellstrom 1999; Fumasoli et al. 2016). By converting volatile ammonia into  $\text{NH}_4^+(\text{l})$  or  $\text{NO}_3^-(\text{l})$ , a sharp reduction in nitrogen losses during distillation and MD were measured (Maurer, Pronk & Larsen 2006; Tun et al. 2016). For example, Fumasoli et al. (2016) operated a pilot-scale nitrification-distillation reactor that was able to produce 20 times concentrated nitrified urine solution, with minimal nitrogen losses, and energy consumption of  $385.2 \pm 111.6 \text{ MJ.m}^{-3}$  of urine.

#### 2.4.3.1 Theory of membrane distillation process

Membrane distillation, which is a hybrid thermal-membrane process, was also investigated as a way to reduce the thermal energy requirements for the distillation process. MD operates by allowing the transport of water vapour through a porous hydrophobic membrane while rejecting all non-volatile compounds (Naidu et al. 2017). As MD can perform at temperatures of 50-70 °C, this thermal requirement could be met by either solar or waste heat integration. The mass transfer in MD is regulated by three essential mechanisms, which are Knudsen diffusion, Poiseuille flow (viscous flow) and molecular diffusion. As such, the mass transfer model used to describe the MD process is that of the dusty gas model (Ashoor et al. 2016).

#### 2.4.3.2 Membrane distillation for urine treatment

Tun et al. studied utilizing direct contact membrane distillation (DCMD) for dewatering source-separated urine to recover nitrogen (Tun et al. 2016). By keeping feed and permeate temperatures of 70 °C and 20 °C, respectively, the process showed low specific ammonia transfer (SAT). It was also revealed that, by increasing the feed temperature from 40 to 70 °C, the SAT value was reduced. This was due to the steeper

increase in water flux compared to ammonia flux. Additionally, acidification and filtration of human urine could inhibit ammonia transfer and prevent the membrane fouling in the DCMD process. When acidification of the urine from pH 9 to 5, the SAT value was reduced from  $2.05 \times 10^{-3}$  to  $6.91 \times 10^{-5}$  g<sub>N</sub>/g<sub>Water</sub>.

Khumalo et al. (2019) also tested MD for water recovery from HU. By reducing the pH to 5, and operating at a feed temperature of 50 °C, a maximum water recovery of 80% was achieved, together with NH<sub>4</sub><sup>+</sup>, Na<sup>+</sup>, K<sup>+</sup> and TOC rejection of 95, 98, 89 and 98% respectively.

However, the economics of HU acidification are questionable as about 230 mmol<sub>H+</sub> are required for every litre of (e.g. 11.3 g of concentrated H<sub>2</sub>SO<sub>4</sub> would be necessary for every litre of urine) which would come at a significant cost (Maurer, Pronk & Larsen 2006). As such, urine nitrification might be a more economical solution to achieve urine acidification. Still, at present, no studies have been conducted to test the effectiveness of MD in dewatering nitrified urine.

#### 2.4.4 Electric potential driven processes

In electrically driven processes the driving force is generated by the electric potential between the anode and cathode. Pairs of anion and cation exchange membranes (AEMs and CEMs, respectively) separate the high from the low concentration solutions. Similarly to RO, if a sufficient external voltage is applied against the ionic concentration gradient, the ions will move from the more dilute side to the concentrated side (ED) (Figure 2-8). The ED process is generally used to achieve up-concentration of an ionic solution.

On the other hand, if no external voltage is applied, ions will flow through the IEMs following the direction of the concentration gradient like FO and the process is called

short-cut ED. Ultimately, if short-cut ED is operated with additional resistance, the process is called RED (Figure 2-8) (Mei & Tang 2018). The RED process has been used to harness the chemical energy gradient between two mixing solutions (e.g., seawater and river water).

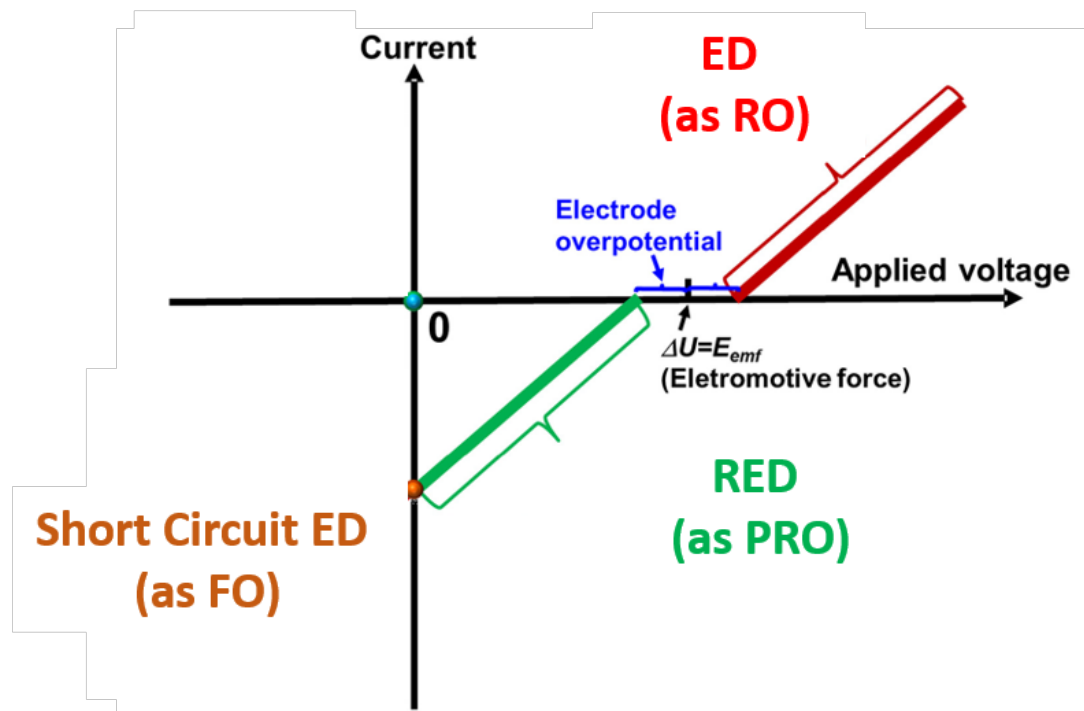


Figure 2-8 Principles of electrically driven processes and how they correlate with pressure-driven processes. Modified from (Mei & Tang 2018).

#### 2.4.4.1 Electrodialysis and reverse electrodialysis for urine treatment

Pronk, Biebow & Boller (2006) studied the use of ED to separate micro-pollutants from nutrients in human urine. Despite being able to achieve almost complete rejection of pharmaceuticals, the maximum achievable urine up-concentration factor was 3.2. After 3.2-time urine concentration, phenomena like osmosis and electro-osmosis caused water transport across the IEMs. Additionally, adsorption of organics on the membrane was observed, causing a decline in the process performances.

To minimise organic fouling, inorganic scaling and to convert the uncharged ammonia into charged  $\text{NH}_4^+$  and  $\text{NO}_3^-$ , De Paepe et al. (2018) combined precipitation, nitrification and electrodialysis to produce a concentrated nutrient solution from HU. During the precipitation step, multivalent cations such as  $\text{Ca}^{2+}$  and  $\text{Mg}^{2+}$ , often responsible for the inorganic scaling on the membrane, were precipitated in the form of struvite and Calcium Phosphate. Afterwards, a moving bed biofilm reactor was used to oxidize the organics and convert ammonia to  $\text{NO}_3^-$ . With these pre-treatments, the ED achieved a final N-P-K concentration factor of 4.3, 2.6 and 4.6. However, this was achieved with a urine solution that was already five times diluted.

In 2019, Mercer et al. (2019) used a combination of MD to extract fresh water from urine, and RED to produce energy from the dilution of the MD concentrate. In this case, cation and anion exchange membranes (CEMs and AEMs) were used to allow only for the transport of ions. By separating the higher concentration urine solution from the lower concentration freshwater through alternated CEMs and AEMs membranes, an ionic flux from the high concentration to the low concentration (Post et al. 2007; Veerman et al. 2011; Vermaas et al. 2013). The ionic flux is then converted into an electrical current thanks to redox reactions occurring at the anode and cathode of the electrode compartment (Veerman et al. 2010). However, both processes have their limitations. While in the first case, the process is only useful for dewatering applications, the MD-RED system was designed only for scenarios where waste heat is available (Mercer et al. 2019).

#### 2.4.5 Membrane-based processes for life support on the ISS

The ISS water recovery system has been operating since November 2008, producing over 30,000 L of water during that time. In this period, on average, 0.21 kg of

disposable hardware, mainly due to the replacement of the media filter, was consumed for every 1 L of water produced (NASA 2015).

The primary challenges with the design and operation during the first ten years were mainly related to the implementation of the technologies described in Figure 2-6 in microgravity. The absence of gravity was found to alter the two-phase fluid dynamics as well as increasing the impact of particulates on the system performances. Additionally, the system's maximum water recovery is strongly affected by the high calcium content in the crew's urine, which was found to cause  $\text{CaSO}_4$  precipitates on the distillation assembly of the UPA (M Smith et al. 2012). New alternatives to overcome the current wastewater treatment challenges and make use of current waste products are described more in detail in the next section.

Currently, the most necessary upgrades for the WRM at the ISS would be:

- I. To increase the water recovery rates beyond 85% and potentially broadening the types of wastewaters that can be processed.
- II. To reduce the reliance on expendable media (e.g., filtration media, sorbents and ion-exchange resins) for minimising the re-supply cost and maximise the use (NASA 2015; Sherwin Gormly & Flynn).

#### 2.4.5.1 Hybrid forward osmosis – reverse osmosis

To increase the water recovery and decrease the reliance on expendable media a combination of forward and reverse osmosis was tested. The hybrid FO-RO system was intended to replace the multibed filtration system.

The double barrier provided by the FO and RO membrane would ensure a high rejection of organics and pollutant. The rationale behind the choice of FO pre-treatment was the higher fouling resiliency, low energy consumption, simplicity and reliability (Cath et al. 2005). However, conventional hydrophilic polymeric FO and RO membranes were not able to achieve sufficient rejection of small and uncharged compounds, such as urea, as well as volatile organic compounds.

#### 2.4.5.2 Hybrid forward osmosis - osmotic distillation/membrane distillation

To obviate the low rejection of urea, OD or MD were proposed as a DS recovery method. The OD/MD membranes are hydrophobic, meaning that only volatile compounds can pass through. Since urea is non-volatile, OD/MD membranes would theoretically have a nearly perfect urea rejection (Cath, Adams & Childress 2005; Cath et al. 2005).

Both MD and OD are membrane distillation processes in which the driving force for the separation is the partial vapour pressure difference across a microporous hydrophobic membrane. However, while OD is an isothermal process, in which the partial vapour pressure difference is induced only by the salinity concentration difference, in MD temperature difference between feed and permeate and/or vacuum (VMD) are used to enhance the water transport (Liu et al. 2016; Zhao et al. 2013). Because of the low water fluxed measured ( $< 1 \text{ L. m}^{-2}.\text{h}^{-1}$ ), OD has not yet proven to be technically and economically feasible (Cath, Adams & Childress 2005; Cath et al. 2005; Gryta 2018; Ongaratto et al. 2018). The average water flux of commercial MD and VMD membranes, on the other hand, are in the range of  $10 - 40 \text{ L.m}^{-2}.\text{h}^{-1}$  (depending on the temperature difference and applied vacuum pressure) (Abu-Zeid et al. 2015; Ashoor et al. 2016; Drioli, Ali & Macedonio 2015).



More recently, Liu et al. (2016) tested the effectiveness of commercial FO and MD membranes in water extraction from real urine. In this paper, it was shown that if FO does not have a near-complete rejection of urea and ammonia the accumulation of those compound in the DS would cause an ammonia permeation in the MD produced water (Liu et al. 2016). Additionally, MD operation temperatures higher than 40 °C are not recommended as the urea in the DS would thermally decompose to ammonia which is volatile and can pass through the MD membrane (Randall et al. 2016).

#### 2.4.5.3 Emerging new materials to improve FO and RO performances

The successes in the fabrication of membranes with the incorporation of novel materials such as Aquaporin vesicles and graphene oxide (GO), has sparked new interest in the application of these new membranes for the treatment of astronauts' wastewater (Buelke et al. 2018; Hali et al. 2017; Tommerup M. 2016).

Aquaporins are a class of transmembrane proteins, found in almost every organism and represented in every major taxonomic group, which act as perme-selective water channels (Agre & Kozono 2003; Tang et al. 2015; Tang et al. 2013; Xie et al. 2018). Once stabilised in a polymeric vesicle they can be embedded in the active layer of conventional thin-film-composite polyamide membranes to enhance their water permeability, salt rejection and organic compounds rejection (Tang et al. 2015; Tommerup et al. 2017). Because of their high rejection capabilities, Aquaporin Inside® hollow fibre (AqP HF) membranes, commercialised by Aquaporin A/S, were tested on Earth and at the ISS as a possible candidate to replace the current multifiltration beds (Hali et al. 2017; Tommerup M. 2016). Initially, NASA tested the TOC and DMSD rejection of Aquaporin Inside® membranes by using a synthetic ISS condensate feed solution developed by Marshall Space Flight Centre (MSFC). 20 psi

of hydraulic pressure was applied. The results showed a rejection of  $61.0 \pm 2.8 \%$  and  $93.3 \pm 0.4 \%$  of TOC and dimethylsilanediol (DMSD), respectively (Tommerup et al. 2016, 2017). These rejections were higher than the targeted 50% rejection (Tommerup et al. 2016, 2017). As a result, the NASA Advanced Exploration System (AES) initiated a program to evaluate the performance of the AqP HF on the ISS. The program aimed at verifying the effect of real wastewater and microgravity in the membrane flux and rejection. Previous studies of Aquaporin FO membranes had shown reduced flux rates in microgravity due to concentration polarization build up on the membrane surface. This was attributed to the absence of buoyancy-driven mixing in space, where all mixing occurs due to Brownian motion (Flynn 2013; Tommerup et al. 2017). Enhanced CP can also affect the contaminant rejection as it increases the concentration difference on the surface of the membrane. The water flux results showed a flux ranging from  $0.7 - 2.3 \text{ L/m}^2\cdot\text{h}^{-1}$ , which is similar to the average flux of  $0.76 \text{ L/m}^2\cdot\text{h}^{-1}$  achieved on-ground tests. Therefore, the effect of microgravity on the flux seems to be less severe than expected. Unfortunately, the concentration of TOC and DMSD measured on Earth are questionable as the samples were heavily delayed and not properly stored. These tests will be repeated in a future flight test for validation (Tommerup et al. 2017).

In a recent paper by Buelke et al., GO-based RO membranes have been proposed due to their stability, non-toxicity and high ion rejection capabilities (Buelke et al. 2018). The authors suggested that GO could enhance the UPA and WPA treatment process is used as 1) adsorbent, 2) membrane or 3) coating solution. If used as an adsorbent, it could replace the activated carbon in the Multifiltration bed due to its higher adsorption capacity (Buelke et al. 2018; Chen et al. 2013; Jiang, Biswas & Fortner 2016). Additionally, GO could be a potentially better candidate to sequester DMSD because

of its similar size and charge to Eosin Y, which is adsorbed at a capacity of 300 mg/g by GO (Buelke et al. 2018).

When GO is incorporated in the active layer of a semi-permeable membrane, this could be operated in RO-mode (i.e., hydraulic pressure is applied to overcome the osmotic pressure of the wastewater) to separate the contaminants from pure water physically. It was suggested that this could potentially make the distillation assembly, particulate filter and gas separator unit redundant. However, this would imply that, firstly, the system should reach hydraulic pressures higher than the osmotic pressure of the concentrated wastewater, at 85% water recovery, which, itself, is a challenge in the absence of gravity. Secondly, there is still a lack of data on the urea rejection proprieties of GO membranes.

Finally, Buelke et al. (2018) proposed to use GO antimicrobial proprieties to mitigate the effect of biomass growth issue that affects the WTA. GO coating could be used as a passive solution to reduce biofilm formation. This, however, would not affect the root cause of microbial growth in the wastewater.

#### 2.4.5.4 Forward osmosis bags for the Water Wall concept

NASA also developed a similar closed-loop concept. Their design, however, focused also on the re-use of concentrated wet wastes as a way to shielding the crew from cosmic radiation (Michael T Flynn et al. 2018; Sherwin Gormly, Michael Flynn & Howe 2012). Their idea was to create a Water Wall comprised of a series of FO membrane bags packed as dry elements integrated into an inflatable habitat structure's wall. After the launch in orbit, the FO bags are filled with produced wastewater to extract potable water from it. Once the FO bags are exhausted or fouled, they are filled

with faeces, solid organic wastes and other wastewater brine residuals. The bags now operates as an anaerobic digestion bags, where the produced  $\text{CH}_4$  and  $\text{CO}_2$  are harvested for  $\text{O}_2$  generation. After the digestion, the stabilised solids are combined with urine brine and become a permanent hydrocarbon/hydrated precipitate radiation shield (Cohen et al. 2014; Sherwin Gormly, Michael Flynn & Howe 2012). Figure 2-9 graphically shows the Water Wall concept. The passive cell-like structures used in the Water Walls concept should be physically integrated into the wastewater management system on-board of the ISS. The key factor of this design is its reliability and redundancy. The spacecraft should depart with all the bags filled with a salt solution and, one by one, they will be used to extract fresh water from wastes and then to protect crew members from ionising radiations.

Reviewing the available technologies for nitrogen cycling in the BLSS Clauwaert et al. concluded that most of the scientific research focused on the recovery of water, oxygen and carbon. At the same time, other (micro) nutrients are often neglected. However, efficient management of nutrients is essential to guarantee quasi-independent extra-terrestrial colonisation as the resupply for an increasing population would not be feasible (Clauwaert et al. 2017).

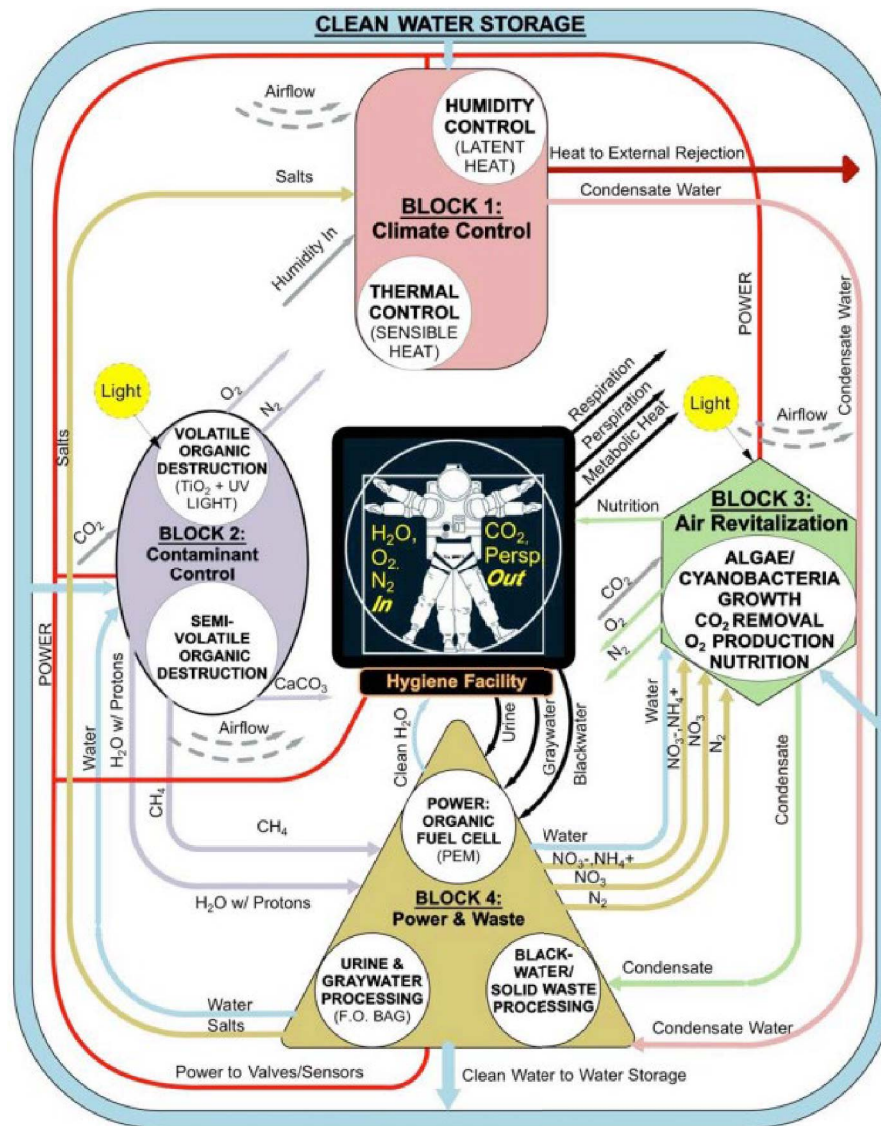


Figure 2-9 Initial concept of Water Wall system architecture. Credit to (Cohen et al. 2014). Permission granted by the copyright holder (Marc M. Cohen).

## 2.5 Current and past implementation of urine source-separation

To conclude this literature review chapter, real-life examples of urine source separation for nutrients recovery are presented.

### 2.5.1 VUNA Ltd. and eTekhwini municipality

Over 75000 urine diversion toilets were installed in 2002 in the eTekhwini municipality (Durban, South Africa) to the under-serviced communities inside the recently extended municipal boundaries. After surveying the users in 2004, it was found that 78% of the responders were satisfied with the system. However, opposite results were registered in 2011 when dissatisfaction was over 70%. Lack of maintenance, poor installation and construction materials might have caused lousy odour, which in turn, decreased the satisfaction levels (Roma et al. 2013).

In response to the dissatisfaction in the eTekhwini municipality, a trans-disciplinary project called VUNA was created. VUNA, which means “harvest” in the isiZulu language and stands for “Valorisation of Urine Nutrients in Africa” aimed at developing the technology and management tools to provide a large scale urine-fertiliser production in Durban. Through this project, a fixed urine-treatment unit was developed (Figure 2-10). The company Vuna Ltd. Later modified the process to develop a mobile treatment unit. The process consists of a nitrification column followed by GAC adsorption and distillation to produce a concentrated liquid fertiliser that was named “Aurin”. Aurin is now sold in Europe and is officially licensed for vegetables and flowers since 2018 by the Swiss Federal Office for Agriculture (Etter 2019; Etter & Udert March 2016).

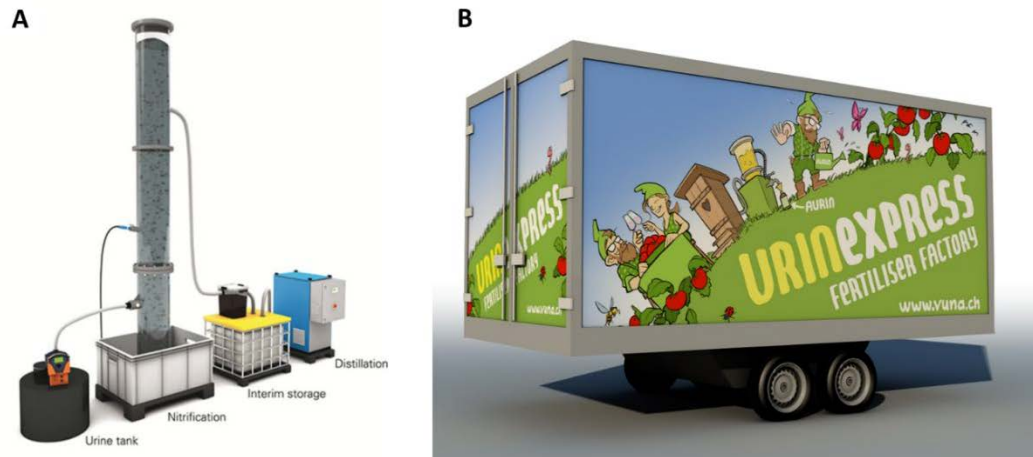


Figure 2-10 Graphic renderings of Aurin fertiliser production (A) and Vuna ltd. ([http://vuna.ch/index\\_en.html](http://vuna.ch/index_en.html)) urine express vehicle (B). Permission granted by the copyright holder (Bastian Etter).

### 2.5.2 GTZ and SANIRESCH program

The German Federal Ministry of Education and Research funded two-phase collaborative project for implementation of novel sanitation concepts in a public office. The objective of the first stage program (2005-2006) was to design and construct the urine separating system in the German agency for technical cooperation (GTZ) main building. This was followed by the SANIRESCH program executed by the Maßalsky GmbH institution which studied the feasibility of implementing an ecological sanitation (ecosan) concept for separate treatment and recycling of urine, brown- and greywater from an urban office building (Winker & Saadoun 2011). The system performance was analysed in according to health and hygiene concerns, environmental impact and local resources availability, operation and implementation complexity, financial and economic feasibility, and social-culture acceptance. It was found upon concluding that the project that, (1) the end product received an end product from the system that is hygienic and safe to use for agricultural

purposes and (2) that both farmers' and consumers' show the willingness to use urine as a liquid fertilizer; and (3) the project is was considered economically feasible in favourable conditions. However, technologies able to enhance the transportability and application efficiency of the urine product need to investigate further.

### 2.5.3 Ecological Sanitation Ethiopia Project

GTZ also funded the Ecological Sanitation Ethiopia Project, which started in 2006. The goal was to demonstrate the technical requirements and economic benefit from the implementation of urine source separation in high population density areas. It was concluded that urine source separation in multi-storey buildings and reuse of human excrete produces in agriculture would contribute to self-sufficiency and food security as well as provide additional income in terms of 1.4 times higher crop yield and productivity. About 25% of capital and operational cost reduction was achieved compared to conventional sanitation systems. This shows an advantage for use alternative sanitation system in higher density areas (Fry et al. 2015; Meinzinger et al. 2009; Meinzinger, Oldenburg & Otterpohl 2009; Simpson-Hebert 2007).

### 2.5.4 UTS Sustainable Sanitation project

The UTS Sustainable Sanitation project conducted by the Institute for Sustainable Futures (ISF) at the University of Technology, Sydney (UTS), in 2013, Australia, investigated the barriers associated with replacing existing sanitation systems to more sustainable urine diversion (UD) systems (Mitchell, Fam & Abeysuriya 2013a). The project consisted of waterless urinals, piping systems for urine sampling, and tanks for urine storage and transportation. The performances of the project were analysed



following regulations and institutions, user practices, operation and implementation, agriculture trials, market and socio-cultural acceptance. It was found that the development of urine diversion system could be hampered by the (I) lack of policies to support or promote the urine diversion and reuse; (II) no guidelines to regulate source-separated urine practices and (III) low market share in sustainable sanitation business.

## 2.6 Conclusions

This Chapter detailed urine composition and transformation under storage and comprehensively reviewed the multiple benefits of source-separating and reusing human urine. It was demonstrated that the savings from having “urine-free” wastewater are significant both from the economic, societal and environmental perspective. It also explained how the recovery of nutrients from urine could significantly reduce our dependency on energy-intensive fertiliser production processes as well as our reliance finite resources.

By reviewing the state-of-the-art processes for the treatment of human urine, several research gaps were identified. Specifically, the use of membrane technologies for the recovery of chemical energy, water and nutrients from urine is still marginal. However, the fact that most membranes have a small footprint, tunable selectivity, strong chemical resistance and versatility in the operation, making them suitable candidates for the treatment of a complex solution like urine.

As such, this Thesis selected membrane distillation, forward osmosis and reverse electrodialysis as emerging membrane technologies for the recovery of water, nutrients and chemical energy (respectively) from human urine. The main research question that this Thesis aims to answer is to whether the emerging technologies elected can provide any additional advantage compared to existing ones. The specific gaps and objective tackled in the Thesis are described in the introduction of each technical chapter.

# Chapter 3: Methodology

---

## 3.1 Introduction

In this thesis, multiple membrane-based technologies were tested. The aim was to investigate their effectiveness in recovering nutrients and water as well as to harness urine chemical energy. As multiple processes were used, this chapter focuses on the commonalities among the diverse experimental investigation, while the detailed experimental procedures for the FO, MBR-MD, FO-MD and RED experiments are described in each relevant chapter.

A common denominator of the experiments was the use of fresh and hydrolysed urine, either synthetically prepared or collected at a building scale. As such, this chapter begins with a description of urine preparation/collection and storage. Moving on the methodology used for the analysis of the urine samples is described. Finally, the analytical techniques used for the characterization of membranes and crystals (i.e., struvite) are detailed.

## 3.2 Experimental Materials

### 3.2.1 Urine solutions preparation

As mentioned before, urine composition varies based on diet, water intake, metabolism and degree of ureolysis (Putnam 1971a). Therefore, the first phase of each experimental investigation was to validate the initial hypothesis and optimise the operating procedure (Figure 3-1), as the errors introduced by the variability in real urine composition had to be avoided. As such, synthetically prepared urine was firstly used as it guaranteed a consistent composition (see section 3.2.1.1). However, synthetic urine lacks the complex organic composition typical of real urine, which means that tests with real urine had to be performed to validate the results and explain any discrepancies. As such, most of the experiments were also performed using real urine and its sampling, storage and usage are described in section 3.2.1.2.

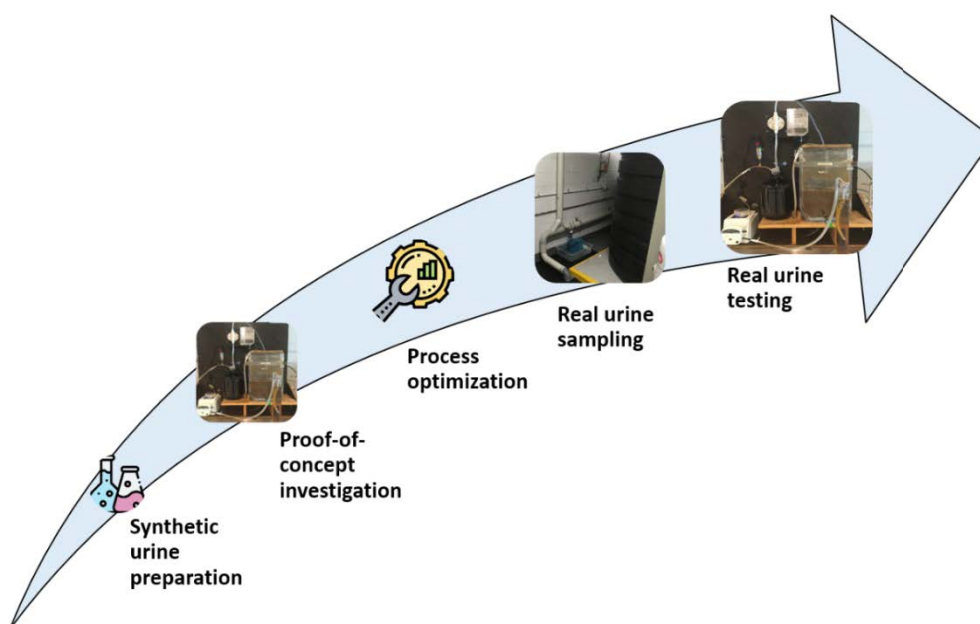


Figure 3-1 Flow diagram of the step-wise process adopted for each investigation.

### 3.2.1.1 Synthetic urine preparation

Simulated synthetic urine was prepared according to the average urine composition in the literature and the composition displayed in Table 3-1 (Etter & Udert March 2016; Putnam 1971a; Udert, Larsen & Gujer 2006). The assumption that no ammonia (g) loss due to volatilisation would occur during the hydrolysis process was made. At these pH values typical of hydrolysed urine, the maximum amount of ammonia (g) is between 25% and 40% of the overall  $\text{NH}_3 + \text{NH}_4^+$ . However, if urine is kept in a closed drum, the TAN (g) concentration the air gap inside the drum quickly reaches saturation levels thereby preventing that all the dissolved TAN in solution entering into the gas phase. Therefore, in reality, less than 5% of the ammonia is lost when the urine is stored in an enclosed drum. Synthetic urine solutions were stored at 4 °C and used within one week from the preparation.

### 3.2.1.2 Real urine collection and storage

The UTS Faculty of Engineering and IT building has built-in, a separate sewage piping network that allows to sample and store the urine collected from over 30 male urinals (Figure 3-2). Urinals are waterless and are cleaned periodically using a commercial biodegradable and chlorine-free detergent and, occasionally, a sulphuric acid-based anti-scaling solution. As the urine collected from the separate sewage network was already hydrolysed, probably due to the presence of urease-producing bacteria inside the pipes, fresh urine had to be collected from anonymous lab members. For fresh urine, the urine was immediately frozen at -80 °C to prevent bacterial growth (Bernini et al. 2011).

Hydrolysed urine, on the other hand, was stored in a 20-litre airtight drum at room temperature and a new batch was collected roughly every month. Every new batch of fresh and hydrolysed urine was analysed for pH, EC, dissolved organic carbon,  $\text{NH}_3/\text{NH}_4^+$ , urea, anions ( $\text{PO}_4^{3-}$ ,  $\text{SO}_4^{2-}$ ,  $\text{Cl}^-$ ) and cations ( $\text{Na}^+$ ,  $\text{K}^+$ ,  $\text{Mg}^{2+}$ ,  $\text{Ca}^{2+}$ ).

Table 3-1 Composition and characteristics of the synthetic fresh and hydrolysed urine feed solutions (Putnam 1971a; Udert, Larsen & Gujer 2006; Zhang, She, et al. 2014b).

Concentration [g/L]	Fresh Urine	Hydrolysed Urine	Characteristics	Fresh Urine	Hydro lysed Urine
Urea	16	-	pH* [-]	4.51	9.14
$\text{NH}_4$ -Acetate	-	9.6	Osmotic Pressure* [kPa]	1340	3010
$\text{NH}_4\text{Cl}$	1.8	-	Alkalinity** [M]	0.02	0.59
$\text{NH}_4\text{HCO}_3$	-	21.4	Ionic Strength** [M]	0.18	0.64
$\text{Na}_2\text{SO}_4$	2.3	2.3			
$\text{NaH}_2\text{PO}_4$	2.9	2.1			
KCl	4.2	4.2			
$\text{MgCl}_2$	0.37	-			
$\text{CaCl}_2$	0.51	-			
NaCl	3.6	3.6			
$\text{C}_4\text{H}_7\text{N}_3\text{O}$	1.1	1.1	(Creatinine)		
$\text{Na}_3\text{C}_6\text{H}_5\text{O}_7 \cdot 2\text{H}_2\text{O}$	0.65	0.65	(Sodium Citrate)		
$\text{Na}_2\text{C}_2\text{O}_4$	0.02	0.02	(Sodium Oxalate)		

\*Calculated with OLI System Analyser. \*\* Based on Udert et al. (Udert, Larsen & Gujer 2006).

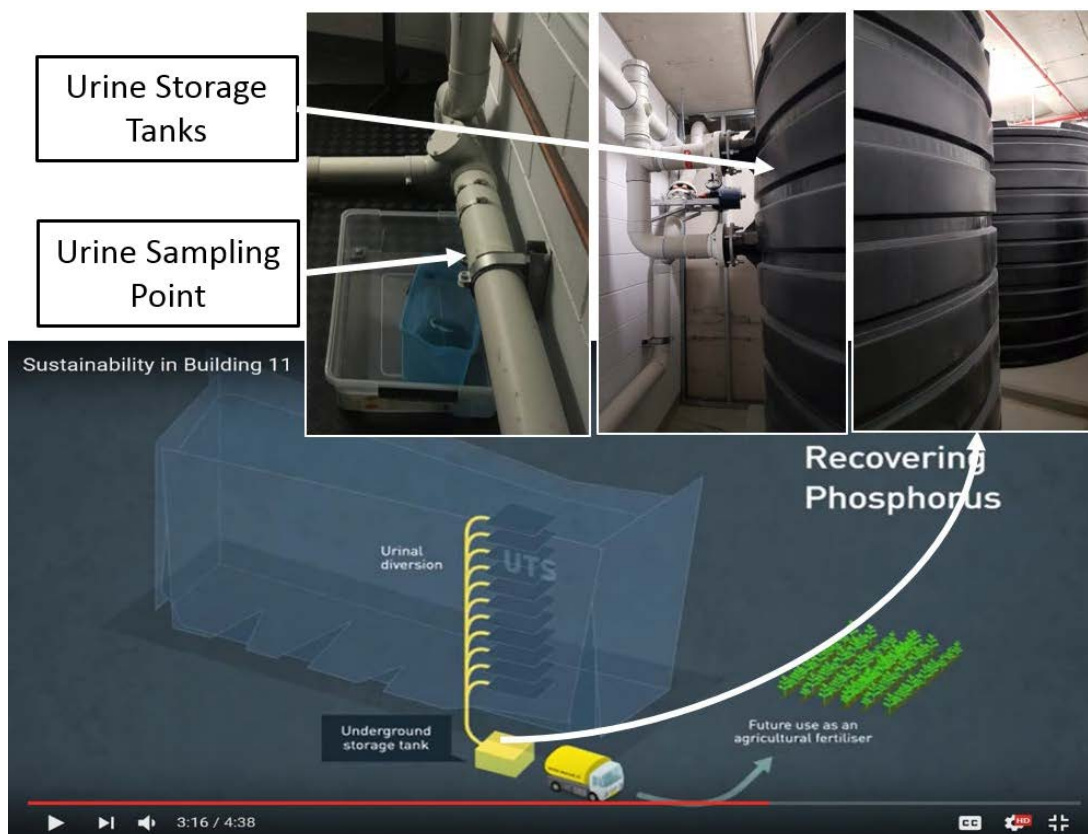


Figure 3-2 Urine storage tanks and urine piping system in the UTS Faculty of Engineering and IT building.

### 3.3 Analytical methods

#### 3.3.1 Water quality and ionic characterisation

Electric conductivity, total dissolved solids and pH of the samples were measured using a portable conductivity and pH meter (HQ14d, HACH, Colorado, US). Thermo Fisher Scientific ionic chromatography (IC, Thermo Fisher Scientific, USA) was used to measure anions such as  $\text{SO}_4^{2-}$ ,  $\text{Cl}^-$ ,  $\text{PO}_4^{3-}$ , while Agilent Technologies microwave plasma atomic emission spectrometry (MP-AES 4100, Agilent, USA) was used for the analysis of cations such as  $\text{Na}^+$ ,  $\text{Ca}^{2+}$ ,  $\text{Mg}^{2+}$ ,  $\text{K}^+$ . On the other hand,  $\text{NO}_3^-$  and  $\text{NO}_2^-$  were measured using a photometric method (Spectroquant Cell Test, NOVA 60, Merck) and ammonia were measured using a spectrophotometer (Spectroquant NOVA

60; Merck KGaA, Darmstadt, Germany), at 340 nm wavelength, using a urea/ammonia Megazyme kit (Megazyme, Australia). Urea was calculated as the amount of ammonia produced after ureolysis.

### 3.3.2 Organics quantification and characterisation

Dissolved organic carbon analysis was used to assess the removal and rejection of organics. The DOC concentration in a given sample was measured using Multi N/C 2000 (Analytikjena, Jena, Germany). Each sample was first filtered using a 0.45 µm cellulose esters filter, and the pH adjusted to be within 5 to 8. DOC standard solutions were prepared with potassium hydrogen phthalate (KHP), per the manufacturer's recommendations.

Size exclusion liquid chromatography coupled with organic carbon detector (DOC-Labor, Germany) was also used to investigate the organic fractionation across the processes. The hydrophilic and hydrophobic fractions were measured using a TSK HW 50-(S) column and 0.028 mol.L<sup>-1</sup> of phosphate buffer.

### 3.3.3 MLSS and MLVSS

MLSS was calculated as the ratio between the dry residue weight and the initial mixed liquor sample volume. The dry residue weight was measured after the filtration of 10 mL of mixed liquor through a 1.2 µm (Millipore, Australia) filter paper. Subsequently, it was oven-dried at 105 °C for two hours and then desiccated for 20 minutes. The dried residue from above was then heated in a furnace at 550 °C for 20 minutes, followed by other 20 minutes of desiccation (Schwarz et al. 2006). The weight of the sample after incineration was used to calculate the mixed liquor volatile suspended solids



(MLVSS). Finally, the ration between MLSS and MLVSS was calculated as an indicator of the inert fraction in the biomass.

### 3.3.4 Extracellular carbohydrates analysis

Extracellular carbohydrates analysis were performed using the phenol-sulphuric acid method with glucose as the standard (Larronde-Larretche & Jin 2017). This analysis was conducted to determine how the carbohydrates released by the algae varied during filtration with different types of DS (Chapter 8:). Firstly, the algae suspension was pelletised during centrifugation at  $6 \times g$  for 20 min; next, the supernatant was collected and filtered through a  $0.2 \mu\text{m}$  hydrophilic nylon filter (Millipore, Australia) (Larronde-Larretche & Jin 2016; Larronde-Larretche & Jin 2017); finally, the EPS concentration was measured and converted from mg/L to mg by multiplying the concentration for the feed volume.

### 3.3.5 SEM-EDX and X-ray diffraction analysis

The surface of membranes (pristine and used) were analysed by scanning electron microscopy (SEM, Zeiss Supra 55VP, Carl Zeiss AG, Germany). Samples were firstly dried under air purging and then coated with Au/Pd. The SEM imaging was performed at an accelerating voltage of 10 kV at different magnifications and various points. For cross-section analysis, the membrane was firstly flash-frozen using liquid nitrogen and then fractured using a sharp blade.

The crystals produced after the FO process (i.e., struvite or  $\text{NH}_4\text{MgPO}_4 \cdot 6 \text{H}_2\text{O}$ ) in Chapter 6: were also analysed using both X-Ray diffraction (Siemens D5000), over Bragg angles ranging from  $6^\circ$  to  $60^\circ$  ( $\text{Cu K}\alpha$ ,  $\lambda=1.54059 \text{ \AA}$ ), and energy-dispersive X-ray spectroscopy (Zeiss Supra 55VP, Carl Zeiss AG, Germany). While EDX provided

the elemental composition of the sample, XRD was used to analyse the structure of the crystals. As such, EDX was used to confirm the 1:1 molar ratio of P to Mg typical of struvite, while the XRD spectrum was used to compare the peaks from the sample with the ones typical of struvite.

## **Chapter 4: FO – MD optimisation to produce distilled water from human urine**

---

**\* This chapter was published in *Journal of Separation and Purification Technology* as:**

**F. Volpin**, S. Phuntsho, N. Ghaffour, J.S. Vrouwenvelder, H. K. Shon, Optimisation of a forward osmosis and membrane distillation hybrid system for the treatment of source-separated urine, *Separation and Purification Technology*, 212 (2019), 368-375.

## 4.1 Summary

Onboard the ISS, water recovery and reuse is a top priority. The reclaimed water is reused for drinking purposes, hygiene and oxygen generation. Human urine is a crucial source of water from the crew, but its current treatment process requires the use of consumables which increases the cost of the system as each kg shipped to the ISS costs up to 10000 USD. As such, this work investigates the combination of FO and MD to extract distilled water from human urine. FO was chosen as MD pre-treatment to increase the overall nitrogen rejection and to prevent wetting of the MD membrane. The goal of this investigation was to tune the FO and MD operating parameters to reduce nitrogen leakage to the MD permeate.

Urine pH, DS salt concentration and operating pressure were varied as a means to enhance the FO performances. Feed temperature, nitrogen concentration and membrane characteristics were investigated to optimise the MD process. With 2.5 M NaCl as DS commercial FO membranes achieved a water flux between 31.5 – 28.7 L.m<sup>-2</sup>.h<sup>-1</sup>. Additionally, a 33% reduction in the nitrogen leakage was observed by applying minimal hydraulic pressure on the DS. However, this was also found to reduce the net transmembrane water flux significantly. Acidification of the feed was also beneficial for both FO and MD nitrogen rejection. Finally, we demonstrated that, by tuning the MD membrane porosity and thickness, higher MD permeate quality could be achieved. To conclude, the hybrid FO-MD process is expected to be an effective solution for the production of clean water and concentrated fertiliser from human urine. This double barrier separation process could be suitable for both water reclamation in space application and resource recovery in a terrestrial application.

## 4.2 Introduction

Wastewater reuse is becoming one of the most sustainable solutions to the freshwater scarcity problem. Besides water, wastewater also contains valuable nutrients which can be extracted and reused to meet the increasingly growing fertiliser demand. However, when yellow, brown and grey waters are combined the recovery of water and nutrients is exceptionally costly due to its large volume and complex composition. On the other hand, several studies have shown that, when up-stream source-separation is adopted, resource recovery is more economically feasible (Alder et al. 2009; Larsen & Gujer 1997; Larsen et al. 2016; Layne et al. 2018).

This explains why source separation has already been widely adopted on board of the ISS, where water recovery has always been a priority (Layne et al. 2018). Water recovered from urine, in particular, is used for crew drinking, hygiene and oxygen generation (Pruitt et al. 2015). As treating the wastewater on board of the ISS accounts for approximately half of the total life support payload, this which means that improving the efficiency of the current processes is paramount (Cath et al. 2005). The ideal life support systems in space must provide the highest possible percentage of water recovery with the lowest energy, operation and maintenance costs (Sherwin Gormly, Michael Flynn & Howe 2012).

In the last two decades, many efforts have been dedicated to the development and optimisation of different physico-chemical processes for the extraction of pure water from source-separated urine (Maurer, Pronk & Larsen 2006; Udert et al. 2015). These processes include (but are not limited to) RO, NF, freeze/thaw concentration and evaporation (Liu et al. 2016; Maurer, Pronk & Larsen 2006; Pronk et al. 2006). Pressure-driven processes, i.e. RO and NF, show promising regarding volume

reduction and rejection of micropollutants but fail to reject well small uncharged compounds like urea and ammonia (Maurer, Pronk & Larsen 2006; Pronk et al. 2006). Hydraulic pressure-driven NF/RO also suffer from membrane fouling or scaling and high operational costs (Amy et al. 2017; Liu et al. 2016). Finally, as the initial urine osmotic pressure is in the range of 10-22 bar, RO can concentrate it up to maximum 3-7 times (Putnam 1971a).

For freeze-thaw, it was calculated that 1100 MJ m<sup>-3</sup> were necessary for a five-fold urine volume reduction. Finally, evaporation is the most straightforward technology for removing water from urine (Maurer, Pronk & Larsen 2006). Despite its simple operation, this technology still suffers from ammonia volatilisation which can jeopardise the final permeate quality and reduce the amount of re-usable nitrogen (Maurer, Pronk & Larsen 2006; Tun et al. 2016). Urine acidification or partial nitrification were found to be effective ways to minimise the nitrogen losses (Maurer, Pronk & Larsen 2006; Udert & Wächter 2012). However, the high buffer capacity of urine makes the acidification process costly while biological oxidation of ammonia requires extensive aeration and process control to be stable (Fumasoli et al. 2016; Udert, Fux, et al. 2003).

More recently, the combination of osmotically and thermally driven membrane processes including FO and MD has been investigated for the treatment of human urine (Cath et al. 2005; Liu et al. 2016; Tun et al. 2016; Zhang, She, et al. 2014b). Although the number of studies is quite limited, initial results demonstrated the feasibility of recovering water and nutrients from source-separated urine. By using FO as MD pre-treatment, a higher quality and more stable MD permeate can be achieved due to the generally high rejection of commercially available FO membrane (Lu et al. 2018; Xie

et al. 2014; Zhang, Wang, et al. 2014; Zhao et al. 2016; Zhao et al. 2014; Zhou et al. 2017). This hybridisation allowed for the purification of wastewater that generally challenging to treat by standalone MD, due to fouling/scaling and wetting problems, such as landfill leachate (Zhou et al. 2017), oily wastewater (Lu et al. 2018; Zhang, Wang, et al. 2014), digested sludge (Nguyen et al. 2016; Xie et al. 2014) As(III) removal (Ge, Han & Chung 2016), wastewater reuse (Husnain et al. 2015; Li, Hou, et al. 2018) and desalination (Luo et al. 2017; Wang et al. 2015).

When it comes to urine treatment via MD, the main issues were related to the permeation of ammonia gas to the produced water and the wetting of the MD membrane due to the presence of surfactants or other wetting agents in the urine collected from urinals (Tun et al. 2016). For urine treatment, the FO process is shown to have an ease of operation and low fouling potential (Volpin, Chekli, et al. 2018; Zhang, She, et al. 2014b). However, if high urine concentration has to be achieved through dewatering, FO draw solution regeneration is deemed necessary. Otherwise, the cost of the DS will make the process prohibitive. A hybrid FO - MD system for the treatment of human urine could provide a double barrier to increase the quality of the final permeate while regenerating DS for continuous operation. However, long-term experiments have revealed that the accumulation of N-compounds with time in the DS remains one of the main limitations, especially when the by-product water from the urine treatment is to be used for drinking (e.g., during space exploration).

The objective of this study was to investigate and optimise a FO-MD hybrid system for the dewatering and concentration of source-separated urine. Based on the results obtained in the few available studies, the emphasis was given on developing strategies to reduce the transport of nitrogen compounds to achieve a final recycled water that

can be used directly on-site (for toilet flushing and fertigation) (Fumasoli et al. 2016; Udert & Wächter 2012). The ultimate goal is to develop a viable system that will contribute positively towards the sustainability of the food-water-energy nexus.

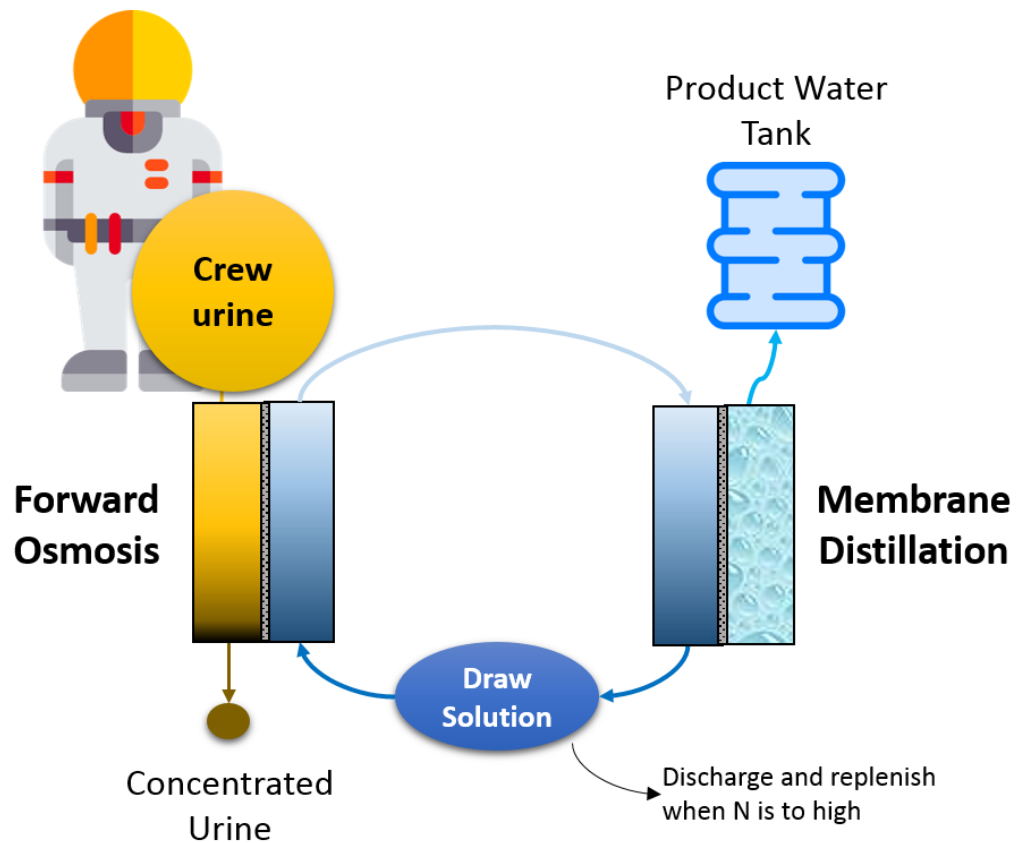


Figure 4-1 Schematic of the source-separated urine treatment system proposed. Water is extracted from the urine solution to the draw solution, through forward osmosis, while the MD system is used to reconcentrate the draw solution and produce distilled water.

### 4.3 Experimental investigation

#### 4.3.1 Feed and draw solutions

Synthetic fresh urine and hydrolysed urine were used in this study as feed solutions. Synthetic solutions were selected against real urine to make sure that the optimisation



of the system was performed under controlled and stable conditions. Synthetic FU and HU solutions were prepared as described in the Methodology Section (0). Even though real urine collected from flushing urinals might have different dilution factors ranging from 1:1 to 1:100, only concentrated FU/HU urine was used as feed for the FO tests (Liu et al. 2014; Udert, Larsen & Gujer 2003). This was chosen to have a conservative estimation of the water and nitrogen flux during FO operations. In fact, if urine is diluted, the FO water flux would likely increase, as the  $\Delta\pi$  between feed and draw would decrease, while the nitrogen flux will increase as the  $\Delta C_N$  between FS and DS will decrease (Fick's law on membrane diffusion rate:  $J_N = D_N \cdot A \cdot \Delta C_N/x$ ). The DS was prepared by dissolving sodium chloride (reagent grade, Sigma Aldrich, Australia) into deionised water at various concentrations ranging from 1 M (i.e. 47.4 bar – seawater RO desalination brine) to 2.5 M (i.e. 131.9 bar – produced water from Oil and Gas operations).

#### 4.3.2 Forward osmosis and membrane distillation membranes

A commercial flat sheet polyamide (PA) TFC membrane from Toray Chemical Inc. (South Korea) was used in this study. The pure water permeability coefficient of the active layer (i.e. A value), as well as the salt rejection (R) and salt permeability coefficient (B) for urea, ammonium and ammonia in both FU and HU, were determined in RO mode at 10 bar applied pressure (Cath et al. 2013; Tiraferri et al. 2011). The difference between the B and R is that B is a constant value based on the intrinsic properties of the membrane, while R depends on the flux or concentration of the salt. The A value was calculated by dividing the average water flux (i.e. of 5 consecutive measurements taken at the 1-minute interval) by the applied pressure. The salt rejection was determined from the difference between the bulk feed concentration

and the final permeate concentration after 1-hour operation. Finally, the B value was determined using the following equation:

$$B = \frac{1 - R}{R} (\Delta P - \Delta \pi) A \quad (4-1)$$

where R is the salt rejection of the targeted compound,  $\Delta P$  is the applied pressure (10 bar in this study),  $\Delta \pi$  is the osmotic pressure of the targeted compound (i.e. urea, ammonia, ammonium) in either FU or SU and A is the pure water permeability coefficient. Table 4-1 shows the pure water permeability (A) and solute permeability (B) of the used membrane. The employed membrane showed both higher A value and lower B values compared to CTA membrane used in a previous study (Zhang, She, et al. 2014b).

Table 4-1 Pure water permeability (A) and solute permeability (B) of the membrane used for the experiments. The B value for urea, ammonium and ammonia in both FU and SU, were determined in RO mode at 10 bar pressure.

		TFC (This study)	CTA (Zhang et al. 2014)
<b>A value (m/s.Pa)</b>		1.54*10 <sup>-11</sup>	2.09*10 <sup>-12</sup>
	Urea - Fresh urine	2.21*10 <sup>-6</sup>	1.12*10 <sup>-5</sup>
	TAN - Fresh urine	6.82*10 <sup>-7</sup>	9.30*10 <sup>-6</sup>
<b>B value (m/s)</b>	NH <sub>4</sub> <sup>+</sup> - Fresh urine	1.97*10 <sup>-7</sup>	-
	TAN - Stored urine	7.09*10 <sup>-7</sup>	1.21*10 <sup>-6</sup>
	NH <sub>4</sub> <sup>+</sup> - Stored urine	2.05*10 <sup>-7</sup>	-

Table 4-2 Proprieties of the MD membranes employed. \* The contact angle was based on a recent study with the same membranes (Silva et al. 2018).

Membrane material	PVDF (Polyvinylidene fluoride)	PTFE (polytetrafluoroethylene)
Manufacturer	Durapore®-GVHP	Fluoropore®-FGLP
Nominal Pore size	0.22 $\mu\text{m}$	0.22 $\mu\text{m}$
Thickness	125 $\mu\text{m}$	150 $\mu\text{m}$
Contact Angle*	131 $\pm$ 1 $^\circ$	146 $\pm$ 1 $^\circ$
Active layer porosity	75%	85%

Also, two different commercial membranes were tested for the MD process. The first was a polyvinylidene fluoride (PVDF) membrane (Durapore®-GVHP, pore size 0.22  $\mu\text{m}$ , thickness 125  $\mu\text{m}$  and porosity 75%) while the second was a polytetrafluoroethylene (PTFE) membrane (Fluoropore®-FGLP, pore size 0.22  $\mu\text{m}$ , thickness 150  $\mu\text{m}$  and porosity 85%). Both were purchased from Merck Millipore.

#### 4.3.3 Bench-scale FO and MD systems

The performance of the FO and MD systems (i.e. water flux and solute transport across the membrane) was evaluated in a batch mode of operation whereby FO feed and draw solutions, and MD permeate solution was recirculated back to their respective tank. Both systems were operated under the counter-current flow mode. The membrane cell for both systems has two symmetric channels on each side (7.7 cm length, 2.6 cm width and 0.3 cm depth) with an active membrane area of 0.002 m<sup>2</sup>. Gear pumps with variable speed (Cole Parmer, USA) were used to circulate the solutions from the tanks to the membrane cell and then back to the tanks. The DS tank for the FO system and

the permeate tank for the MD system were placed on a digital scale connected to a computer. Weight measurements allowed for the determination of the transmembrane water flux. pH and conductivity probes were connected to the feed tank of the FO system and to the permeate tank of the MD system to record the change of pH and conductivity in the FS and permeate solution.

The FO experiments were conducted under the active layer facing the FS mode (AL-FS). A new membrane was used for each new test and was stabilised with DI water on both sides for 30 minutes prior to the start of the experiment. After stabilisation, both feed and draw solutions were replaced, and the water flux was measured continuously every 3 minutes. Tests were conducted at a cross-flow velocity of 8.5 cm/s at a constant temperature of 25°C maintained with a temperature-controlled bath connected to a heating/chilling unit. For the MD experiments, the DCMD configuration was chosen due to its higher performance (i.e. water flux) and relative ease of setting up (Lee et al. 2017). A new membrane was also used for each new experiment. The membrane cell was placed horizontally with the feed flowing on the top side. The feed temperature was varied from 40 to 60°C by a heating bath. Deionised water was used on the permeate side and kept at 25°C using a chiller. Both feed and permeate solutions were allowed to recirculate for about 30 minutes before starting the experiments to reach the targeted temperature. The cross-flow velocity on both sides was maintained at 8.5 cm/s.

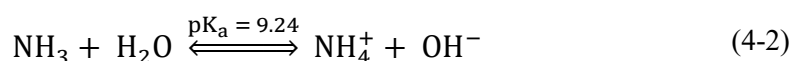
#### 4.3.4 Experimental protocol

##### 4.3.4.1 Optimisation of the FO process

Optimisation of the FO process was carried out for both FU and SU solutions. The optimisation focused on reducing the transport of nitrogen compounds through the

membrane. For FU, urea was the targeted nitrogen compounds while for SU, it was mainly ammonia. In fact, for the combined FO-MD system, TAN is the main issue if it accumulates in the DS side since ammonia can pass through the MD membrane together with water vapour.

It was hypothesised that applying a little hydraulic pressure on the DS would lessen the urea diffusion to the FS. In fact, similarly to pressure-assisted osmosis (Blandin et al. 2013) whereby pressure is applied on the feed side to increase the water flux and reduce the reverse salt flux from the DS; here, applying pressure on the DS would theoretically reduce the transport of salts from the feed to the draw solution. To test that, pressure (up to 2 bar) was applied on the DS side using a pressure valve connected to the DS outlet pipe (a pressure gauge was also installed to control more accurately the change in pressure). For experiments with stored urine, the pH was varied from initial pH (i.e. 8.87) down to pH 6 to shift the equilibrium  $\text{NH}_3/\text{NH}_4^+$  towards  $\text{NH}_4^+$  (reaction 2) and thus reduce the concentration of TAN in the feed solution.



#### 4.3.5 Optimisation of the MD process

Apart from testing different feed temperatures and MD membrane types, feed urine solutions with different dilution (1:1, 1:10 and 1:100) were tested to evaluate the effect of initial nitrogen compounds concentration on the quality of the final permeate. In fact, by using FO as a pre-treatment, nitrogen compounds will accumulate on the DS side, which will affect the performance of the MD process. Also, both PTFE and PVDF based membranes were employed for the experiments and their performances evaluated. PVDF and PTFE are among the most widely used membranes for MD due

to their hydrophobic nature and high thermal stability. The water droplet contact angle on a PTFE surface varies from 108° to 115° while for PVDF membrane was found to be 107° (Tomaszewska 1996; Zhang et al. 2010).

#### 4.3.6 Analytical methods

Samples were taken from the draw solution side in FO experiments and from the permeate side in MD experiments. Ammonia and Urea were measured as described in the Methodology.

### 4.4 Results and discussion

The direct application of MD for the concentration of human urine is questionable as, in the majority of urine collection systems, real urine is mixed with detergents and surfactants. Surfactants can lower the surface tension of the membrane, thereby causing fouling and pore wetting which would jeopardise the whole process (Chew et al. 2017). However, if forward osmosis is chosen as a “pre-treatment”, surfactants can be almost entirely removed (the rejection was found above 99.8%) (Zhao et al. 2015), thereby providing an optimal solution for the MD process to work with. Additionally, FO should reduce the amount of ammoniacal nitrogen leaching to the MD feed, which in turns would increase the quality of the MD permeate.

#### 4.4.1 FO performances in dewatering fresh and stored urine

In this section, the FO water flux was measured using fresh or stored urine as FS and different NaCl concentration as DS. Afterwards the nitrogen transport, as  $\text{NH}_3/\text{NH}_4^+/\text{Urea}$ , through the membrane per litre of treated water was investigated. Figure 4-2 displays the achieved water flux when SU or FU is used. FU higher water flux is expected to be due to its lower osmotic pressure compared to SU (i.e., 13.7

versus 29.1 bar). However, Figure 4-3 shows that FU also exhibits higher nitrogen leakage. This can be explained by looking at equation (4-3). It can be seen that the solute transport coefficient for urea is higher than both  $\text{NH}_3$  and  $\text{NH}_4^+$ . The low rejection of urea is due to the combination of having a low molecular weight, absence of charge, high diffusivity ( $D_{\text{urea}} = 1.32 \cdot 10^{-10} \text{ m}^2 \cdot \text{s}^{-1}$ ) as well as a high concentration in the feed solution (Lee & Lueptow 2001).

$$\begin{aligned} B_{\text{urea}} &= 2.21 \cdot 10^{-6} \frac{\text{m}}{\text{s}} > B_{\text{NH}_3} = 7.09 \cdot 10^{-7} \frac{\text{m}}{\text{s}} > B_{\text{NH}_4^+} \\ &= 2.05 \cdot 10^{-7} \frac{\text{m}}{\text{s}} \end{aligned} \quad (4-3)$$

Additionally, Figure 4-3 shows that the nitrogen flux decreases with the increase in DS concentration. A possible explanation can be given by looking at equation (4-4), where  $J_W$  is the water flux and  $B_N$  the permeability of the selected nitrogen compound (Zhang, She, et al. 2014b). Equation (4-4) shows that the rejection is directly proportional to the water flux. In particular, if the water flux increases, so does the rejection.

$$R [\%] = J_W / (J_W + B_N) \quad (4-4)$$

$$\text{Nitrogen Transport [gN/L of treated water]} = \frac{\frac{\Delta m_{N, \text{Draw}}}{A \cdot \Delta T}}{\overline{J_W}} \quad (4-5)$$

Equation (4-5)(4-4) was then used to calculate the nitrogen flux depicted in Figure 4-2. Where,  $\Delta m_{N, \text{Draw}}$  is the nitrogen mass increase in the draw solution,  $A$  the membrane area and  $\Delta T$  the sampling time interval and  $\overline{J_W}$  the average water flux between the samples.

$$R_N[\%] = \left( 1 - \frac{m_{N,Draw}}{m_{N,Feed}} \right) * 100 \quad (4-6)$$

Eq. 4-6 was then used to calculate the nitrogen rejection as the ration between the concentration of nitrogen in the draw  $C_{N, Draw}$  and the initial concentration of nitrogen in the feed  $C_{N, Feed}$  (Xie et al. 2018).

To summarise, due to its lower osmotic pressure, FU exhibited a water flux on average 13% greater than the one of SU. On the other hand, it also exhibited higher nitrogen transport. Finally, as urea and  $NH_4^+$  are non-volatile, they will accumulate in the draw solution over time. Therefore, DS purging/replenishment will be necessary.

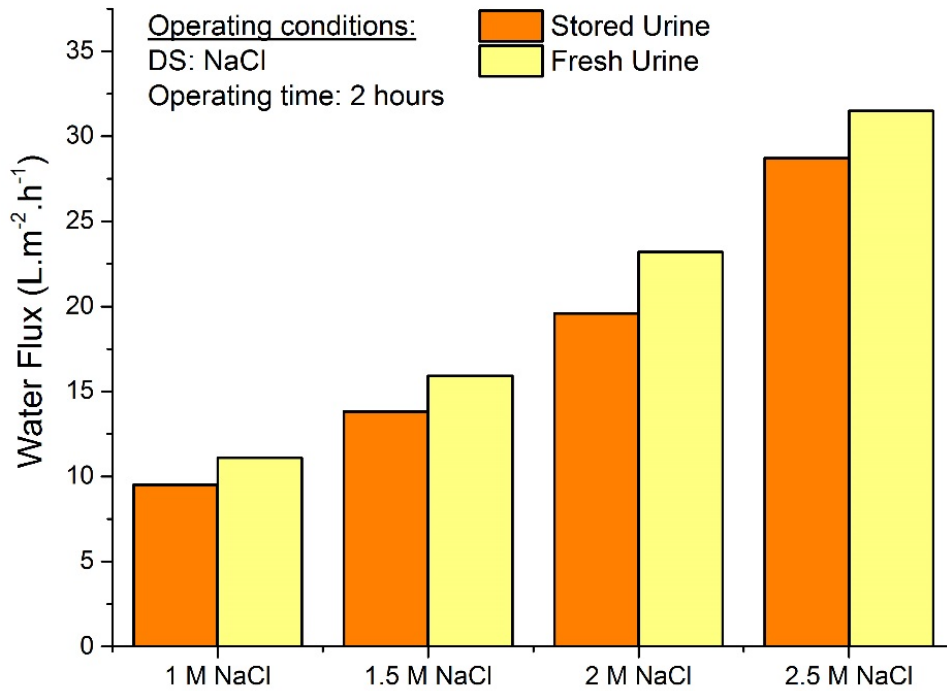


Figure 4-2 Forward osmosis water flux using fresh or stored urine as feed, and NaCl at different concentrations as draw solution.



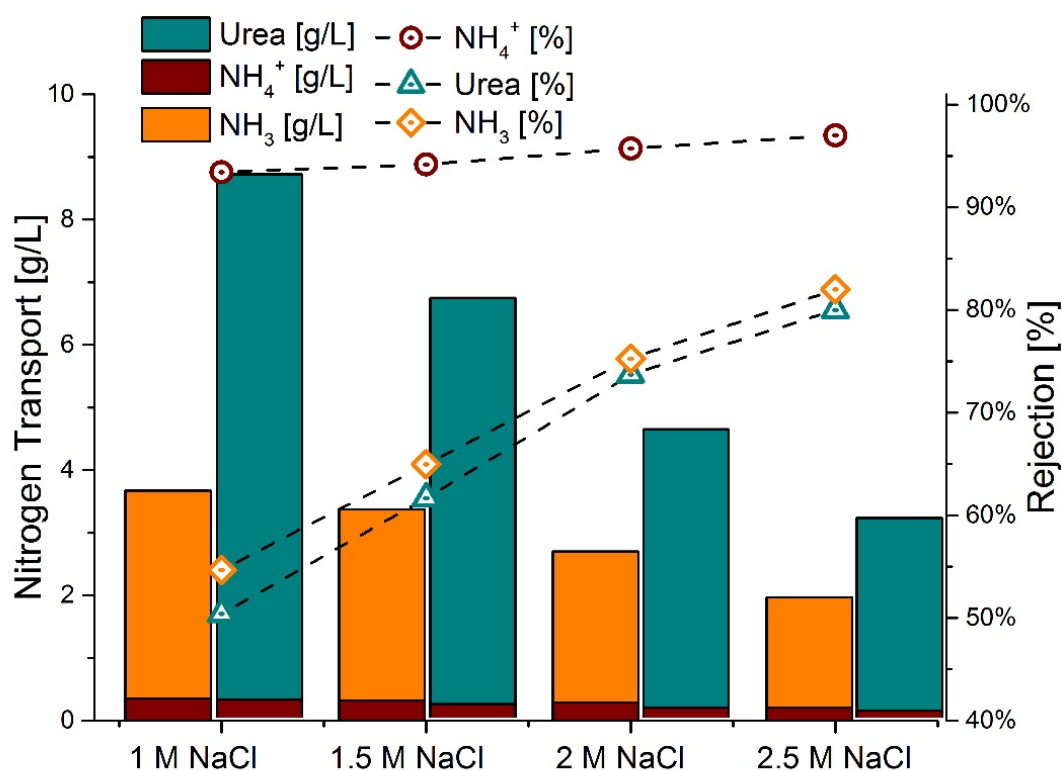


Figure 4-3 Nitrogen rejection (right axis) and transport from feed to draw per volume of treated water (left axis). For every draw concentration, the stacked column on the left refers to the fresh urine while the column on the right to the hydrolysed urine.

#### 4.4.2 Optimisation of the FO process

##### 4.4.2.1 Fresh urine: Effect of hydraulic pressure applied to the draw solution side

In this section, the effect of DS pressure and FS pH on the transmembrane FO nitrogen flux was investigated. A 1.5 M NaCl was used as DS. This DS concentration was chosen to match the flux of FO with the one of MD. Applying pressure on the feed side (i.e., pressure assisted osmosis) was often found to decrease the reverse diffusion of ions from the DS to the FS (Coday et al. 2013). Other studies explained this phenomenon as the effect of enhanced convective flux that drives the draw solutes away from the membrane due to back diffusion (Sahebi et al. 2015). Here, the same

principle was tested as a means to reduce the forward diffusion of urea to the DS. Specifically, pressures ranging from 0.5 to 2 bar were applied on the draw side and the forward flux of urea measured. It was found that the specific urea flux could be decreased by about 30% when a pressure of 2 bar is applied on the draw side. Nevertheless, the water flux was also found to drop by 42%.

To sum up, nitrogen rejection can be boosted by simply applying back pressure on the DS, the downside of that is that it would also decrease the effective driving force.

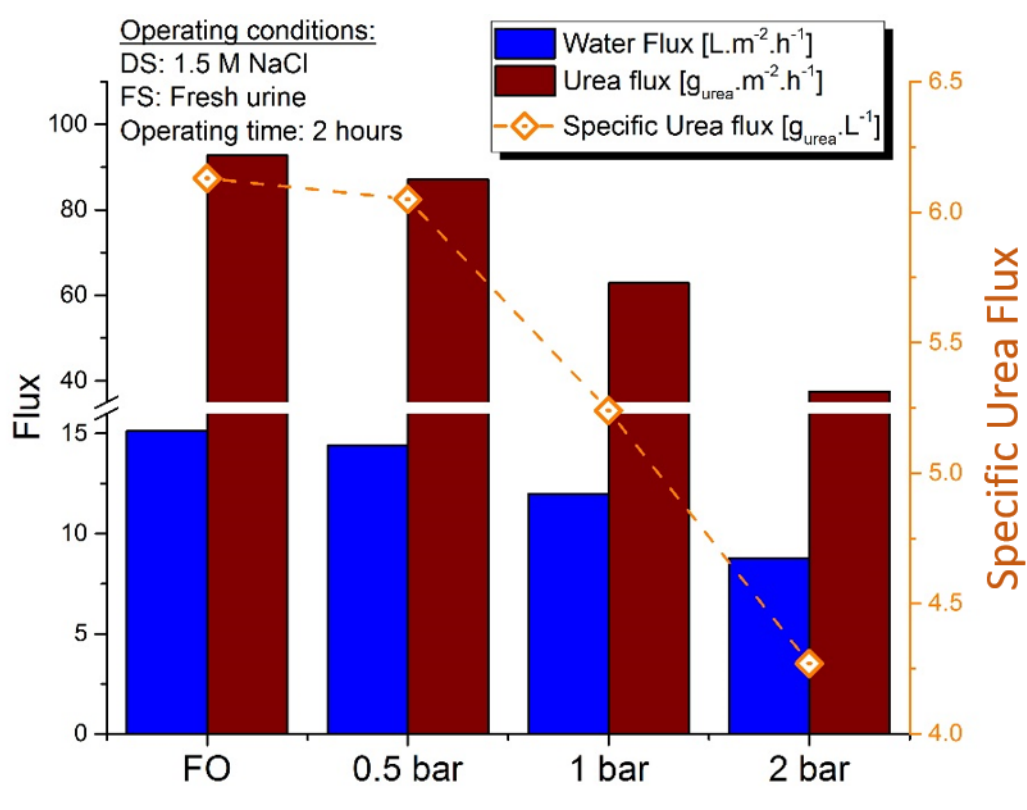


Figure 4-4 Water and urea flux as a function of transmembrane pressure exerted on the draw side. The operating conditions are also detailed in the picture.

#### 4.4.2.2 Stored urine: Effect of feed solution pH

Urine acidification has been extensively investigated as a means to reduce the ammonia permeation in both FO and MD. Shifting the equilibrium  $\text{NH}_3 \xrightleftharpoons{\text{pK}_a=9.25} \text{NH}_4^+$  to the ionic  $\text{NH}_4^+$  would enhance the nitrogen rejection of the polyamide active-layer due to electrostatic repulsion (Donnan effect) of charged ammonium. On the other hand, the rejection of uncharged ammonia would be only regulated by size exclusion mechanism. The nitrogen rejection by MD would also increase when the pH of the urine is 7 or less as  $\text{NH}_4^+$  is non-volatile while ammonia is a gas with a boiling point of  $-33.3^\circ\text{C}$ . However, it has to be noted that it would be preferable to acidify urine when it is fresh to prevent urea hydrolysis. In fact, the high buffer capacity of hydrolysed urine would increase the required acid to reach pH neutralisation four times (i.e., about  $230 \text{ mmol H}^+ \cdot \text{l}^{-1}_{\text{urine}}$ ) (Maurer, Pronk & Larsen 2006).

Figure 4-5 (A) confirms the hypothesis of the effect of the pH on nitrogen transport. With the decrease in the pH, the concentration of charged  $\text{NH}_4^+$  ions in the urine increases thereby leading to a lower total nitrogen flux. However, the addition of acid (in this case HCl) also increases the salinity of the urine and, therefore, its osmotic pressure. As a consequence, the FO water flux was also found to decrease with the decrease in the pH. In fact, the protonation of ammonia is not expected to influence the FO flux as the diffusivity coefficients of  $\text{NH}_3$  and  $\text{NH}_4^+$  are very close (i.e.,  $D_{\text{NH}_4^+} = 1.82 \cdot 10^{-9} \frac{\text{m}^2}{\text{s}} \sim D_{\text{NH}_3} = 2.07 \cdot 10^{-9} \frac{\text{m}^2}{\text{s}}$ ). The lowering of the FO water flux caused a slight increase in the nitrogen transport rate through the membrane as nitrogen transport is the ratio between nitrogen flux ( $\text{g}_\text{N} \cdot \text{m}^{-2} \cdot \text{h}^{-1}$ ) and water flux. Additionally, the stability of the polyamide active layer might be compromised under alkaline conditions due to hydrolysis via the direct nucleophilic addition of  $\text{OH}^-$  to the

carbonyl group (Lee et al. 2015). Therefore, operating under pH of 6-7 is also recommended from the membrane stability point of view.

Finally, at high pH membrane scaling might be more severe due to carbonates and phosphate precipitation of the membrane active layer. When real urine is used, the effect of pH in the co-precipitation of inorganic and organic foulants on the membrane should be further investigated.

It can be concluded that, despite the lower water flux, acidified stored urine is preferable to ensure a stable higher ammonium rejection.

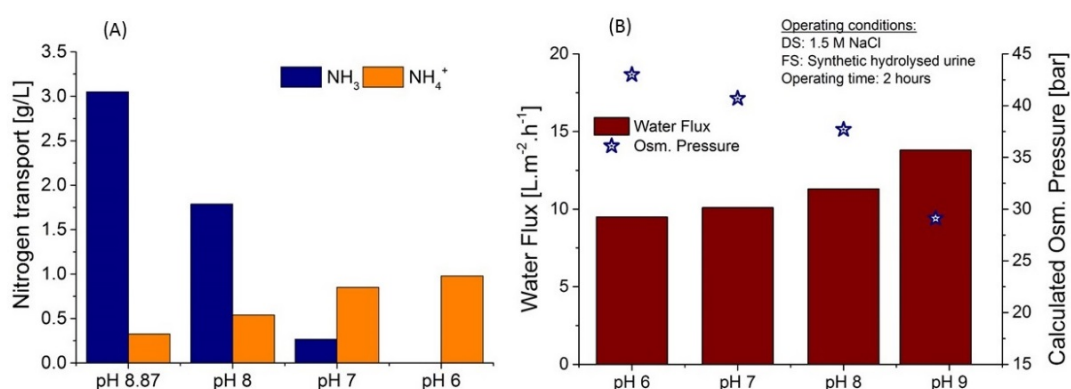


Figure 4-5 Impact of feed acidification in the transport of nitrogen (A) and water (B) across the TFC-FO membrane. Figure (B) also displayed the calculated feed osmotic pressure as a function of the pH. The osmotic pressure of the solution was calculated using ROSA software (Version 9.1, Dow Filmtech, USA).

#### 4.4.3 Optimisation of the MD process

##### 4.4.3.1 Effect of feed temperature and membrane types on the water permeation

The optimal MD operation was studied to minimise the N transport in the permeate. In this section, the water flux of the PVDF and PTFE commercial MD membranes was

tested and compared. The membranes were tested at with 1.5 M NaCl as feed and having a temperature ranging from 40 °C to 60 °C. Afterwards, the optimal feed temperature was used to investigate the ammonia transport to the MD produced water. It can be seen that the  $\Delta T$  between the feed and the permeate should be above 40 °C, for PVDF, and above 30 °C for PTFE for the MD to have the same FO water permeation rate. This can also be avoided by increasing the MD membrane area. Figure 4-5 also shows how the employed PTFE membranes achieved, on average, 35% higher water flux compared to PVDF membranes. One possible explanation is the higher porosity of PTFE over PVDF (i.e., 85% compared to 75%) and hydrophobicity (determined by contact angle) i.e., 146° compared to 131°. Similar results were found by Silva T. et al (Silva et al. 2018).

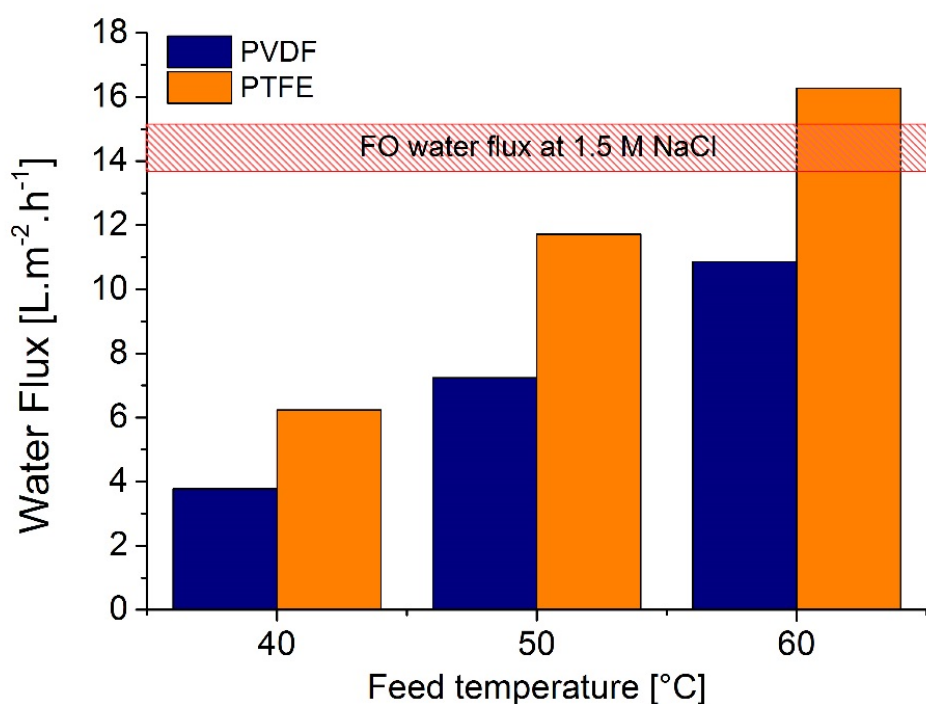


Figure 4-6 Water flux of PVDF and PTFE MD membranes using 1.5M NaCl as DS and feed temperature of 40, 50 or 60 °C. Permeate temperature was kept at 20 °C.

#### 4.4.3.2 Effect of feed solutes concentration on the permeate quality

Once the optimal  $\Delta T$  between feed and permeate was determined, the mass transfer of nitrogen was measured as a function of ammonia concentration and membrane material. To do so, stored urine with different dilution factors (1:1, 1:10 and 1:100) were tested to evaluate the effect of initial nitrogen compounds concentration on the quality of the final permeate (as explained in section 2). New solutions were used for the MD tests to ensure a consistent feed for each replicate. Ammonia concentration, pH and temperature are the dominant factors in the ammonia permeation rate (Tun et al. 2016). The ammonia vapour pressure increases with the increase in ammonia concentration and solution temperature. The pH, in particular, regulates the amount of ammonia (gas) over  $\text{NH}_4^+$  (liquid). High concentrations of gaseous ammonia would significantly increase the nitrogen leakage to the produced water. Several studies have proven that ammonia leakage can be minimised if the urine is acidified to pH below 6 (Liu et al. 2016; Tun et al. 2016; Zhao et al. 2013). In this study, the performance of PVDF and PTFE membranes were benchmarked in the worst-case scenario, i.e., high feed temperature, pH and concentration.

Membrane pore size and thickness were found to be the dominant factors in the ammonia flux through the MD membrane. The membrane thickness is inversely proportional to the ammonia mass transfer (Ding et al. 2006; Tun et al. 2016). In this case, the employed membranes have the same pore sizes, 0.22  $\mu\text{m}$ , while the thickness of the PTFE membranes was higher than the PVDF ones. Therefore, it was expected that the TAN transfer would be lower when the PTFE membrane is used. Additionally, the higher water flux of PTFE would also lower the nitrogen to water transfer rate. Overall, if FO can reject >95% of the ammoniacal nitrogen, PTFE membrane is expected to ensure a low nitrogen concentration in the permeate.

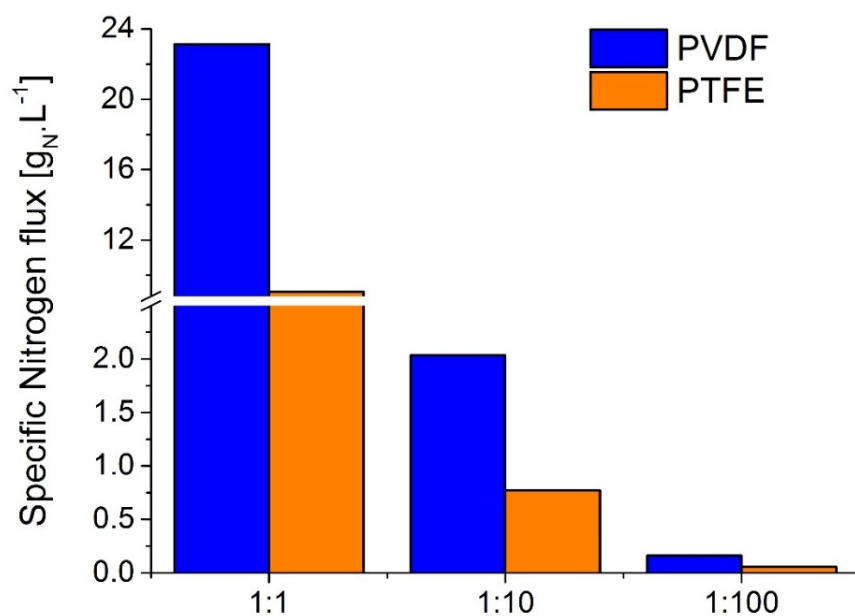


Figure 4-7 Specific nitrogen flux from the urine solution ( $T = 60\text{ }^{\circ}\text{C}$ ,  $\text{pH} = 8.87$ ) to the de-ionised water permeate ( $T = 20\text{ }^{\circ}\text{C}$ ) using PVDF or PTFE MD membranes. The feed solution consists of stored urine with a dilution factor of 1:1, 1:10 and 1:100.

## 4.5 Conclusions

In this work, FO was used as a pre-treatment to MD to concentrate FU and HU and produce distilled water. With 2.5 M NaCl as DS commercial FO membranes achieved a water flux of 31.5 (FU) – 28.7 (HU)  $\text{L.m}^{-2}.\text{h}^{-1}$ , a  $\text{NH}_4^+$  flux of  $0.1 \text{ gNH}_4^+.\text{m}^{-2}.\text{h}^{-1}$ , and TAN flux of  $1.8 \text{ gNH}_3.\text{m}^{-2}.\text{h}^{-1}$  and an urea flux of  $2.9 \text{ gUrea.m}^{-2}.\text{h}^{-1}$ . Additionally, the application of moderate back pressure on the DS was able to reduce the nitrogen flux by up to 30%. This is expected to be due to the convective flux from the DS to the FS that drives the  $\text{NH}_4^+/\text{NH}_3$ /urea solutes away from the membrane. However, this led also to a decrease in the water flux. Further investigation should be done to assess the impact of high back pressure on the membrane stability, especially on the possibility of active layer delamination. During the recovery of the DS via MD, the use of PTFE membranes was found beneficial in reducing the nitrogen leakage to the permeate solution. The higher porosity and thickness of PTFE membranes over PVDF showed to achieve higher water flux and lower ammonia flux. In particular, the thickness of the membrane was found to be inversely proportional to the ammonia mass transfer.

Overall, the high nitrogen rejection of FO during HU filtration can significantly decrease the nitrogen leakage to the final permeate water during the MD process. This double barrier separation process could be suitable for both water reclamation on the ISS as well as for urine dewatering for nutrients mining.





## **Chapter 5: Hybrid MBR - MD to produce concentrated fertiliser and distilled water**

---

**This chapter published in the *Journal of Cleaner Production* as:**

**F. Volpin**, J. Jiang, I. E. Saliby, M. Preire, S. Lim, M.A.H. Johir, J. Cho, D. S. Han, S. Phuntsho, H. K. Shon, Sanitation and dewatering of human urine via membrane bioreactor and membrane distillation and its reuse for fertigation, *Journal of Cleaner Production*, p. 122390.

## 5.1 Summary

In this work, undiluted urine was stabilised, sanitised, and dewatered through biological oxidation, ultrafiltration and MD. The result was a fertiliser with nutrients concentrations similar to commercial liquid products. Finally, the concentrated fertiliser was used to grow leafy vegetables hydroponically. The MBR reactor was able to achieve over 95% dissolved organic carbon removal and almost 50% of TAN to  $\text{NO}_3^-$  conversion. As urine was used to buffer the pH of the reactor, adjusting the HRT was found to be an effective strategy to cope with the risk of  $\text{NO}_2^-$  accumulation caused by the high TAN loading rate. MD was able to concentrate the nitrified urine up to  $280 \text{ g.L}^{-1}$ , but severe flux decline was observed after 80% water recovery.

The use of alkaline cleaning was effective in removing the thick membrane fouling layer and fully recover the initial flux. Additionally, as low feed temperatures were used ( $55^\circ\text{C}$ ), the  $\text{pK}_a$  of  $\text{NH}_4^+$  was kept relatively high, which in turn, led to about 99% rejection of ammoniacal nitrogen. Lastly, the application of produced nutrients from urine showed promising results in growing lettuce and Pak Choi. The biomass obtained was often similar to the one from commercial fertilisers.

## 5.2 Introduction

Most of the excess nutrients that human ingest are excreted through urine, which makes it a suitable raw material for fertiliser production. As such, urine to fertiliser conversion is increasingly investigated as a means to reduce wastes, and reliance on finite mineral fertilisers. In this context, a growing number of agricultural trials were performed, showing that crops' yields significantly increased when fertilised with urine, and they were often similar in quantity to the one obtained with synthetic fertilisers (Bonvin et al. 2015; McHunu, Odindo & Muchaonyerwa 2018; Pandorf, Hochmuth & Boyer 2019; Viskari et al. 2018). The use of urine as fertiliser source has also shown to be an effective way to achieve both biomass production as well as wastewater phytoremediation (Kamyab et al. 2017; Rezania et al. 2016; Yang et al. 2015).

Besides, an upstream urine separation is also expected to benefit the downstream sewage treatment processes. As urine contributes up to 80% of the TAN in wastewater, its separation would reduce the aeration energy required for biological oxidation of ammonia to form nitrate thereby resulting in smaller, less energy-intensive and more effective wastewater treatment plant (Jacquin et al. 2018; Larsen et al. 2009; Larsen et al. 2016; Maurer, Schwegler & Larsen 2003a; Udert & Wächter 2012). Additionally, urine separation could help in reducing the pharmaceutical compounds coming with the sewage before and after its treatment and discharge (Lienert, Güdel & Escher 2007; Pronk et al. 2006).

Given that untreated urine is generally a poorly accepted fertiliser solution, the best chance to enhance its fertiliser value is to produce safe, effective and odourless fertilisers product (Mkhize et al. 2017; Okem et al. 2013; Udert & Wächter 2012). As

such, several signs of progress were made by the scientific community in developing and optimising a wide range of technologies to produce safe fertilisers from urine (Larsen, Udert & Lienert 2013; Maurer, Pronk & Larsen 2006; Randall & Naidoo 2018). Still, one major bottleneck for producing commercial fertilisers from urine is its low nutrient concentration (i.e., 10-1000 times lower depending on the dilution factor) compared to the commercial liquid fertiliser (Maurer, Pronk & Larsen 2006). Therefore, much attention was put on selectively extracting single elements (i.e., N, P and K) from urine, or on recovering all the ions by stabilising and concentrating urine directly. When focusing on the recovery of single ions, adsorption, electrochemical ammonia stripping and struvite precipitation have been the most widely investigated approaches (Etter et al. 2011; Tarpeh et al. 2018; Tarpeh, Udert & Nelson 2017). Even though these approaches were successful in the recovery of P as struvite or N as  $(\text{NH}_4)_2\text{SO}_4$  or  $\text{NH}_4\text{HCO}_3$ , each process recovers mainly one single ion, neglecting all the others (Jermakka et al. 2018). While this can be useful for some applications, complete urine re-use would mean no discharge of waste by-products, a higher degree of nutrients recovery and above all, environmentally more sustainable.

In this context, (Udert & Wächter 2012) proposed a combination of biological urine oxidation to reduce organics and pH, followed by thermal distillation to produce a stable, highly concentrated fertiliser solution with only distilled water as a by-product. In the first stage of the process, a sequence batch reactor was used to achieve partial  $\text{NH}_3/\text{NH}_4^+$  conversion to  $\text{NO}_3^-$  and removal of malodorous organics. During nitrification, the alkalinity in the urine was also consumed, causing a reduction in pH from about 9.2 (typical pH of hydrolysed urine) to 5.5 - 6.5. The pH of the reactor was maintained by adjusting the HRT as feeding raw urine increased the pH while nitrification reduced it. In the second stage, the stabilised and acidified urine was

thermally evaporated to remove water and increase its dissolved solids concentration. (Fumasoli et al. 2016) later investigated the effect of pH set-point in the nitrification performance and biomass selection, pathogen inactivation performance and mechanisms (Bischel, Schertenleib, et al. 2015) and operational costs of the system. Recently, other groups have looked at the use of an MBR followed by electrodialysis (De Paepe et al. 2018) or by microalgae cultivation (Coppens et al. 2016) to achieve full nutrients recovery. However, only the nitrification – distillation process is currently operated in a semi-large scale, by the company VUNA GmbH, and the urine fertiliser commercialised under the trademark of “Aurin”(Etter 2019). Aurin production is a clear demonstration of the real potential of urine separation and re-use.

Nonetheless, the high energy required to operate such system i.e.,  $107 \pm 31 \text{ Wh.L}^{-1}$  for distillation and  $35 \pm 24 \text{ W}\cdot\text{g N}^{-1}$  for nitrification reduces the net revenue from the sale of the fertiliser product, thereby hindering the expansion of such system (Fumasoli et al. 2016). As up to 82% of the energy demand to run the process is due to the mechanical vapour compression distillation unit, this work aimed at investigating the potential use of a lower temperature thermal process to concentrate the nitrified urine. Direct contact membrane distillation was chosen as an alternative to mechanical vapour compression as it can operate at temperatures of 50-70 °C, and this thermal requirement could be met by either solar or waste heat integration (Al-Obaidani et al. 2008). However, to match the current system, DCMD should be able to dewater urine to over  $250 \text{ mS.cm}^{-1}$  of electric conductivity which, in turn, means DOC concentrations up to  $1000 \text{ mg.L}^{-1}$ . These conditions imply a high risk of severe organic fouling and inorganic scaling on the porous hydrophobic membrane (Naidu et al. 2017). As such, for the first time, an in-depth investigation of the nature and reversibility of MD fouling, after a nitrified urine concentration factor of 20 was

reached. Additionally, the effectiveness of the produced N-P-K fertiliser was tested in growing lettuce and Pak Choi.

### 5.3 Experimental Investigation

A UF - MBR reactor was operated using real, undiluted urine collected from the male's urinals at the University of Technology Sydney (UTS) (see 0 for the urine sampling strategy), and its permeate was dewatered using MD. UF-MBR was chosen over the sequence batch reactor to have an improved quality of the stabilised urine as UF can reject bacteria and viruses (that would not be killed in the MD process due to the low operating temperatures). MD permeate flux, maximum urine concentration factor, nutrients rejection rates, membrane fouling and cleaning requirements were all measured in the study. Figure 5-1 shows the schematic drawing of the process.

Finally, the concentrated fertiliser was used to grow lettuce (*Lactuca Sativa L.*) and Pak Choi (*Brassica Chinensis*) in a vertical garden. These plants were selected for their adaptability to hydroponic systems, short life-cycle and extensive data on their cultivation under different conditions and scenarios (Chekli et al. 2017; Yang et al. 2015). The biomass weight produced using urine fertiliser was benchmarked with the biomass from a commercial nutrient's solution and a standard formulation as a control.

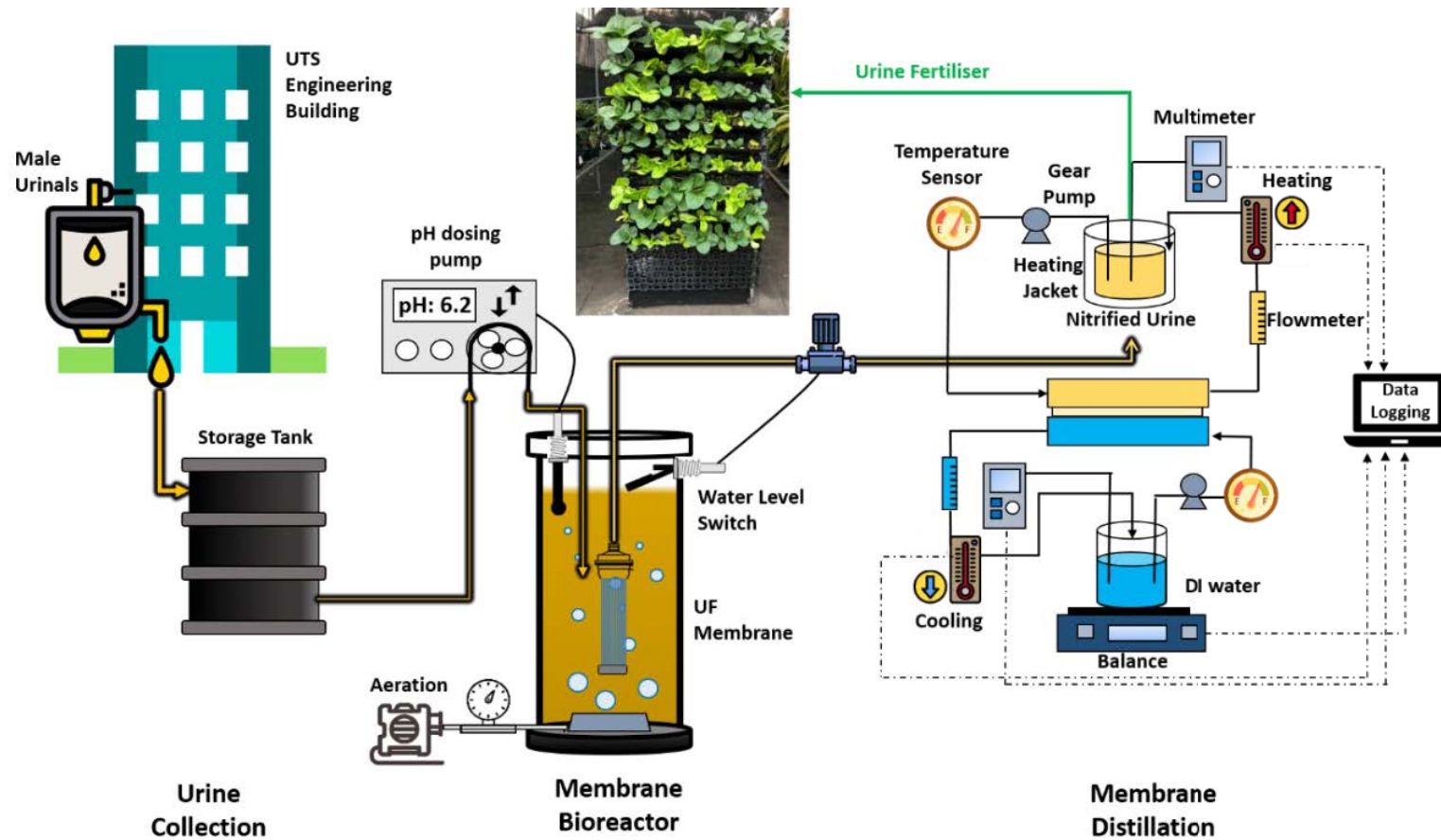


Figure 5-1 Schematic diagram showing the collection, nitrification via MBR, dewatering via DCMD and testing of urine fertiliser on a vertical garden.



### 5.3.1 Nitrification membrane bioreactor start-up and operation

A 5 L MBR was employed for the biological oxidation of urine as presented in Figure 5-1. Braided PVDF hollow fibre membrane modules from Lotte Chemical (Daejeon, Republic of Korea) were potted, in house, with an active filtration area of 0.042 m<sup>2</sup>. The nominal pore diameter of the membrane was 0.03 µm with an inner and outer diameter of 0.8 cm and 2.1 cm, respectively. The compressed air (0.2 m<sup>3</sup>/h) was supplied through an air diffuser to provide fine bubble aeration. The aeration served to guarantee levels of O<sub>2</sub> always higher than 6 mgO<sub>2</sub>.L<sup>-1</sup>, full reactor mixing and membrane air scrubbing. As the pH in the reactor decreases, due to the consumption of alkalinity during the oxidation of TAN to NO<sub>3</sub><sup>-</sup>, raw urine was pumped to bring back the pH to the desired set-point. A dosing pump (BL7916-1, Hanna Instruments, Australia) connected to a pH meter (HI6100405, Hanna, Australia) was used to regulate the reactor's pH.

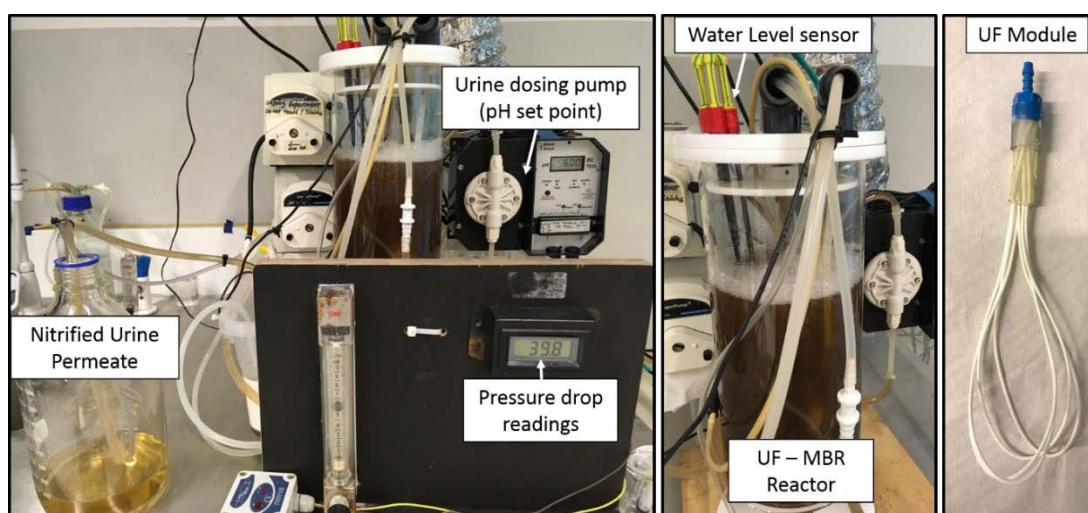


Figure 5-2 Picture of the membrane bioreactor unit used to nitrify real human urine.

Given that urea hydrolyses giving 1 mol of  $\text{HCO}_3^-$  and 2 mol of ammonia, without additional alkalinity, the maximum theoretical ammonia to  $\text{NO}_3^-$  conversion rate in urine is 50% (Udert & Wächter 2012). A water level switch was used to activate a peristaltic pump, (Longer BT100 2 J) connected to the UF membrane, to pump the treated urine out of the reactor. Also, a high resolution ( $\pm 0.1$  kPa) pressure sensor (Keller, Reinacherstrasse, Basel, Switzerland) was installed to monitor the TMP, ensuring a sub-critical flux operation to avoid fouling of the UF module. Given the high fouling potential of urine (Jacquin et al. 2018), the UF module was operated at a flux of about  $0.5 \text{ L.m}^{-2}.\text{h}^{-1}$  which led to low TMP development ( $3.2 \pm 2.3$  kPa) which is not an optimised operational flux. The MLSS of the reactor was measured weekly and maintained to approximately  $5 \pm 1 \text{ g.L}^{-1}$  that allowed to keep the MLSS/MLVSS ratio above 0.85. About 10 mL of sludge was discarded daily to do so (i.e., solid retention time of  $\sim 500$  d). HRT changed depending on the ammonia concentration and pH set-point. During stable operations, at pH of 6.2, the measured HRT was  $14 \pm 5 \text{ d}^1$ . Finally, the UF-MBR permeate was collected in a 2 L glass bottle and stored at  $4^\circ\text{C}$  in a 20 L canister ready to be used for the MD tests.

### 5.3.2 Membrane distillation set-up and operation

DCMD configuration was chosen due to its higher flux compared to vacuum or air gap MD and ease of set up (Lee et al. 2017). In each experiment, 3 L of urine collected from MBR (MBR effluent) and 1 L of DI water were recirculated, in counter-current flow mode, inside the acrylic membrane cell. The acrylic membrane cell used had two symmetric channels, each with 7.7 cm length, 2.6 cm width and 0.3 cm depth, allowing for an active membrane area of  $0.002 \text{ m}^2$ . Durapore®-GVHP PVDF flat sheet membranes were used for the experiments. Their nominal pore size is  $0.22 \mu\text{m}$ , thickness of  $125 \mu\text{m}$ , a contact angle of  $131 \pm 1^\circ$  and active layer porosity of 75%. The

dense layer of the membrane always faced the feed solution. A heating jacket, connected to a heater, was used to maintain the urine temperature at 55 °C while a heat exchanger, connected to a chilling unit, was used to keep the DI water temperature at 20 °C. A moderate feed temperature was chosen to minimise organic fouling and shift the  $\text{NH}_3$  (g) /  $\text{NH}_4^+$  (l) equilibrium towards the latter (Bates & Pinching 1950; Naidu et al. 2017; Naidu et al. 2014). Before starting the experiments, feed and permeate were recirculated, bypassing the membrane cell, for about 30 min to reach the targeted temperature. After that, the cross-flow velocity used to flow the solutions inside the membrane cell was of 8.5 cm.s<sup>-1</sup>. All the experiments were then run upon reaching 95% water recovery. Finally, as real nitrified urine contains HCl (even if in low concentrations), only acid resistance plastic tubing and fittings were used for the experiments to prevent any corrosion (Etter & Udert March 2016).

### 5.3.3 Membrane performance evaluation and cleaning

The performance of the MD process was measured in terms of water flux and solute transport. The flux was calculated based on the step increase in the permeate weight over time. This was recorded with the aid of a balance connected to a computer for continuous data logging. Permeate conductivity and pH were also continuously recorded as they are considered useful parameters to assess the TAN transport (measured by the pH increase) and membrane wetting (sharp permeate conductivity increase). Additionally, permeate samples were taken at a regular interval to measure for the anion/cation, TAN and DOC rejection. The rejection was calculated based on Eq. (5-1 below displayed). Where  $C_{p,f}$  and  $V_{p,f}$  are the concentration of the targeted compound in the final permeate, and the final permeate volume respectively. Similarly, the concentration and volume in of the initial feed are expressed by the variables  $C_{f,i}$  and  $V_{f,i}$ .

$$R [\%] = 1 - \frac{(C_{p,f} \cdot V_{p,f})}{(C_{f,i} \cdot V_{f,i})} \cdot 100 \quad (5-1)$$

Membrane fouling reversibility was evaluated by inspecting the performance and morphology of the membrane before and after the cleaning. First, a membrane coupon was used to concentrate urine over 95% (i.e., EC > 250 mS.cm<sup>-1</sup>). The coupon was then cut in three pieces, each cleaned with a different solution: (I) DI water, (II) 0.1 M citric acid or (III) 0.1 M NaOH. Cleaning was done by placing the coupon in a beaker, filled with the cleaning solution and agitated on an orbital shaker. After four hours, the membrane was extracted, washed with DI water and dried. After drying, the coupon was soaked in ethanol, frozen with liquid nitrogen and cut with a sharp blade. The resulting cross-sections were analysed using an SEM. Based on the visual inspection of the cleaned membranes, NaOH showed the highest degree of “brown layer” removal. However, to assess the effectiveness of NaOH in restoring the initial flux, the repeated cycles of MD operation and cleaning were performed while keeping the same membrane.

#### 5.3.4 Analytical measurements

Anions (NO<sub>3</sub><sup>-</sup>, NO<sub>2</sub><sup>-</sup>, PO<sub>4</sub><sup>3-</sup>, SO<sub>4</sub><sup>2-</sup>, Cl<sup>-</sup>), cations (Na<sup>+</sup>, K<sup>+</sup>, Mg<sup>2+</sup>, Ca<sup>2+</sup>), TAN and organics were measured as described in the Methodology Section (0). Given the high nitrogen, sodium and potassium concentration in the urine, prior to the analysis, the samples had to be diluted 50 times.

#### 5.3.5 GSky Versa Wall and plant response assessment

The GSky Versa Wall (TPR Group, Sydney, Australia) system was chosen, among others, due to its flexibility, versatility and wide application in vertical gardens. The experiment was carried out from 23-04-2019 to 13-06-2019 at the Royal Botanical

Garden Sydney Nursery on a west-facing outdoor GSKy Vertical Wall module, covered with a twin-wall polycarbonate sheet to minimise the effect of rainfall on nutrient solutions. Lettuce ‘All Year Round’ (*Lactuca sativa*, Mr Fothergill’s seeds, Australia) and Pak Choi ‘Hei Xia F1’ (*Brassica rapa* Var. *chinensis*, Johnsons-Seeds, Australia) were germinated in different growing media, grown in a controlled temperature (18-27 °C) glasshouse for about three weeks and fed with the respective nutrient solutions before being transferred to the wall. Climatic data were recorded, and they could be summarised by a minimum temperature of  $11 \pm 3$  °C, a maximum of  $26 \pm 4$  °C and a 9 am humidity of  $67 \pm 9\%$ .

Urine fertiliser performance as nutrient solution 1 (Us) was benchmarked with a commercial hydroponic solution (Optimum Grow twin pack hydroponic nutrient, Growth Technology, Australia) as nutrient solution 2 (Cs) and a control hydroponic solution tailored for lettuce and Pak Choi (i.e., Half-strength Hoagland’s solution) as nutrient solution 3 (Hs). The composition of Optimum Grow and Half-strength Hoagland’s solutions can be found elsewhere (Chekli et al. 2017). Three different growing media were used for the experiments. The growing media used were (i) a 44 mm peat moss cylindrical media (Jiffy-7®, Garden City Plastics, Australia) as potting media 1 (PM1), (ii) a 50 mm coir cubic media (Jiffy® Coir Grow Block, Garden City Plastics, Australia) as potting media 2 (PM2) and (iii) a Vermiculite fine grade (Ausperl, Australia) / Perlite P400 (Ausperl, Australia) / Orchiata Pine bark 6-9 mm (Garden City Plastics, Australia) (ratio 1/1/1) filled in a 105 mm MIDI pot (Garden City Plastics, Australia) (Figure 5-3) as potting media 3 (PM3). In each of the three nutrient solutions treatments, lettuce and Pak Choi were grown in different media (PM1, PM2 and PM3) and randomly placed in the trays. Individual plants were placed on the wall with a density of 56 plants per square meter and fed with nutrient solutions

delivered to the top tray of plants. The three nutrient solutions' treatments consisted of three trays (rows) of eight plants each. Nutrient solutions were pumped (AquaPro Submersible pump, AP1050) from a 10 L container through a 13 mm low-density polyethylene pipe fitted with pressure compensating drippers that delivered 30 L.h<sup>-1</sup> of nutrient solution to each treatment. Nutrient solutions drained by gravity from the top tray to the lower trays through a 19 mm drainage hole and through a drainage pipe back to the nutrient solution containers which was placed below the bottom tray of each treatment. The recirculation allows for the solution to have enough dissolved oxygen (Chekli et al. 2017).

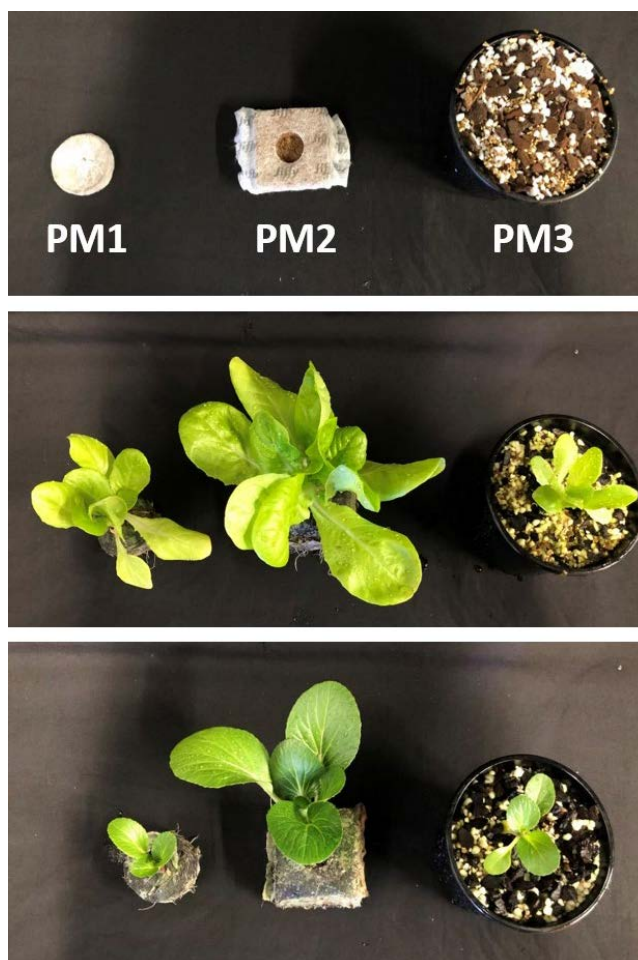


Figure 5-3 potting mix used for the hydroponic experiments. PM1 is a cylindrical media made of special mix material mainly composed of Peatmoss, PM2 is a cubic

media made of Cocopeat and PM3 is a vermiculite fine grade/Perlite P400/Orchiata Pine bark 6-9 mm (ratio 1/1/1) filled in a 105 mm MIDI pot.

Overall, each combination of nutrient solution-substrate-plant was grown in triplicate, meaning that 81 plants were grown in total (Figure 5-12). Each nutrient solution was diluted with deionised water to achieve a nitrogen concentration of about  $110 \text{ mg-N.L}^{-1}$  (~500 times concentrate urine dilution), and their final elemental composition is displayed in Table 5-3. Finally, the diluted solutions were replenished every week based on the water level and EC, while the pH was adjusted using KOH or  $\text{H}_3\text{PO}_4$  to keep it at  $6.1 \pm 0.2$  (TPS -Aqua CPA, V6819).

#### 5.3.6 Data collection and analysis of growth performance

At the end of the experiment, roots and shoots of each plant were separated to assess fresh biomass. Fresh weight (FW) of samples was recorded using an EJ Series scale (AND, EJ-610, A&D Co LTD, Korea). Leaves and roots samples were also placed in paper bags in a Memmert GmbH oven (Model 400, Germany) at  $60^\circ\text{C}$  for 72 h (Chekli et al. 2017; Li, Li, et al. 2018) and then weighted again (DW) to measure the dry biomass. Finally, roots to shoots ratio (RSR) was also calculated as the ratio between roots dry weight and shoots dry weight.

## 5.4 Results and Discussion

### 5.4.1 Nitrification bioreactor

The MBR reactor was started in October 2018. The seed sludge was collected from a wastewater treatment plant (Central Park Sydney, Ultimo, NSW, Australia) and, for the first 20 weeks of operation, the sludge was gradually acclimatised to the new substrate. As the salinity, C/N ratio and pH of urine differed significantly from municipal wastewater, urine was initially diluted 100 times and the pH corrected to 7 by addition of HCl (Fumasoli et al. 2016; Jacquin et al. 2018; Udert & Wächter 2012). Following the increase in the abundance and activity of ammonia and nitrite oxidising bacteria (AOBs and NOBs), estimated through the amount of  $\text{NO}_3^-$  produced per gram of MLSS, urine dilution was gradually decreased. Once 4 times urine dilution was reached, automatic urine dosing to the bioreactor was introduced. In this mode of operation, the high alkalinity of raw urine was enough to keep in check the pH of the reactor. To reduce the risk of  $\text{NO}_2^-$  accumulation, the pH set-point was set between 5.8 and 6.6 (Fumasoli et al. 2017). High throughput operation was achieved by increasing the pH set-point to 6.4 – 6.6, thereby reducing the HRT of the system. That is because as the bioreactor pH approaches neutral the nitrification rate increases, which causes higher alkalinity consumption and, therefore, faster urine dosage to buffer the pH drop (Udert & Wächter 2012). However, higher urine dosage is associated with higher TAN loading rate which can then result in a higher  $\text{NO}_2^-$  accumulation rate due to an imbalance between AOB and NOB, in favour of the AOB (Fumasoli et al. 2017; Fumasoli et al. 2016). When the AOB population outnumbers the NOB, the excess  $\text{NO}_2^-$  produced by the AOB would inevitably accumulate in the bioreactor which over time further inhibits the NOB activity (Fumasoli et al. 2016; Udert & Wächter 2012). Conversely, operating at lower pH range (pH 5.8 – 6.2) minimised the risk of  $\text{NO}_2^-$



accumulation but at the expense of the HRT. (Fumasoli et al. 2017) also showed that, at low pH, (i.e., lower than 5.4), acid-tolerant  $\gamma$ -proteobacterial AOB accumulates while the microbial community responsible for high-rate nitrification reduction which possibly causes the emission of hazardous NO compounds.

#### 5.4.2 Nitrite accumulation events

Two nitrite accumulation events occurred during the reactor operations. The first  $\text{NO}_2^-$  accumulation event ( $\text{NO}_2^- \text{-N} > 100 \text{ mg.L}^{-1}$  in the MBR permeate) happened when urine dilution was reduced from 4 to 2 (i.e. TAN increased from 800 to 1600  $\text{mg.L}^{-1}$ ). Here, a failure in the pH regulation system caused the pH to increase to 7.5-8 for over 24 h. Feeding was then interrupted to allow for the conversion of the  $\text{NO}_2^-$  in the bioreactor system to  $\text{NO}_3^-$ , and the pH was corrected using HCl. For the following 6 weeks, the reactor was operated at high HRT of  $35 \pm 5$  days and a pH of  $6.1 \pm 0.1$ . During this period, the  $\text{NO}_2^-$  concentrations were still higher than 20  $\text{mg-N.L}^{-1}$  but slowly decreased to less than 1  $\text{mg-N.L}^{-1}$ . The second  $\text{NO}_2^-$  accumulation event, visible in Figure 5-4 (B), happened when operating the bioreactor with undiluted urine. In this case, the reactor was re-stabilised in about three weeks only by pH set-point adjustment. Although, both the DOC removal and  $\text{NH}_4^+$  to  $\text{NO}_3^-$  conversion rate dropped during this event, the DOC reduction always remained above 85% (Figure 5-4 (A)).

In the last 8 weeks of stable operation, only minimal pH set-point adjustments had to be made and an average HRT of  $20 \pm 3$  days was reached with an ammonia conversion rate of  $65.2 \pm 21.5 \text{ mg-N.L}^{-1}.\text{d}^{-1}$ . Overall, an average DOC removal rate of 95% and 50%  $\text{NH}_4^+$  to  $\text{NO}_3^-$  conversion rate (which is the theoretical maximum conversion

indicated by urine alkalinity) was achieved. Table 5-1 also shows that the essential plant macronutrients (i.e., N, P and K) were all preserved in the final permeate.

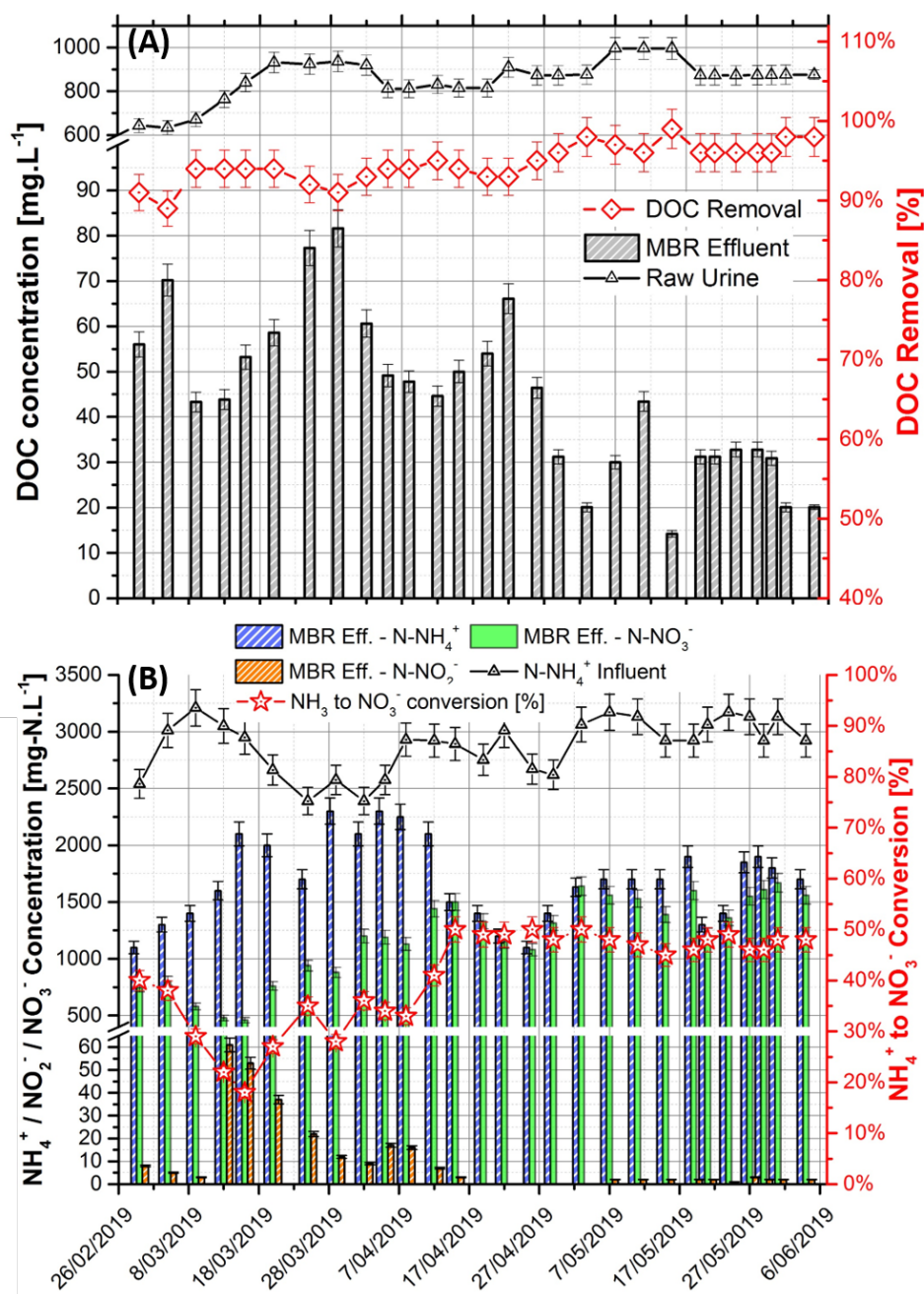


Figure 5-4 Performance of the MBR when using raw undiluted urine as feed. The top graph (A) shows the removal of DOC while the bottom (B) the conversion of NH<sub>3</sub> to NO<sub>2</sub><sup>-</sup> and NO<sub>3</sub><sup>-</sup>. The operating pH was 6.2 ± 0.2.

Table 5-1 Characteristics and composition of urine before and after MBR and MD.

		Raw untreated urine	Urine after MBR	Concentrated urine	MD Permeate*
EC	[mS.cm <sup>-1</sup> ]	32 ± 5	39 ± 10.5	> 250	0.16 ± 0.1
pH	[-]	9.1 ± 1	6.1 ± 3	4.5 ± 2	9.1 ± 1
DOC	[mg.L <sup>-1</sup> ]	865 ± 265	40 ± 15	920 ± 115	1.1 ± 0.1
TAN	[mg.L <sup>-1</sup> ]	3040 ± 271	1740 ± 475	31300 ± 1650	22 ± 1.1
NO <sub>3</sub> <sup>-</sup> -N	[mg.L <sup>-1</sup> ]	n.d.	1560 ± 104	29641 ± 1865	2.9 ± 0.1
NO <sub>2</sub> <sup>-</sup> -N	[mg.L <sup>-1</sup> ]	n.d.	<1	n.d.	n.d.
Cl <sup>-</sup>	[mg.L <sup>-1</sup> ]	1410 ± 71	1410 ± 71	24800 ± 740	n.d.
PO <sub>4</sub> <sup>3-</sup> -P	[mg.L <sup>-1</sup> ]	230 ± 51	247 ± 34	4770 ± 230	n.d.
SO <sub>4</sub> <sup>2-</sup>	[mg.L <sup>-1</sup> ]	780 ± 120	800 ± 58	12000 ± 320	n.d.
Na <sup>+</sup>	[mg.L <sup>-1</sup> ]	1220 ± 258	979 ± 278	19400 ± 5471	1.7 ± 0.1
K <sup>+</sup>	[mg.L <sup>-1</sup> ]	1020 ± 240	896 ± 180	17900 ± 896	2.4 ± 0.1
Mg <sup>2+</sup>	[mg.L <sup>-1</sup> ]	2 ± 5	3 ± 2	30 ± 21	n.d.
Ca <sup>2+</sup>	[mg.L <sup>-1</sup> ]	51 ± 12	31 ± 21	465 ± 23	n.d.

\* MD permeate was measured after 95% urine concentration rate. n.d. = not detected.

### 5.4.3 Organics transformation within the reactor

The fractionation of organics present in the raw urine and the MBR effluent was characterised via LC-OCD analysis. Depending on the elution time, the instrument identified four hydrophilic DOC fractions: (I) biopolymers (BPOCD), with size < 20,000 g.mol<sup>-1</sup>, (II) Humic substances and their degradation by-products (HS + BB<sub>OCD</sub>), with size between 1000 and 300 g.mol<sup>-1</sup>, (III) low molecular weight acids (LMW-AOCD) and neutrals (LMW-NOCD), having a size smaller than 350 g.mol<sup>-1</sup>. Based on mass balance, the remaining DOC was categorised as hydrophobic (Huber et al. 2011). Table 5-2 shows that urine is mainly composed of LMW organics (i.e., < 350 g.mol<sup>-1</sup>), with little HS+BB<sub>OCD</sub> and almost a negligible amount of BP<sub>OCD</sub>. A distinct signal from the OCD was detected after 75 min of raw urine elution time (Figure 5-5). This peak, attributed to LMW-A compounds, was probably due to the high concentration of organic acids such as acetic acid, uric acid, hippuric acid, glucuronic and lactic acid which have a concentration ranging from 30 to > 500 mg.L<sup>-1</sup> (Putnam 1971a). However, the LMW-A peak is restricted to monoprotic acids, diprotic or triprotic acids such as oxalic or citric acid will elute in the building block fraction due to their charge density (Huber et al. 2011). This might be the cause for the high building blocks fraction in raw urine (14%).

After the MBR the OCD signal of urine showed a higher fraction of humic-like substances and building blocks. This could be due to microbial by-products (SMP or EPS) released in the reactor as well as the aggregation of smaller organics (Jacquin et al. 2018). Organics with MW > 1000 Da were all retained by the UF membrane. (Jacquin et al. 2018) also found that the retention of DOM compounds by the membrane was essential to avoid substrate limitation, which could affect biomass stability. Overall, whatever the organic fraction, the concentrations measured in raw

urine were reduced 80-99% by the UF-MBR. Among the different fractions, the reduction of LMW-A was the highest, 99.6%, while 94.4% of the LMW-N were removed.

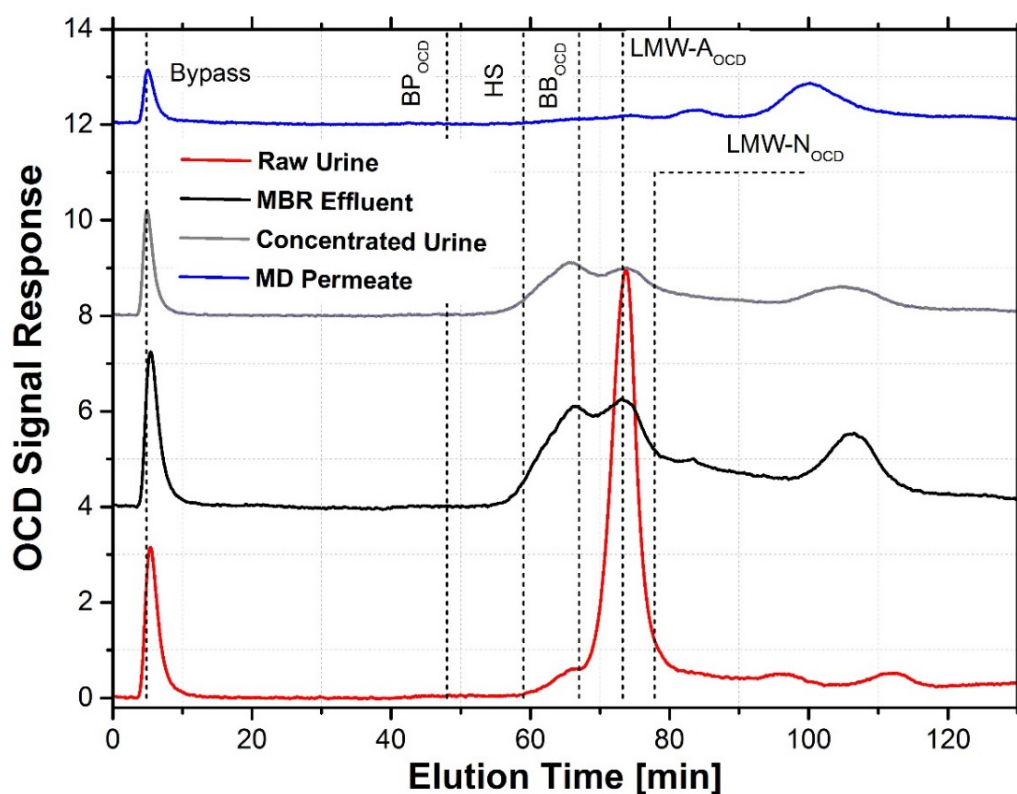


Figure 5-5 OCD signals obtained by analysing urine before and after the MBR as well as the MD concentration and permeate.

#### 5.4.4 Membrane distillation performance

In this section, the urine dewatering performance of a DCMD system was investigated. MD flux decline, permeate quality, and membrane fouling and cleaning were investigated using both synthetic and real nitrified urine. For the real urine experiments, the MBR effluent was fed to the DCMD system without any additional pre-treatment.

		Approximate molecular weights (g/mol):						
		>> 20,000	~1000	~300-500	< 350	< 350		
		DOC	Biopolymers	Humic substances	Building blocks	LMW neutrals	LMW acids	DOC Reduction
<b>Raw Urine</b>	mgC/L	987.0	7.8	26.7	138.1	360.4	453.9	
	% DOC		0.8%	2.7%	14.0%	36.5%	46.0%	
<b>Urine after MBR</b>	mgC/L	38.7	0.1	5.2	11.2	20.2	2.0	96.1%
	% DOC		0.3%	12.4%	26.5%	47.9%	4.6%	
<b>Urine after MD</b>	mgC/L	1920.5	20.1	640.1	242.5	985.4	32.4	
	% DOC		1.0%	30.4%	11.5%	46.9%	1.5%	
<b>MD Permeate</b>	mgC/L	1.13	0.01	n.q.	0.13	0.99	0.01	99.9%
	% DOC		0.4%	--	11.1%	87.8%	0.7%	

Table 5-2 LC-OCD data of raw urine, MBR permeate (during stable operation), and MD permeate. Samples from MD permeate and concentrate were collected at 95% urine concentration factor.

#### 5.4.4.1 MD Flux decline and maximum concentration factor

At a temperature difference ( $\Delta T$ ) between urine and permeate water of 35 °C, an initial water flux of about 15 L.m<sup>-2</sup>.h<sup>-1</sup> was achieved for both synthetic and real urine as MD feed. Within 120-130 h of MD operation, 4.75 L of the urine (of initial 5 L used) permeated to the cold side, thereby achieving 95% water recovery from the urine. In both cases, the EC of concentrated urine exceeded 250 mS.cm<sup>-1</sup>, which is the upper limit of the EC meter used.

Additionally, the permeate conductivity and the ions rejection values indicates that membrane wetting did not occur during the 130 h of MD operation. The initial increase in the permeate EC was due to the pervaporation of ammonia to the permeate side. As the permeate has little to no buffer capacity, the ammonia permeation caused a steep pH increase, which stabilised at 9.2 after about 5% urine concentration. The EC stabilisation after about 30% urine concentration was probably because, as pH increases, a higher fraction of NH<sub>4</sub><sup>+</sup> is changed in the form of uncharged ammonia.

It was clear that the MD flux decline was also very severe, especially after about 80% water recovery. In fact, by the end of both experiments, MD fluxes were less than 1 L.m<sup>-2</sup>.h<sup>-1</sup> (i.e., >94% flux decline). While the water flux for synthetic urine was almost constant until about 80% recovery rate after which it showed a sharp decline, the real urine induced a flux decline throughout the whole experiment, gradual at the beginning and rapidly towards the end. In both cases, the high salinity reached after 80% concentration (>150 mS.cm<sup>-1</sup>) caused a reduction in the vapour pressure, which affected the transmembrane flux (Tijing et al. 2015). Though, in the case of real urine, flux decline was also due to the high amount of organics deposited on the surface of

the membrane, and of the spacers. When approaching 90% concentration, however, inorganic scaling would also occur. Organic fouling accompanied by salt crystals was observed also by (Zhao et al. 2013). In fact, by computing the scaling tendencies of synthetic urine at a function of the concentration factor, through OLI Studio Analyser (Version 9.5, Oli Systems Inc., USA), it was found that after 80% urine concentration, compounds like  $\text{KNO}_3$ ,  $\text{K}_2\text{SO}_4$  and  $\text{NaHCO}_3$  would start to precipitate. As on the membrane interface the contractions would be higher due to concentration polarisation, scaling was even more rapid. For example, at 55° C and 90% water recovery, about 6.6% of the  $\text{KNO}_3$  is expected to be in crystal form, and its solubility would also drastically decrease at a lower temperature. The precipitation of these compounds is expected to be the reason for the sharp flux decline, for both synthetic and real urine, in the low end of the dewatering process.



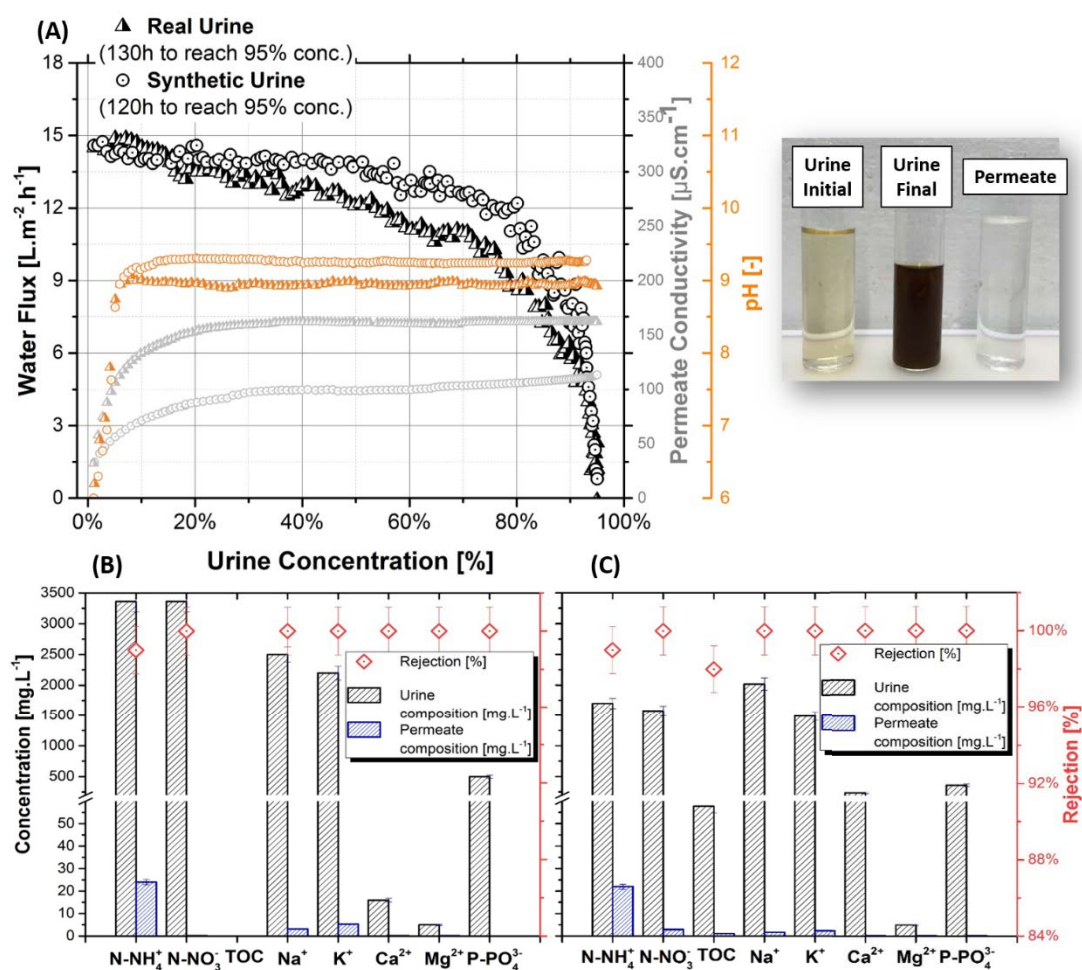


Figure 5-6 Above: Permeate flux and electric conductivity of synthetic and real nitrified urine as a function of urine concentration factor ( $T_f = 55^\circ\text{C}$ ,  $T_p = 20^\circ\text{C}$ ,  $V_{f,p} = 0.06 \text{ m} \cdot \text{s}^{-1}$ ). Below: Anions, cations and organics concentration in the urine and the final MD permeate using synthetic urine (Fig. B) and real urine (Fig. C). Relative rejection is plotted in red.

#### 5.4.4.2 Quality of MD permeate and concentrate

Although the presence of ammonical nitrogen in the permeate water from MD is not an issue for water reuse such as toilet flushing or irrigation, in the latter might even be desirable, curtailing the ammoniacal nitrogen transport out of the urine would allow for higher nutrients recovery. As the acid dissociation constant of ammonia ( $\text{pK}_a$  of

ammonia) is temperature-dependent, it decreases at higher temperatures (Bates & Pinching 1950). As such, at higher urine temperatures, the equilibrium  $H_2O + NH_3(gas) \xrightleftharpoons{pK_a} OH^- + NH_4^+(liquid)$  was dominated by the reverse reaction, causing more volatile ammonia gas to vaporise and become part of the permeate (Figure 5-7 (B)). By operating at lower temperatures (55 °C) compared to conventional mechanical vapour compression distillation (MVC) (70-100 °C) and low pH (6.2), less than 2% of the ammonia was, theoretically, in the form of volatile ammonia. This explains why only 1.4% of the initial ammoniacal nitrogen was lost in the process. Figure 5-6 (B) and (C) also showed that all the other ions ( $NO_3^-$ ,  $Na^+$ ,  $K^+$ ,  $Ca^{2+}$ ,  $Mg^{2+}$ ,  $PO_4^{3-}$ ) were entirely rejected by both MD, which confirms that membrane wetting did not occur as noted by Naidu et al. (2017). Finally, Table 5-1 shows that the ions concentration in concentrated urine is proportional to the ions in diluted urine, meaning that the nutrients were all well retained in the process. The decrease observed in the urine from 6.2 to 4.5 following MD is likely to be due to the removal of alkali ammonia in the process. As commercial fertilisers are generally acidic, this is not expected to be an issue when it comes to the use of urine fertiliser.

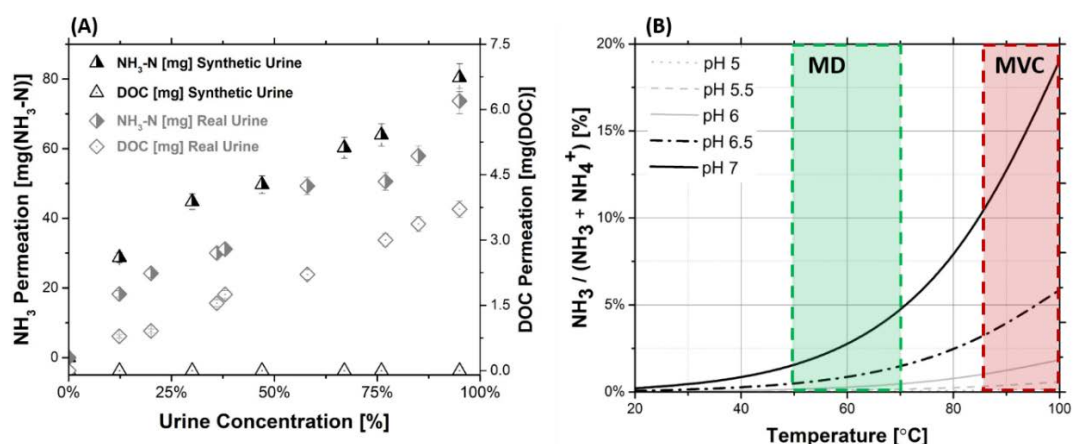


Figure 5-7 (A) Amount of ammoniacal nitrogen and DOC transported to the permeate side from real and synthetic urine using membrane distillation. (B) Theoretical fractionation of ammoniacal nitrogen into NH<sub>3</sub> and NH<sub>4</sub><sup>+</sup> based on the pH and temperature. The pKa coefficient at different temperature was obtained using OLI Studio Analyser (Version 9.5, Oli Systems Inc., USA) and from the literature (Bates & Pinching 1950).

#### 5.4.4.3 Organics rejection

Table 5-2 and Figure 5-5 show that the vast majority (87.8%) of the organics in the MD permeate were LMW-N. This was expected as between the different organic fractions, LMW-N had the highest concentration, followed by BB and humic-like substances. However, as volatility is generally inversely proportional to the MW, LMW-N is most likely to move to the gas phase and permeate through the membrane. This is expected to be the leading cause for the visible fouling layer that persists on the membrane even after DI-water flush (Figure 5-8 and Figure 5-9). Naidu et al. (2014) demonstrated that LMW humics could penetrate the membrane pores causing severe membrane fouling in a DCMD operation. As the large majority of organics in the nitrified urine are LMW-N, they are probably the cause for the severe membrane

pore blockage. Overall, the organic fraction that permeated through the membrane was less than 2%, which explains why the OCD signal of concentrated urine in Figure 5-5 shows peaks very similar to diluted nitrified urine.

#### 5.4.4.4 Membrane cleaning and flux recovery

Fouling reversibility tests were conducted by comparing two successive MD operation cycles of real urine concentration each time up to 95%, followed by DI water (control) or 0.1 M NaOH cleaning before using the same membrane for the next cycle. NaOH was chosen as the pore blocking foulants described in the previous section are expected to be LMW organics (Srisurichan, Jiraratananon & Fane 2005; Tijing et al. 2015). Our previous studies on urine concentration using hydrophilic membranes also showed that NaOH could entirely remove the organic fouling layer (Volpin, Heo, et al. 2019). As Figure 5-9 and Figure 5-8 clearly show that the membrane was still fouled after DI water cleaning and citric acid cleaning. As such, the cyclic flux recovery tests were conducted only after NaOH cleaning.

The SEM cross-section of the membrane before and after alkaline cleaning showed that the fouling deposits indicated by rough and irregular surface profile on the membrane seem to have been eliminated (Figure 5-9 (C and D)). This can also be visually confirmed through naked eyes observation of the membrane before and after cleaning. Also, similar MD permeate flux pattern was observed for the two subsequent cycles of operation, thereby demonstrating the effectiveness of NaOH cleaning strategy.

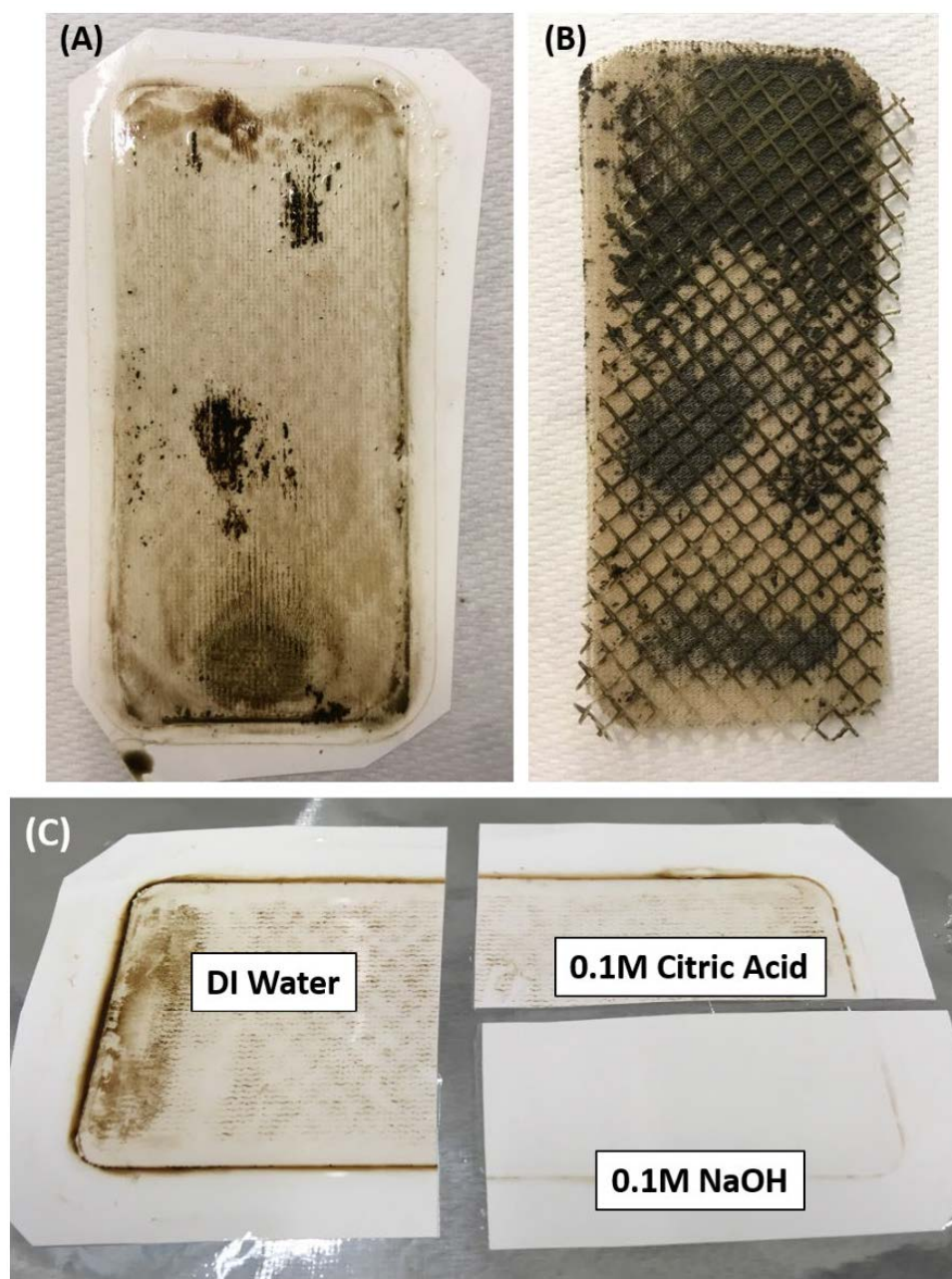


Figure 5-8 Pictures A and B show the MD membrane (B) and spacers (C) after reaching 95% real urine concentration. Picture C shows the membrane after cleaning with DI water, citric acid and sodium hydroxide.

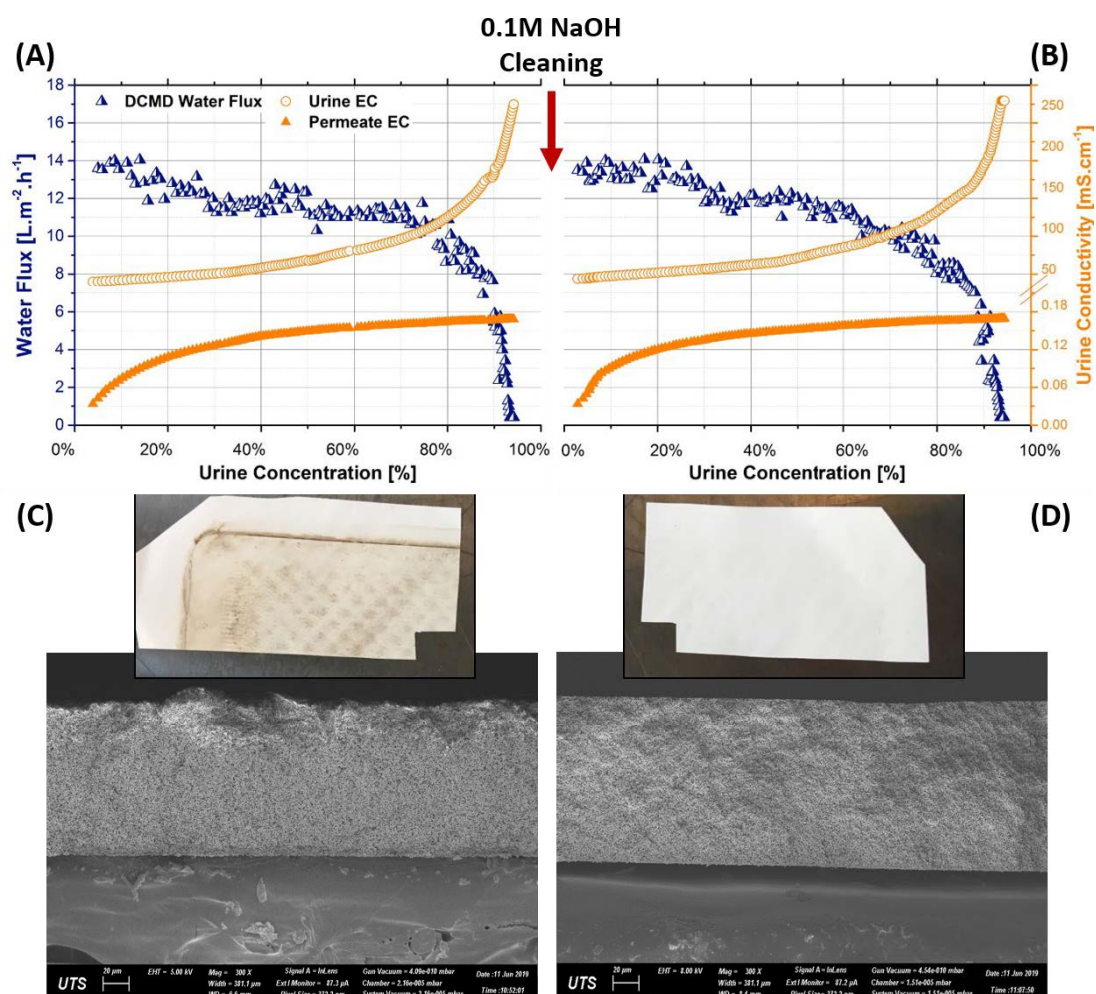


Figure 5-9 Above: MD permeate flux, feed and permeate conductivity for two repeated cycles (A and B) of real urine concentration, with 0.1 M NaOH cleaning procedure. Below: SEM images of the MD used for real urine concentration, after DI-water flushing (C) and after alkaline with 0.1 M of NaOH (D).



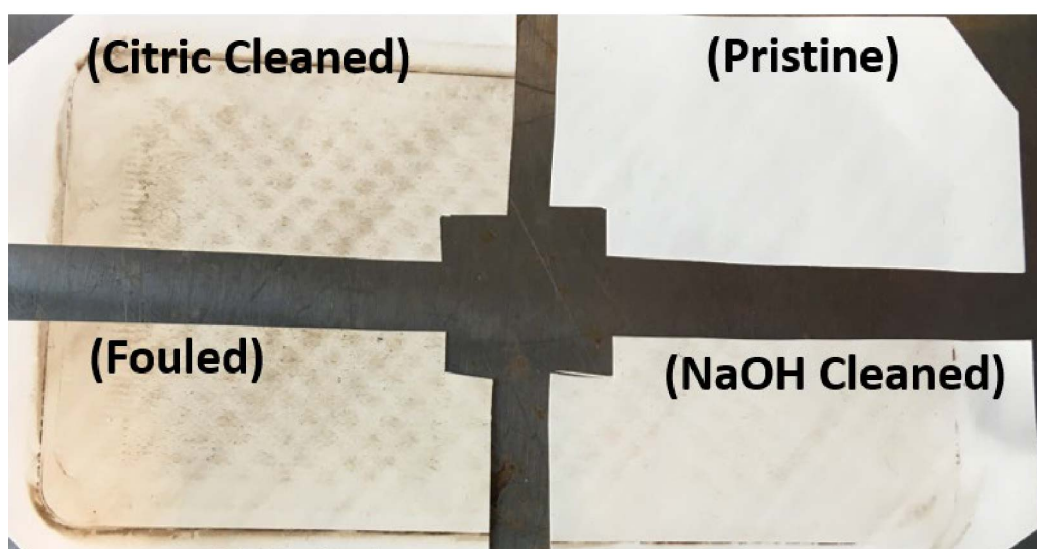


Figure 5-10 Picture of the pristine membrane and the fouled membrane before and after NaOH and Citric Acid cleaning.

### 5.5 Lettuce and Pak Choi plants growth

The concentrated nitrified urine product (95% of the water removed or concentrated 20 times) obtained from a combined MBR-MD process was compared with the half-strength Hoagland solution and Optimum Grow (commercial hydroponic nutrient solution) for growing lettuce and Pak Choi in a vertical garden module at the Sydney Royal Botanical Garden (Figure 5-12). The concentrated urine and the Optimum Grow solutions were diluted to reach  $110 \text{ mg-N.L}^{-1}$  and matching the nitrogen in the half-strength Hoagland solution. At this dilution, the diluted urine solution was found to have about 4 to 7 times less phosphorous, 4 to 5 times less potassium and over 100 times less calcium and magnesium compared to the other two commercial fertiliser solutions (Table 5-3).

Table 5-3 Concentration of the elements in the nutrient solutions before and after dilution.

	Treatment 1		Treatment 2		Treatment 3	
	<b>Half-strength Hoagland solution</b>		<b>Urine fertiliser UTS</b>		<b>Optimum Grow</b>	
Element (g/L)	Concentrate	Feed solution	Concentrate	Feed solution	Concentrate	Feed solution
<b>N</b>	22.75	0.11375	50	0.11	43.1	0.10775
<b>P</b>	6.56	0.0328	2.1	0.00462	8	0.02
<b>K</b>	27.81	0.13905	15	0.033	60.1	0.15025
<b>Ca</b>	22.32	0.1116	0.4	0.00088	36	0.09
<b>Mg</b>	2.44	0.0122	0.04	0.000088	10	0.025
<b>S</b>	3.223	0.016115	1.6	0.00352	13.2	0.033
<b>Fe</b>	0.77	0.00385	0.0005	0.0000011	0.44	0.0011
<b>Cu</b>	0.0013	0.0000065	0.0003	0.00000066	0.03	0.000075
<b>Zn</b>	0.0045	0.0000225	0.015	0.000033	0.04	0.0001
<b>B</b>	0.005	0.000025	0.016	0.0000352	0.06	0.00015
<b>Mn</b>	0.048	0.00024	0.096	0.0002112	0.18	0.00045
<b>Mo</b>	0.001	0.000005	0.002	0.0000044	0.01	0.000025

This is due to the exceptionally high concentration of nitrogen in the urine compared to other elements. The nitrogen concentration was used as a benchmark for dilution because higher nitrogen concentrations are detrimental to plants as it can cause foliage dehydration and burn (Broadley et al. 2003). Because of the high dilution required for



the urine to lower the nitrogen concentration, the EC of the diluted urine is also 3 to 4 times lower compared to the others (i.e.,  $336 \pm 20$  vs  $1055 \pm 79 \text{ mS.cm}^{-1}$ ) (Figure 5-11).

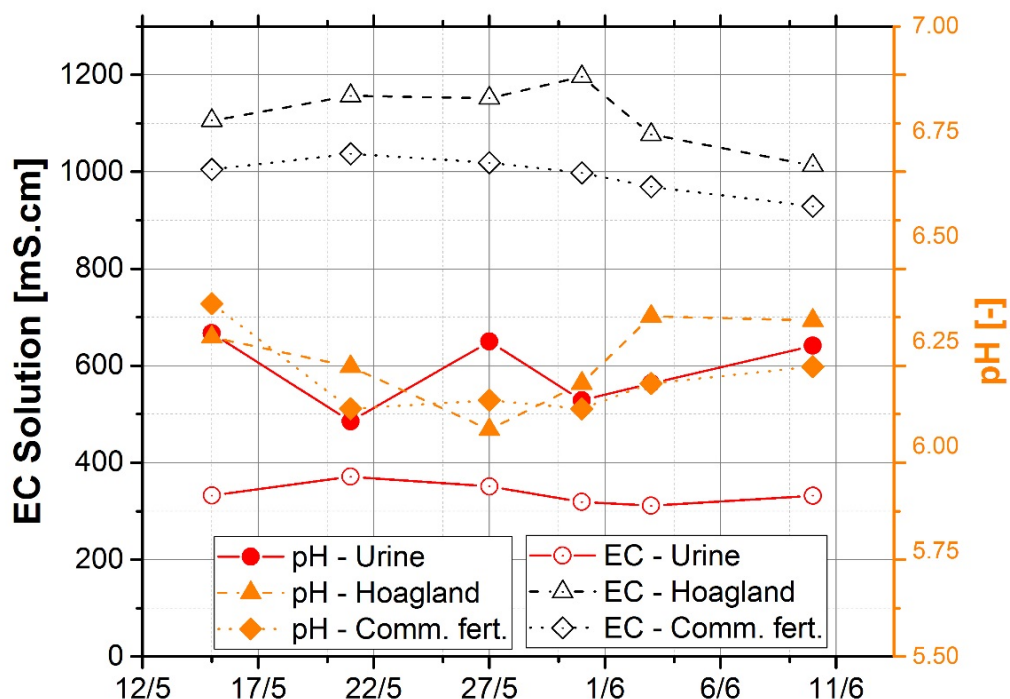


Figure 5-11 Electrical conductivity and pH of the fertiliser solutions during part of the growing experiment.

However, this could be an advantage for the farmers using urine fertiliser with lower salt-index, as farmers must meet strict EC discharge guidelines to prevent environmental pollution.

When all the solutions were used as fertiliser, similar growth values were obtained using the three different potting mixes (Figure 5-13 and Figure 5-14). Specifically, Figure 5-13 shows that the Pak Choi roots and aerial parts biomass results obtained with urine fertiliser were statistically the same as ones obtained with commercial fertiliser and the half-strength Hoagland solution. The Pak Choi fresh aerial parts yield

obtained using just urine was 41.7 g ( $\pm$  13.3 g) while the weight of the root was 5.7 g ( $\pm$  1.6 g). Figure 5-13 also shows that there are no apparent signs of yellowing or scorching of older leaves, a sign of nitrogen, potassium or calcium deficiency, or stunting, a sign of phosphorous or nitrogen deficiency (Chekli et al. 2017). However, the plants grown in the bottom tray are visibly smaller. This could be due to uneven flow distribution in the module. As the water flowed in the trays from top to bottom, plants growing in the top tray likely captured and used more nutrients compared to plants in trays 2 and 3. The installation of drippers in every tray might be more suitable to provide similar nutrients for the downstream plants. At this stage, however, that is still quite speculative and needs to be further tested.

The biomass yield of lettuce using urine nutrient solution was, on average, slightly lower than the biomass yield produced with Half-strength Hoagland's solution, 16.1 g ( $\pm$  2.9 g) compared to 34.4 g ( $\pm$  9.5 g) respectively but similar to the biomass yield with the commercial fertiliser 24.4 g ( $\pm$  4.8 g). This could be due to the lower concentration of phosphorous and potassium in the urine (Neocleous & Savvas 2019). Here, however, urine has a P concentration of 0.005 g $\cdot$ L<sup>-1</sup>, which might be the cause for the reduced yield. Nonetheless, the lettuce roots/shoots average values were found to be similar or higher compared to the one reported in the literature (i.e., 0.11  $\pm$  0.2) (Li, Li, et al. 2018).

Overall, urine fertiliser was shown to be more effective in growing Pak Choi compared to lettuce. When using urine for growing lettuce, the addition of phosphate and potassium might be required to enhance the biomass yield.



Figure 5-12 Picture of the GSky Versa Wall set up with the different growing media. The first three rows (A) were fertilised with Half-strength Hoagland's solution (Hs), the second three (B) with urine (Us) and the bottom three (C) with the commercial nutrients solution (Cs).

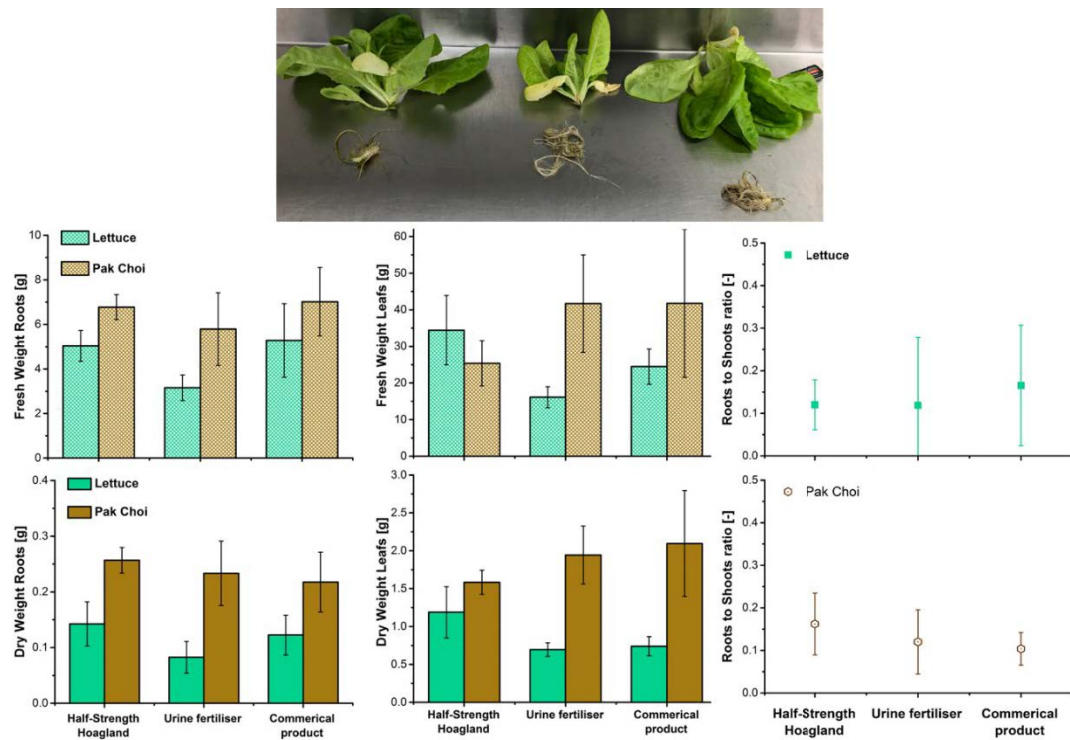


Figure 5-13 Fresh and dry weight of aerial parts and roots for lettuce (green) and Pak Choi (brown) grown in PM1. Roots to shoots ratio are also displayed in the column on the right. A picture of the separation between leaves (aerial parts) and roots of lettuce is shown at the top.

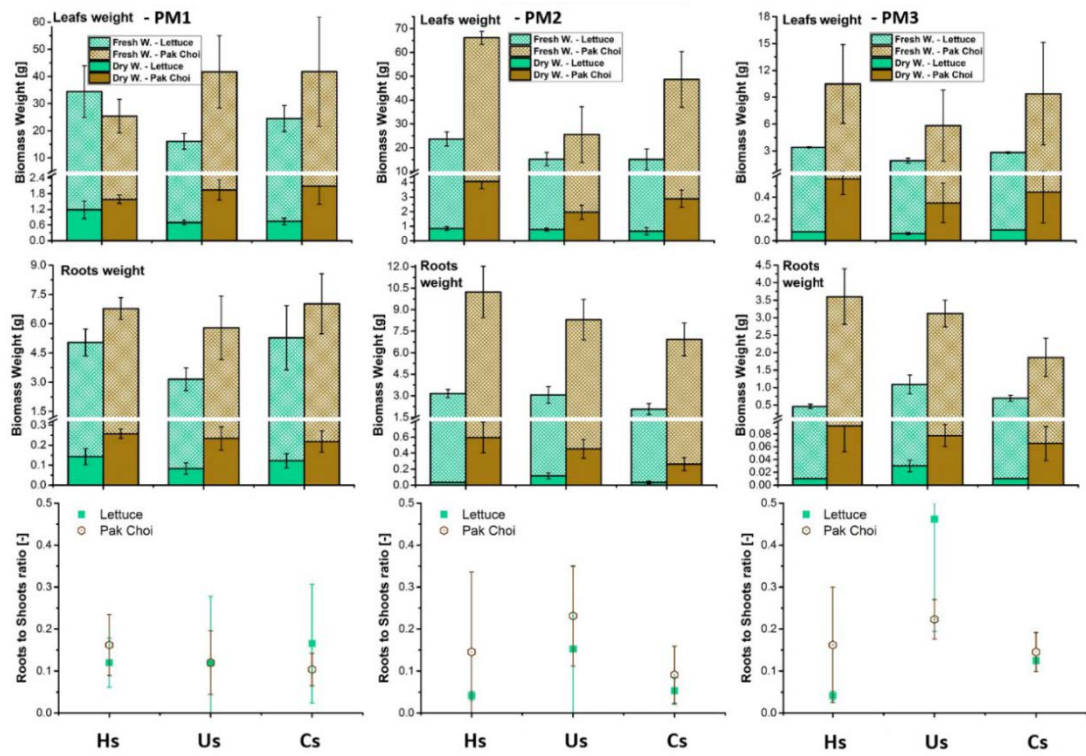


Figure 5-14 Fresh and dry weight of shoots and roots for lettuce (green) and Pak Choi (brown). Roots to shoots ratio are also displayed in the last row.

## 5.6 Conclusions

In this work, the human urine effluent from a UF-MBR was dewatered using the DCMD process and tested as a nutrient solution to grow lettuce and Pak Choi in a vertical garden. Overall, it was proven that DCMD is able to reach 20 times urine concentration, achieving a dissolved solids concentration of up to  $280 \text{ g.L}^{-1}$ . Also, the  $\text{NO}_2^-$  accumulation events frequent during urine nitrification, were easily counteracted by tuning the pH set-point of the reactor. This allowed achieving a stable 95% DOC removal and 50% TAN to  $\text{NO}_3^-$  oxidation. LC-OCD analysis also found that, while most of the LMW organics in raw urine are LMW-A, the MBR effluent was mainly composed of LMW-N. The high fouling potential of LMW organics had a significant impact on the MD flux decline during the dewatering step. In fact, a thick fouling layer deposited on the membrane surface, especially after 80% water recovery, causing the water flux to decline from  $15 \text{ L.m}^{-2}.\text{h}^{-1}$  to about  $1 \text{ L.m}^{-2}.\text{h}^{-1}$ . Even though alkaline cleaning successfully restored the initial DCMD performances, the chemical cleaning cost should be accounted for when benchmarking MD with distillation.

Finally, encouraging results were observed when growing lettuce and Pak Choi using just MD concentrate as a nutrient solution. In fact, all three solutions tested yielded similar Pak Choi biomass. This was despite the lower EC of urine fertiliser compared to the commercial nutrient solutions and control solution. However, more extensive trials are recommended to understand how to enhance the yield of crops fertigated with urine, and whether changes in the upstream process could improve the quality of the fertiliser.

## Chapter 6: Nitrogen and phosphorus recovery from fresh urine via fertiliser driven forward osmosis

---

This chapter was published in the articles below:

**F. Volpin**, L. Chekli, S. Phuntsho, J. Cho, N. Ghaffour, J.S. Vrouwenvelder, H. K. Shon, Simultaneous phosphorous and nitrogen recovery from source-separated urine: A novel application for fertiliser drawn forward osmosis, *Chemosphere*, 203 (2018) 482-489.

**F. Volpin**, H. Heo, M. A. H. Johir, J. Cho, S. Phuntsho, H. K. Shon, Techno-economic feasibility of recovering phosphorus, nitrogen and water from dilute human urine via forward osmosis, *Water Research*, 150 (2019), 47-55.



## 6.1 Summary

The high phosphorus (P) and nitrogen (N) content of human urine means that urine is a suitable raw material for fertiliser production. However, most of the urine-diverting toilets, or male urinals, dilute the urine 2 to 10 times which decreases the efficiency in the precipitation of P and stripping of N. In this work, a commercial fertiliser blend was used as a FO draw solution to concentrate real diluted urine. During the concentration, the urea in the urine is recovered as it diffuses to the fertiliser while the magnesium concentration in the dewatered urine increases due to the reverse  $\text{Mg}^{2+}$  flux from the DS, leading to higher  $\text{PO}_4^{3-}$  as struvite. The results show that, with 50% water recovery, 93% of the P was recovered without the addition of an external source of  $\text{Mg}^{2+}$ . XRD and SEM – EDX analysis confirmed that P was precipitated as mineral struvite. Concurrently, 50% of the N was recovered in the diluted fertiliser DS. An economic analysis was performed to understand the feasibility of this process. It was found that the revenue from the produced fertilisers could potentially offset the operational and capital costs of the system. Additionally, if the reduction in the downstream nutrients load is accounted for, the total revenue of the process would be over 5.3 times of the associated costs.



## 6.2 Introduction

The latest report from the United Nations Food and Agriculture Organisation estimates that between 2015 - 2018, the world demand for fertilisers (N,  $P_2O_5$ ,  $K_2O$ ) has increased, on an average, 1.8 percent per annum (FAO 2017a). This means that every year, extra 3'351'300 tonnes are added to the current 184'017'000 tonnes of fertiliser already consumed. With a world population expected to reach 11.2 billion people by 2100, this trend is anticipated to keep rising (United Nations 2017). The rise in the need for fertilisers would affect both the raw material availability as well as the greenhouse gas (GHG) emissions and eutrophication. In fact, at present, 1 - 2% of the world primary energy consumption is due to the production of ammonia fertiliser (130 million tonnes in 2008) (Bicer et al. 2017; Canfield, Glazer & Falkowski 2010). As a by-product, about 2 to 3 tons of  $CO_2$  are released for each ton of ammonia produced. This means that the ammonia production industries is responsible for about 0.93% of the world greenhouse gasses emission (Bicer et al. 2017). At the same time, the high quality and high-grade phosphate rock reserves, which constitute the primary source of P fertilisers, are depleting. However, the projections of P depletion rates vary, with a recent estimate that suggests a 20 - 60% resource depletion by 2100 (Elser & Bennett 2011; Mogollón et al. 2018; Van Vuuren, Bouwman & Beusen 2010).

The current growth in the size and density of cities is leading to increasing nutrients discharge to downstream treatment plants. The conventional biological oxidation and reduction of ammonium ( $NH_4^+$ ) to unreactive nitrogen gas ( $N_2$ ) is an energy-intensive process due to the high amount of oxygen required for the ammonia and nitrite oxidising bacteria (Kavvada et al. 2017; Ma et al. 2016). Recent investigations determined a theoretical energy requirement of 1.2 – 12.5 kWh.kg $_N^{-1}$  (Batstone et al.

2015; Maurer, Schwegler & Larsen 2003a; Wett et al. 2013) (lowest Sharon-Anammox, highest nitrification-denitrification) for the removal of N, and a unit cost of 93 – 134 \$.kgp<sup>-1</sup> for the removal of P (via Integrated Fixed-Film Activated Sludge Systems with Enhanced Biological Phosphorus removal IFAS-EBPR) (Bashar et al. 2018). Consequently, two challenges are likely to become increasingly relevant to achieve sustainable waste management. First, finding new nutrient sources and, second, reducing the costs associated with WW treatment.

One of the proposed approaches to pursue these goals it is to “shortcut” the N and P cycles by recovering TAN and PO<sub>4</sub><sup>3-</sup> directly from the WW (Larsen & Gujer 1997; Larsen et al. 2016; Maurer, Pronk & Larsen 2006). In particular, if the different WW streams (i.e., faeces, urine, light and heavy greywater) are separated at source, the economics of nutrients and water recovering might be more favourable (Larsen et al. 2016). Among them, source-separated human urine could be a suitable raw material for fertiliser production due to its high nutrients concentration (i.e. more than 5 kg<sub>N</sub>/m<sup>3</sup> and up to 0.5 kg<sub>P</sub>/m<sup>3</sup>) (Fumasoli et al. 2016; Maurer, Pronk & Larsen 2006; Maurer, Schwegler & Larsen 2003b). The phosphorous in urine can be recovered individually via struvite crystallisation (de Boer, Hammerton & Slootweg 2018; Etter et al. 2011). In this process, an external magnesium (Mg<sup>2+</sup>) source is added to hydrolysed urine (pH > 9) to trigger the precipitation of a magnesium ammonium phosphate salt (i.e., struvite). Vegetables grown using struvite produced from human urine showed an insignificant human health risk (de Boer, Hammerton & Slootweg 2018). Currently, the primary issue with this process is that, in most male urinals, urine is heavily diluted with flushing water, which decreased the P-recovery efficiency (Liu et al. 2014; Udert, Larsen & Gujer 2003). Additionally, only about 3% of the N in the urine can be recovered via struvite precipitation (Maurer, Pronk & Larsen 2006). Therefore, there

is a need to find suitable technologies to concentrate urine for N and P recovery while keeping the energy consumption is low.

Among the different processes that can be used to concentrate urine to recover N and P forward osmosis is one of the more promising. FO is a process that relies on the osmotic pressure difference between two solutions, separated by a semi-permeable membrane, to drive the water transport. As the solutes are not able to diffuse through the membrane, the water in the low concentration solution (FS) will dilute to the high concentration solution (DS) until the thermodynamic equilibrium is reached (Phuntsho, Shon, Majeed, et al. 2012). Additionally, when fertiliser is used as a DS, which is called fertiliser-drawn FO, the final diluted solution can be directly used for irrigation. As no DS recovery, as well as no high-pressure pumping, are required, the operational costs of the process are low (Van Der Bruggen & Luis 2015). However, the major drawback of this process is the occurrence of reverse diffusion of the ions in the DS to the FS, also called RSF. This happens due to the non-ideality of the available FO membranes (i.e., the ionic rejection is not 100%).

Here a Mg-based fertiliser was used for simultaneous urine concentration, urea/ ammonia and  $\text{PO}_4^{3-}$  recovery. Urea and ammonia recovery are achieved due to a combination of the concentration gradient between FS and DS combined with the low urine/ ammonia rejection of commercial FO membranes. At the same time, the combination of urine concentration and reverse  $\text{Mg}^{2+}$  flux from the fertiliser to the urine increases the recovery rates of  $\text{PO}_4^{3-}$  as struvite.

This work investigated the performances of the process, in terms of water and nitrogen flux, when using a commercial liquid fertiliser as DS. Membrane fouling/scaling was also investigated. Finally, the data obtained were used to calculate the payback period

of the plant. OPEX and CAPEX were benchmarked with the revenue from the produced fertiliser. The savings due to the reduction in the downstream nutrients load was also considered.

## **6.3 Experimental Investigation**

### **6.3.1 Process description**

Figure 6-1 shows the schematic representation of the process. Real fresh (i.e., non-hydrolysed) urine was used as FS while pure and blended fertilisers were used as DS. The solutions were separated by a commercial TFC polyamide (PA) membrane (Toray Chemical Korea Inc., South Korea), with the active layer was oriented towards the feed solution (i.e., AL-FS, FO mode).

The osmotic gradient between the two solutions allows for the permeation of water from the urine to the fertiliser, thereby diluting it. Urea would diffuse to the fertiliser side due to the combination of the concentration gradient, low urea molecular weight and absence of charge. Phosphorous, on the other hand, is crystallised after the FO in the DS. The increase in the  $\text{PO}_4^{3-}$  concentration plus the  $\text{Mg}^{2+}$  reverse flux from the DS allowed for the precipitation of phosphorus as struvite. This would happen once the pH of the concentrated urine rose to 8.5 – 9 as a consequence of the hydrolysis of the remaining urea (M. Fidaleo & R. Lavecchia 2003; Randall et al. 2016; Ray, Saetta & Boyer 2018).

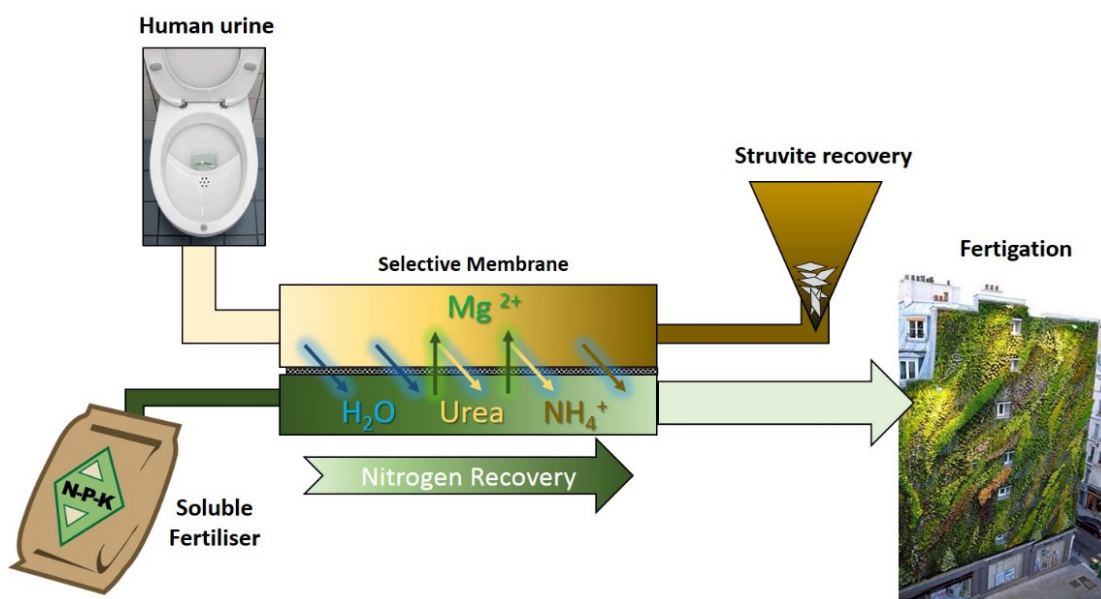


Figure 6-1 Schematic representation of the process.

### 6.3.2 Urine collection, fertiliser preparation, storage and characterisation

Real urine was collected and analysed, as described in the Methodology Section (0). The urine composition is given in Table 6-1. Magnesium nitrate hexahydrate and a commercial fertiliser blend were used as DS. Firstly, magnesium nitrate hexahydrate ( $\text{Mg}(\text{NO}_3)_2 \cdot 6\text{H}_2\text{O}$ ) was employed as a control solution due to the (I) high solubility of  $\text{Mg}(\text{NO}_3)_2 \cdot 6\text{H}_2\text{O}$ , which generates high osmotic pressure, (II) high  $\text{Mg}^{2+}$  content and (III) high water flux. Afterwards, a commercial fertiliser blend was used to simulate real applications such as fertigation of the green wall or other hydroponic applications. The commercial hydroponic nutrient solution (Optimum Grow - twin pack hydroponic nutrient) used in this study as DS was obtained from Fernland Agencies Pty Ltd (Queensland, Australia). The composition of the fertiliser solution is displayed in Table 6-1.

### 6.3.3 Experimental plan and performance evaluation

Experiments were first conducted using 0.5 M  $\text{Mg}(\text{NO}_3)_2 \cdot 6\text{H}_2\text{O}$  as DS. Afterwards, the commercial fertiliser blend was used to conduct long-term experiments (i.e. > 10 days). The concentration of the DS was chosen to achieve a water flux similar to the one generated by the commercial fertiliser. The first set of experiments aimed at assessing the optimal pH of urine to avoid struvite precipitation on the membrane surface. In this regards, the pH of fresh urine was adjusted to 6, 6.5, 6.75, 7 and 7.5 using 1 M NaOH or 1 M citric acid. FO flux decline was measured over time, and the used membrane was analysed by scanning electron microscopy as described in section 3.3.5.

Table 6-1 Ionic composition, osmotic pressure, pH and EC of fresh urine and the commercial liquid fertiliser used in this study.

	Urea [mg/L]	TAN	NO <sub>3</sub> <sup>-</sup> -N	TN	PO <sub>4</sub> <sup>3-</sup> -P	SO <sub>4</sub> <sup>2-</sup>	K <sup>+</sup>	Mg <sup>2+</sup> +	Ca <sup>2+</sup>	Osmotic pressure <sup>1</sup> [bar]	EC [mS/cm]	pH
Undiluted Urine	6590 ± 2370	133 ± 55	n.d.	4220 ± 384	28 ± 14	723 ± 170	1200 ± 200	70 ± 12	90 ± 13	9 ± 2	16 ± 4	6.3 ± 0.5
Commercial Fertiliser	n.d.	1,800 ± 36	8,700 ± 174	12,000 ± 24	9,000 ± 180	12,900 ± 258	36,800 ± 736	100 ± 206	n.d.	66 ± 3	107 ± 1	4.3 ± 0.3
Drinking water <sup>2</sup>	n.d.	n.d.	n.d.	n.d.	n.d.	n.d.	2 ± 0.4	7 ± 3	14 ± 3	n.d.	19 ± 2	7.9 ± 0.1

<sup>1</sup> The osmotic pressure was calculated using OLI Studio Analyser (Version 9.5, Oli Systems Inc., USA), <sup>2</sup> Based on lab analysis and Sydney Water potable water quality report (Sydney Water 2019), n.d. = not detected.

#### 6.3.3.1 Long-term experiments with commercial fertiliser blend

After preliminary tests, a long-term experiment (i.e. two weeks) was carried out with 5 L of diluted urine (1:5) as FS and 0.35 L of the commercial fertiliser as DS. Tap water was used for the dilutions, and its composition is presented in Table 6-1. The experiment was run until ~ 50% urine concentration and about eight times fertiliser dilution was reached. To avoid microbial growth in the FS and DS, 0.5 mL of hydrogen peroxide (30% v/v) was added once a week. The outcomes from this test were used for the economic analysis below discussed.

#### 6.3.3.2 Modelling of the water flux

To better identify the impact of fouling of the transmembrane flux, the theoretical FO water flux was modelled via the classical solution-diffusion model coupled with the diffusion-convection transport in the membrane support layer (Ali et al. 2018; Tang et al. 2010). Equation (6-6) was used for predicting the water flux (see Table 6-2 for the input data). Equation (6-6) was obtained by solving Eq. (6-1), (6-2), (6-4) and (6-5). Where the first 2 equations describe the water and salt transport across the semipermeable non-porous active layer, while the last 2 equations accounts for the effect of concentration polarisation (Ali et al. 2018; Tang et al. 2010).

$$J_W = A(\pi_{draw}^m - \pi_{feed}^m) \quad (6-1)$$

$$J_S = B(C_{draw}^m - C_{feed}^m) \quad (6-2)$$

$$B = \left( \frac{1-R}{R} \right) \cdot (\Delta P - \Delta \pi) \cdot (A) \quad (6-3)$$

$$C_{Feed}^m = C_{Feed}^b \exp\left(\frac{J_W}{k_F}\right) \text{ (Active Layer - FS)} \quad (6-4)$$



$$C_{Draw}^m = C_{Draw}^b \exp\left(\frac{J_w}{K_D}\right) \text{ (Active Layer – FS)} \quad (6-5)$$

$$\text{Combining Eq. (6-1)(6-2)(6-4)(6-5)} \quad (6-6)$$

$$J_w = \sigma K_m \ln\left(\frac{A\pi_D + B_s}{A\pi_F + J_w + B_s}\right)$$

Where A is the pure water permeability, B the solute diffusivity,  $\pi^m$  and  $C^m$  the osmotic pressure and concentration on the membrane interface layer.  $\Delta P$  is the applied pressure (bar), R the rejection (as  $R = 1 - C_{\text{permeate}}/C_{\text{feed}}$ ), and  $\Delta\pi$  osmotic pressure difference.  $C_{Feed}^b$  is the concentration in the bulk feed solution and  $C_{Draw}^b$  in the bulk draw solution.  $k_F$  the mass transfer coefficient and  $K_m$  the diffusivity coefficient.

Finally,  $\sigma$  is the reflection coefficient, assumed as unity (complete rejection of the solute),  $K_m$  is the mass transfer coefficient, of the selected DS, given by the ratio between the diffusivity of the salt and the structural parameter (S) of the membrane (i.e.  $K_m = D/S$ ). The transport coefficients for water and solutes are expressed as A and B<sub>s</sub>. Finally,  $\pi_D$  and  $\pi_F$  are the DS and FS bulk osmotic pressure, respectively.

Table 6-2 Input parameters used for the modelling of water flux. Osmotic pressure and diffusivity were estimated using OLI Studio Analyser (Version 9.5, Oli Systems Inc., USA) while rejection, A and S are based on experimental data. The A value was measured by applying 10 bar of hydraulic pressure and recording the transmembrane flux. To calculate the B value of the commercial fertiliser, the membrane rejection of a 500 mg/L fertiliser solution was measured under 10 bar operating pressure.

	Osmotic Pressure, $\pi_D$ [bar]	Diffusivity, D [m <sup>2</sup> .h <sup>-1</sup> ]	Rejection, R [%]	Selectivity, B <sub>s</sub> [L.m <sup>-2</sup> .h <sup>-1</sup> ]
Fertiliser Blend	66.3	$2.50 \times 10^{-6}$	98.8	0.46
A [L.m <sup>-2</sup> .h <sup>-1</sup> .bar <sup>-1</sup> ]	3 ± 0.3			
S [μm]	419			

#### 6.3.3.3 Membrane fouling and scaling

After each experiment, the membrane was cleaned with a solution of 0.1 M NaOH (pH = 12) for 10 minutes and then flushed with de-ionised water (Kim et al. 2014; Mi & Elimelech 2008). Alkaline cleaning procedure was chosen as most of the fouling layer was resulting from organic deposition (e.g., creatinine). After cleaning, membrane flux recovery test was conducted using 0.5 M NaCl solution and de-ionised water, as DS and FS respectively.

#### 6.3.4 Economic analysis

Understanding the economic feasibility of this process is crucial for practical application. The cost of the system as OPEX and CAPEX was analysed and benchmarked with the revenues from the products (i.e., urea/ ammonia and struvite). Additionally, the theoretical savings of reducing the nutrients load to the downstream treatment plant were included in the analysis.

Finally, an economic analysis was performed to investigate the investment return period with different process performances. OPEX and CAPEX assumptions are displayed in Table 6-3. Construction and equipment costs were also included (Kim, Phuntsho, et al. 2017). The construction cost includes pressure vessels, pumps, piping and others (i.e., civil engineering, intakes, working capital and contingencies) while the equipment cost includes membranes and materials (Chekli et al. 2017; Valladares Linares et al. 2016). The required membrane area was calculated based on the plant capacity and average measured flux. CAPEX amortization costs were then calculated as follows:

$$\text{Amortized CAPEX (\$. m}^{-3}\text{)} = \frac{\text{CAPEX} \times i}{1 - (1 - i)^{-n}} \times \frac{1}{Q \times 365} \quad (6-7)$$

Where  $i$  is the interest rate,  $n$  is the plant lifetime, and  $Q$  is the plant capacity.

For the pumping energy calculations, pressure losses of 2 bar, for the feed channel, and of 0.5 bar for the draw channel were assumed (Kim, Phuntsho, et al. 2017). The revenue from the recovery of urea/ ammonia and struvite was calculated using the recovery rates measured in this work and the commercial prices of urea and struvite (World Bank Group 2018),(Forrest et al. 2008). All the other assumptions for the revenue calculations are displayed in Table 6-3. Finally, for the economic analysis, the plant construction time was hypothesised to be one year with the construction costs distributed during the construction year.

Table 6-3 Summary of the main assumptions used to calculate the OPEX/CAPEX cost of operating an FDFO plant (Valladares Linares et al. 2016). Australian Energy Market Commission data were used for the New South Wales energy prices (AEMC 2013).

<b>OPEX/CAPEX assumptions</b>	
Plant availability due to downtime	0.95
Pump Efficiency	0.85
Power cost (\$/kWh) <sup>a</sup>	0.29
Interest rate (%)	6
Plant lifetime (years)	20
Capacity (m <sup>3</sup> /day)	10
Feed pressure (bar)	2
FO element cost (\$/element)	1000
Number of elements per pressure vessel (PV)	6
PV cost (\$/PV) with 6 elements per PV	1000
Membrane area per element (m <sup>2</sup> )	15.3
Number of membrane elements	3.97
Total membrane area (m <sup>2</sup> )	60.75
Replacement rate (%)	10

Table 6-4 Summary of the main assumptions used to calculate the revenue and savings of operating an FDFO plant to recover N and P from human urine.

Revenue/Savings assumptions	
Average TP Initial [kg-P/m <sup>3</sup> ] <sup>a</sup>	0.30
Average TN Initial [kg-N/m <sup>3</sup> ] <sup>a</sup>	4.50
Struvite Price [\$/kg] <sup>b</sup>	0.33
Urea Price [\$/kg] <sup>c</sup>	0.29
Total N Recovery [%] <sup>a</sup>	50
N removal cost [MJ/kg <sub>N</sub> ] <sup>d</sup>	30
Total P Recovery [%] <sup>a</sup>	93
P removal cost [MJ/kg <sub>P</sub> ] <sup>e</sup>	28

<sup>a</sup> Based on measured values in this study. <sup>b</sup> Based on the paper by Forrest et al. about the optimisation of struvite production for phosphate recovery in WWTP (Forrest et al. 2008). <sup>c</sup> Based on the World Bank commodities prices index (World Bank Group 2018). <sup>d-e</sup> Based on the average values proposed by M. Maurer et al. on the energetic aspects of the removal of nitrogen via nitrification/denitrification-Anammox and the removal of phosphorous via enhanced biological phosphorus removal (Maurer, Schwegler & Larsen 2003a).

## 6.4 Results and discussion

### 6.4.1 Effect of pH of urine on struvite production and FO performance

The solubility of struvite crystals is strongly dependant on the pH of the solution. Struvite solubility decreases at pH > 6, reaching the minimum solubility at pH above 9 (Doyle & Parsons 2002). As most commercial fertilisers contain Mg<sup>2+</sup>, some of which might back diffuse during the FO filtration process, it is crucial to understand what the optimal urine pH is to avoid membrane scaling caused by struvite formation



membrane scaling. On the right side, an SEM picture of the fouled membrane is also displayed.

#### 6.4.2 Effect of urine dilution on the water flux and membrane cleaning

The concentration of  $\text{PO}_4^{3-}$  and  $\text{Mg}^{2+}$  in the urine significantly affects the P recovery efficiency via struvite crystallisation. Previous studies found that diluted urine often shows less P-recovery as struvite as well as lower struvite crystals size under the same experimental conditions (i.e. at same pH and  $\text{Mg}^{2+}$  load) (Liu et al. 2014; Udert, Larsen & Gujer 2003). This assumption was confirmed, experimentally, and the results are displayed in Figure 6-3. It was found that P removal was less than 73% when the urine was diluted five times, compared to a 99.5% removal of P with the undiluted urine.

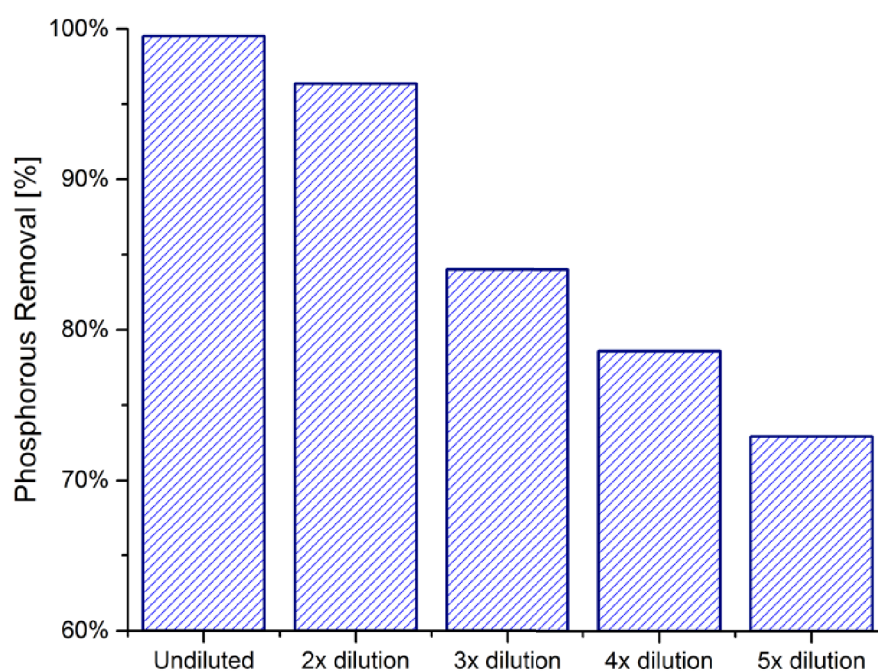


Figure 6-3 Phosphorus removal via struvite precipitation with different urine dilution factors.

Afterwards, the effectiveness of FO in concentrating different urine solutions was investigated. Water flux and membrane cleaning effectiveness were evaluated for urine diluted to 1, 2 and 5 times. The following average fluxes were achieved:  $6.6 \text{ L.m}^{-2}.\text{h}^{-1}$  (undiluted, 50% concentration, 67.5 h),  $8.6 \text{ L.m}^{-2}.\text{h}^{-1}$  (2 times dilution, 50% concentration, 64.5 h),  $8.1 \text{ L.m}^{-2}.\text{h}^{-1}$  (5 times dilution, 80% concentration, 93 h). Figure 6-5 (A) shows the temporal variation of water flux as a function of the urine concentration factor. Flux decline was attributed to the combination of DS dilution, urine concentration and membrane fouling. Particularly at high urine concentration factor (i.e.,  $> 15 \text{ mS/cm}$ ), the formation of a brown layer was observed on top of the membrane surface (Figure 6-4). Membrane cleaning with de-ionised water only partially removed the brown layer. However, the brown layer was removed entirely when alkaline cleaning with  $0.1 \text{ M NaOH}$  was conducted for 10 minutes. Figure 6-5 (B) confirms the effectiveness of the cleaning strategy by showing that the flux of the clean membrane was nearly the same to that of the virgin membrane with a minor variation of  $\pm 5\%$ . This was despite the different experimental time and urine concentration factor. It can be then concluded that real urine can be concentrated over 2 times without any pre-treatment. Alkaline cleaning was found to be effective in fully restoring the initial water flux.





Figure 6-4 Picture of the membrane coupon before and after the alkaline cleaning. The feed solution was real urine while the draw was commercial fertiliser. The experimental run time was 11 days.

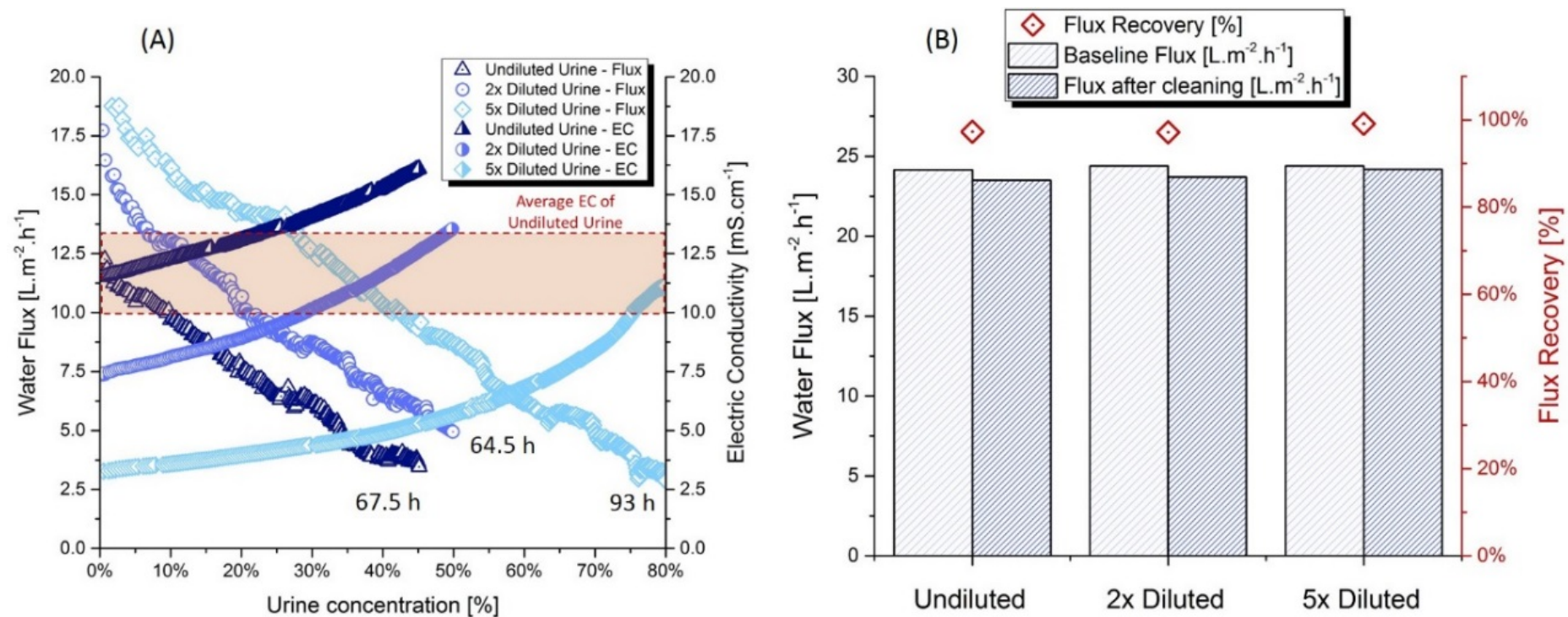


Figure 6-5 On the left (Fig. A), forward osmosis water flux having as FS urine with different dilution factors (i.e., 1, 2 and 5 times) and 0.5 M  $\text{Mg}(\text{NO}_3)_2 \cdot 6\text{H}_2\text{O}$  as DS. The time necessary to reach the urine concentration factor was displayed at the end of the plot. On the right (Fig. B) it is shown the water flux before and after the urine tests, and subsequent membrane cleaning, using 0.5 M NaCl as DS and DI-water as feed.

### 6.4.3 Nutrients flux and recovery for different urine dilution factors

Nitrogen and phosphorus recovery are vital parameters for understanding the economic feasibility of the urine concentration process. Hence, the nitrogen flux from the urine to the fertiliser solution together with the P recovery after struvite precipitation was investigated.

The urine dilution factor strongly influences the urea/ammonia flux. This can be explained by Fick's law, as it regulates the membrane diffusion rate (i.e.,  $J_N = D_N \cdot A \cdot \Delta C_N/x$ ) where the concentration difference  $\Delta C_N$  is a dominant factor in the diffusion rate  $J_N$ . In this case, the nitrogen diffusivity  $D_N$ , membrane area  $A$  [m<sup>2</sup>] and thickness  $x$  [m] is the same for each experiment. Therefore, the high initial concentration of urea/ammonia in undiluted urine is responsible for the higher diffusion rate. Additionally, the higher water flux ( $J_w$ ) (in the case of diluted urine) also lowers the specific nitrogen flux. Figure 6-6 shows the linear relationship between the urine concentration factor and the total nitrogen recovery (as the sum of urea and ammonia).

Because of the same principle, the  $Mg^{2+}$  reverse flux was almost the same in all cases. In fact,  $\Delta C_{Mg}$  depends only on the  $Mg^{2+}$  concentration in the DS, which was the same in each test. The experiments showed that the recovery of P and N was ~99% and 40-65%, respectively (Figure 6-7 B). The total N recovery was found to be 1-2% lower than the sum of urea-N and TAN. This is because of the  $NO_3^-$  reverse salt flux from the  $Mg(NO_3)_2 \cdot 6H_2O$  DS to FS (Volpin, Chekli, et al. 2018). Also, due to the  $Mg^{2+}$ -RSF and P concentration factor, the removal of phosphorous was high (>99%) in all the concentrated urine solutions without any addition of additional magnesium

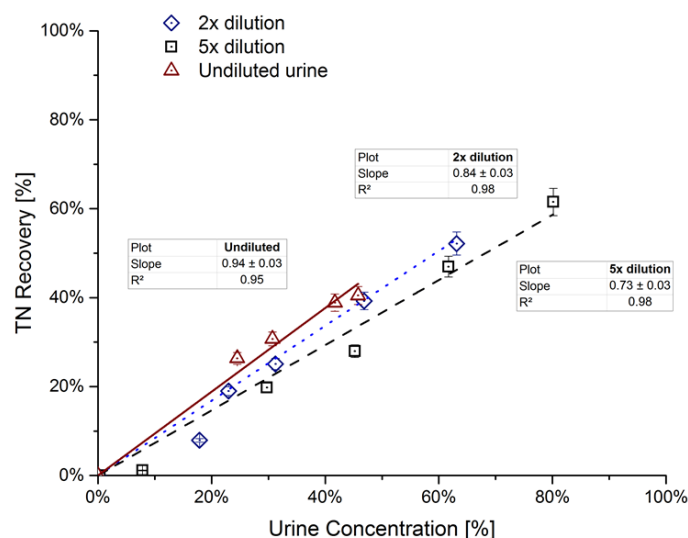


Figure 6-6 Statistical correlation between the total nitrogen (TN) recovery from the urine and the urine concentration during the FO process.

Figure 6-8 shows the XRD spectrum of the precipitates while Figure 6-9 shows the SEM - EDX. In the XRD, the peaks of the sample match quite well with the standard peaks of struvite, according to the literature, while the EDX shows that the molar ratio of Mg and P is almost 1:1 (Xie et al. 2014; Xu et al. 2015). The crystals obtained with both fertilisers were identical at the SEM – EDX and XRD spectrum.

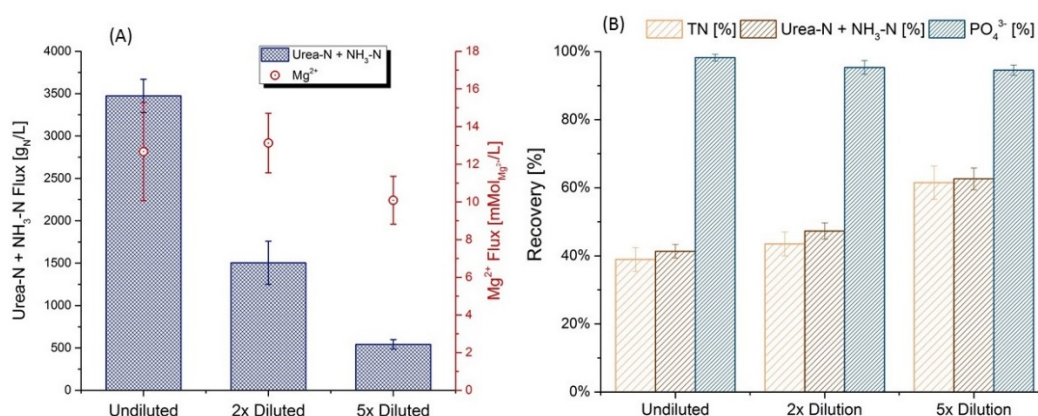


Figure 6-7 (A) Nitrogen and magnesium flux. The blue columns represent the average specific nitrogen flux, in the form of urea and TAN, from the urine to the fertiliser

solution. The red dots represent the specific reverse magnesium flux from the fertiliser (i.e.,  $\text{Mg}(\text{NO}_3)_2 \cdot 6\text{H}_2\text{O}$ ) to the urine. (B) Measured recovery of phosphorus ( $\text{PO}_4^{3-}$ ), total nitrogen (TN) and urea + ammonia at the end of each experiment.

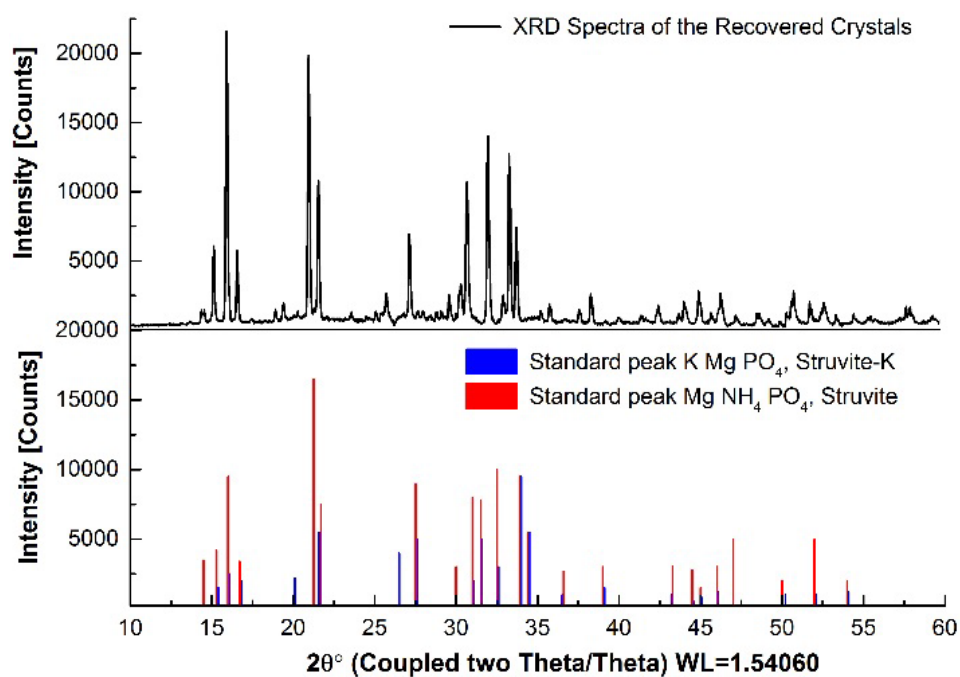


Figure 6-8 XRD spectrum of the precipitates obtained from the concentrated FS after FO filtration.

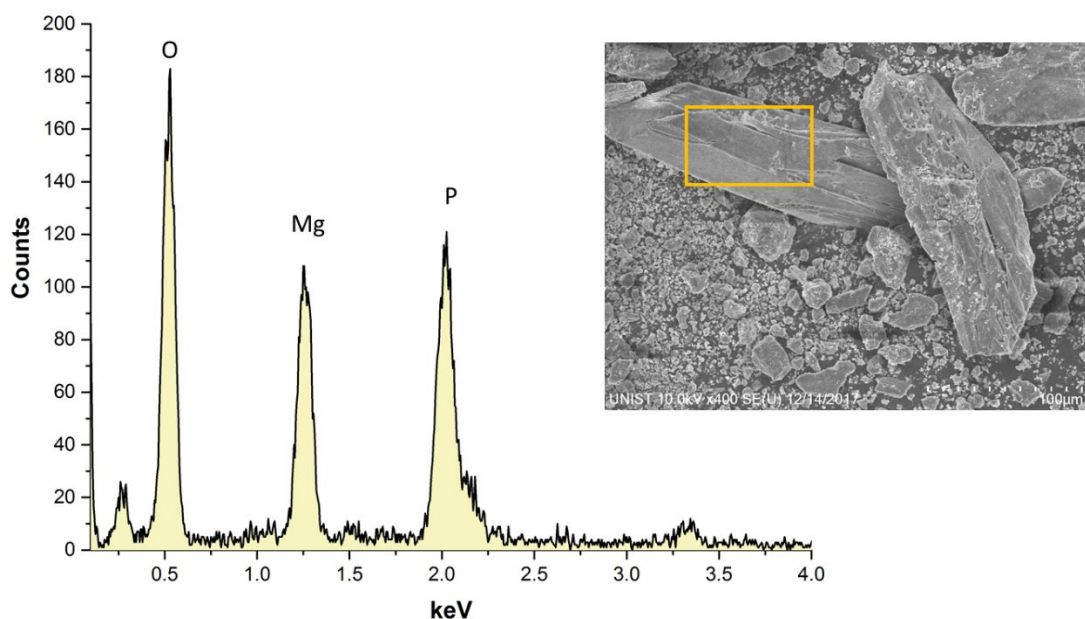


Figure 6-9 SEM picture and EDX spectrum of the precipitates obtained after filtration of the concentrated urine.

#### 6.4.4 Diluted real urine with commercial fertiliser as the draw solution

After having tested the effectiveness of a pure fertiliser, a commercial fertiliser blend was used for dewatering real diluted urine. A long-term experiment (i.e., over 11 days) was performed to investigate:

- i. Achievable urine concentration and fertiliser dilution,
- ii. Clean in place effectiveness, and
- iii. Nitrogen and phosphorus recovery.

The results obtained in the long-term test were used for the economic analysis described in the following section. Figure 6-10 shows the temporal variation of flux over the urine concentration factor. The average flux to achieve 50% urine concentration was about  $4.2 \text{ L.m}^{-2}.\text{h}^{-1}$ . The gradual flux decline is mainly attributed to

the decrease in the osmotic driving force ( $\Delta\pi$ ), as over time, the fertiliser gets diluted, and the urine gets concentrated. However, membrane fouling could also play an essential role. To assess the effect of membrane fouling on the flux decline, flux modelling and clean in place (CIP) with 0.1 M NaOH were conducted. The impact of flux loss due to fouling can be noticed after 20% urine concentration, and it becomes more severe in the final part of the filtration. By looking at the flux improvement after the CIP, at about 33% urine concentration, a 29% flux improvement was measured (i.e., from 3.3 to 4.6 L.m<sup>-2</sup>.h<sup>-1</sup>). This corresponds to an 88% flux recovery compared to the theoretical flux.

On the other hand, Figure 6-10 shows the calculated N and P recovery based on nutrients mass balance. The results show that over 93% of the P was removed after struvite precipitation, and over 50% of the N was recovered in the fertiliser. This is in line with the previous results using Mg(NO<sub>3</sub>)<sub>2</sub>.6H<sub>2</sub>O as DS (Figure 6-7).

To conclude, urine was concentrated 50% using a commercial fertiliser as DS, while fouling was observed. About 93% of the P and 50% of the N were removed after the filtration-precipitation without the addition of additional Mg<sup>2+</sup> source. Assisting the process with hydraulic pressure (pressure-assisted osmosis or PAO), especially at the end of the filtration, could improve the overall average flux (Chekli et al. 2017). However, the impact that the hydraulic pressure would have on the N/P recovery and fouling should be further investigated.



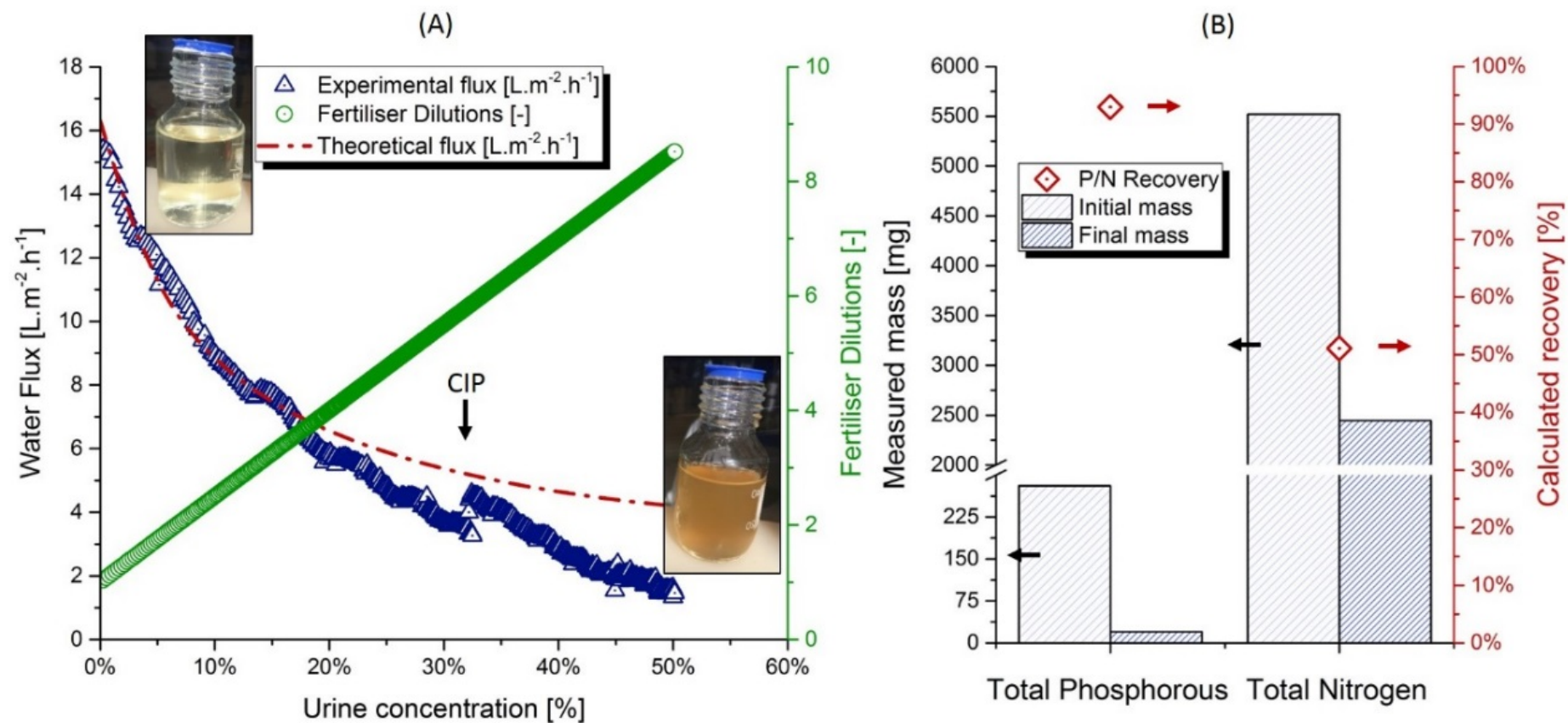


Figure 6-10 (A) Theoretical and experimental water flux and fertiliser dilution as a function of the urine concentration factor. Clean in place (CIP) with 0.1 M NaOH was performed after about 33% urine concentration. (B) Total nitrogen and phosphorus in the urine.



#### 6.4.5 Assessment of the system's economic feasibility

In this section, the costs associated with the construction and operation (i.e., CAPEX and OPEX respectively) were benchmarked with the revenue from the produced fertiliser and the downstream WW treatment savings. The impact of the average water flux in return in the capital investment was also analysed. Scenario A uses  $J_w = 4.2 \text{ L.m}^{-2}.\text{h}^{-1}$  as input (measured value), scenario C uses  $J_w = 8 \text{ L.m}^{-2}.\text{h}^{-1}$  (ideal no fouling process) and scenario B used  $J_w = 6.5 \text{ L.m}^{-2}.\text{h}^{-1}$  (moderate fouling, in between A and C).

Figure 6-11 shows that, without accounting for the reduction in the N and P discharge, the payback period for Scenario A is of over 20 years. That is because the revenue from the struvite and urea/ ammonia recovery is only 0.8% higher than the OPEX of the system (Figure 6-11A). This is because membrane replacement costs account for the most significant portion of the OPEX, i.e., 64% (Figure 6-12). However, Figure 6-11B shows that just by increasing the average flux to 6.5 or 8  $\text{L.m}^{-2}.\text{h}^{-1}$  (scenario B and C) the payback period can be moved to 5.5 or 2.7 years, respectively. This could be achieved by having more frequent CIP or by assisting the process with hydraulic pressure. Chekli et al. (2017) showed that by applying a small pressure (e.g., 2 - 4 bar) at the end of the filtration, the flux can be increased by over 57% (Chekli et al. 2017). This should be investigated further as a means to reduce the overall OPEX and CAPEX of the system.

Regarding the returns from the process, Figure 6-13 shows that struvite and urea/ ammonia would yield similar revenues. It can be argued that the urea recovered is

already mixed with the fertiliser draw solution. Therefore, instead of revenue, its recovery would be more of saving in the addition of nitrogen to the fertiliser solution to meet the required concentration. For a more conservative estimation, the savings from the water extracted from the urine were not included in the calculation.

Finally, the theoretical savings on the reduced nutrient load to the downstream treatment plant were calculated. The results are shown in Figure 6-11 A and B. Due to the high nitrogen content of urine, and the relatively high cost to oxidise  $\text{NH}_4^+$  to  $\text{NO}_3^-$  and reduce  $\text{NO}_3^-$  back to unreactive  $\text{N}_2$ , a 50% reduction in the N load from urine was found to have a significant impact on the economics of the process. In particular, the savings in the downstream treatment costs can be as high as 6.2 \$/m<sup>3</sup> of urine (which is 3.5 times higher than the sum of CAPEX and OPEX).

To conclude, a preliminary economic analysis was performed to estimate the economic viability of this process. Even though with current fertiliser prices, the direct revenues from the extracted fertiliser would only be adequate to offset the FDFO process costs, if the savings to the downstream treatment plant are included, the total revenue was calculated to be over 4.3 times of the process costs. However, that is currently not the case in Australia, where there is no economic incentive on reducing the nitrogen discharge to the sewers by users.

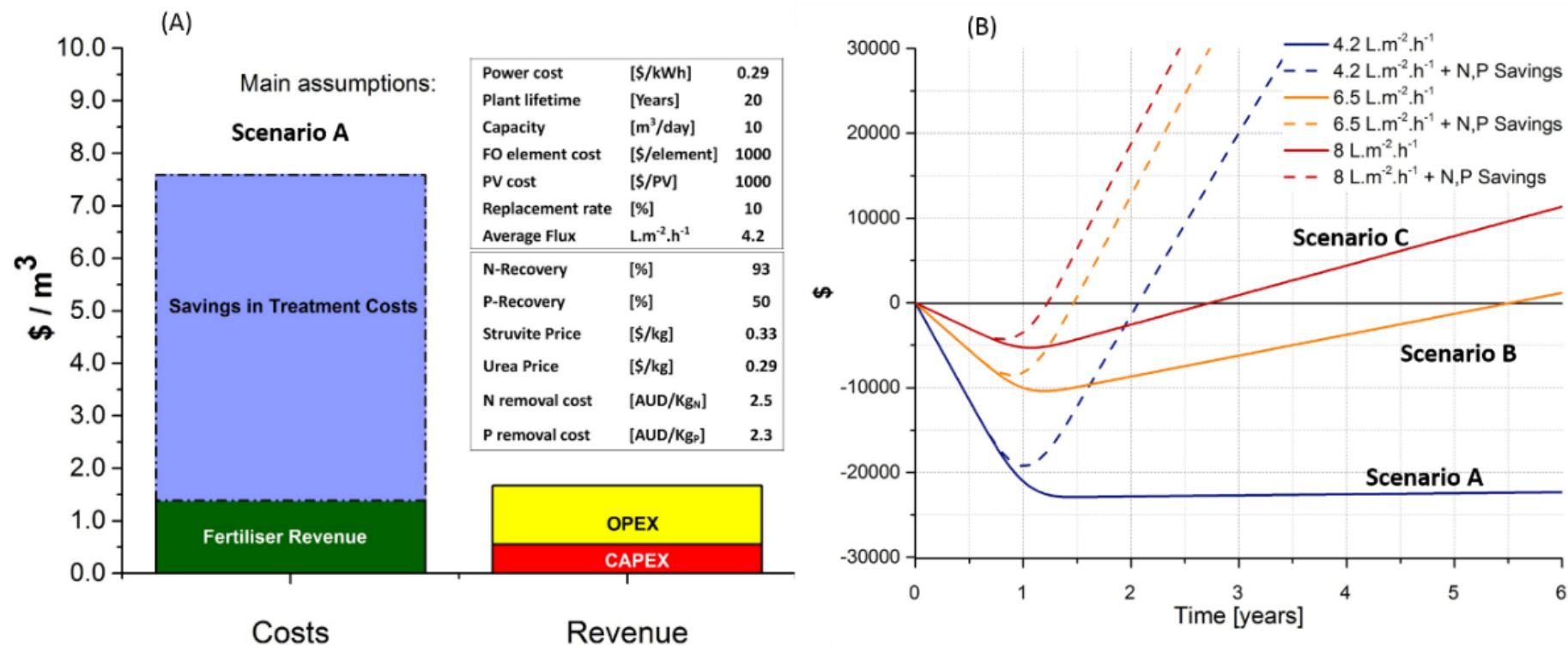


Figure 6-11 (A) shows the comparison of the estimated costs and revenues of this process. (B) shows the economic analysis of using FDFO, assuming that the construction of the plant is finalised in 1 year. For both analyses, the costs consist of the sum of OPEX and CAPEX while the revenues as the sum of produced fertiliser (urea + struvite) and downstream WW treatment savings.

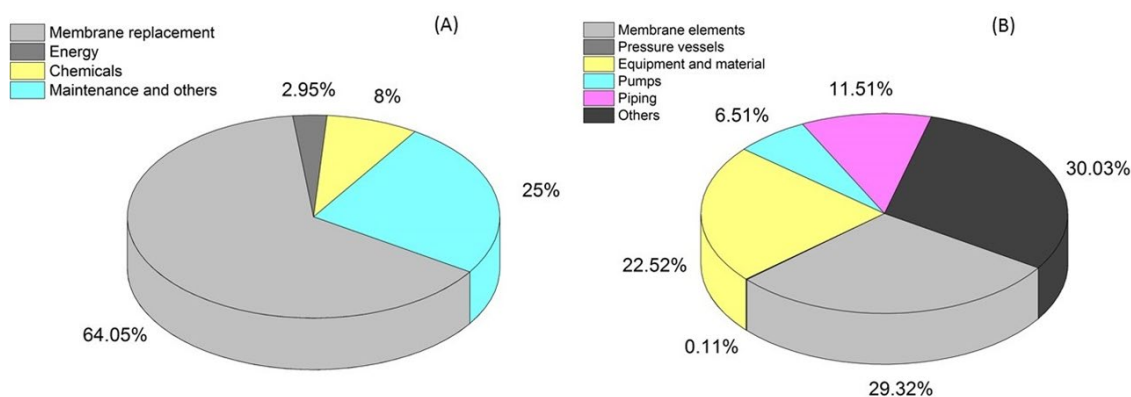


Figure 6-12 Breakdown of the operational costs (A) and capital costs (B).

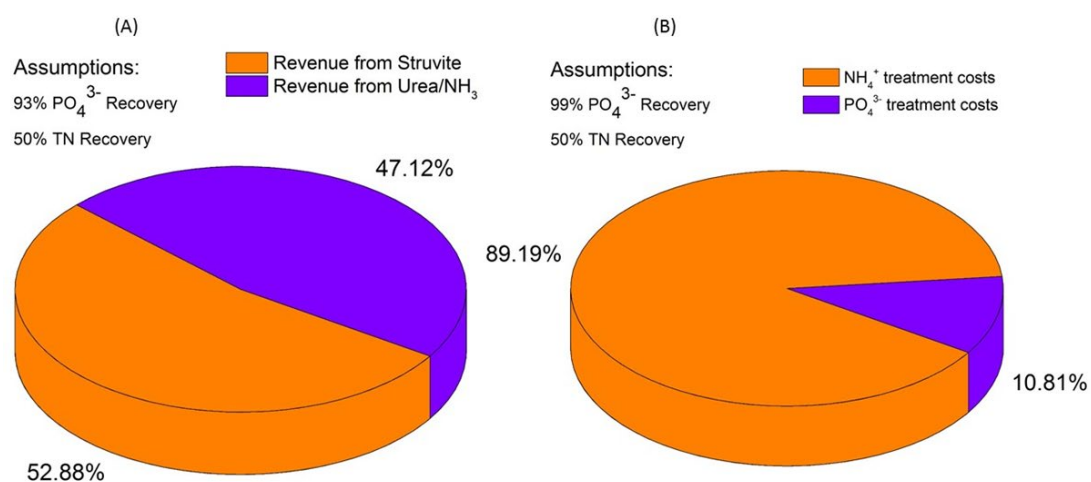


Figure 6-13 Breakdown of fertiliser revenue (A) and downstream nitrogen and phosphorous removal savings (B).

## 6.5 Conclusions

Forward osmosis (FO) was successfully utilised in dewatering real human urine, diluted five times, using a commercial fertiliser blend as DS. Phosphorus recovery from the urine was achieved without the addition of an external  $\text{Mg}^{2+}$  source. Instead, the combination of over 50% urine concentration, reverse  $\text{Mg}^{2+}$  flux from the DS and the  $\text{Mg}^{2+}$  present in the tap water were found to be adequate to remove 93% of the P present in the urine. Simultaneously, about 50% of the N was recovered in the diluted fertiliser DS. Organic foulants in the urine were found to affect the FO water flux, especially at high urine concentration factors. However, alkaline cleaning with 0.1 M NaOH was able to recover the initial flux values. Inorganic scaling, on the other hand, was effectively avoided by keeping the urine pH below 6.5.

The experimental outcomes were used to perform an economic analysis of the process. The low average filtration flux was found to yield high OPEX costs, mainly due to the membrane replacement cost. With the average flux measured in this study (i.e.,  $4.2 \text{ L.m}^{-2}.\text{h}^{-1}$ ), the payback period for this plant would be over 20 years. However, if the average flux is increased to  $8 \text{ L.m}^{-2}.\text{h}^{-1}$  (via fouling mitigation or pressure-assisted osmosis), the return on the investment can be reached after 2.7 years. Finally, if the savings to the downstream treatment plant are included, even with an average flux of  $4.2 \text{ L.m}^{-2}.\text{h}^{-1}$ , the total revenue of the process would be over 4.3 times of the associated OPEX and CAPEX costs.

# **Chapter 7: Energy recovery through reverse electro dialysis: Harnessing the salinity gradient from the flushing of human urine**

---

**\* This chapter was submitted for publication in the Journal *Water Research*.**

## 7.1 Summary

Urine dilution is often performed to avoid clogging or scaling of pipes, which occurs due to urine  $\text{Ca}^{2+}$  and  $\text{Mg}^{2+}$  precipitating under the alkaline conditions created by ureolysis. The large salinity gradient between urine and flushing water is, theoretically, a source of potential energy which is currently unexploited. As such, this work explored the use of a compact reverse electrodialysis (RED) system to convert the chemical potential energy of urine dilution into electric energy. Urine composition and ureolysis state as well as solution pumping costs were all taken into account. Despite having almost double its electric conductivity, real hydrolysed urine obtained net energy recoveries  $E_{\text{Net}}$  of 0.053 - 0.039 kWh/m<sup>3</sup>, which is similar to energy recovered from real fresh urine. The reduced performances of hydrolysed urine were linked to its higher organic fouling potential and possible volatilisation of ammonia due to its high pH. However, the higher-than-expected performance achieved by fresh urine is possibly due to the fast diffusion of uncharged urea to the freshwater side. Real urine was also tested as a novel electrolyte solution and its performance compared with a conventional  $\text{K}_4\text{Fe}(\text{CN})_6/\text{K}_3\text{Fe}(\text{CN})_6$  couple. While  $\text{K}_4\text{Fe}(\text{CN})_6/\text{K}_3\text{Fe}(\text{CN})_6$  outperformed urine in terms of power densities and energy recoveries, net chemical reactions seemed to have occurred in urine when used as an electrolyte solution, leading to TOC, ammonia and urea removal of up to 13%, 6% and 4.4%, respectively. Finally, due to the migration of  $\text{K}^+$ ,  $\text{NH}_4^+$  and  $\text{PO}_4^{3-}$ , the low concentration solution could be utilised for fertigation. Overall, this process has the potential of providing off-grid urine treatment or energy production at a household or building level.

## 7.2 Introduction

The latest WHO/UNICEF joint monitoring program for water supply, sanitation and hygiene shows that more than 30% of the world population still does not have access to essential sanitation services (WHO and UNICEF 2017). However, in areas like urban slums, centralised wastewater (WW) treatment is not practical as sewage pipelines cannot be laid. As such, on-site sanitation is the only option. One commonly proposed approach for improving decentralised sanitation is to treat human urine separately from the remaining WW. This is because urine separation would reduce up to 81% of the nitrogen (N) and 50% of the phosphorus (P) in the remaining WW, thereby making it easier to treat (Maurer, Pronk & Larsen 2006; Putnam 1971b; Rose et al. 2015). The reported concentration of nitrogenous compounds in typical urine can exceed 8000 mg-N/L, while total phosphorus levels can add up to 500 mg/L (Larsen et al. 2016; Larsen, Udert & Lienert 2013; Udert, Larsen & Gujer 2006). That is because urine contains over 6000 mgN/L of urea (which hydrolyses into ammonia during storage), 300 mg/L of uric acid, 250 mg/L of creatine and 1400 mg/L creatinine (Putnam 1971a). This makes urine almost as saline as seawater (Volpin, Yu, et al. 2019). As urine is generally mixed with flushing water, which has an average total dissolved solids (TDS) between 0.1 and 1 g/L, there is a large salinity gradient of mixing, which could be converted into chemical potential energy.

While several articles have looked at the energy recovery from the mixing of saline industrial wastewaters, mainly using processes like pressure retarded osmosis (PRO) and reverse electrodialysis (RED), so far there are only a few articles that look into the recovery of urine chemical potential energy (Han et al. 2020; Ma et al. 2020; Mehdizadeh et al. 2020).

For example, in one case, urine was used as a draw solution for forward osmosis (FO) to dewater a microalgae culture (Volpin, Yu, et al. 2019). There, urine was used to draw water



from the algae solution as its osmotic pressure was higher than that the one of the algae solutions. However, this approach is only useful for dewatering applications. To extract water and energy from urine, Mercer et al. (2019) used a combination of membrane distillation (MD) and RED. Here, urine is firstly concentrated urine MD, and the MD concentrate is then used to power the RED process. In RED, cation and anion exchange membranes (CEMs and AEMs) were used to allow only for the transport of ions. By separating the higher concentration urine solution from the lower concentration (LC) freshwater through alternated CEMs and AEMs membranes, an ionic flux from HC to LC is created (Post et al. 2007; Veerman et al. 2011; Vermaas et al. 2013). The ionic flux is then converted into an electrical current thanks to redox reactions occurring at the anode and cathode of the electrode compartment (Veerman et al. 2010). However, the hybrid RED-MD process was designed only for scenarios where waste heat is available.

However, if used as a stand-alone process, RED is possibly more competitive compared to other salinity gradient-driven energy recovery processes such as PRO in the recovery of energy from urine. That is because RED here has the advantage of being able to operate at low flow rates, of requiring lower capital investment (given that no turbine or pressure exchangers are necessary) and is easily scalable (Post et al. 2007; Yip & Elimelech 2014). As reduced process complexity and cost is paramount if energy is to be recovered from urine at a household/building level, RED seems to be the best candidate for this job.

That is why the goal of this work is to explore the use of stand-alone RED to recover energy from the dilution of real fresh and hydrolysed urine.

Also, for the first time, real urine was used both as a high-concentration solution and as an electrolyte solution. This would reduce the costs of the process, as no additional chemicals e.g, electrolytes would be required. Additionally, the net chemical reactions occurring at the

electrode compartment when urine is used as electrolyte solution could promote organics and nitrogen removal. Finally, the transport of plant macronutrients (N, P, K) from urine to the freshwater was also investigated to understand if the low concentration solution could then be used as fertigation solution.

## 7.3 Experimental Investigations

### 7.3.1 Experimental plan

#### 7.3.1.1 Process Description

Two different process operation modes were adopted and compared. While the first approach is expected to maximise the energy recovery (i.e., System A), the second does not need any additional chemical (i.e., System B) (see Figure 7-1):

- System A: A mixture of  $\text{K}_4\text{Fe}(\text{CN})_6/\text{K}_3\text{Fe}(\text{CN})_6$  and  $\text{NaCl}$  was recirculated as electrolyte solution (ES)
- System B: Urine was flowed, in single-pass, as ES

Both systems were tested with fresh and hydrolysed human urine as HC solutions. That is because fresh and hydrolysed urine are chemically very different as, when stored without any pH adjustment, the urea in the fresh urine hydrolyses into ammonia and bicarbonate causing a significant increase in urine ionic strength and pH (Randall et al. 2016; Ray, Saetta & Boyer 2018; Volpin, Yu, et al. 2019). In this work, we refer to the urine before ureolysis as FU and after as HU. Also, each test was firstly run with synthetic urine solution (Table S1) and afterwards, a real solution. The model solutions were used to provide an upper boundary in the maximum energy extractable from human urine. That is because synthetic urine resembles the ionic strength and composition of real urine without its complex, and high fouling, organic matrix. All the experimental investigations were run were in triplicates.

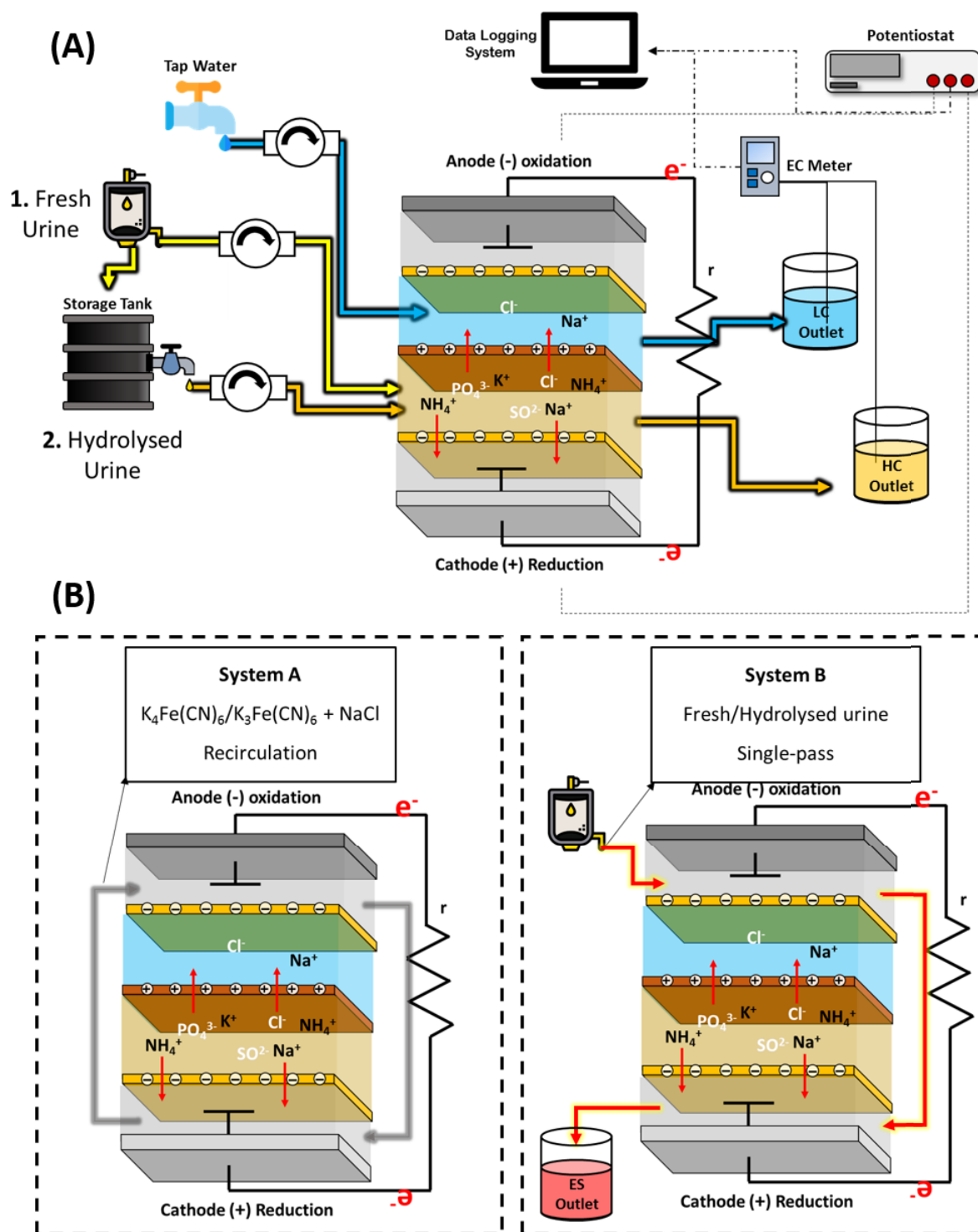


Figure 7-1 (A) Schematic drawing of the single-pass RED experiments using fresh and hydrolysed urine. (B) Schematics of the two different configurations used for the experiments. In the first configuration, (System A)  $K_4Fe(CN)_6/K_3Fe(CN)_6$  are used as ES and recirculated

in the anode and cathode chamber. In the second configuration (System B), real fresh or hydrolysed urine is used as ES.



Figure 7-2 Picture of the RED setup used for the experiments.

### 7.3.2 HC and LC solutions

The collection, characterization and storage of urine is described in 0 Before the feeding in the module, HU was pre-filtered using a 0.1  $\mu\text{m}$  hollow fibre microfiltration module to remove the carbonates and phosphates salts that typically precipitate during urine hydrolysis. This was done to prevent clogging of the RED flow channels.

Before running the experiments with real urine, synthetic FU and HU solutions were prepared as per Table 3-1 and fed to the RED stack. The results from these tests were used to compare OCV and  $PD_{gross}$  of synthetic and real urine, as well as to analyse the transport of monovalent and multivalent anions and cations from the HC to the LC solution. Each stack was also tested with synthetic seawater (0.6 M NaCl) before and after the urine experiments to ensure similar stack baseline performances and measure any loss in performance after the urine tests. All the standard tests were performed using 0.015M NaCl as LC solution. However, to have consistent results, real freshwater (Table 6-1) was also tested with real FU and HU before the analysis of the fouled membrane. This was done to see if any of the  $Ca^{2+}$  or  $Mg^{2+}$  in the freshwater would precipitate on the IEMs. However, the results might differ if harder water is used.

Finally, both the LC and HC solutions were fed to the RED cell, in single-pass and counter-current flow, using peristaltic pumps (Longer BT100 2 J). Flow rates of 5, 10, 15, 25 and 35 mL/min were used and kept the same for both HC and LC solutions at all conditions. According to equation (7-1), where  $A_{cs}$  is the channels' cross-section area (as spacer thickness multiplied by channel width) and  $\phi$  is the spacer' open area, the above flowrates translate in linear velocities of 2.82, 5.65, 8.47, 14.1 and 19.8 cm/s.

$$v \left[ \frac{cm}{s} \right] = \frac{Q \left[ \frac{mL}{min} \right]}{60 \cdot A_{cs} [cm^2] \cdot \phi [\%]} \quad (7-1)$$

### 7.3.3 Electrolyte solutions

The experiments for System A (Figure 7-1 B) were conducted recirculating a mixture of the reversible redox couple  $K_3Fe(CN)_6/K_4Fe(CN)_6$  (0.05 M) combined with 0.5 M NaCl, while in System B real FU or HU were used both as HC and ES solution (Figure 7-1 B). In both cases,

the ES solutions were recirculated with a flow rate of 5 mL/min independently of the HC and LC solution flow rates.

#### 7.3.4 Reverse electrodialysis cell

The RED cell consisted of a 20 cell pair stack, each with an area of 19.63 cm<sup>2</sup>, with an overall active membrane area of 0.039 m<sup>2</sup>. Each membrane pair was separated by a reinforced glass fibre gasket and a woven mesh PTFE spacer having a thickness of 100 µm to create an adequate flow channel. The lab-scale RED stack was provided by Jeju Global Research Center (JGRC) of Korea Institute of Energy Research (KIER). The spacer had an open area of 51% with a porosity of 70%. The electrode compartments (HCs), sitting at the anode and cathode of the cell, comprised a Pt/Ti mesh (coating thickness, 3 µm, Wesco Electrode, South Korea) welded to a titanium rod which was then connected to the source meter (Keithley 2400, Ohio, USA) (Kim, Jeong, et al. 2019). Type I Fujifilm AEMs and CEMs were used for the experiments. The first characteristics are displayed in the table below (Table 7-1). New pristine membranes were used after each test with real human urine.

Table 7-1 Characteristic and proprieties of Fujifilm Type I membranes.

Proprieties	AEM-Type I	CEM-Type I	Unit
Membrane type	Homogeneous	Homogeneous	-
Thickness	125	135	μm
Permeselectivity:			
KCl (0.05 - 0.5M)	92	93	%
NaCl (0.05-0.5M)	92	92	%
Electrical Resistance:			
2M NaCl	0.8	1.3	Ω.cm <sup>-2</sup>
0.5M NaCl	1.3	2.7	Ω.cm <sup>-2</sup>
Water permeation	6	10	kg.cm <sup>-2</sup>
pH Stability	2 to 10	4 to 12	-

### 7.3.5 Theoretical and experimental electrochemical calculations

#### 7.3.5.1 Specific extractable energy from human urine

The theoretical energy, as maximum Gibbs free energy ( $\Delta G_{\max}$ ), from the dilution of human urine, was calculated as in Lin S. (2014) (Lin, Straub & Elimelech 2014). This was done to calculate the energy efficiency ( $\eta$ ) of the process.  $\eta$  was calculated via equation (7-2), where  $E_{\text{Net}}$  is the measured recovered energy.

$$\eta [\%] = \frac{E_{\text{Net}} \left[ \frac{\text{kWh}}{\text{m}^3} \right]}{\Delta G_{\max} \left[ \frac{\text{kWh}}{\text{m}^3} \right]} \cdot 100 \quad (7-2)$$

To define  $\Delta G_{\max}$ , some initial assumption had to be made. Firstly, the osmotic pressure of the solutions was approximated using the van't Hoff equation  $\pi(c) = vRTc$ , where  $v$ , is the van't Hoff factor for strong electrolytes,  $R$  and  $T$  are ideal gas constant and temperature, respectively. An activity coefficient of one was used for the calculations. Using an activity coefficient of one, Lin S. (2014) (Lin, Straub & Elimelech 2014) showed less than 10% error on the  $\Delta G$  of RO brine/river water mixing. As urine is even more dilute than seawater, it is expected that the

error would be even lower. Finally, a maximum HC/LC mixing fraction of  $\phi = 50\%$  was used for the calculations as both solutions were pumped at the same rate (i.e., at equilibrium 50% of the solutes in the HC solution will be moved to the LC solution). Once these assumptions were made, the  $\Delta G_{\max}$  for synthetic FU and HU was calculated using equation (7-3) (Lin, Straub & Elimelech 2014; Straub, Deshmukh & Elimelech 2016; Volpin, Gonzales, et al. 2018; Yip & Elimelech 2012). The osmotic pressure of FU and HU is shown in Table 3-1.

$$\Delta G_{\max} = \Delta G(\phi = 0.5) = \pi_M \ln(\pi_M) - \phi \pi_{LC} \ln(\pi_{LC}) - (1 - \phi) \pi_{HC} \ln(\pi_{HC}) \quad (7-3)$$

### 7.3.6 Power density and energy recovery

Gross power densities measurements were conducted using a source meter (Keithley 2400, Ohio, USA) as galvanostat. A linear current from 0 to 100 mA was swept, with 5 mA step and 30 seconds of delay, and Keithley KickStart software (Tektronix, Oregon, USA) was used to record the voltage (V). Equation (7-4) was used to calculate the gross power density ( $PD_{Gross}$ ) (Nam et al. 2018). For each experiment, an initial stabilisation period of at least 10 minutes was used to obtain stable OCV measurements. Afterwards, the slope of the I-V curve (where V is the voltage and i the specific current density) gave the value of  $R_{stack}$ .

$$PD_{Gross} \left[ \frac{W}{m^2} \right] = V \cdot i \quad (7-4)$$

The net power density ( $PD_{Net}$ ) was then calculated by subtracting the energy of pumping the HC and LC solutions (i.e.,  $2 \cdot P_{pumping}$ ) to the  $PD_{Gross}$  value (Eq. (7-5)). After measuring the pressure drop via a high resolution ( $\pm 0.1$  kPa) pressure sensor (Keller, Reinacherstrasse, Basel, Switzerland), the pumping energy was calculated as assuming 70% pump efficiency.

$$PD_{Net} \left[ \frac{W}{m^2} \right] = PD_{Gross} - \frac{2 \cdot P_{pumping}}{A_t} \quad (7-5)$$



Finally,  $E_{Net}$  was calculated as the produced power per urine flow rate pumped through the stack (Eq. (7-6)).

$$E_{Net} \left[ \frac{kWh}{m^3} \right] = \frac{PD_{Net} \cdot A_t}{Q_{Urine}} \quad (7-6)$$

### 7.3.7 Nutrients recovery and removal

#### 7.3.7.1 Chemical analysis

Anions, cation and organics were measured as described in 0

#### 7.3.7.2 Mass balance calculations for nutrients recovery

The transport of ions (and urea) from the HC to the LC solution were measured for each different feed solution, operating mode and linear velocities. As both HC and LC solutions were pumped with the same flow-rate, and assuming a negligible water transport due to osmosis, mass balance equations were used to calculate the recovery of each targeted species (Eq. (7-7)).

$$C_{i,recovery}[\%] = 1 - \frac{C_{i(HC,Eff)} \left[ \frac{mg}{L} \right]}{C_{i(Urine)} \left[ \frac{mg}{L} \right]} \approx \frac{C_{i(LC,Eff)} \left[ \frac{mg}{L} \right]}{C_{i(Urine)} \left[ \frac{mg}{L} \right]} \quad (7-7)$$

Here,  $C_{i(HC,Eff)}$  and  $C_{i(LC,Eff)}$  are the concentration of the targeted species (i), in HC and LC solutions, after passing through the stack.  $C_{i(Urine)}$  is the initial concentration of the species (i) in the urine. If the difference between the mass balance in the HC and LC solution was less than 5%, an average between the two values was taken. HC and LC effluents were sampled after operating the stack for at least 15 minutes at the amperage that maximises  $PD_{gross}$ . During this period, voltage and pressure losses were continuously measured to ensure that the system was operated in steady-state conditions.

Finally, the difference in the TDS between the inlet urine and the HC and LC effluents was also measured to calculate the overall TDS recovery using equation (7-7).

#### 7.3.7.3 TOC, nitrogen and chloride removal calculations

In the case of Scenario B, similar mass balance calculations were performed. This time, though, any change in the  $\text{NH}_3/\text{NH}_4^+$ , urea, TN, TOC and  $\text{Cl}^-$  concentrations in the urine before and after passing through the stack was attributed to the redox reactions occurring inside the ECs. Also, in this case, a sample was taken only after reaching stable voltage readings.

$\text{NO}_2^-$  and  $\text{NO}_3^-$  concentrations at the effluent were also measured as  $\text{NH}_4^+$  could be directly oxidised to those species (Tarpeh et al. 2018). Overall, the removal of the selected compounds (i) was calculated as  $C_{i,\text{removal}} [\%] = 1 - (C_{i (\text{Urine, Effluent})} [\text{mg/L}] / C_{i (\text{Urine, Influent})} [\text{mg/L}])$ .

#### 7.3.8 Membrane characterization

Pristine and fouled AEMs and CEMs were analysed as described in 0.

## 7.4 Results and Discussion

### 7.4.1 System's A performance

In this section, the outcomes from the experiments that employed  $\text{K}_3\text{Fe}(\text{CN})_6$ /  $\text{K}_4\text{Fe}(\text{CN})_6$  as ES are discussed. The change in  $\text{PD}_{\text{Net}}$ ,  $\text{E}_{\text{Net}}$  and N/P/K recovery at increasing urine flow rate were investigated. Baseline tests using synthetic seawater were also conducted and the results shown in Figure 7-4A and Figure 7-3. The goals of the section were:

- To describe and discuss the differences in the outcomes using fresh and hydrolysed urine,
- To provide an optimal stack operating condition to balance the trade-off between power density and energy/nutrients recovery.

### 7.4.2 Baseline NaCl tests

As a benchmark for the experiments, the baseline performance of the RED stack was firstly assessed using 0.6M NaCl as HC solution and 0.015M NaCl as LC solution. Performance parameters such as: OCV [V], stack resistance [ $\Omega$ ], pressured drop [bar], maximum  $\text{PD}_{\text{Gross}}/\text{PD}_{\text{Net}}$  [ $\text{W.m}^{-2}$ ], transport of ions from the HC to the LC solution [%],  $\text{E}_{\text{Net}}$  [ $\text{kWh.m}^{-3}$ ] and  $\eta$  [%] are all displayed in Figure 7-3. The error bars in the graphs of Figure 7-3 show the variability in the results from all the NaCl experiments. NaCl experiments were conducted before and after each experiment with synthetic and real urine. This was to ensure that each new stack had similar baseline performances and it gave an indication on whether organic or inorganic depositions on the IEMs had an impact on the stack's performance. From the results it seems that the change in the baseline performances was never above 10%.

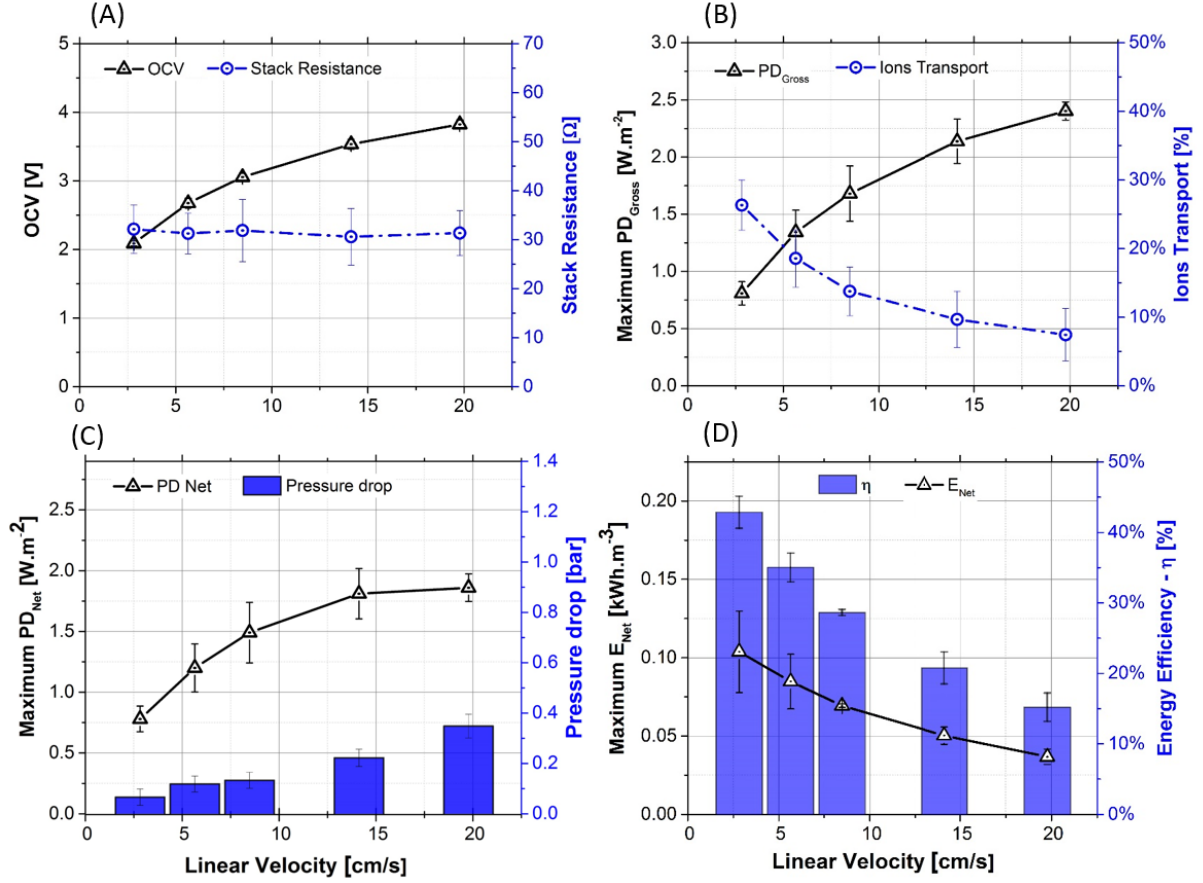


Figure 7-3 Baseline performances of the RED stack operated with an 0.6M NaCl solution as HC solution and  $K_3Fe(CN)_6$ /  $K_4Fe(CN)_6$  as ES. HC and LC solutions were flowed inside the stack in single-pass and with flow rates of 5, 10, 15, 25 and 35 mL.min<sup>-1</sup>.

### 7.4.3 Energy Recovery and Energy Efficiency

#### 7.4.3.1 Synthetic vs real urine

Synthetic FU and HU were tested to provide an upper boundary in the maximum energy extractable from human urine. In fact, Figure 7-4 shows that between real and synthetic FU there is a 10-12% drop in RED performances, which increases up to 90% in the case of HU. While the effect of organic fouling on the AEMs and spacers would be the main reason for the drop in the FU performances (Rijnaarts et al. 2019), real HU also suffered from higher ohmic resistance due to its lower EC values compared to synthetic HU. That is because the synthetic

recipe used to simulate HU overestimated its ionic strength as it disregarded the ammonia losses due to volatilisation. Regarding the effect of organic fouling on the RED performance, Rijnaarts T. (2019) found a 15-20% decrease in RED performances after operating it with natural river water for over a 12 day (Rijnaarts et al. 2019). Of that, only 2-4% was due to an increase in AEMs resistance and decrease in its permselectivity due to sorption of humic-like substances. The remaining was due to spacer fouling. Despite that our experiments were run only for a maximum of 8 hours, the concentration of LMW organics and humic-like substances in real urine is up to 50 times higher compared to river water (Jacquin et al. 2018). As such, AEMs performance drop is highly likely when using real urine. The characterisation of IEM fouling when using real urine will be explained more in details below.

Comparing the performances of real urine, fresh and hydrolysed, with synthetic seawater, a common RED benchmark, it is clear that urine achieved rather low current densities (60-70% less  $PD_{Gross}$ ). This translates in much higher capital costs as more stacks will be required. However, in the case of HU, there seems to be a large margin of improvement as synthetic HU achieved performances similar to seawater. As such, the next section focuses on the comparison between the performances of fresh and hydrolysed urine.

The open circuit voltage is a measurement of the driving force for the RED process, given by the sum of the Donnan potential steps across all membranes in the system. Figure 7-4 reveals that the driving force is similar for all cases, with the exception of real hydrolysed urine, whereby the open circuit voltage seems to be approximately 0.5 V lower than all other cases. This could be ascribed to organic fouling changing the surface charge of the membranes. Moreover, the  $i$ -V curves for HU (both synthetic and real) display higher slopes than the seawater benchmark, despite having similar or higher ionic conductivities. This again leads to the hypothesis of organic fouling introducing additional resistance.

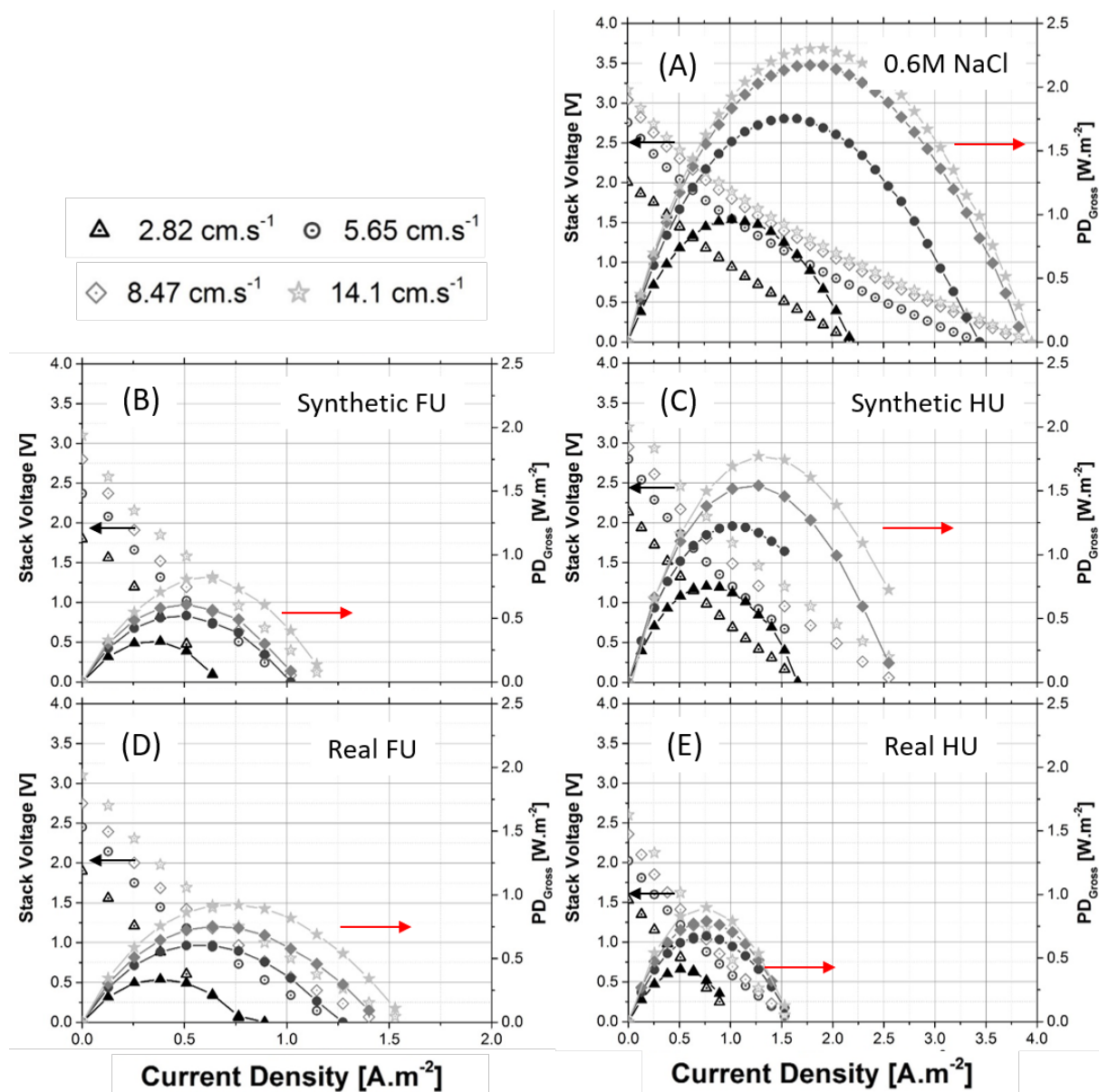


Figure 7-4 Performances of the RED stack operated with an 0.6M NaCl solution, Synthetic FU and HU and real FU and HU. The solutions were flowed inside the stack in single-pass and with flow rates of 5, 10, 15, 25 and 35 mL.min<sup>-1</sup> and K<sub>3</sub>Fe(CN)<sub>6</sub>/ K<sub>4</sub>Fe(CN)<sub>6</sub> was used as ES.

#### 7.4.3.2 Real FU vs HU performances

Figure 7-5 also shows that the performances of real HU are just  $13 \pm 4\%$  higher than FU, even though HU has 40% higher salinity compared to FU (i.e., 33.1 vs 20.1 mS/cm) and a much

lower concentration of multivalent ions (as almost half of the  $\text{PO}_4^{3-}$  and all the  $\text{Ca}^{2+}$  and  $\text{Mg}^{2+}$  precipitates during storage). The explanation for this could be twofold.

The most plausible reason is that HU has higher fouling tendency compared to FU due to the bacterial-aided transformation of the organics in urine during storage. In fact, Figure 7-12 shows a significantly higher amount of coloured compounds deposited on the AEMs tested with real HU, though fouling did not cause any steep increase in the urine channel's pressure drop, which increased linearly at increasing flow velocity (Figure 7-5 A).

Additionally, we here propose another mechanism that could have enhanced FU performances. The hypothesis we make is that the high flux of urea from the HC to LC solution in FU could accelerate the ionic transport to the LC solution, as urea molecules could have helped to push the ions through the IEMs. In fact, the uncharged nature, high diffusivity coefficient (i.e.,  $1.38 \cdot 10^9 \text{ m}^2/\text{s}$ ) and high concentrations of urea in FU would mean that a significant amount would diffuse through the IEMs following a pure diffusion-driven model (Ma et al. 2018). This can be observed by looking at the high TN in the LC effluent when using FU (Figure 7-7B). However, at this stage, this hypothesis still has to be experimentally validated.

Overall, at the tested flow rates, real FU achieved  $\text{OCV} = 1.6 - 3.3 \text{ V}$ ,  $\text{PD}_{\text{Net}} = 0.32 - 0.75 \text{ W.m}^{-2}$ ,  $\text{E}_{\text{Net}} = 0.006 - 0.039 \text{ kWh.m}^{-3}$  and overall energy efficiency  $\eta = 5 - 22\%$  (assuming  $\Delta\text{G}_{\text{FU,Max}} = 0.140 \text{ kWh.m}^{-3}$ ). For real HU,  $\text{OCV} = 1.53 - 2.75 \text{ V}$ ,  $\text{PD}_{\text{Net}} = 0.40 - 0.70 \text{ W.m}^{-2}$ ,  $\text{E}_{\text{Net}} = 0.018 - 0.053 \text{ kWh.m}^{-3}$  and  $\eta = 7 - 20\%$  were obtained ( $\Delta\text{G}_{\text{SU,Max}} = 0.262 \text{ kWh.m}^{-3}$ ). Both energy values are quite low in comparison with other renewable energies. For example, assuming an average power density of  $17 \text{ W/m}^2$  for a commercial solar panel,  $1 \text{ m}^2$  of solar panel would be equivalent to approximately the daily amount of energy produced by a group of over 20 people.

The only other available benchmark to these results is from a recent article from Mercer et al. (2019). Their experimental conditions, however, were quite different. Firstly, they operated in co-current mode and used an 0.25 M NaCl as the electrode rinse solution. Additionally, the authors concentrated real HU twice (i.e., from EC of 12.4 mS/cm to 24.1 mS/cm) using MD. As MD is a thermal process and HU has over 30% of its nitrogen in the form of volatile ammonia, it is expected that some of the ammonia would be lost in the MD permeate during the concentration process. The combination of all the above could explain why the authors achieved lower performances (i.e.,  $OCV \approx 0.79 - 0.9$  V and  $PD_{Gross} \approx 0.2 - 0.3$  W.m<sup>-2</sup>).

Finally, given the trade-off between power density and energy recovery, this section aimed at suggesting an optimal operating range to achieve relatively high  $PD_{Net}$  and  $E_{Net}$ . Overall, the results showed that low flow velocities, i.e. 2.5 – 7.5 cm/s are recommended to obtain reasonable PD and  $E_{Net}$  values.

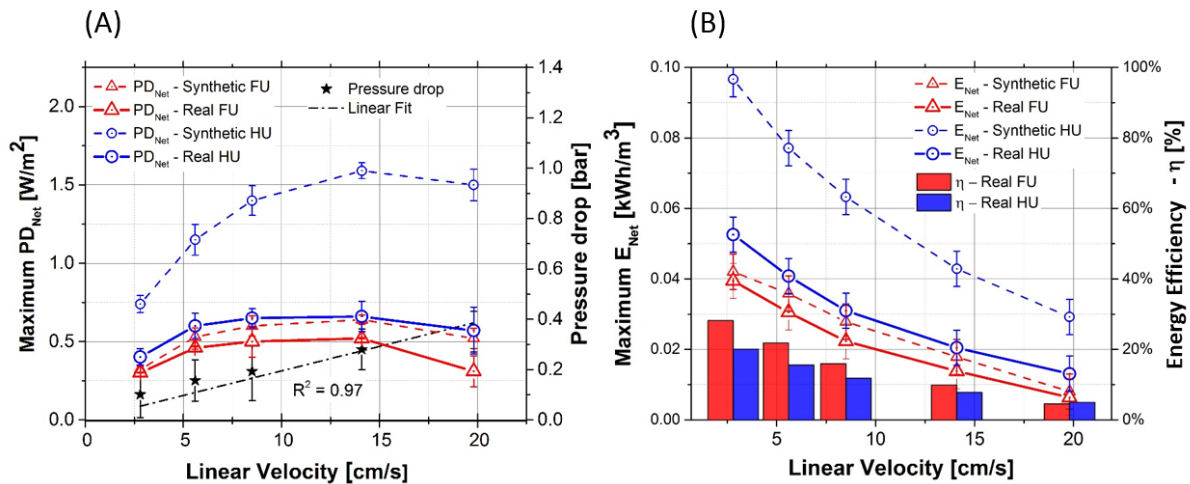


Figure 7-5 (A) shows the net power densities achieved ( $PD_{Net}$ ), Figure (D) displays the energy recovered  $E_{Net}$  and energy efficiency  $\eta$  are displayed. HC and LC solutions were flowed inside the stack in single-pass and with flow rates of 5, 10, 15, 25 and 35 mL.min<sup>-1</sup> and  $K_3Fe(CN)_6/K_4Fe(CN)_6$  was used as ES.



## 7.4.4 Ionic Transport

### 7.4.4.1 Synthetic Urine

The transport of the main species through the IEMs was firstly analysed at different linear velocities. Figure 7-6 shows a characterisation of the transport of different species when synthetic FU (Figure 7-6A) and synthetic HU (Figure 7-6B) were used. Synthetic solutions were used to eliminate the effect of membrane fouling. As expected, the transport rate of multivalent ions (e.g.,  $\text{SO}_4^{2-}$ ,  $\text{PO}_4^{3-}$ ) is 2 to 5 times lower compared to monovalent ions (e.g.,  $\text{Na}^+$ ,  $\text{K}^+$ ,  $\text{Cl}^-$ ). Interestingly, HU has higher  $\text{Cl}^-$  and slightly lower  $\text{Na}^+$  and  $\text{K}^+$  transport compared to FU. This could be to balance the more significant flow of  $\text{NH}_4^+$  ions in HU, as they account for over 70% of all the cations in HU, compared to only 10% in FU.

By focusing on the total nitrogen transport, FU shows a lower decrease in the TN transport at increasing flow velocities. This could be due to the high concentration of urea, which is uncharged, whose transport is regulated solely by the concentration difference in the HC-LC channels as it follows the solution-diffusion transport mechanism (Ma et al. 2018) solely. As such, the flow rate would have an effect on the urea transport only when it increases the HRT enough to allow for a higher  $\Delta C_{\text{Urea}}$  inside the stack.

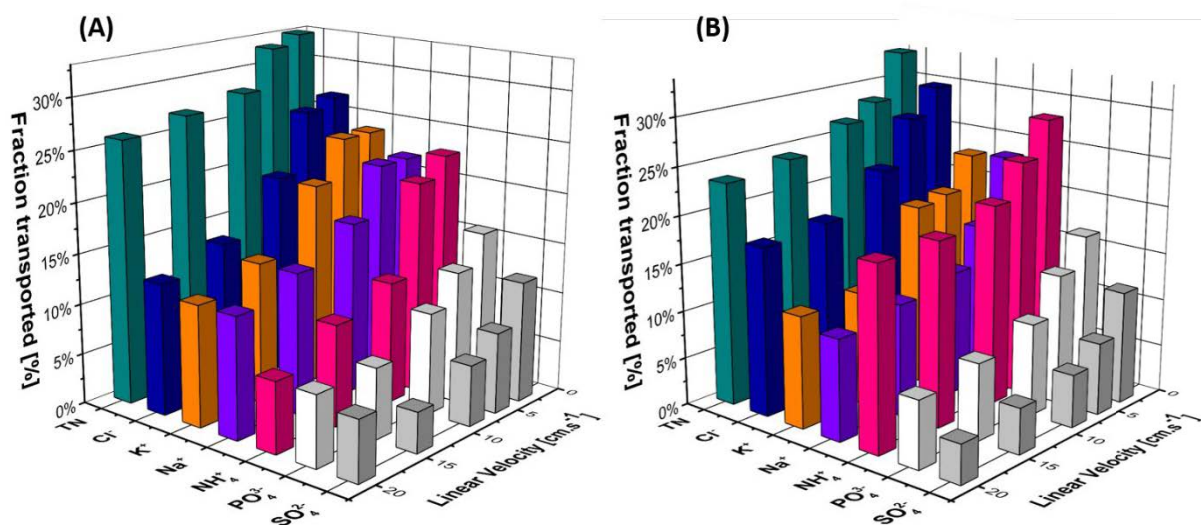


Figure 7-6 Single ion species transport from HC to LC at different flow velocities. In Figure (A) synthetic FU was used while synthetic HU was used in Figure (B).

#### 7.4.4.2 Real Urine

Figure 7-7 A shows that the relative ionic transport from the real urine to the LC solution. The widening gap between FU and HU results at increasing flow velocities could also be the results of lower AEMs permselectivity due to more severe fouling deposition in AEMs fouled with HU. These EC data, however, provide only a piece of information on the electrolyte transport, while neglecting ammonia and urea. As such, Figure 7-7 B shows the overall transport of TN,  $\text{PO}_4^{3-}$  and  $\text{K}^+$  (i.e., N/P/K). N, P, K analysis were chosen as it is hypothesised that the LC effluent could be used as fertigation water.

Overall, by operating at 5.61 cm/s, which has been previously identified as an optimal velocity to maximise the stack's performance, about  $30 \pm 5\%$  of nitrogen,  $5 \pm 2.1\%$  for phosphorus, and  $31 \pm 4\%$  for potassium were recovered in the LC solution.

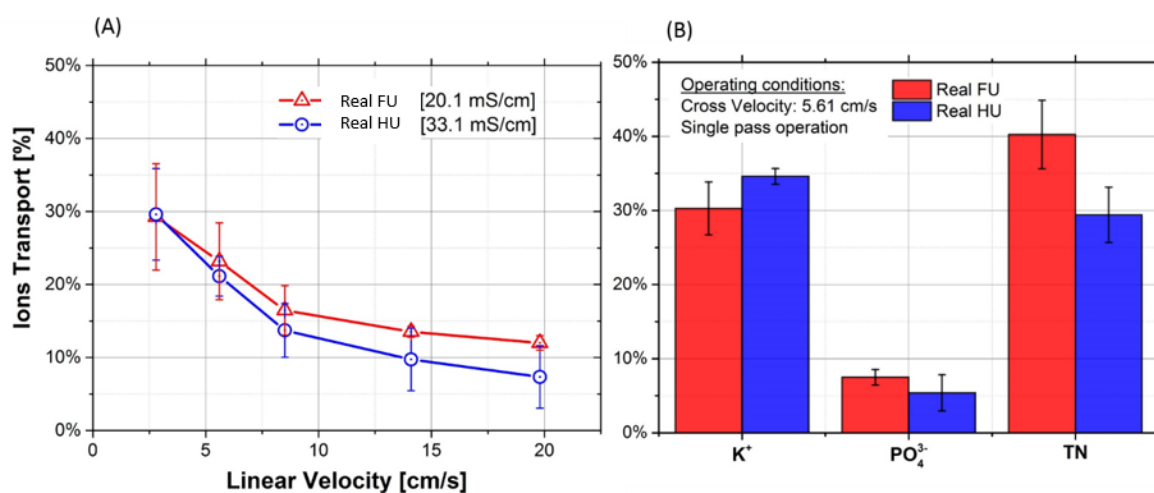


Figure 7-7 (A) shows the overall ions transport, based on electric conductivity measurements, from the HC to the LC solution at increasing urine flow rate. The overall nutrients recovery,

measured as the transport of nitrogen/phosphorus/potassium from urine to the Lc solution, is displayed in Figure (B).

#### 7.4.5 System's B performance

In this section, the outcomes from the experiments that employed urine as ES are discussed. The principal goal of this configuration was to compare the power densities achievable with urine as ES and whether TOC or TN removal can occur at the electrode chambers.

##### 7.4.5.1 Energy Recovery, Energy Efficiency and ionic transport

Figure 7-9 and Figure 7-8 show that despite only having a decrease in OCV of just 10 - 20% compared to synthetic urine, the reduction in  $PD_{Gross}$ ,  $PD_{Net}$  and  $E_{Net}$  in real urine was between 80 – 110%. Additionally, a 10 - 50% decrease in ionic transport was also observed (Figure 7-10A).

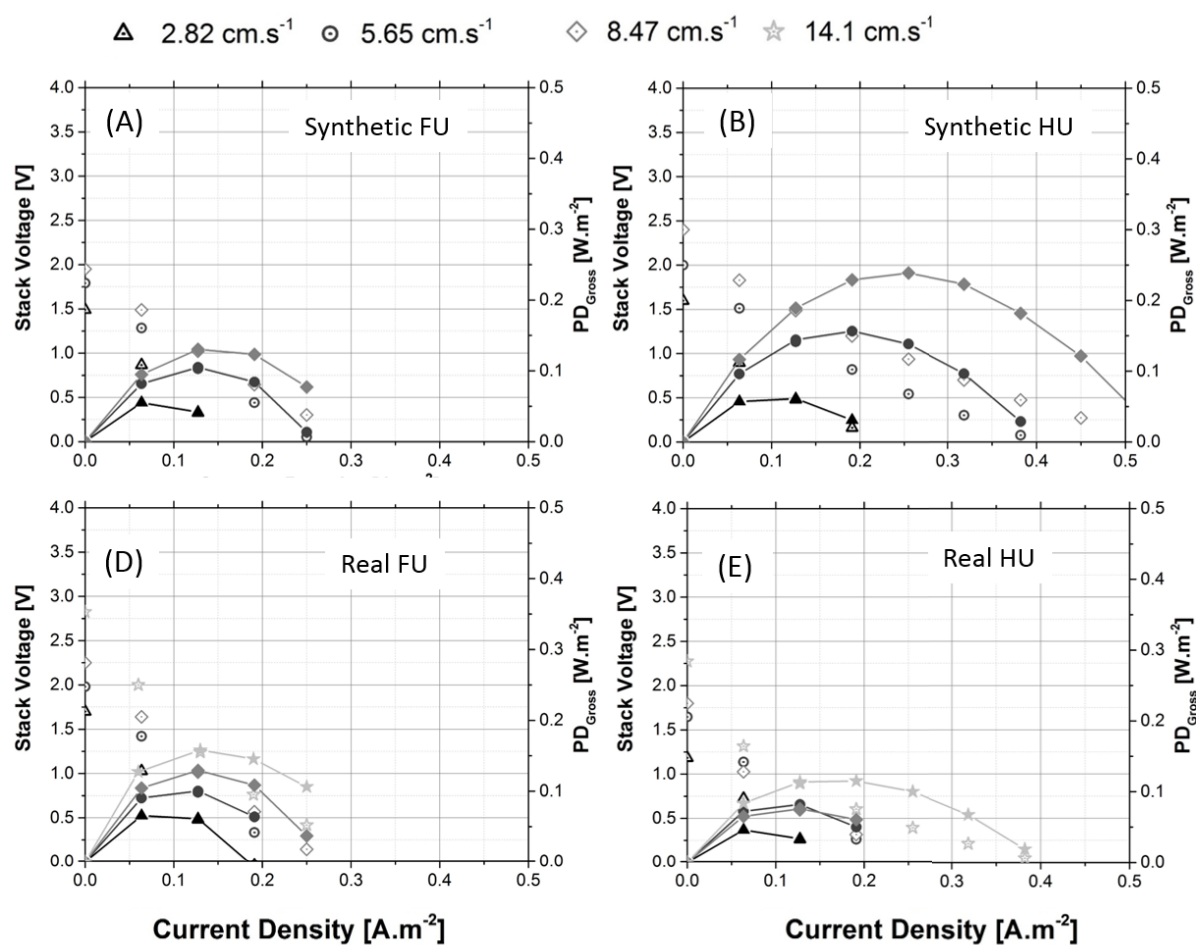


Figure 7-8 Performances of the RED stack operated with a Synthetic FU and HU and real FU and HU as both HC and ES solution. HC and LC solutions were flowed inside the stack in single-pass and with flow rates of 5, 10, 15, 25 and 35 mL.min<sup>-1</sup> while the ES solution flowed at 5 mL.min<sup>-1</sup>.

While the reduction the OCV and ionic transport could be explained by urine higher ohmic resistance, compared to  $K_3Fe(CN)_6/K_4Fe(CN)_6 + NaCl$ , the decrease in power and energy recovery was also due to the electromotive force and overpotentials of the oxidation and reduction reactions occurring at the ECs. This is also confirmed by the reduction in  $NH_4^+$ , urea and TOC concentrations in Figure 7-11.

As the relative ionic transport decreases compared to System A, the recovery of  $K^+$  and  $PO_4^{3-}$  from real urine was also found to be about 2 – 5 times lower. That is probably because the transport of uncharged urea and ammonia from the HC to the LC solution would not be affected by the increase in ohmic resistances as is purely regulated by their concentration profile.

Overall, utilising urine as ES drastically decreases the energy efficiency and nutrients recovery of the process as it increases the stacks resistance and the voltage losses due to net chemical reactions at the electrodes.

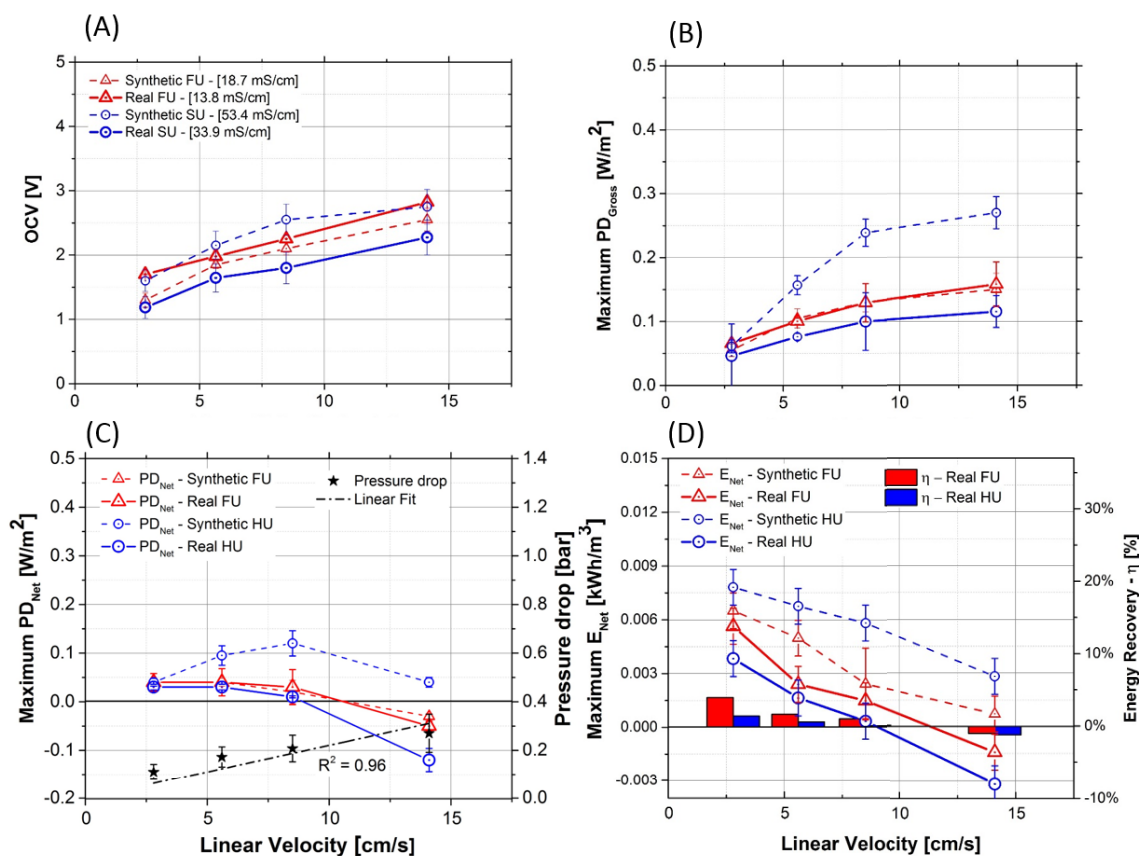


Figure 7-9 Baseline performances of the RED stack tested with synthetic and real FU and HU solutions both as HC and ES solutions. HC and LC solutions were flowed inside the stack in single-pass and with flow rates of 5, 10, 15, 25 and 35 mL.min<sup>-1</sup> while ES was pumped with a flow rate of 5 mL.min<sup>-1</sup>.

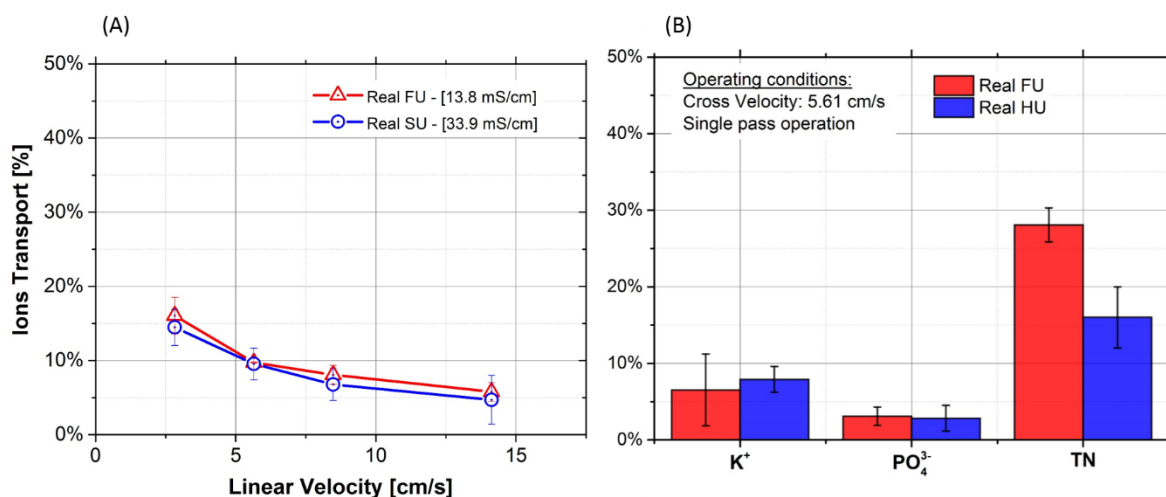


Figure 7-10 (A) shows the overall ions transport, based on electric conductivity measurements, from the HC to the LC solution at increasing urine flow rate. The overall nutrients recovery, measured as the transport of nitrogen/phosphorus/potassium from urine to the LC solution, is displayed in Figure (B).

#### 7.4.5.2 Change in the Cl<sup>-</sup>, NH<sub>4</sub><sup>+</sup>, urea and TOC in the electrolyte solution

Here, urine mass balance results, before and after flowing through the ECs of the RED stack, are presented. The stack was always operated at the current densities that maximise the power densities (Figure 7-8). The initial hypothesis was that the sharp reduction in the stack's performances was a result of net chemical reactions occurring at the ECs.

The open-circuit voltages as shown in Figure 7-9 are in most cases higher than the minimum voltage to achieve water splitting (i.e., 1.229 V) or anodic chloride formation coupled to cathodic hydrogen evolution (i.e., 1.358 V). However, that does not necessarily mean that reactive oxygen species or free chlorine species were produced (Katsounaros et al. 2012; Tarpeh et al. 2018), as activation overpotentials could have played a major role. Indeed, Figure 7-11 shows that the Cl<sup>-</sup> mass balance in the urine before and after the flowing through the anode and cathode is closed, indicating no loss to chlorine gas or chlorinated by-products. As such, it

is suggested that no free chlorine was produced. This is a positive result as Zöllig H. (2015) demonstrated that the formation of  $\text{Cl}_2$  (gas) in urine can lead to the formation of dangerous chlorination by-products (Zöllig et al. 2015).

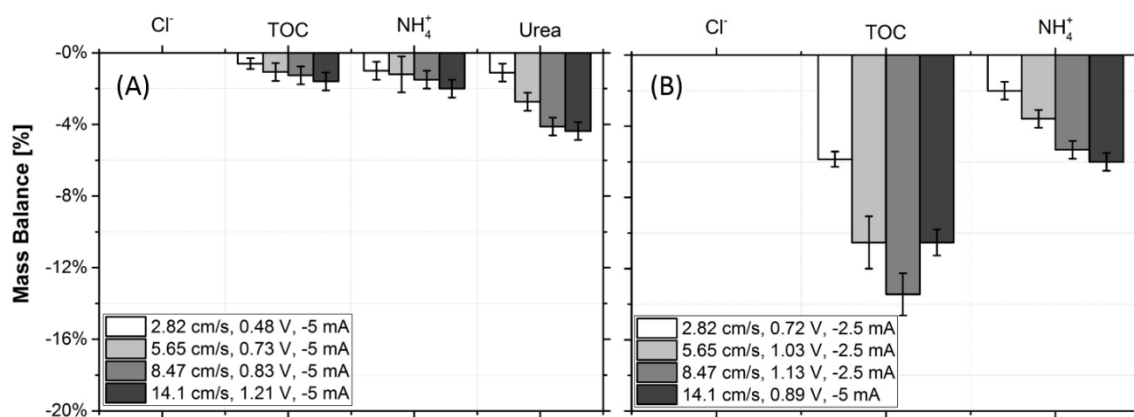
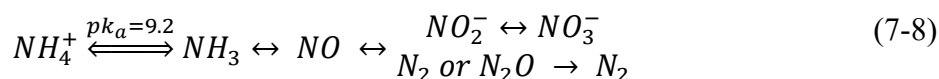
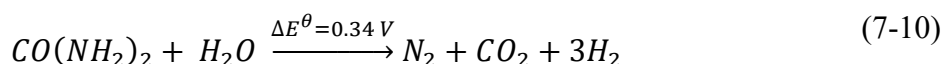
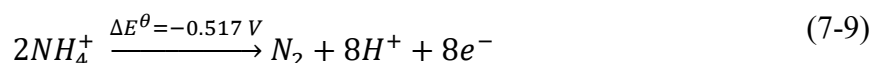


Figure 7-11 Mass balance of the  $\text{Cl}^-$ , TOC,  $\text{NH}_4^+$  and urea in the urine used as electrolyte solution at different stack's voltage and current. The mass balance was calculated as per section 2.3.3, and the ES was pumped with a flow rate of 5 mL/min. Figure A shows the results for real FU while real HU is shown in Figure B.

Figure 7-11 shows that  $\text{NH}_4^+$  removal ranged from 0% - 5% and it was highest when using HU. On the other hand, up to 4.4% of the initial urea was removed (i.e., 397 mg/L of urea) in FU. In the case of ammonia, if no free  $\text{Cl}_2$  was produced, indirect oxidation through monochloramine should not have occurred (Candido & Gomes 2011). One other hypothesis is the direct ammonia oxidation through  $\text{NO}_2^-/\text{NO}_3^-$  (Eq. (7-8) (Candido & Gomes 2011; Tarpeh et al. 2018). In fact, platinum-based electrodes, like the one used in this study, have often proven to be an effective electro-catalyst for the oxidation of  $\text{NH}_4^+$  to  $\text{NO}_3^-$  or  $\text{N}_2$  gas (Bunce & Bejan 2011).



Also, it was found that the ammonia removal for HU was about 3 times higher compared to FU, and  $NO_3^-$  and  $NO_2^-$  concentrations of  $4.5 \pm 0.4$  mg/L and  $0.1 \pm 0.04$  mg/L were measured in HU effluents but not in FU effluents. That is probably because of the high concentration of ammonia in HU, whose lone electron pair makes it easier to be oxidised compared to  $NH_4^+$  ion (Cheng, Scott & Christensen 2005). While ammonia adsorbs onto the surface of the electrode before being oxidised to  $N_2$ , at pH < 7 no adsorption/oxidation occurs, and  $NH_4^+$  is directly decomposed to  $N_2$  as per reaction below (Eq. (7-9)) (Candido & Gomes 2011). In the case of urea, Eq. (7-10) was suggested as a possible degradation pathway (Ye et al. 2018).



Finally, TOC removal of up to 13% was measured in HU. At this stage, though, it is still unknown whether the mineralisation has occurred through direct electrochemical oxidation, indirect oxidation due to water splitting and the formation of reactive oxygen species (ROS) or a combination of both. Also, the TOC removal in HU is over 6 times higher than FU. That might be because of the high concentration of LMW acids and neutrals (MW < 350 Da) in urine ( $62 \pm 16\%$  of the TOC) which are generally more efficient in alkaline media as it occurs with lower overpotential (Jacquin et al. 2018; Munoz et al. 2015).

To conclude, the mass balance of  $NH_4^+$ , urea and TOC showed that some degree of removal was achieved, which would also explain the lower stack's performances when urine was used as ES. However, the redox reactions occurring at the anode and cathode compartments are still quite speculative and should be investigated further. Additionally, it should be noted that, with



the stack's scale-up and optimisation, higher voltages are expected which could lead to the formation of chlorine, peroxides, persulfate species. This, together with the effect of electrode material, HRT and current density, should be optimised to achieve a higher degree of nutrients removal.

#### 7.4.6 Characterisation of used AEMs and CEMs

The high concentration of LMW organic acids, such as oxalic, uric, citric, hippuric, lactic and acetic acid (Putnam 1971a), in urine, makes it a solution with high fouling potential (Nam et al. 2018). This is particularly true for HU as during storage anaerobic microorganisms can use the creatinine, fatty acids and other organic acids in urine as an electron donor to grow and possibly release high fouling potential polymeric substances (Udert, Larsen & Gujer 2006). The results of the interaction between organics and the AEMs is evident when looking at Figure 7-12. There, the change in AEMs colour before and after testing the stack with real urine is quite evident (especially for HU). Given the negative charge density of LMW acids, it is expected that the positive fix charge in AEMs would allow them to migrate through and possibly accumulate on the membrane's surface (Rijnaarts et al. 2019). This was confirmed both by analysing the TOC transport to the LC effluent and by analysis FTIR analysis (Figure 7-12). FTIR analysis, in particular, show that in the AEMs after being in contact with FU and HU shows a new peak appears between 1040 and 1240  $\text{cm}^{-1}$  wavelength. This is generally attributed to the presence of C-O bonds due to ethers, carboxylic acids and polysaccharides (Cho et al. 1998). On the other hand, there is no difference between the CEMs' FTIR analyses. This suggests that only negatively charged low MW organics were able to pass through the non-porous IMEs.

Also, the EDX spectra for both CEMs and AEMs show no significant difference between pristine and fouled membrane, indicating that phosphate scaling has not occurred during the

short experimental period. This was expected as no significant increase in pressure drop was observed during the experiments. Over time, however, the transport of  $\text{PO}_4^{3-}$  to the tapwater side, or the uphill transport of  $\text{Mg}^{2+}$  and  $\text{Ca}^{2+}$  to the urine, could trigger carbonates and phosphates precipitation, especially in the alkaline environment of HU.

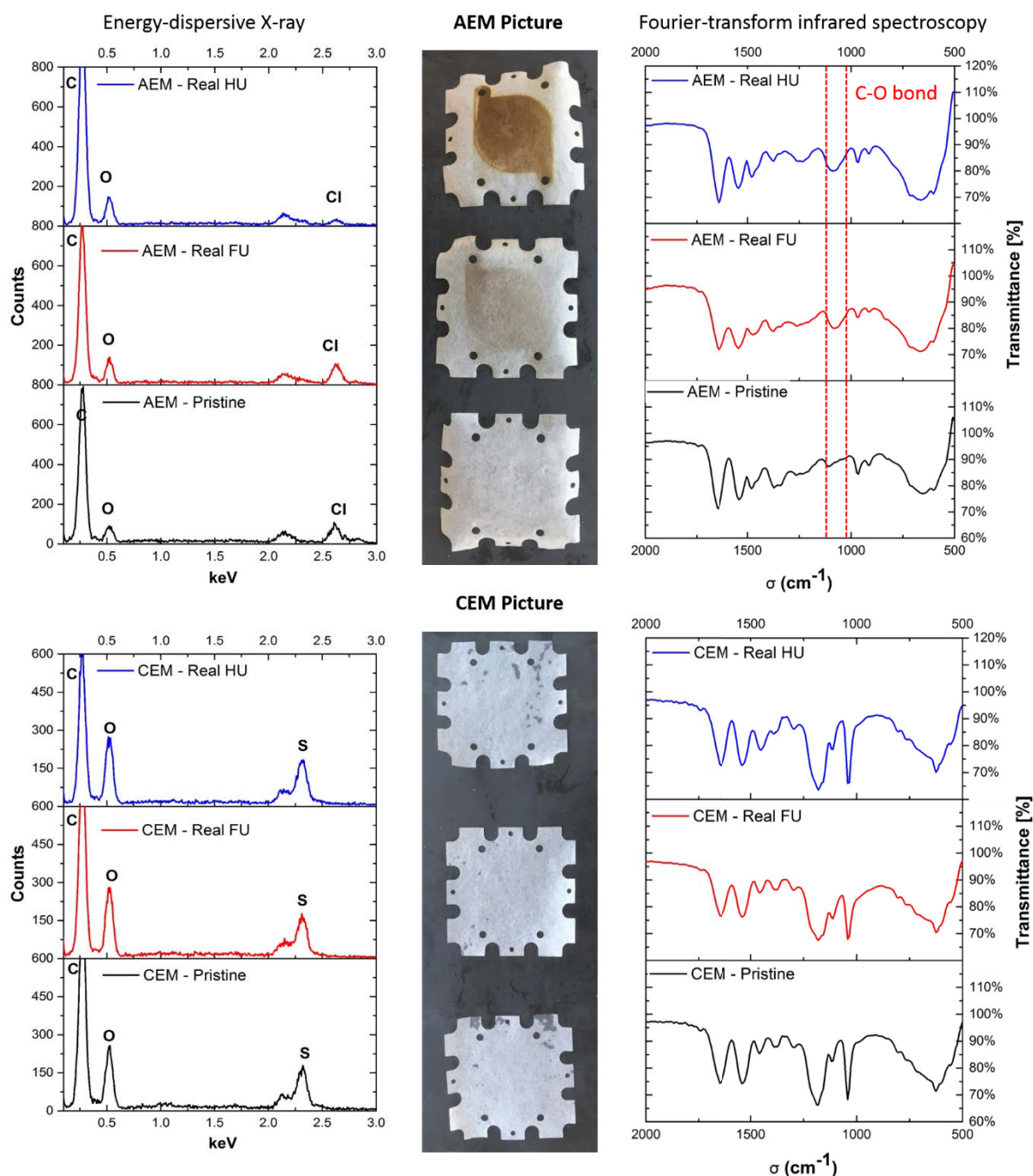


Figure 7-12 Characterisation of the AEMs (top) and CEMs (bottom) before and after the tests with real fresh and hydrolysed urine. Each picture shows the pristine membrane at the bottom, the membrane fouled with HU at the top, and the membrane fouled with FU in the middle. Energy dispersive X-Ray spectra are displayed on the left-hand side while Fourier-transform infrared spectra are shown on the right-hand side.

## 7.5 Conclusions

This study proved that RED could effectively be used to convert the ionic gradient between urine and flushing water into potential energy. The results showed that (i) a maximum  $E_{\text{Net}}$  of 0.053 - 0.039 kWh per  $\text{m}^3$  of real urine can be achieved when utilising homogenous redox couples as ES, while (ii) a TOC, ammonia and urea removal of up to 13%, 6% and 4.4% can be obtained when real FU and HU are used as ES. On the other hand, in the experiments with  $\text{K}_3\text{Fe}(\text{CN})_6/\text{K}_4\text{Fe}(\text{CN})_6$ , relatively high OCV and power densities were achieved. In fact,  $\eta \approx 5 - 22 \%$  and  $\text{PD}_{\text{Net}} \approx 0.3 - 0.7 \text{ W.m}^{-2}$  were obtained using real solutions. It should be noted that despite its higher EC, HU performed similarly to FU. The principal explanation for that was the higher AEMs fouling with real HU, probably due to sorption of LMW acids and humic substances on the membrane surface. This was also confirmed by visually observing the darker colour of AEMs after flowing HU. Though, despite the sorption of organics on the AEMs, no significant pressure drop was measured during the experiments.

Overall, an important outcome from this work is that organics and nitrogen removal can be achieved when urine is used as ES and RED driving force simultaneously. This opens the possibility of designing a gravity-driven and decentralised urine treatment unit to, partially, sanitise urine in-situ before it is discharged in the combined sewage network.



## **Chapter 8: Human urine as a forward osmosis draw solution for the application of microalgae dewatering**

---

**This chapter was published in Journal of *Hazardous Material* as:**

**F. Volpin**, H. Yu, J. Cho, C. Lee, S. Phuntsho, N. Ghaffour, J. S. Vrouwenvelder, H. K. Shon,  
Human urine as a forward osmosis draw solution for the application of microalgae dewatering,  
*Journal of Hazardous Materials*, 378 (2019).

## 8.1 Summary

Human urine is a unique solution that has the right composition to constitute both a severe environmental threat and a rich source of nitrogen and phosphorous. In fact, between 1-4% of urine mass consists of ions, such as  $K^+$ ,  $Cl^-$ ,  $Na^+$  or  $NH_4^+$ . Because of its high ionic strength, urine osmotic pressure can reach values of up to 2000 kPa. With this in mind, this work aimed to study the effectiveness of real urine as a novel draw solution for forward osmosis. Water flux, reverse nitrogen flux and membrane fouling were investigated using fresh or hydrolysed urine. Water flux as high as  $16.7 \pm 1.1 \text{ L.m}^{-2}.\text{h}^{-1}$  was recorded using real hydrolysed urine.

Additionally, no support layer membrane fouling was noticed in over 20 hours of experimentation. Urine was also employed to dewater a *Chlorella vulgaris* culture. A fourfold increase in algal concentration was achieved while having an average flux of  $14.1 \text{ L.m}^{-2}.\text{h}^{-1}$ . During the algae dewatering, a flux decrease of about 19% was noticed; this was mainly due to a thin layer of algal deposition on the active side of the membrane. Overall, human urine was found to be an effective draw solution for forward osmosis.

## 8.2 Introduction

Sustainable urban water management is shaping the design of future water and wastewater infrastructure (Larsen & Gujer 1997; Larsen et al. 2016). Specifically, the source-separation of urine, brown water, greywater and stormwater could open up numerous opportunities for the recovery of nutrients, energy and water from wastes (Larsen et al. 2009; Larsen et al. 2016). Despite its low volume relative to the overall wastewater flow, human urine on average contributes more than two-thirds of the N and half of the P and K present in sewage (Chrispim et al. 2017; Ishii & Boyer 2015; Maurer, Pronk & Larsen 2006; Udert & Wächter 2012). This high concentration of nutrients results in substantial costs during downstream wastewater treatment (Maurer, Schwegler & Larsen 2003a). However, despite its high nutrient concentration, the direct application of urine as a raw fertiliser is hindered by its non-ideal N/P/K ratio (the concentration of N is much higher relative to that of P and K), its high concentration of ammonia and organic acids (resulting in the characteristic unpleasant smell), and the possible presence of hormones and pharmaceuticals (Maurer, Pronk & Larsen 2006). Nonetheless, if we could adequately mine and transform these nutrients into marketable products, the potential economic and environmental benefits would be enormous (Ishii & Boyer 2015; Mehta et al. 2015; Tarpeh, Udert & Nelson 2017).

One approach to simultaneously treating urine and transforming it into a valuable product is microalgae cultivation (He et al. 2019). In this concept, microalgae are grown in the nutrient-rich urine, which is later harvested and converted into feedstock for the production of valuable chemicals (e.g., Poly-3-hydroxybutyrate, pigments) or biofuel (Chang et al. 2013; Cuellar-Bermudez et al. 2017; Hempel et al. 2011; Tuantet et al. 2014; Wijffels, Barbosa & Eppink 2010; Zhang, Lim, et al. 2014). Previous work from de Wilt et al. (2016) has shown that in an algae photobioreactor, 60–100% of pharmaceuticals such as diclofenac, ibuprofen and paracetamol could be removed via biodegradation and photolysis (de Wilt et al. 2016).



Consequently, sustainable urban water management and nutrient recycling could also be achieved.

However, the high pH and free ammonia concentration (i.e. 2–8 g N/L) of urine were found to inhibit microalgal growth (Chang et al. 2013; Tuantet et al. 2014; Zhang, Lim, et al. 2014). A minimum dilution of 100% was found to be necessary for stable algal growth (Tuantet et al. 2014). In addition, a further barrier to the feasibility of algal cultivation is lack of access to a low-cost and efficient algal dewatering process. In fact, 20-40% of the production cost for microalgae is generally associated with the harvesting process (Barros et al. 2015; Buckwalter et al. 2013; Larronde-Larretche & Jin 2016). Harvesting algae is costly because of low algal density; this makes many commercial dewatering technologies, e.g. centrifugation, belt filtration and flocculation, either very energy- and chemical-intensive or capable of affecting the final biomass quality (Larronde-Larretche & Jin 2016; Mo et al. 2015).

Meanwhile, membrane-based filtration processes have gained attention as an alternative dewatering approach due to their lower energy consumption and footprint (Mo et al. 2015). However, one of the downsides of pressure-driven algae filtration is the high chance of irreversible membrane fouling (Larronde-Larretche & Jin 2016; Rickman, Pellegrino & Davis 2012; Sharma et al. 2013). One alternative membrane-based process, which relies on the osmotic pressure gradient rather than the hydraulic pressure difference, is forward osmosis (FO). In FO, the transport of water across the membrane occurs due to the osmotic pressure difference between a solution with low osmotic pressure (i.e. the feed) and one with high osmotic pressure (i.e. the draw). Specifically, water moves from the feed to the draw until the osmotic equilibrium is reached (Chekli et al. 2017; Phuntsho, Shon, Hong, et al. 2012; Valladares Linares et al. 2016; Volpin, Chekli, et al. 2018). The absence of hydraulic pressure

has a number of positive effects on the filtration, including lowering the operational costs and reducing the chance of irreversible fouling (Kim et al. 2014; Van Der Bruggen & Luis 2015).

The high salinity of human urine causes its osmotic pressure to range between 1100-1800 kPa when fresh and up to 2200-3000 kPa when hydrolysed, making it a completely unexplored FO draw solution (Liu et al. 2016; Maurer, Pronk & Larsen 2006; Volpin, Chekli, et al. 2018). Moreover, as urine is generally considered a waste product, the cost of using it as a DS is expected to be minimal. In light of the above, the present work aimed to investigate the feasibility of utilising real urine as an FO draw solution to dewater a *Chlorella vulgaris* culture.

### **8.3 Experimental Investigation**

#### **8.3.1 Experimental plan**

To understand the effectiveness of real urine as an FO draw solution, experiments using fresh and hydrolysed urine (real and synthetic) were initially conducted. First, the effects of urea hydrolysis on the electric conductivity (EC) and ion concentration of urine were measured. Based on this analysis, the van 't Hoff equation was used to calculate the osmotic pressure of fresh and hydrolysed urine. Next, the effectiveness of different fresh and hydrolysed urine samples, which have distinct EC values, was investigated. FO experiments were performed using 500 mL of real and synthetic urine as DS and 500 mL of de-ionised water as FS. The goal was to identify a correlation between the initial urine EC and the FO water flux.

It should be noted that despite the correlation between the EC and osmotic pressure, a high EC does not necessarily mean a high FO flux, as the diffusivity of the species in the DS has a significant impact on the concentration polarisation effect and, therefore, the flux itself. During these tests, the nitrogen reverse salt flux of fresh and hydrolysed urine was also measured. Given the heterogeneous composition of urine, long-term experiments (i.e., > 20 hours in

length) were then conducted to study the support layer fouling (if any) of the membrane (Mi & Elimelech 2008). In these experiments, the pristine membrane was first tested with DI water and 0.5 M NaCl; the experiment was then operated again with real urine instead of NaCl, flushed with water, and finally re-tested with NaCl. The difference between the flux of the first and last NaCl test was used as an indication of membrane fouling.

After measuring the maximum flux achievable with urine as DS, urine was used to dewater a microalgae culture (Figure 8-1). 500 mL of 0.2 g/L *C. vulgaris* was employed as FS and 2 L of urine as DS. This concentration was chosen to benchmark the present results against the outcomes from other published studies (Buckwalter et al. 2013; Larronde-Larretche & Jin 2016). Synthetic seawater was also used as a benchmark for the results. During these tests, fouling of the active layer was also investigated, and the EPS was measured before and after the filtration. Analysis of the EPS concentration was performed to elucidate the response of microalgae to the reverse salt flux (RSF) of the compounds present in the urine, in particular to urea and ammonia, as well as to the algal stress occurring due to pumping and FO filtration (Larronde-Larretche & Jin 2017). To summarise, the following investigations were performed:

- Impact of urine hydrolysis in the EC and osmotic pressure;
- Maximum achievable FO flux using real fresh and hydrolysed urine;
- Membrane support layer fouling when urine DS is used;
- The effectiveness of urine DS in concentrating a microalgae solution.

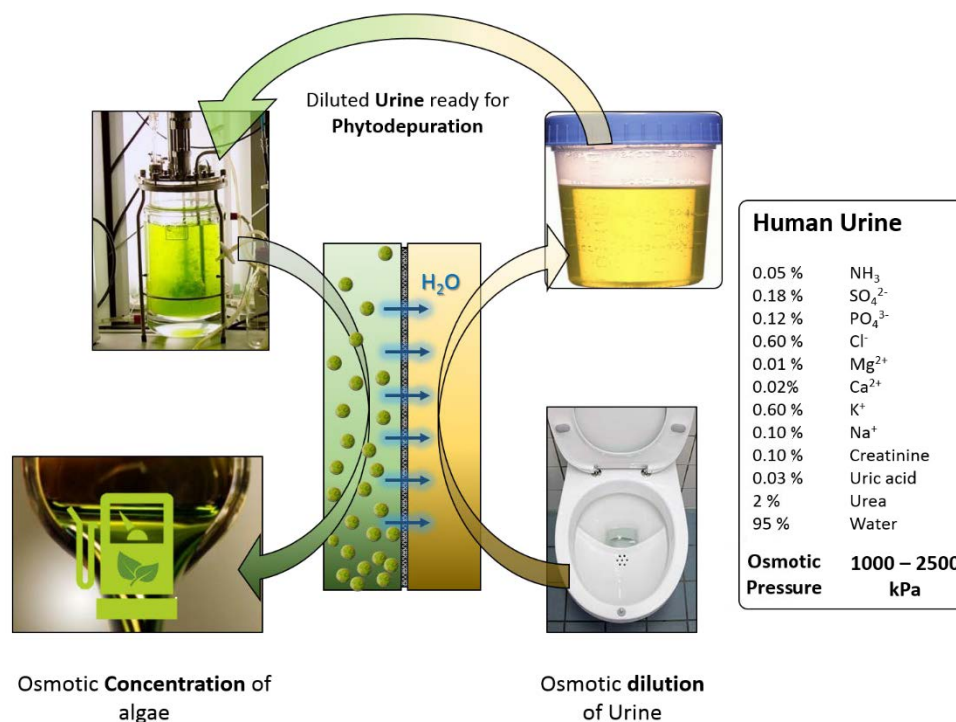


Figure 8-1. Conceptual design of the process where urine is used as DS to concentrate a microalgae solution.

### 8.3.2 Forward osmosis set-up and feed and draw solution preparation

Toray Chemical Korea Inc. supplied the TFC polyamide (PA) FO membranes that were used for the experiments. Measured pure water permeability (A) was found to be  $6.64 \text{ L.m}^{-2}.\text{h}^{-1}.\text{bar}^{-1}$ , NaCl selectivity (B) was  $1.17 \text{ L.m}^{-2}.\text{h}^{-1}$ , and the structural parameter (S) was  $409 \text{ }\mu\text{m}$ . The membrane was tested in an acrylic testing cell that exposed an area of  $20 \text{ cm}^2$  to the FS and DS solutions. The system was operated in counter-current mode, with the urine facing the porous support layer and the microalgae or DI-water solutions facing the PA membrane active layer. The DS weight increase (i.e. water flux) was continuously measured via a digital scale that was connected to a computer for continuous data recording. Each set of experiments was carried out in triplicate. Real urine was compared to synthetic urine to study the effect of the trace

organics present in real urine (e.g. carbohydrates and proteins) on the FO flux. Synthetic and real FU and HU solutions were prepared/sampled as described in the Methodology Section (0).

Finally, the urine hydrolysis process was continuously monitored to facilitate understanding of the transformation of urea into ammonia. Throughout the monitoring, the urine was continuously analysed for urea, ammonia, EC and pH until it was fully hydrolysed (Figure 8-2).

### 8.3.3 Microalgae cultivation and characterisation

*Chlorella vulgaris* KCTC AG 10002 was purchased from the Korean Collection for Type Cultures (KCTC) and cultivated in a modified Bristol medium (per litre distilled water: 157 mg  $\text{NH}_4\text{Cl}$ , 25 mg  $\text{CaCl}_2 \cdot 2\text{H}_2\text{O}$ , 75 mg  $\text{MgSO}_4 \cdot 7\text{H}_2\text{O}$ , 75 mg  $\text{K}_2\text{HPO}_4$ , 175 mg  $\text{KH}_2\text{PO}_4$ , 25 mg  $\text{NaCl}$ , and 1 mL trace element solution) (Stephenson et al. 2010). The trace element solution contained (per litre DI-water) 0.49 mg  $\text{Co}(\text{NO}_3)_2 \cdot 6\text{H}_2\text{O}$ , 8.82 mg  $\text{ZnSO}_4 \cdot 7\text{H}_2\text{O}$ , 1.44 mg  $\text{MnCl}_2 \cdot 4\text{H}_2\text{O}$ , 0.71 mg  $\text{MoO}_3$ , 1.57 mg  $\text{CuSO}_4 \cdot 5\text{H}_2\text{O}$ , 11.42 mg  $\text{H}_3\text{BO}_3$ , 50 mg EDTA, 31 mg KOH, 4.98 mg  $\text{FeSO}_4 \cdot 7\text{H}_2\text{O}$ , and 0.001 mL  $\text{H}_2\text{SO}_4$  (98%, v/v). The medium was sterilised by autoclaving at 121°C for 15 min. The microalgal cultivation was conducted in 500 mL Erlenmeyer flasks at room temperature (20 – 25°C) under white light-emitting diode illumination (1000 lux) with a 16 h light and 8 h dark cycle. The flasks were continuously aerated with ambient air at a flow rate of 170 mL/min via magnetic stirring at 200 rpm. The *C. vulgaris* culture was harvested at a volatile suspended solids concentration of 0.2 g/L and adjusted to  $\text{pH } 7.0 \pm 0.3$  with 3 M NaOH solution before use in the dewatering experiments.

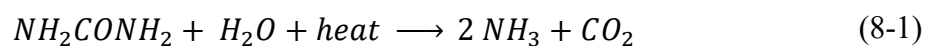
### 8.3.4 Analytical methods

The EPS analysis and ions/urea analysis was performed as described in the Methodology Section (0).

## 8.4 Results and discussion

### 8.4.1 Urine composition and hydrolysis process

Firstly, the effect of the storage on urine EC and osmotic pressure was investigated. This was crucial in determining the stage of hydrolysis at which the urine performs best as an FO DS. During the enzymatic hydrolysis of one mole of urea, two moles of ammonia plus one mole of  $\text{CO}_2$  are produced (reaction 1). As the osmotic pressure is a colligative property of the solution, the increase in the net amount of dissolved species leads to an increase in the osmotic pressure of the urine. This process is inevitable if the urine is stored in non-sterile conditions.



To calculate the osmotic pressure, the urine composition was measured before and after storage. The results are shown in Table 8-1.

Table 8-1. Ionic composition, pH and conductivity of fresh and hydrolysed urine.

Urine Composition											
	Urea	TAN	PO <sub>4</sub> <sup>3-</sup> -P	Cl <sup>-</sup>	SO <sub>4</sub> <sup>2-</sup>	K <sup>+</sup>	Mg <sup>2+</sup>	Ca <sup>2+</sup>	Na <sup>+</sup>	Cond.	pH
	[mg/L]									[mS/cm]	[-]
<i>Fresh</i>	9049 ±			3210 ±	723 ±	1177 ±		90 ±	1943 ±		6.3 ±
	1489	96 ± 33	420 ± 190	410	170	200	70 ± 12	13	500	15.6 ± 3.1	0.5
<i>Hydrolysed</i>		6272 ±		3210 ±	723 ±	1177 ±		46 ±	1943 ±		9.1 ±
	< 10	712	370 ± 190	410	170	200	19 ± 7	16	500	27.84 ± 4.4	0.2

Subsequently, the pH, EC, urea, and TAN of the fresh urine were continuously measured during the hydrolysis process (Figure 8-2). Cations and anions were also measured to enable calculation of the osmotic pressure of the solution. The OLI Stream Analyser 3.1 software was used for computing the osmotic pressure calculations. In theory, one mmole of urea generates about 2.4 kPa, while two mmols of ammonia plus 1 mol of  $\text{H}_2\text{CO}_3$  generates 7.2 kPa. This explains why the osmotic pressure of hydrolysed urine was found to be almost double that of fresh urine. Figure 8-2 A and B also show that the measured parameters follow a semi-logistic function trend; in particular, there is a clear lag-phase and exponential growth phase, which is due to microbial ureolysis (Udert, Larsen, et al. 2003).

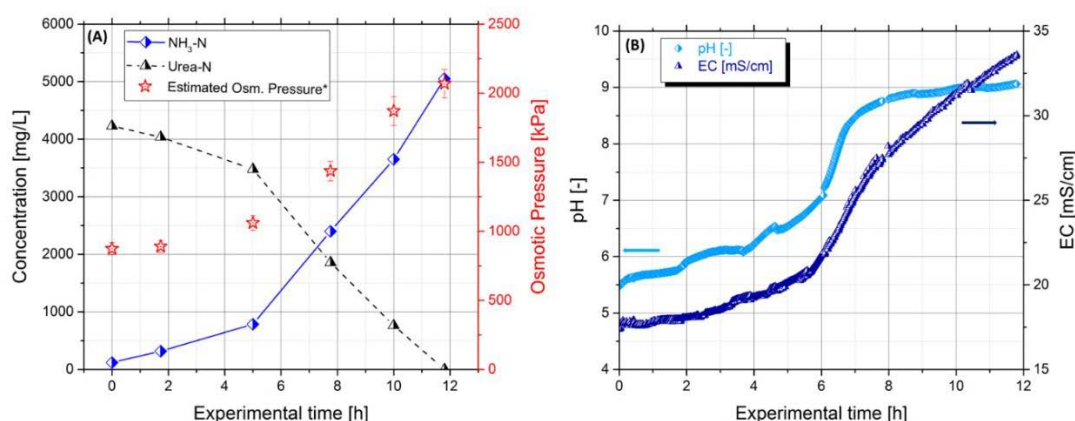


Figure 8-2. Measured urea and ammonia (A), pH and conductivity (B) during urine storage. \* The osmotic pressure of the urine was calculated using OLI Stream Analyser 3.1 software based on the chemical analysis of the urine during storage (OLI Systems Inc., Morris Plains, NJ, USA).

#### 8.4.2 Real and synthetic urine FO performance

However, the osmotic pressure of a solution is not sufficient on its own to predict the FO water flux. The internal concentration polarisation effect (ICP) and reverse salt



flux are major factors hindering the water transport from FS to DS. The ICP, in particular, is a function of the diffusivities of the ionic species in the DS. The higher the diffusivity ( $D$ ) of the ions, the lower the ICP and, therefore, the higher the water flux ( $J_w$ ) will be (Phuntsho, Shon, Majeed, et al. 2012). In this case:

$$\begin{aligned} D_{urea} &= 1.32 \cdot 10^{-10} \frac{m^2}{s} < D_{NH_3} = 2.21 \cdot 10^{-9} \frac{m^2}{s} < D_{NaCl} \\ &= 1.48 \cdot 10^{-9} \frac{m^2}{s} \end{aligned} \quad (8-2)$$

It can readily be observed that hydrolysed urine, compared to fresh urine, has both higher osmotic pressure and a higher concentration of ions with a greater self-diffusivity coefficient. Thus, hydrolysed urine should generate higher fluxes than fresh urine.

By looking at Figure 8-3, it can be seen that, as predicted, the water flux generated by hydrolysed urine is almost double that generated by fresh urine. More specifically, an average of  $9.5 \pm 0.7 \text{ L.m}^{-2}.\text{h}^{-1}$  was achieved with real fresh urine compared to  $16.7 \pm 1.1 \text{ L.m}^{-2}.\text{h}^{-1}$  with real hydrolysed urine as DS. Statistically, the water flux generated by fresh urine was the same when using real or synthetic solutions. On the other hand, synthetic hydrolysed urine solution achieved higher fluxes compared to the actual urine (Figure 8-3 A). One of the reasons might be that, given that  $pK_{a_{NH_4^+}} = 9.24$  and that ammonia is a volatile compound, ammonia volatilisation might have occurred during the urine storage and testing process due to the high pH. This explains why the theoretical concentration of ammonia in the hydrolysed synthetic urine is often higher than that in actual hydrolysed urine solutions. Figure 8-4 (B) depicts the total nitrogen (TN), total organic carbon and SRSF when different urine solutions are used as DS. Given its low molecular weight and absence of charge, any polyamide membrane often

performs poorly at removing urea. This explains why fresh urine had a higher TN and TOC specific reverse salt flux. The higher SRSF of fresh urine also contributes to its lower water flux. In summary, hydrolysed urine outperformed fresh urine, with a high water flux (i.e. up to  $20 \text{ L.m}^{-2}.\text{h}^{-1}$ ) and a lower SRSF (i.e.,  $0.4 \text{ gN/L}$ ).

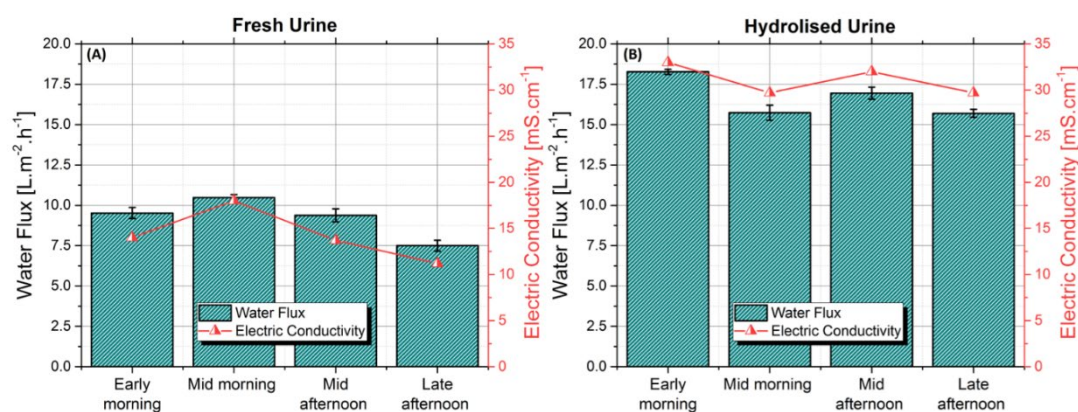


Figure 8-3 Histograms representing the water flux and EC of several samples of fresh (A) and hydrolysed (B) urine. The red triangles indicate the EC of the samples tested. These experiments were run for one hour, using 500 mL of DS (urine) and 500 mL of FS (DI-water).

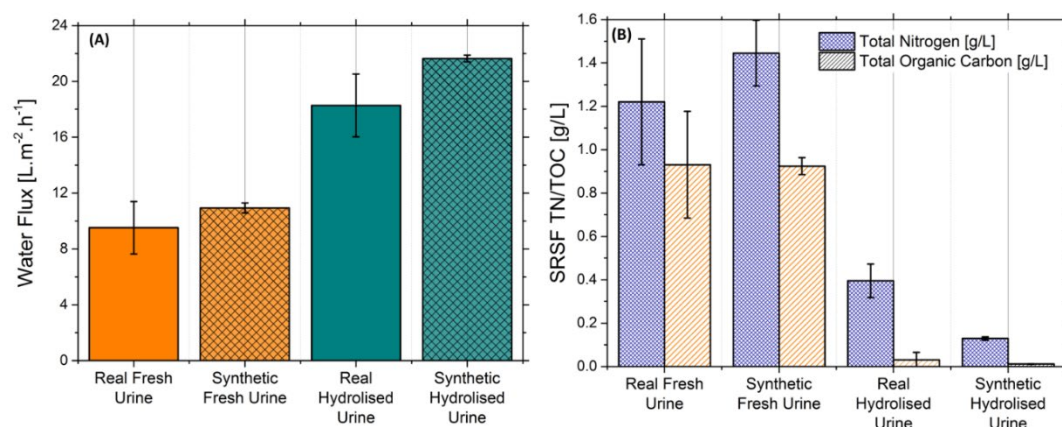


Figure 8-4 Summary of the experiments conducted with real, synthetic, fresh and hydrolysed urine using DI-water as FS. The water flux is presented in (A), while the SRSF of TN and TOC are displayed in (B).

### 8.4.3 Support layer fouling while using real urine draw solution

Urine, due to its high concentration of creatinine, carbohydrates, organic acids, and suspended solids (e.g.,  $\text{CaPO}_4$ , struvite), is a solution with a high fouling potential (Ouma et al. 2016; Putnam 1971a). As urine is facing the porous support layer of the membrane in these experiments, it is critical to assess whether this may cause severe flux decline and irreversible fouling. A recent paper has shown that when urine is facing the active layer of the membrane, the fouling is reversible (Volpin, Heo, et al. 2019); however, no investigations into support layer fouling when urine is used as a draw solution have yet been published.

The experiments were run for 20 hours, reaching a final draw dilution over 70%, and benchmarked with the performance of a pure 0.6M NaCl solution. Figure 8-5 A shows that no rapid flux decline occurred when real hydrolysed urine was used as a draw solution; in fact, the observed flux decline occurred only due to the dilution of the draw solution. Figure 8-5 B shows that 98%-99% of the initial flux was recovered after fouling the membrane with urine as DS, meaning that the irreversible fouling on the membrane support is negligible. One explanation for this could be that the transmembrane water flux prevents the foulants from being entrapped in the porous support layer. Therefore, allowing for the shear force exerted by the cross-flow to preventing any fouling compaction (Coday, Almaraz & Cath 2015; Kim, Lee & Hong 2012). This phenomenon is similar to the effect of osmotic backwashing described by Kim C. et al. when describing the cleaning of a fouled FO membrane operated in AL-DS mode (active layer facing the draw side) (Kim, Lee & Hong 2012).

Finally, Figure 8-6 shows the image of a pristine membrane support layer (B) and the support layer after filtration. Both the picture of the membrane and the SEM image

shows that there is no clear deposition of any crystal, gels or colloids on the membrane surface, reinforcing the idea that the support layer fouling is negligible.

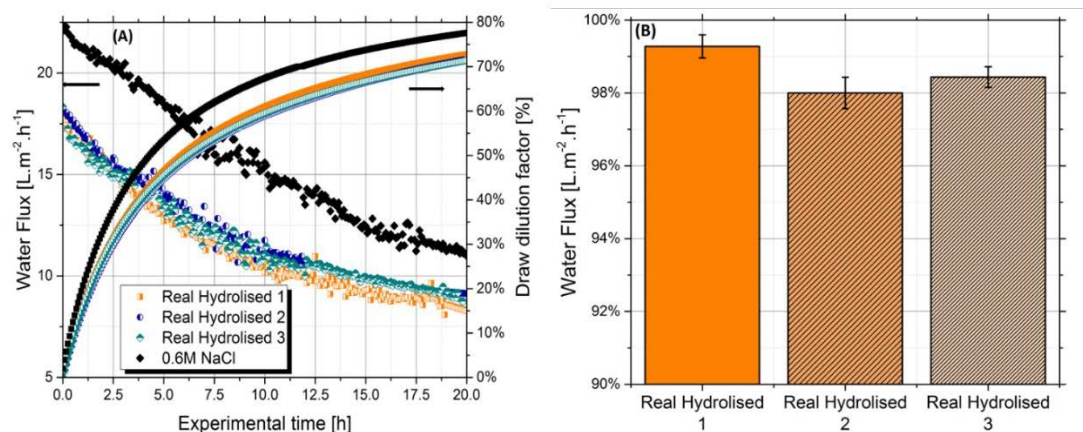


Figure 8-5. Experiments with real hydrolysed urine as draw solution and deionised water as feed. The tests were performed until  $> 70\%$  DS dilution (A). The membrane was tested with standard  $0.5\text{ M NaCl}$  as DS and DI – water as FS before and after the experiments. The differences in flux before and after the urine tests are displayed in Figure 8-5 (B).

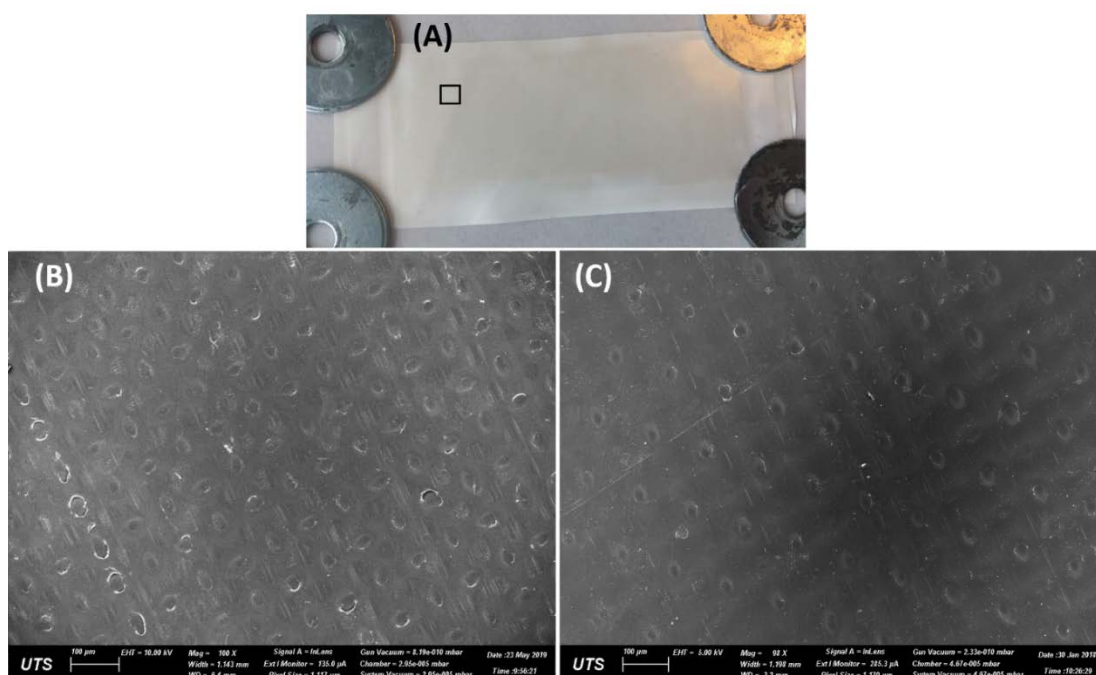


Figure 8-6. (A) Picture of the support layer after using real hydrolysed urine as DS and DI-water as FS. SEM image of the pristine membrane support layer (B) and SEM image of the support layer after FO experiments with hydrolysed urine as DS and DI-water as FS (C).

#### 8.4.4 Microalgae dewatering using real human urine as the draw solution

The third leading research question was to understand the effectiveness of urine when used in concentrating a *C. vulgaris* solution. Both real and synthetic urine were tested. Additionally, synthetic seawater, i.e. 0.6M NaCl, was used as a benchmark. Seawater was chosen because it has been extensively investigated as a suitable draw solution for microalgae dewatering (Buckwalter et al. 2013; Honda et al. 2015; Larronde-Larretche & Jin 2016; Larronde-Larretche & Jin 2017; Zhang, She, et al. 2014b).

Synthetic seawater yielded the highest flux, followed by synthetic hydrolysed urine, real hydrolysed urine and fresh urine (Figure 8-7). Although seawater and synthetic hydrolysed urine have similar osmotic pressures (2700 and 3100 kPa respectively),

NaCl, which has very high self-diffusivity (see equation (8-2)), is the predominant constituent of seawater. This is why seawater outperformed all the other urine solutions. However, the difference between real hydrolysed urine and seawater is just 5 L.m<sup>-2</sup>.h<sup>-1</sup>.

In respect of the membrane fouling, none of the DSs showed a faster flux decline. Nonetheless, Figure 8-8 shows that a mild layer of algae was deposited on the membrane surface after the filtration. The circular shape of the algae matched with the shape of *C. vulgaris* (Larronde-Larretche & Jin 2017), which indicates that membrane fouling occurred during algae dewatering, especially when a higher feed concentration was targeted (i.e. > 75%). It should be noted that Honda et al. showed that alkaline cleaning with NaOH at a pH of 11 was enough to fully restore the FO water flux after dewatering *C. vulgaris* (Honda et al. 2015). Overall, the algal concentration was increased fourfold, from 0.2 to 0.8 g/L, with an average flux of 7.6 L.m<sup>-2</sup>.h<sup>-1</sup> for fresh urine and 14.1 L.m<sup>-2</sup>.h<sup>-1</sup> for hydrolysed urine.

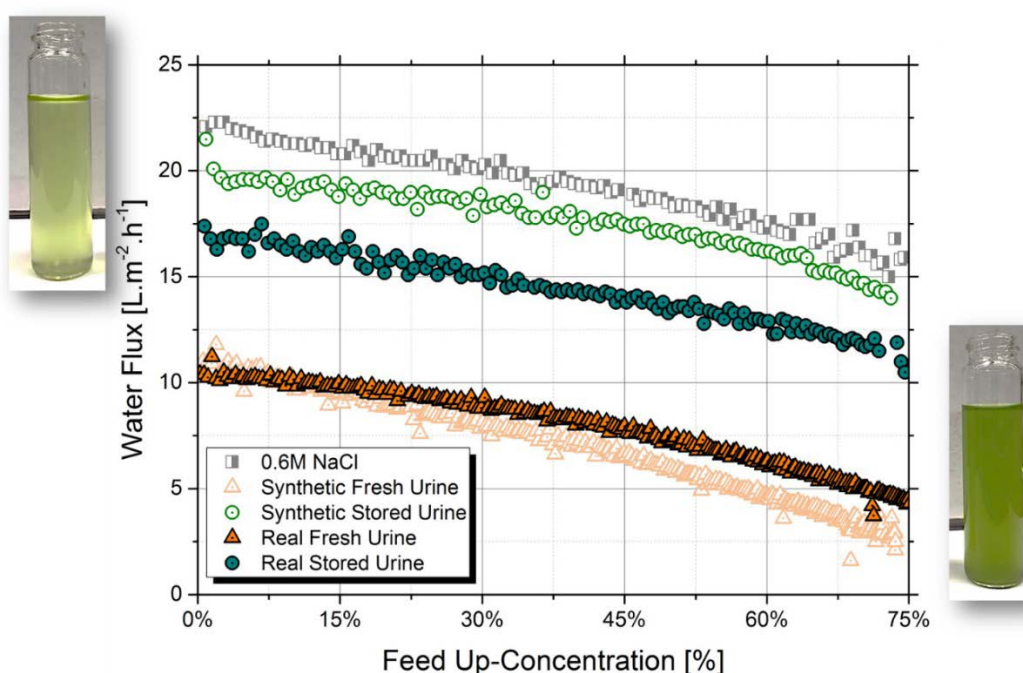




Figure 8-7. Long-term testing (>20 hours) of real and synthetic urine in dewatering a 0.2 g/L solution of *Chlorella vulgaris*. The experiments were carried out using 2 L of draw solution and 500 mL of feed until the FS was concentrated four times. Synthetic seawater (0.6 M NaCl) was also tested as a benchmark for the results.

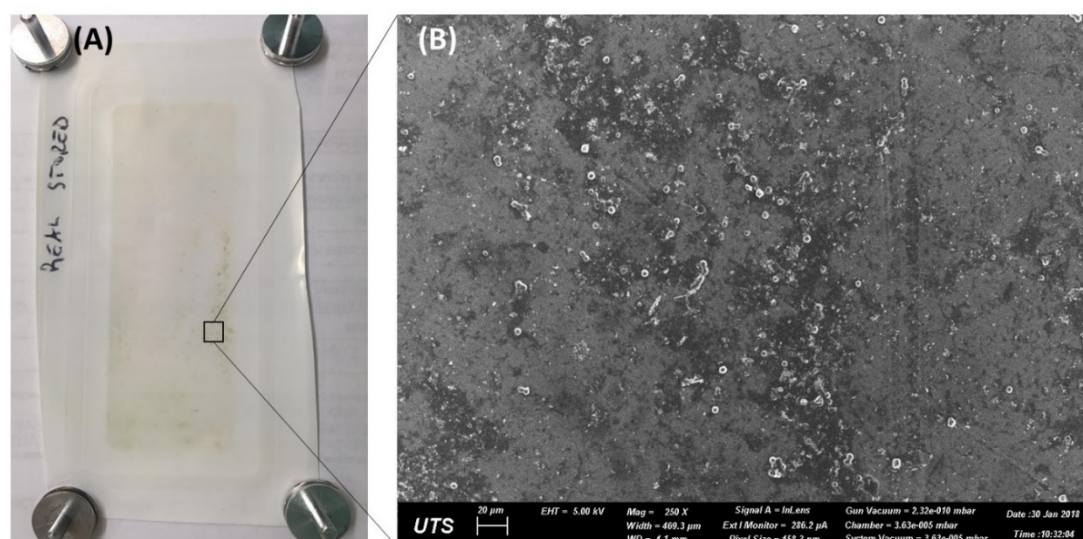


Figure 8-8. Photo (A) and SEM picture (B) of the active layer of the FO membrane after microalgae filtration.

#### 8.4.5 Extracellular carbohydrates production during algal filtration

Algae can release storage compounds, such as carbohydrates, to adjust their growth during changing environmental conditions (Markou, Angelidaki & Georgakakis 2012). One explanation for this EPS increase is the accumulation of intracellular carbohydrates with low molecular weight, such as trehalose, sucrose, etc., which puts the internal algal osmotic pressure in equilibrium with the outside (Markou, Angelidaki & Georgakakis 2012). This increase in carbohydrate content protects the algae from salt harms (Markou, Angelidaki & Georgakakis 2012). This means that, in this work, the change in the algae growing solution due to ammonia-RSF and feed up-

concentration could result in EPS release. Particularly in the presence of divalent cations such as  $\text{Ca}^{2+}$ , EPSs are reported to bind with the carboxylate functional group of the algal cell-EPS interface, creating a gel network (Gao et al. 2010; Larronde-Larretche & Jin 2017). This gel network can provide a surface for the further adherence of organic or inorganic foulants, thereby promoting membrane fouling, which could jeopardise the filtration process. Therefore, it is essential to assess the extent of EPS released by the algal solution when urine is used as DS during the FO process.

Figure 8-9 shows that there is no noticeable difference between fresh and hydrolysed urine in terms of EPS production. In both cases, the final EPS mass in the FS was about 8-10 times higher than at initialisation. The RSF of ammonia is suggested as the primary cause for EPS release. Figure 8-9 shows the difference between the initial and final amount of nitrogen in the culture. High free ammonia concentration can interfere with the photosynthesis process in isolated chloroplasts (Crofts 1966; Källqvist & Svenson 2003). M. Larronde-Larretche also speculated that a higher localised concentration of  $\text{Ca}^{2+}$  could interfere with the “ $\text{Ca}^{2+}$  signal”, which is also involved in the photosynthesis process (Larronde-Larretche & Jin 2017), (Hetherington & Brownlee 2004). Nonetheless, the ammonia RSF from hydrolysed urine, which was higher compared to fresh urine, appeared not to increase the algal EPS release.

When synthetic urine was tested, 35% fewer EPS were found in the feed. One possible explanation might be the RSF of carbohydrates from the urine to the feed. A low concentration of carbohydrates may be found even in the urine of a healthy individual. However, this argument requires further investigation, as carbohydrates are generally well rejected by the FO membrane due to their large size. Finally, synthetic seawater



induced EPS uptake rather than release. This last result was also observed in the literature (Larronde-Larretche & Jin 2016; Larronde-Larretche & Jin 2017).

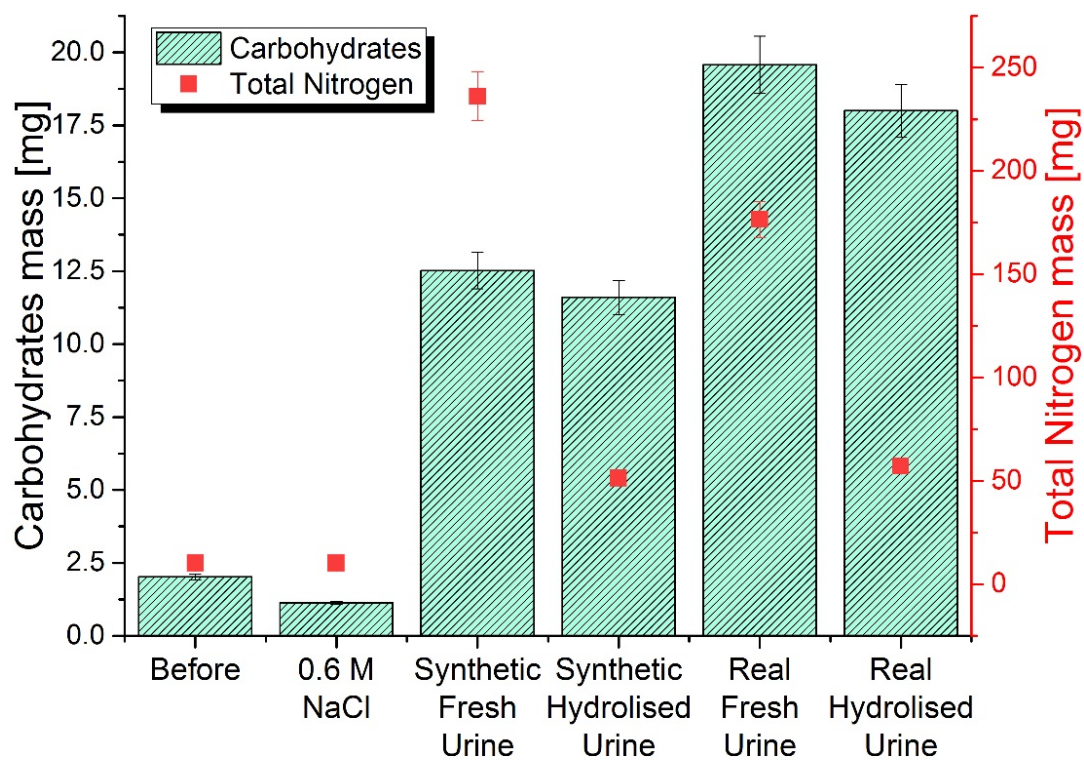


Figure 8-9. Extracellular carbohydrate content (histograms) and total nitrogen (red squares) in the solution before dewatering and after the FO concentration, using different draw solutions.

## 8.5 Conclusions

Real urine was investigated as a novel DS for forward osmosis. The experimental results showed that, when hydrolysed, real urine had an osmotic pressure of up to 2000 kPa which led to a water flux of over  $16 \text{ L.m}^{-2}.\text{h}^{-1}$ . Support layer fouling was also mild and easy to remove by simple flushing. Additionally, this work proposed the application of a urine draw solution in the field of microalgae biotechnology, specifically in the dewatering of microalgae solutions. That is because, contrary to conventional draw solution such as seawater, the availability of human urine is not constrained by the geographical location of the plant and the exhausted DS, i.e. diluted urine, could itself be used as microalgae growth media. A solution of  $0.2 \text{ g/L}$  *C. vulgaris* was concentrated fourfold (up to  $0.8 \text{ g/L}$ ) using real fresh and hydrolysed urine with an average flux of  $7.6 \text{ L.m}^{-2}.\text{h}^{-1}$  for fresh urine and  $14.1 \text{ L.m}^{-2}.\text{h}^{-1}$  for hydrolysed urine. A mild active layer fouling was confirmed by SEM analysis and attributed to the release of EPS by the algae during the filtration.

Finally, if urine is intended to be used for microalgae dewatering, several research questions are yet to be addressed. Among them, we have identified the following: (I) the effect of pharmaceuticals and hormones on the growth and dewatering of algae solutions; (II) the effect of high urea RSF on the growth rate of the algae culture; finally, (III) membrane fouling and cleaning strategies when longer experiments are performed.



# Chapter 9: Conclusions and Recommendations

---

This Thesis is aimed at valorising human urine through new treatment configurations of forward osmosis, membrane distillation, reverse electrodialysis and membrane bioreactor. Water, nutrients or energy recovery were targeted depending on urine ureolysis state, dilution, targeted product and mode of use. Concluding remarks and recommendations for each process are below described. Figure 9-1 uses the framework proposed in Figure 1-3 to show the primary outcomes of each process.

## 9.1 Distilled water production from urine through FO – MD

Onboard of the ISS, urine is a valuable source of water. There, the goal is to extract potable water from fresh human urine while minimising the use of expendable materials to reduce the resupply cost. In this context, the double membrane barrier of FO-MD processes could be a versatile, lightweight and reliable alternative. In this configuration, the role of FO is to filter-out the volatile nitrogen species before they come in contact with the gas-permeable MD membrane. This would ensure high-quality MD product water as all non-volatile compounds can be entirely rejected by the PTFE and PVDF test membranes.

Permeation of nitrogen from the urine feed to the DS is one of the challenges of FO process. However, by applying moderate back pressure on the draw side of the FO membrane, a reduction of nitrogen flux by up to 30% was measured. When it comes to DS regeneration by MD process, the choice of PTFE membranes over PVDF seems

to be preferable due to its higher porosity and thickness, which contributed to achieving a higher water flux and lower ammonia flux.

Despite these positive results, FO-MD still needs further evaluation to overcome its critical drawbacks. The nitrogen accumulation in the DS, possible FO active-layer delamination in back-pressures operation and product water contamination in the event of membrane wetting were found to be the most important ones.

## **9.2 Hybrid MBR - MD to produce fertiliser and distilled water**

In this work, it was proven that an odourless, safe and valuable concentrated liquid fertiliser can be produced through UF-MBR-MD, using undiluted hydrolysed human urine as raw material. The automation of the HRT in the biological nitrification as pre-treatment resulted in a stable 95% DOC removal and 50% ammonia to  $\text{NO}_3^-$  oxidation rate, while effectively coping with sudden  $\text{NO}_2^-$  accumulation events. Also, DCMD was able to reach up to 20 times urine concentration, thereby producing a final concentrated product with a TDS concentration of  $280 \text{ g.L}^{-1}$ . The encouraging results achieved by growing lettuce and Pak Choi using the treated urine product showed that this process has a significant potential for real application.

Despite the stability of the process and the quality of the produced fertiliser, DCMD was found to suffer from severe membrane fouling after 80% water recovery, causing the water flux to decline from  $15 \text{ L.m}^{-2}.\text{h}^{-1}$  to about  $1 \text{ L.m}^{-2}.\text{h}^{-1}$ . The fouling layer mainly comprised of LMW-N organics and alkaline cleaning was determined to be able to restore the initial DCMD performances.

Overall, the UF-MBR-MD hybrid process seems to be a promising candidate for the production of fertiliser in an urban context. However, the possible presence of pharmaceuticals and MD fouling could be a challenge which needs addressing.

### **9.3 N and P recovery from fresh urine via FDFO**

Here, the techno-economic feasibility of using FDFO process to produce struvite and liquid fertiliser from diluted fresh human urine was investigated. By using a commercial liquid fertiliser as DS and real diluted FU as feed and at 50% urine concentration, 93% P recovery as struvite and 50% N recovery as dilute fertiliser were achieved. The economic analysis showed that downstream WWTP savings greatly exceed the revenue from the produced fertiliser. That is because of the relatively low price of commercial fertilisers and high costs associated with the biological nitrogen removal. On the other hand, membrane replacement costs seem to dominate the OPEX of the system. Overall, if the average flux of the process is increased to  $8 \text{ L.m}^{-2}.\text{h}^{-1}$ , the ROI of the system can be reached after 2.7 years.

That being said, the high concentration of LMW organic in urine and the risk of struvite crystallisation on the membrane surface are still major challenges. While membrane scaling can be prevented by maintaining the pH of the solution below 6.5, the occurrence of organic fouling seems to be inevitable (though recoverable through alkaline cleaning).

Finally, given the ubiquitous nature of urease enzyme, this process might only be feasible in a context where urine is stored for a minimal amount of time to prevent ureolysis and consequent loss of urea and increase of the pH.

#### 9.4 Energy recovery from urine dilution through RED

In this study, the energy of mixing urine with flushing water was successfully harnessed through RED. This ionic gradient was enough to obtain a maximum  $E_{\text{Net}}$  of 0.053 - 0.039 kWh per  $\text{m}^3$  of real urine. Promising results were, in fact, obtained using  $\text{K}_3\text{Fe}(\text{CN})_6/\text{K}_4\text{Fe}(\text{CN})_6$  as ES and urine as HC solution. There  $\text{PD}_{\text{Net}}$  up to 0.3 - 0.7  $\text{W.m}^{-2}$  were measured, with efficiencies  $\eta$  of 5 - 22 %. Interestingly, while FU has lower ionic strength compared to HU, the two solutions performed similarly. While more severe fouling of AEMs with LMW acids and humic substances undoubtedly played a role when using real HU, it was proposed that the fast transport of urea in FU might also have increased its power densities. In addition, it was demonstrated for the first time that using urine as both HC solution and ES can achieve a TOC, ammonia and urea removal of up to 13%, 6% and 4.4%.

#### 9.5 Urine as a FO draw solution to dewater microalgae

Here, urine draw solution was investigated in a FO setup as another novel solution for the harnessing urine chemical energy. Urine high osmotic pressure (up to 2000 kPa) and high concentration of high-diffusivity species allowed to achieve pure water flux of over 16  $\text{L.m}^{-2}.\text{h}^{-1}$  and an osmotic gradient high-enough to concentrate a 0.2 g/L *C. vulgaris* four times. During the algal concentration, an average flux of 7.6  $\text{L.m}^{-2}.\text{h}^{-1}$  for FU and 14.1  $\text{L.m}^{-2}.\text{h}^{-1}$  for HU was measured. Support layer fouling was also mild and easy to remove by simple flushing. It was suggested that contrary to other low-cost DS such as seawater, the availability of human urine is not constrained by the geographical location of the plant. This, together with the fact that the exhausted DS could itself be used as microalgae growing media or just discharged in the sewage, makes it industrial application worth investigating further.

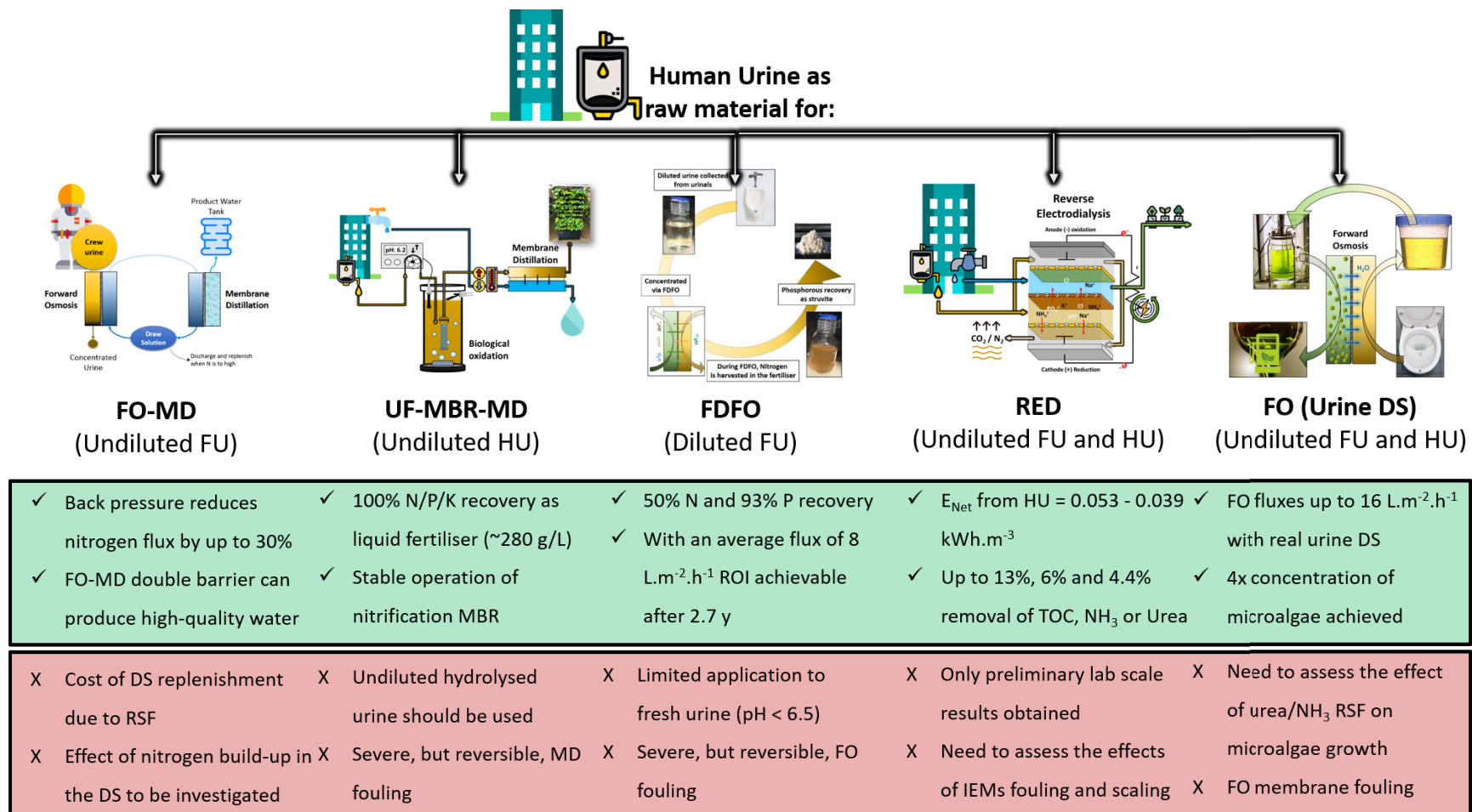


Figure 9-1 Schematic diagram of the main benefits (green) and limitation (red) of the processes presented in the five technical chapters.



## 9.6 Recommendation for future work

The road to begin the implementation of urine separation and recovery in an urban context comes with both regulatory, economic and technological challenges. When focusing on the production of fertiliser from urine via MBR-MD or FDFO process, the following regulatory and oversight challenges have been identified:

- How to set water quality standards, issue permits, and provide operational oversight of the urine-treatment facilities,
- Type of on-going water quality monitoring and reporting to be implemented,
- The categorisation of urine as a substance distinct from sewage water, to allow for different regulations and certifications.

From an economic point of view, it is also crucial to:

- Develop a business model for the manufacture and marketing of urine-derived fertilisers,
- Develop visibility of urine-diverting toilets through collaboration with architects, building owners and design engineers
- Identify multiple methods for the collection and conveyance of urine (centralised, decentralised, hybrid) and their associated costs.
- Assess the long-term impact of urine-derived fertilisers on soil health to produce guidance for users on how and where to apply such fertilisers.

Overall, Figure 9-2 offers an idea of a roadmap for the successful scaling up of urine fertiliser technology, which includes the co-participation of four pillars, namely

technology, business, policy/regulation and society. This was developed by combining the knowledge gained during this Thesis, with the experience shared by Vuna Ltd. (2020) and Rich Earth Institute (2020). Both of which are established players in the field of urine separation and recovery.

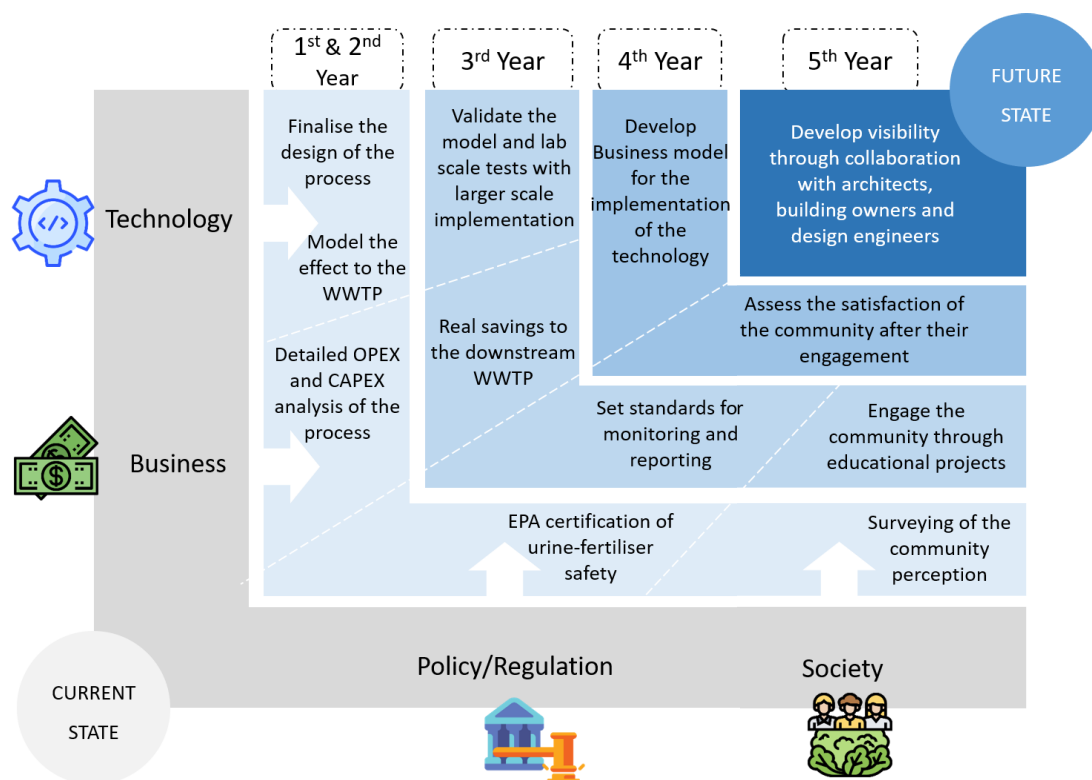


Figure 9-2 Proposed roadmap for the implementation of urine-derived fertilisers.

Finally, if membrane technology is to be used to treat urine, future research should look into the development of membranes that are more resistant toward fouling from LMW organics and carbonates and phosphates scaling. This is especially important when reaching a high degree of urine dewatering with MD. Additionally, it is worth investigating new alternative options to process the ammonia in the urine into a product with an added value higher than fertilisers. If successful, this would positively affect the business opportunities with urine separation, as fertilisers are commodities with a low-profit margin. One example would be extracting the ammonia stored in the

urine to fuel the ammonia-to-hydrogen process. The produced hydrogen, in turn, could be used as an energy source such as for hydrogen fuel cell vehicles or be utilized in solid oxide fuel cells, in an internal combustion engine or a gas turbine (Giddey et al. 2017).

## **9.7 Concluding remarks**

Overall, this Thesis looked at multiple technologies for the valorisation of human urine. While MD and RED were effective in extracting clean water or energy from urine but limited to such use, FO turned out to be the most adaptable one as it can be used to achieve both water, nutrients or energy recovery. However, it is essential to place the practical feasibility of each solution in a real context. It is important to remember that:

- When it comes to nutrients recovery, the practical experience gained during this Thesis seems to point in the direction of the MBR-MD process. That is because of its ability to handle all kinds of urine solution, whether it is FU, HU, diluted or concentrated (though that is all at the expense of the OPEX). This makes MBR-MD possibly more resilient and reliable than the FDFO process, which can handle just diluted FU.
- When it comes to water recovery, at present the high cost and complexity linked with the extraction of water from human urine appears to limit its use for only space application. There the FO-MD process could potentially reduce the current cost of resupply while maintaining the same water quality. However, assessing the occurrence of membrane wetting during long-term operations in microgravity is crucial to validate the reliability of the process.

- Finally, despite being at a very early stage, the research on urine energy recovery is worth investigating particularly for areas where electric energy is either not readily available or expensive. However, both RED and FO still must prove their reliability in the long-term operation as well as their capital and operational costs.



# Bibliography

---

- Abey Suriya, K., Fam, D. & Mitchell, C. 2013, 'Trialling urine diversion in Australia: technical and social learnings', *Water Science and Technology*, vol. 68, no. 10, pp. 2186-94.
- Abu-Zeid, M.A.E.-R., Zhang, Y., Dong, H., Zhang, L., Chen, H.-L. & Hou, L. 2015, 'A comprehensive review of vacuum membrane distillation technique', *Desalination*, vol. 356, pp. 1-14.
- AEMC 2013, 'Final Report: 2013 Residential Electricity Price Trends', *Australian Energy Market Commission (AEMC)*.
- Agre, P. & Kozono, D. 2003, 'Aquaporin water channels: molecular mechanisms for human diseases', *FEBS Letters*, vol. 555, no. 1, pp. 72-8.
- Al-Obaidani, S., Curcio, E., Macedonio, F., Di Profio, G., Al-Hinai, H. & Drioli, E. 2008, 'Potential of membrane distillation in seawater desalination: Thermal efficiency, sensitivity study and cost estimation', *Journal of Membrane Science*, vol. 323, no. 1, pp. 85-98.
- Alder, A.C., Eggen, R.I., Maurer, M. & Lienert, J. 2009, 'Source Separation: Will We See a Paradigm Shift in Wastewater Handling? ', *Environmental Science Technology*, vol. 43, pp. 6121-5.
- Ali, S.M., Kim, J.E., Phuntsho, S., Jang, A., Choi, J.Y. & Shon, H.K. 2018, 'Forward osmosis system analysis for optimum design and operating conditions', *Water Research*, vol. 145, pp. 429-41.
- Amy, G., Ghaffour, N., Li, Z., Francis, L., Linares, R.V., Missimer, T. & Lattemann, S. 2017, 'Membrane-based seawater desalination: Present and future prospects', *Desalination*, vol. 401, pp. 16-21.
- Andreev, N., Ronteltap, M., Boincean, B., Wernli, M., Zubcov, E., Bagrin, N., Borodin, N. & Lens, P.N.L. 2017, 'Lactic acid fermentation of human urine to improve its fertilizing value and reduce odour emissions', *J Environ Manage*, vol. 198, no. Pt 1, pp. 63-9.
- Ashley, K., Cordell, D. & Mavinic, D. 2011, 'A brief history of phosphorus: From the philosopher's stone to nutrient recovery and reuse', *Chemosphere*, vol. 84, no. 6, pp. 737-46.
- Ashoor, B.B., Mansour, S., Giwa, A., Dufour, V. & Hasan, S.W. 2016, 'Principles and applications of direct contact membrane distillation (DCMD): A comprehensive review', *Desalination*, vol. 398, pp. 222-46.

- Barros, A.I., Gonçalves, A.L., Simões, M. & Pires, J.C.M. 2015, 'Harvesting techniques applied to microalgae: A review', *Renewable and Sustainable Energy Reviews*, vol. 41, pp. 1489-500.
- Bashar, R., Gungor, K., Karthikeyan, K.G. & Barak, P. 2018, 'Cost effectiveness of phosphorus removal processes in municipal wastewater treatment', *Chemosphere*, vol. 197, pp. 280-90.
- Bates, R.G. & Pinching, G.D. 1950, 'Dissociation Constant of Aqueous Ammonia at 0 to 50° from E. m. f. Studies of the Ammonium Salt of a Weak Acid', *Journal of the American Chemical Society*, vol. 72, no. 3, pp. 1393-6.
- Batstone, D.J., Hülsen, T., Mehta, C.M. & Keller, J. 2015, 'Platforms for energy and nutrient recovery from domestic wastewater: A review', *Chemosphere*, vol. 140, pp. 2-11.
- Bernini, P., Bertini, I., Luchinat, C., Nincheri, P., Staderini, S. & Turano, P. 2011, 'Standard operating procedures for pre-analytical handling of blood and urine for metabolomic studies and biobanks', *Journal of Biomolecular NMR*, vol. 49, no. 3-4, pp. 231-43.
- Bicer, Y., Dincer, I., Vezina, G. & Raso, F. 2017, 'Impact Assessment and Environmental Evaluation of Various Ammonia Production Processes', *Environmental Management*, vol. 59, no. 5, pp. 842-55.
- Bischel, H.N., Özel Duygan, B.D., Strande, L., McArdeell, C.S., Udert, K.M. & Kohn, T. 2015, 'Pathogens and pharmaceuticals in source-separated urine in eThekweni, South Africa', *Water Research*, vol. 85, pp. 57-65.
- Bischel, H.N., Schertenleib, A., Fumasoli, A., Udert, K.M. & Kohn, T. 2015, 'Inactivation kinetics and mechanisms of viral and bacterial pathogen surrogates during urine nitrification', *Environmental Science: Water Research & Technology*, vol. 1, no. 1, pp. 65-76.
- Blandin, G., Verliefde, A.R.D., Tang, C.Y., Childress, A.E. & Le-Clech, P. 2013, 'Validation of assisted forward osmosis (AFO) process: Impact of hydraulic pressure', *Journal of Membrane Science*, vol. 447, pp. 1-11.
- Bonvin, C., Etter, B., Udert, K., Frossard, E., Nanzer, S., Tamburini, F. & Oberson, A. 2015, 'Plant uptake of phosphorus and nitrogen recycled from synthetic source-separated urine', *AMBIO - A Journal of the Human Environment*, vol. 44, pp. 217-27.
- Broadley, M.R., Seginer, I., Burns, A., Escobar-Gutiérrez, A.J., Burns, I.G. & White, P.J. 2003, 'The nitrogen and nitrate economy of butterhead lettuce (*Lactuca sativa* var. *capitata* L.)', *Journal of Experimental Botany*, vol. 54, no. 390, pp. 2081-90.
- Buckwalter, P., Embaye, T., Gormly, S. & Trent, J.D. 2013, 'Dewatering microalgae by forward osmosis', *Desalination*, vol. 312, pp. 19-22.

- Buelke, C., Alshami, A., Casler, J., Lewis, J., Al-Sayaghi, M. & Hickner, M.A. 2018, 'Graphene oxide membranes for enhancing water purification in terrestrial and space-born applications: State of the art', *Desalination*, vol. 448, pp. 113-32.
- Bunce, N.J. & Bejan, D. 2011, 'Mechanism of electrochemical oxidation of ammonia', *Electrochimica Acta*, vol. 56, no. 24, pp. 8085-93.
- Calero-Cáceres, W., Melgarejo, A., Colomer-Lluch, M., Stoll, C., Lucena, F., Jofre, J. & Muniesa, M. 2014, 'Sludge As a Potential Important Source of Antibiotic Resistance Genes in Both the Bacterial and Bacteriophage Fractions', *Environmental Science & Technology*, vol. 48, no. 13, pp. 7602-11.
- Candido, L. & Gomes, J.A.C.P. 2011, 'Evaluation of anode materials for the electro-oxidation of ammonia and ammonium ions', *Materials Chemistry and Physics*, vol. 129, no. 3, pp. 1146-51.
- Canfield, D.E., Glazer, A.N. & Falkowski, P.G. 2010, 'The Evolution and Future of Earth's Nitrogen Cycle', *Science*, vol. 330, no. 6001, pp. 192-6.
- Cath, T.Y., Adams, D. & Childress, A.E. 2005, 'Membrane contactor processes for wastewater reclamation in space: II. Combined direct osmosis, osmotic distillation, and membrane distillation for treatment of metabolic wastewater', *Journal of Membrane Science*, vol. 257, no. 1, pp. 111-9.
- Cath, T.Y., Elimelech, M., McCutcheon, J.R., McGinnis, R.L., Achilli, A., Anastasio, D., Brady, A.R., Childress, A.E., Farr, I.V., Hancock, N.T., Lampi, J., Nghiem, L.D., Xie, M. & Yip, N.Y. 2013, 'Standard Methodology for Evaluating Membrane Performance in Osmotically Driven Membrane Processes', *Desalination*, vol. 312, pp. 31-8.
- Cath, T.Y., Gormly, S., Beaudry, E.G., Flynn, M.T., Adams, V.D. & Childress, A.E. 2005, 'Membrane contactor processes for wastewater reclamation in space: Part I. Direct osmotic concentration as pretreatment for reverse osmosis', *Journal of Membrane Science*, vol. 257, no. 1-2, pp. 85-98.
- Chang, Y., Wu, Z., Bian, L., Feng, D. & Leung, D.Y.C. 2013, 'Cultivation of *Spirulina platensis* for biomass production and nutrient removal from synthetic human urine', *Applied Energy*, vol. 102, pp. 427-31.
- Chekli, L., Kim, J.E., El Saliby, I., Kim, Y., Phuntsho, S., Li, S., Ghaffour, N., Leiknes, T. & Kyong Shon, H. 2017, 'Fertilizer drawn forward osmosis process for sustainable water reuse to grow hydroponic lettuce using commercial nutrient solution', *Separation and Purification Technology*, vol. 181, pp. 18-28.
- Chen, Y., Chen, L., Bai, H. & Li, L. 2013, 'Graphene oxide-chitosan composite hydrogels as broad-spectrum adsorbents for water purification', *Journal of Materials Chemistry A*, vol. 1, no. 6, pp. 1992-2001.



- Cheng, H., Scott, K. & Christensen, P.A. 2005, 'Paired electrolysis in a solid polymer electrolyte reactor—Simultaneously reduction of nitrate and oxidation of ammonia', *Chemical Engineering Journal*, vol. 108, no. 3, pp. 257-68.
- Cherkasov, N., Ibhaddon, A.O. & Fitzpatrick, P. 2015, 'A review of the existing and alternative methods for greener nitrogen fixation', *Chemical Engineering and Processing: Process Intensification*, vol. 90, pp. 24-33.
- Chew, N.G.P., Zhao, S., Loh, C.H., Permogorov, N. & Wang, R. 2017, 'Surfactant effects on water recovery from produced water via direct-contact membrane distillation', *Journal of Membrane Science*, vol. 528, pp. 126-34.
- Cho, J., Amy, G., Pellegrino, J. & Yoon, Y. 1998, 'Characterization of clean and natural organic matter (NOM) fouled NF and UF membranes, and foulants characterization', *Desalination*, vol. 118, no. 1, pp. 101-8.
- Chrispim, M.C., Tarpeh, W.A., Salinas, D.T.P. & Nolasco, M.A. 2017, 'The sanitation and urban agriculture nexus: Urine collection and application as fertilizer in São Paulo, Brazil', *Journal of Water Sanitation and Hygiene for Development*, vol. 7, no. 3, pp. 455-65.
- Clauwaert, P., Muys, M., Alloul, A., De Paepe, J., Luther, A., Sun, X., Ilgrande, C., Christiaens, M.E.R., Hu, X., Zhang, D., Lindeboom, R.E.F., Sas, B., Rabaey, K., Boon, N., Ronsse, F., Geelen, D. & Vlaeminck, S.E. 2017, 'Nitrogen cycling in Bioregenerative Life Support Systems: Challenges for waste refinery and food production processes', *Progress in Aerospace Sciences*, vol. 91, pp. 87-98.
- Coday, B.D., Almaraz, N. & Cath, T.Y. 2015, 'Forward osmosis desalination of oil and gas wastewater: Impacts of membrane selection and operating conditions on process performance', *Journal of Membrane Science*, vol. 488, pp. 40-55.
- Coday, B.D., Heil, D.M., Xu, P. & Cath, T.Y. 2013, 'Effects of Transmembrane Hydraulic Pressure on Performance of Forward Osmosis Membranes', *Environmental Science & Technology*, vol. 47, no. 5, pp. 2386-93.
- Cohen, M.M., Matossian, R.L., Levy, F. & Flynn, M.T. 2014, 'Water Walls Life Support Architecture: System Overview', paper presented to the 44th International Conference on Environmental Systems, Tucson, Arizona.
- Coppens, J., Lindeboom, R., Muys, M., Coessens, W., Alloul, A., Meerbergen, K., Lievens, B., Clauwaert, P., Boon, N. & Vlaeminck, S.E. 2016, 'Nitrification and microalgae cultivation for two-stage biological nutrient valorization from source separated urine', *Bioresource Technology*, vol. 211, pp. 41-50.
- Cordell, D. & White, S. 2014, 'Life's Bottleneck: Sustaining the World's Phosphorus for a Food Secure Future', *Annual Review of Environment and Resources*, vol. 39, no. 1, pp. 161-88.

- Crofts, A.R. 1966, 'Uptake of ammonium ion by chloroplasts, and the mechanism of amine uncoupling', *Biochemical and Biophysical Research Communications*, vol. 24, no. 1, pp. 127-34.
- Cuellar-Bermudez, S.P., Aleman-Nava, G.S., Chandra, R., Garcia-Perez, J.S., Contreras-Angulo, J.R., Markou, G., Muylaert, K., Rittmann, B.E. & Parra-Saldivar, R. 2017, 'Nutrients utilization and contaminants removal. A review of two approaches of algae and cyanobacteria in wastewater', *Algal Research*, vol. 24, pp. 438-49.
- Dang, H. & Chen, C.-T.A. 2017, 'Ecological Energetic Perspectives on Responses of Nitrogen-Transforming Chemolithoautotrophic Microbiota to Changes in the Marine Environment', *Frontiers in Microbiology*, vol. 8, p. 1246.
- Daniel Hellstrom, E.J., Kerstin Grennberg 1999, 'Storage of human urine acidification as a method to inhibit decomposition of urea', *Ecological Engineering*, vol. 12, pp. 253-69.
- de Boer, M.A., Hammerton, M. & Slootweg, J.C. 2018, 'Uptake of pharmaceuticals by sorbent-amended struvite fertilisers recovered from human urine and their bioaccumulation in tomato fruit', *Water Research*, vol. 133, pp. 19-26.
- De Paepe, J., Lindeboom, R.E.F., Vanoppen, M., De Paepe, K., Demey, D., Coessens, W., Lamaze, B., Verliefde, A.R.D., Clauwaert, P. & Vlaeminck, S.E. 2018, 'Refinery and concentration of nutrients from urine with electrodialysis enabled by upstream precipitation and nitrification', *Water Research*, vol. 144, pp. 76-86.
- de Wilt, A., Butkovskyi, A., Tuantet, K., Leal, L.H., Fernandes, T.V., Langenhoff, A. & Zeeman, G. 2016, 'Micropollutant removal in an algal treatment system fed with source separated wastewater streams', *Journal of Hazardous Materials*, vol. 304, pp. 84-92.
- Deng, S., Xie, B. & Liu, H. 2016, 'The recycle of water and nitrogen from urine in bioregenerative life support system', *Acta Astronautica*, vol. 123, pp. 86-90.
- Ding, Z., Liu, L., Li, Z., Ma, R. & Yang, Z. 2006, 'Experimental study of ammonia removal from water by membrane distillation (MD): The comparison of three configurations', *Journal of Membrane Science*, vol. 286, no. 1, pp. 93-103.
- Doyle, J.D. & Parsons, S.A. 2002, 'Struvite formation, control and recovery', *Water Research*, vol. 36, no. 16, pp. 3925-40.
- Drioli, E., Ali, A. & Macedonio, F. 2015, 'Membrane distillation: Recent developments and perspectives', *Desalination*, vol. 356, pp. 56-84.
- Elser, J. & Bennett, E. 2011, 'Phosphorus cycle: A broken biogeochemical cycle', *Nature*, vol. 478, no. 7367, pp. 29-31.

- Escher, B.I., Pronk, W., Suter, M.J.F. & Maurer, M. 2006, 'Monitoring the Removal Efficiency of Pharmaceuticals and Hormones in Different Treatment Processes of Source-Separated Urine with Bioassays', *Environmental Science & Technology*, vol. 40, no. 16, pp. 5095-101.
- Etter, B. 2019, *Vuna* ([http://www.vuna.ch/aurin/index\\_en.html](http://www.vuna.ch/aurin/index_en.html)), <[http://www.vuna.ch/aurin/index\\_en.html](http://www.vuna.ch/aurin/index_en.html)>.
- Etter, B., Tilley, E., Khadka, R. & Udert, K.M. 2011, 'Low-cost struvite production using source-separated urine in Nepal', *Water Research*, vol. 45, no. 2, pp. 852-62.
- Etter, B. & Udert, K. March 2016, *VUNA Handbook on Urine Treatment*.
- FAO 2017a, 'World fertilizer trends and outlook to 2020', *Food and Agriculture Organization of the United Nations (FAO)*, p. 66.
- FAO 2017b, 'World fertilizer trends and outlook to 2020: Summary report', *Food and Agriculture organization of the United Nations (FAO), Rome*.
- Flynn, M.T. 2013, 'Microgravity Testing of the Forward Osmosis Bag (FOB), A Personal Water Purification Device', *43rd International Conference on Environmental Systems*, American Institute of Aeronautics and Astronautics.
- Foley, J., de Haas, D., Hartley, K. & Lant, P. 2010, 'Comprehensive life cycle inventories of alternative wastewater treatment systems', *Water Research*, vol. 44, no. 5, pp. 1654-66.
- Forrest, A.L., Fattah, K.P., Mavinic, D.S. & Koch, F.A. 2008, 'Optimizing Struvite Production for Phosphate Recovery in WWTP', *Journal of Environmental Engineering*, vol. 134, no. 5, pp. 395-402.
- Fritzmann, C., Löwenberg, J., Wintgens, T. & Melin, T. 2007, 'State-of-the-art of reverse osmosis desalination', *Desalination*, vol. 216, no. 1, pp. 1-76.
- Fry, D., Mideksa, D., Ambelu, A., Feyisa, Y., Abaire, B., Cunliffe, K. & Freeman, M.C. 2015, 'Adoption and sustained use of the arborloo in rural Ethiopia: a cross-sectional study', *Journal of Water, Sanitation and Hygiene for Development*, vol. 5, no. 3, pp. 412-25.
- Fumasoli, A., Bürgmann, H., Weissbrodt, D.G., Wells, G.F., Beck, K., Mohn, J., Morgenroth, E. & Udert, K.M. 2017, 'Growth of Nitrosococcus-Related Ammonia Oxidizing Bacteria Coincides with Extremely Low pH Values in Wastewater with High Ammonia Content', *Environmental Science & Technology*, vol. 51, no. 12, pp. 6857-66.
- Fumasoli, A., Etter, B., Sterkele, B., Morgenroth, E. & Udert, K.M. 2016, 'Operating a pilot-scale nitrification/distillation plant for complete nutrient recovery from urine', *Water Science and Technology*, vol. 73, no. 1, pp. 215-22.

- Gao, D.W., Zhang, T., Tang, C.Y.Y., Wu, W.M., Wong, C.Y., Lee, Y.H., Yeh, D.H. & Criddle, C.S. 2010, 'Membrane fouling in an anaerobic membrane bioreactor: Differences in relative abundance of bacterial species in the membrane foulant layer and in suspension', *Journal of Membrane Science*, vol. 364, no. 1-2, pp. 331-8.
- Ge, Q., Han, G. & Chung, T.-S. 2016, 'Effective As(III) Removal by A Multi-Charged Hydroacid Complex Draw Solute Facilitated Forward Osmosis-Membrane Distillation (FO-MD) Processes', *Environmental Science & Technology*, vol. 50, no. 5, pp. 2363-70.
- Giddey, S., Badwal, S.P.S., Munnings, C. & Dolan, M. 2017, 'Ammonia as a Renewable Energy Transportation Media', *ACS Sustainable Chemistry & Engineering*, vol. 5, no. 11, pp. 10231-9.
- Gòdia, F., Albiol, J., Montesinos, J.L., Pérez, J., Creus, N., Cabello, F., Mengual, X., Montras, A. & Lasseur, C. 2002, 'MELISSA: a loop of interconnected bioreactors to develop life support in Space', *Journal of Biotechnology*, vol. 99, no. 3, pp. 319-30.
- Gregson, N., Crang, M., Fuller, S. & Holmes, H. 2015, 'Interrogating the circular economy: the moral economy of resource recovery in the EU', *Economy and Society*, vol. 44, no. 2, pp. 218-43.
- Gryta, M. 2018, 'The long-term studies of osmotic membrane distillation', *Chemical Papers*, vol. 72, no. 1, pp. 99-107.
- Hali, L.S., Michael, F., David, B., Kevin, H., Brian, K., Thomas, A., Kim, K., Jörg, V. & Jurek, P. 2017, 'Multifiltration Bed Replacement (MFBR) System for the International Space Station using Aquaporin Membranes and Humidity Condensate Ersatz Wastewater', *47th International Conference on Environmental Systems*.
- Han, J.-H., Jeong, H., Hwang, K.S., Kim, C.-S., Jeong, N. & Yang, S. 2020, 'Asymmetrical electrode system for stable operation of a large-scale reverse electrodialysis (RED) system', *Environmental Science: Water Research & Technology*.
- Hanford, A. & Ewert, M. 2006, 'Exploration Life Support Baseline Values and Assumptions Document', *Document #NASA CR-2006-213693*.
- Harper, L.D., Neal, C.R., Poynter, J., Schalkwyk, J.D. & Wingo, D.R. 2016, 'Life Support for a Low-Cost Lunar Settlement: No Showstoppers', *New Space*, vol. 4, no. 1, pp. 40-9.
- He, M., Chen, W.-J., Tian, L., Shao, B. & Lin, Y. 2019, 'Plant-microbial synergism: An effective approach for the remediation of shale-gas fracturing flowback and produced water', *Journal of Hazardous Materials*, vol. 363, pp. 170-8.

- Heer, C., Kamps, N., Biener, C., Korr, C., Boerger, A., Zittermann, A., Stehle, P. & Drummer, C. 1999, 'Calcium Metabolism in Microgravity', *European Journal of Medical Research*, vol. 4, pp. 357-60.
- Heitland, P. & Köster, H.D. 2004, 'Fast, simple and reliable routine determination of 23 elements in urine by ICP-MS', *Journal of Analytical Atomic Spectrometry*, vol. 19, no. 12, pp. 1552-8.
- Hempel, F., Bozarth, A.S., Lindenkamp, N., Klingl, A., Zauner, S., Linne, U., Steinbüchel, A. & Maier, U.G. 2011, 'Microalgae as bioreactors for bioplastic production', *Microbial Cell Factories*, vol. 10, no. 1, p. 81.
- Henze, M., Harremoës, P., Jes la Cour, J. & Arvin, E. 2002, *Wastewater Treatment – Biological and Chemical Processes*, Springer-Verlag Berlin.
- Hetherington, A.M. & Brownlee, C. 2004, 'THE GENERATION OF Ca<sup>2+</sup> SIGNALS IN PLANTS', *Annual Review of Plant Biology*, vol. 55, no. 1, pp. 401-27.
- Honda, R., Rukapan, W., Komura, H., Teraoka, Y., Noguchi, M. & Hoek, E.M.V. 2015, 'Effects of membrane orientation on fouling characteristics of forward osmosis membrane in concentration of microalgae culture', *Bioresource Technology*, vol. 197, pp. 429-33.
- Hotta, S. & Funamizu, N. 2008, 'Inhibition factor of ammonification in stored urine with fecal contamination', *Water Sci Technol*, vol. 58, no. 6, pp. 1187-92.
- Huber, S.A., Balz, A., Abert, M. & Pronk, W. 2011, 'Characterisation of aquatic humic and non-humic matter with size-exclusion chromatography – organic carbon detection – organic nitrogen detection (LC-OCD-OND)', *Water Research*, vol. 45, no. 2, pp. 879-85.
- Husnain, T., Liu, Y., Riffat, R. & Mi, B. 2015, 'Integration of forward osmosis and membrane distillation for sustainable wastewater reuse', *Separation and Purification Technology*, vol. 156, pp. 424-31.
- Ikematsu, M., Kaneda, K., Iseki, M. & Yasuda, M. 2007, 'Electrochemical treatment of human urine for its storage and reuse as flush water', *Sci Total Environ*, vol. 382, no. 1, pp. 159-64.
- Ishii, S.K.L. & Boyer, T.H. 2015, 'Life cycle comparison of centralized wastewater treatment and urine source separation with struvite precipitation: Focus on urine nutrient management', *Water Research*, vol. 79, pp. 88-103.
- Jackson, W., Thompson, B., Sevanthi, R., Morse, A., Meyer, C. & Callahan, M. 2017, 'Biologically Pre-Treated Habitation Waste Water as a Sustainable Green Urine Pre-Treat Solution', paper presented to the 47th International Conference on Environmental Systems, Charleston, South Carolina, 16-20 July, <<https://ntrs.nasa.gov/search.jsp?R=20170004969> 2018-08-30T08:22:27+00:00Z>.

- Jackson, W.A., Barta, D.J., Anderson, M.S., Lange, K.E., Hanford, A.J., Shull, S.A. & Carter, D.L. 2014, 'Water Recovery from Brines to Further Close the Water Recovery Loop in Human Spaceflight', *Proceedings of the 44th International Conference on Environmental Systems. ICES-2014-186*.
- Jacquin, C., Monnot, M., Hamza, R., Kouadio, Y., Zaviska, F., Merle, T., Lesage, G. & Héran, M. 2018, 'Link between dissolved organic matter transformation and process performance in a membrane bioreactor for urinary nitrogen stabilization', *Environmental Science: Water Research & Technology*, vol. 4, no. 6, pp. 806-19.
- Jermakka, J., Thompson Brewster, E., Ledezma, P. & Freguia, S. 2018, 'Electro-concentration for chemical-free nitrogen capture as solid ammonium bicarbonate', *Separation and Purification Technology*, vol. 203, pp. 48-55.
- Jiang, Y., Biswas, P. & Fortner, J.D. 2016, 'A review of recent developments in graphene-enabled membranes for water treatment', *Environmental Science: Water Research & Technology*, vol. 2, no. 6, pp. 915-22.
- Källqvist, T. & Svenson, A. 2003, 'Assessment of ammonia toxicity in tests with the microalga, *Nephroselmis pyriformis*, Chlorophyta', *Water Research*, vol. 37, no. 3, pp. 477-84.
- Kampschreur, M.J., Temmink, H., Kleerebezem, R., Jetten, M.S.M. & van Loosdrecht, M.C.M. 2009, 'Nitrous oxide emission during wastewater treatment', *Water Research*, vol. 43, no. 17, pp. 4093-103.
- Kamyab, H., Chelliapan, S., Din, M.F.M., Shahbazian-Yassar, R., Rezaia, S., Khademi, T., Kumar, A. & Azimi, M. 2017, 'Evaluation of *Lemna minor* and *Chlamydomonas* to treat palm oil mill effluent and fertilizer production', *Journal of Water Process Engineering*, vol. 17, pp. 229-36.
- Katsounaros, I., Schneider, W.B., Meier, J.C., Benedikt, U., Biedermann, P.U., Auer, A.A. & Mayrhofer, K.J.J. 2012, 'Hydrogen peroxide electrochemistry on platinum: towards understanding the oxygen reduction reaction mechanism', *Physical Chemistry Chemical Physics*, vol. 14, no. 20, pp. 7384-91.
- Kavvada, O., Tarpeh, W.A., Horvath, A. & Nelson, K.L. 2017, 'Life-Cycle Cost and Environmental Assessment of Decentralized Nitrogen Recovery Using Ion Exchange from Source-Separated Urine through Spatial Modeling', *Environmental Science & Technology*, vol. 51, no. 21, pp. 12061-71.
- Khumalo, N., Nthunya, L., Derese, S., Motsa, M., Verliefe, A., Kuvarega, A., Mamba, B.B., Mhlanga, S. & Dlamini, D.S. 2019, 'Water recovery from hydrolysed human urine samples via direct contact membrane distillation using PVDF/PTFE membrane', *Separation and Purification Technology*, vol. 211, pp. 610-7.

- Kim, C., Lee, S. & Hong, S. 2012, 'Application of osmotic backwashing in forward osmosis: mechanisms and factors involved', *Desalination and Water Treatment*, vol. 43, no. 1-3, pp. 314-22.
- Kim, D., Min, K.J., Lee, K., Yu, M.S. & Park, K.Y. 2017, 'Effects of pH, molar ratios and pre-treatment on phosphorus recovery through struvite crystallization from effluent of anaerobically digested swine wastewater', *Environmental Engineering Research*, vol. 22, no. 1, pp. 12-8.
- Kim, H., Jeong, N., Yang, S., Choi, J., Lee, M.-S., Nam, J.-Y., Jwa, E., Kim, B., Ryu, K.-s. & Choi, Y.-W. 2019, 'Nernst–Planck analysis of reverse-electrodialysis with the thin-composite pore-filling membranes and its upscaling potential', *Water Research*, vol. 165, p. 114970.
- Kim, J.E., Kuntz, J., Jang, A., Kim, I.S., Choi, J.Y., Phuntsho, S. & Shon, H.K. 2019, 'Techno-economic assessment of fertiliser drawn forward osmosis process for greenwall plants from urban wastewater', *Process Safety and Environmental Protection*, vol. 127, pp. 180-8.
- Kim, J.E., Phuntsho, S., Chekli, L., Hong, S., Ghaffour, N., Leiknes, T., Choi, J.Y. & Shon, H.K. 2017, 'Environmental and economic impacts of fertilizer drawn forward osmosis and nanofiltration hybrid system', *Desalination*, vol. 416, pp. 76-85.
- Kim, Y., Elimelech, M., Shon, H.K. & Hong, S. 2014, 'Combined organic and colloidal fouling in forward osmosis: Fouling reversibility and the role of applied pressure', *Journal of Membrane Science*, vol. 460, pp. 206-12.
- Kir, M., Topuz, M., Sunar, M.C. & Topuz, H. 2016, 'Acute toxicity of ammonia in Meagre (*Argyrosomus regius* Asso, 1801) at different temperatures', *Aquaculture Research*, vol. 47, no. 11, pp. 3593-8.
- Kirchmann, H. & Pettersson, S. 1994, 'Human urine - Chemical composition and fertilizer use efficiency', *Fertilizer research*, vol. 40, no. 2, pp. 149-54.
- Kümmerer, K. 2009, 'Antibiotics in the aquatic environment – A review – Part I', *Chemosphere*, vol. 75, no. 4, pp. 417-34.
- Landry, K.A. & Boyer, T.H. 2013, 'Diclofenac removal in urine using strong-base anion exchange polymer resins', *Water Research*, vol. 47, no. 17, pp. 6432-44.
- Larronde-Larretche, M. & Jin, X. 2016, 'Microalgae (*Scenedesmus obliquus*) dewatering using forward osmosis membrane: Influence of draw solution chemistry', *Algal Research*, vol. 15, pp. 1-8.
- Larronde-Larretche, M. & Jin, X. 2017, 'Microalgal biomass dewatering using forward osmosis membrane: Influence of microalgae species and carbohydrates composition', *Algal Research*, vol. 23, pp. 12-9.

- Larsen, T.A., Alder, A.C., Eggen, R.I.L., Maurer, M. & Lienert, J. 2009, 'Source separation: Will we see a paradigm shift in wastewater handling?', *Environmental Science and Technology*, vol. 43, no. 16, pp. 6121-5.
- Larsen, T.A. & Gujer, W. 1996, 'Separate management of anthropogenic nutrient solutions (human urine)', *Water Science and Technology*, vol. 34, no. 3, pp. 87-94.
- Larsen, T.A. & Gujer, W. 1997, 'The concept of sustainable urban water management', *Water Science and Technology*, Article, vol. 35, pp. 3-10, <<https://www.scopus.com/inward/record.uri?eid=2-s2.0-0030737881&doi=10.1016%2fS0273-1223%2897%2900179-0&partnerID=40&md5=6e8ab7b106889ae557768b9ba5aa2529>>.
- Larsen, T.A., Hoffmann, S., Lüthi, C., Truffer, B. & Maurer, M. 2016, 'Emerging solutions to the water challenges of an urbanizing world', *Science*, vol. 352, no. 6288, pp. 928-33.
- Larsen, T.A., Udert, K.M. & Lienert, J. 2013, *Source Separation and Decentralization for Wastewater Management*, IWA Publishing.
- Layne, C., Jennifer, P., Christopher, A.B., Ryan, S. & Lyndsey, B. 2015, 'Status of ISS Water Management and Recovery', *45th International Conference on Environmental Systems*.
- Layne, C., Jill, W., Christopher, B., Jesse, B., Daniel, G., Ryan, S. & Frank, T. 2018, 'Status of ISS Water Management and Recovery', *48th International Conference on Environmental Systems*.
- Ledezma, P., Kuntke, P., Buisman, C.J.N., Keller, J. & Freguia, S. 2015, 'Source-separated urine opens golden opportunities for microbial electrochemical technologies', *Trends in Biotechnology*, vol. 33, no. 4, pp. 214-20.
- Lee, J.-G., Alsaadi, A.S., Karam, A.M., Francis, L., Soukane, S. & Ghaffour, N. 2017, 'Total water production capacity inversion phenomenon in multi-stage direct contact membrane distillation: A theoretical study', *Journal of Membrane Science*, vol. 544, pp. 126-34.
- Lee, K.P., Zheng, J., Bargeman, G., Kemperman, A.J.B. & Benes, N.E. 2015, 'pH stable thin film composite polyamine nanofiltration membranes by interfacial polymerisation', *Journal of Membrane Science*, vol. 478, pp. 75-84.
- Lee, S. & Lueptow, R.M. 2001, 'Membrane Rejection of Nitrogen Compounds', *Environmental Science & Technology*, vol. 35, no. 14, pp. 3008-18.
- Li, J., Hou, D., Li, K., Zhang, Y., Wang, J. & Zhang, X. 2018, 'Domestic wastewater treatment by forward osmosis-membrane distillation (FO-MD) integrated system', *Water Science and Technology*, vol. 77, no. 6, pp. 1514-23.



- Li, Q., Li, X., Tang, B. & Gu, M. 2018, 'Growth Responses and Root Characteristics of Lettuce Grown in Aeroponics, Hydroponics, and Substrate Culture', vol. 4, no. 4, p. 35.
- Liakopoulos, V., Leivaditis, K., Eleftheriadis, T. & Dombros, N. 2012, 'The kidney in space', *International Urology and Nephrology*, vol. 44, no. 6, pp. 1893-901.
- Lienert, J., Bürki, T. & Escher, B.I. 2007, 'Reducing micropollutants with source control: Substance flow analysis of 212 pharmaceuticals in faeces and urine', *Water Science and Technology*, Conference Paper, vol. 56, pp. 87-96, <<https://www.scopus.com/inward/record.uri?eid=2-s2.0-34948835228&doi=10.2166%2fwst.2007.560&partnerID=40&md5=8a92e34b5b42f7a0a0e19789d8a59549>>.
- Lienert, J., Güdel, K. & Escher, B.I. 2007, 'Screening Method for Ecotoxicological Hazard Assessment of 42 Pharmaceuticals Considering Human Metabolism and Excretory Routes', *Environmental Science & Technology*, vol. 41, no. 12, pp. 4471-8.
- Lin, S., Straub, A.P. & Elimelech, M. 2014, 'Thermodynamic limits of extractable energy by pressure retarded osmosis', *Energy & Environmental Science*, vol. 7, no. 8, pp. 2706-14.
- Liu, Q., Liu, C., Zhao, L., Ma, W., Liu, H. & Ma, J. 2016, 'Integrated forward osmosis-membrane distillation process for human urine treatment', *Water Research*, vol. 91, pp. 45-54.
- Liu, X., Hu, Z., Zhu, C., Wen, G., Meng, X. & Lu, J. 2014, 'Effect of contact to the atmosphere and dilution on phosphorus recovery from human urine through struvite formation', *Environmental Technology*, vol. 35, no. 3, pp. 271-7.
- Lu, D., Liu, Q., Zhao, Y., Liu, H. & Ma, J. 2018, 'Treatment and energy utilization of oily water via integrated ultrafiltration-forward osmosis-membrane distillation (UF-FO-MD) system', *Journal of Membrane Science*, vol. 548, pp. 275-87.
- Luo, W., Phan, H.V., Li, G., Hai, F.I., Price, W.E., Elimelech, M. & Nghiem, L.D. 2017, 'An Osmotic Membrane Bioreactor-Membrane Distillation System for Simultaneous Wastewater Reuse and Seawater Desalination: Performance and Implications', *Environmental Science & Technology*, vol. 51, no. 24, pp. 14311-20.
- M Smith, S., McCoy, T., Gazda, D., L L Morgan, J., Heer, M. & R Zwart, S. 2012, *Space Flight Calcium: Implications for Astronaut Health, Spacecraft Operations, and Earth*, vol. 4.
- M. Fidaleo & R. Lavecchia 2003, 'Kinetic Study of Enzymatic Urea Hydrolysis in the pH Range 4-9', *Chem. Biochem. Eng. Q.*, vol. 17, no. 4, pp. 311-8.

- Ma, B., Wang, S., Cao, S., Miao, Y., Jia, F., Du, R. & Peng, Y. 2016, 'Biological nitrogen removal from sewage via anammox: Recent advances', *Bioresource Technology*, vol. 200, pp. 981-90.
- Ma, L., Gutierrez, L., Vanoppen, M., Lorenz, D.N., Aubry, C. & Verliefde, A. 2018, 'Transport of uncharged organics in ion-exchange membranes: experimental validation of the solution-diffusion model', *Journal of Membrane Science*, vol. 564, pp. 773-81.
- Ma, P., Hao, X., Galia, A. & Scialdone, O. 2020, 'Development of a process for the treatment of synthetic wastewater without energy inputs using the salinity gradient of wastewaters and a reverse electrodialysis stack', *Chemosphere*, vol. 248, p. 125994.
- Magureanu, M., Piroi, D., Mandache, N.B., David, V., Medvedovici, A. & Parvulescu, V.I. 2010, 'Degradation of pharmaceutical compound pentoxifylline in water by non-thermal plasma treatment', *Water Research*, vol. 44, no. 11, pp. 3445-53.
- Magureanu, M., Piroi, D., Mandache, N.B. & Parvulescu, V. 2008, 'Decomposition of methylene blue in water using a dielectric barrier discharge: Optimization of the operating parameters', *Journal of Applied Physics*, vol. 104, no. 10, p. 103306.
- Markou, G., Angelidaki, I. & Georgakakis, D. 2012, 'Microalgal carbohydrates: an overview of the factors influencing carbohydrates production, and of main bioconversion technologies for production of biofuels', *Applied Microbiology and Biotechnology*, vol. 96, no. 3, pp. 631-45.
- Maurer, M., Pronk, W. & Larsen, T.A. 2006, 'Treatment processes for source-separated urine', *Water Research*, vol. 40, no. 17, pp. 3151-66.
- Maurer, M., Schwegler, P. & Larsen, T.A. 2003a, 'Nutrients in urine: Energetic aspects of removal and recovery', *Water Science and Technology*, Conference Paper, vol. 48, pp. 37-46, <<https://www.scopus.com/inward/record.uri?eid=2-s2.0-0042405010&partnerID=40&md5=f97827b654c99b682af352ba49c3b94f>>.
- Maurer, M., Schwegler, P. & Larsen, T.A. 2003b, 'Nutrients in urine: energetic aspects of removal and recovery', *Water Science and Technology*, vol. 48, no. 1, pp. 37-46.
- Max, R. & Hannah, R. 2020, *How many people does synthetic fertilizer feed?*, <<https://ourworldindata.org/fertilizers>>.
- McBride, M.B. & Spiers, G. 2001, 'TRACE ELEMENT CONTENT OF SELECTED FERTILIZERS AND DAIRY MANURES AS DETERMINED BY ICP-MS', *Communications in Soil Science and Plant Analysis*, vol. 32, no. 1-2, pp. 139-56.

- McHunu, N., Odindo, A. & Muchaonyerwa, P. 2018, 'The effects of urine and urine-separated plant nutrient sources on growth and dry matter production of perennial ryegrass (*Lolium perenne*. L)', *Agricultural Water Management*, vol. 207, pp. 37-43.
- Mehdizadeh, S., Yasukawa, M., Suzuki, T. & Higa, M. 2020, 'Reverse electrodialysis for power generation using seawater/municipal wastewater: Effect of coagulation pretreatment', *Desalination*, vol. 481, p. 114356.
- Mehta, C.M., Khunjar, W.O., Nguyen, V., Tait, S. & Batstone, D.J. 2015, 'Technologies to recover nutrients from waste streams: A critical review', *Critical Reviews in Environmental Science and Technology*, vol. 45, no. 4, pp. 385-427.
- Mei, Y. & Tang, C.Y. 2018, 'Recent developments and future perspectives of reverse electrodialysis technology: A review', *Desalination*, vol. 425, pp. 156-74.
- Meinzinger, F., Oldenburg, M., Lisanework, A.A., Gutema, K., Otterpohl, R., Krusche, P. & Jebens, O. 2009, 'Implementation of urine-diverting dry toilets in multi-storey apartment buildings in Ethiopia', *3rd International Dry Toilet Conference*, vol. 12, pp. 2009-15.08.
- Meinzinger, F., Oldenburg, M. & Otterpohl, R. 2009, 'No waste, but a resource: Alternative approaches to urban sanitation in Ethiopia', *Desalination*, vol. 248, no. 1, pp. 322-9.
- Mercer, E., Davey, C.J., Azzini, D., Eusebi, A.L., Tierney, R., Williams, L., Jiang, Y., Parker, A., Kolios, A., Tyrrel, S., Cartmell, E., Pidou, M. & McAdam, E.J. 2019, 'Hybrid membrane distillation reverse electrodialysis configuration for water and energy recovery from human urine: An opportunity for off-grid decentralised sanitation', *Journal of Membrane Science*, vol. 584, pp. 343-52.
- Mi, B. & Elimelech, M. 2008, 'Chemical and physical aspects of organic fouling of forward osmosis membranes', *Journal of Membrane Science*, vol. 320, no. 1, pp. 292-302.
- Michael T Flynn, Marc M Cohen, Renee L. Matossian, Sherwin Gormly, Rocco Mancinelli, Jack Miller, Jurek Parodi & Grossi, E. 2018, 'Water Walls Architecture: Massively Redundant and Highly Reliable Life Support for Long Duration Exploration Missions'.
- Mihelcic, J.R., Fry, L.M. & Shaw, R. 2011, 'Global potential of phosphorus recovery from human urine and feces', *Chemosphere*, vol. 84, no. 6, pp. 832-9.
- Mitchell, C., Fam, D. & Abey Suriya, K. 2013a, 'Transitioning to sustainable sanitation: a transdisciplinary pilot project of urine diversion'.
- Mitchell, C.A., Fam, D.M. & Abey Suriya, K. 2013b, *Transitioning to sustainable sanitation: a transdisciplinary pilot project of urine diversion*, pp. 1-137, Institute for Sustainable Futures, UTS, Sydney.

- Mkhize, N., Taylor, M., Udert, K.M., Gounden, T.G. & Buckley, C.A. 2017, 'Urine diversion dry toilets in eThekweni Municipality, South Africa: acceptance, use and maintenance through users' eyes', *Journal of Water, Sanitation and Hygiene for Development*, vol. 7, no. 1, pp. 111-20.
- Mo, W., Soh, L., Werber, J.R., Elimelech, M. & Zimmerman, J.B. 2015, 'Application of membrane dewatering for algal biofuel', *Algal Research*, vol. 11, pp. 1-12.
- Mogollón, J.M., Beusen, A.H.W., van Grinsven, H.J.M., Westhoek, H. & Bouwman, A.F. 2018, 'Future agricultural phosphorus demand according to the shared socioeconomic pathways', *Global Environmental Change*, vol. 50, pp. 149-63.
- Munoz, F., Hua, C., Kwong, T., Tran, L., Nguyen, T.Q. & Haan, J.L. 2015, 'Palladium–copper electrocatalyst for the promotion of the electrochemical oxidation of polyalcohol fuels in the alkaline direct alcohol fuel cell', *Applied Catalysis B: Environmental*, vol. 174-175, pp. 323-8.
- Naidu, G., Jeong, S., Choi, Y. & Vigneswaran, S. 2017, 'Membrane distillation for wastewater reverse osmosis concentrate treatment with water reuse potential', *Journal of Membrane Science*, vol. 524, pp. 565-75.
- Naidu, G., Jeong, S., Kim, S.-J., Kim, I. & Vigneswaran, S. 2014, 'Organic fouling behavior in direct contact membrane distillation', *Desalination*, vol. 347, pp. 230-9.
- Nam, J.-Y., Hwang, K.-S., Kim, H.-C., Jeong, H., Kim, H., Jwa, E., Yang, S., Choi, J., Kim, C.-S., Han, J. & Jeong, N. 2018, 'Assessing the behavior of the feed-water constituents of a pilot-scale 1000-cell-pair reverse electrodialysis with seawater and municipal wastewater effluent', *Water Research*.
- NASA 2015, *Technology Roadmaps: Human Health, Life Support, and Habitation Systems.*, vol. 6, National Aeronautics and Space Administration.
- National Minerals Information Center 2019, *Phosphate Rock Statistics and Information*, USGS, <<https://www.usgs.gov/centers/nmic/phosphate-rock-statistics-and-information>>.
- Neocleous, D. & Savvas, D. 2019, 'The effects of phosphorus supply limitation on photosynthesis, biomass production, nutritional quality, and mineral nutrition in lettuce grown in a recirculating nutrient solution', *Scientia Horticulturae*, vol. 252, pp. 379-87.
- Nguyen, D.V., Ho, P.Q., Pham, T.V., Nguyen, T.V. & Kim, L. 2019, 'Treatment of surface water using cold plasma for domestic water supply', *Environmental Engineering Research*, vol. 24, no. 3, pp. 412-7.
- Nguyen, N.C., Nguyen, H.T., Ho, S.-T., Chen, S.-S., Ngo, H.H., Guo, W., Ray, S.S. & Hsu, H.-T. 2016, 'Exploring high charge of phosphate as new draw solute in a forward osmosis–membrane distillation hybrid system for concentrating

high-nutrient sludge', *Science of The Total Environment*, vol. 557-558, pp. 44-50.

- Okem, A.E., Xulu, S., Tilley, E., Buckley, C. & Roma, E. 2013, 'Assessing perceptions and willingness to use urine in agriculture: a case study from rural areas of eThekwin municipality, South Africa', *Journal of Water, Sanitation and Hygiene for Development*, vol. 3, no. 4, pp. 582-91.
- Ongaratto, R.S., Menezes, L., Borges, C.P. & Laranjeira da Cunha Lage, P. 2018, 'Osmotic distillation applying potassium pyrophosphate as brine', *Journal of Food Engineering*, vol. 228, pp. 69-78.
- Ouma, J., Septien, S., Velkushanova, K., Pocock, J. & Buckley, C. 2016, 'Characterization of ultrafiltration of undiluted and diluted stored urine', *Water Science and Technology*, vol. 74, no. 9, pp. 2105-14.
- Pahore, M.M., Ushijima, K., Ito, R. & Funamizu, N. 2012, 'Fate of nitrogen during volume reduction of human urine using an on-site volume reduction system', *Environ Technol*, vol. 33, no. 1-3, pp. 229-35.
- Pandorf, M., Hochmuth, G. & Boyer, T.H. 2019, 'Human Urine as a Fertilizer in the Cultivation of Snap Beans (*Phaseolus vulgaris*) and Turnips (*Brassica rapa*)', *Journal of Agricultural and Food Chemistry*, vol. 67, no. 1, pp. 50-62.
- Patange, A., Boehm, D., Giltrap, M., Lu, P., Cullen, P.J. & Bourke, P. 2018, 'Assessment of the disinfection capacity and eco-toxicological impact of atmospheric cold plasma for treatment of food industry effluents', *Science of The Total Environment*, vol. 631-632, pp. 298-307.
- Peerapong, P. 2018, 'Removal of Organic Contaminants by Argon Plasma Jet: A Prospective Treatment of Urine on Spacecraft', paper presented to the 9th International Conference on Mechanical and Aerospace Engineering, Budapest, Hungary.
- Peter-Fröhlich, A., Pawlowski, L., Bonhomme, A. & Oldenburg, M. 2007, 'EU demonstration project for separate discharge and treatment of urine, faeces and greywater – Part I: Results', *Water Science and Technology*, vol. 56, no. 5, pp. 239-49.
- Phuntsho, S., Shon, H.K., Hong, S., Lee, S., Vigneswaran, S. & Kandasamy, J. 2012, 'Fertiliser drawn forward osmosis desalination: The concept, performance and limitations for fertigation', *Reviews in Environmental Science and Biotechnology*, vol. 11, no. 2, pp. 147-68.
- Phuntsho, S., Shon, H.K., Majeed, T., El Saliby, I., Vigneswaran, S., Kandasamy, J., Hong, S. & Lee, S. 2012, 'Blended fertilizers as draw solutions for fertilizer-drawn forward osmosis desalination', *Environmental Science and Technology*, vol. 46, no. 8, pp. 4567-75.

- Pietrzyk, R.A., Jones, J.A., Sams, C.F. & Whitson, P.A. 2007, 'Renal Stone Formation Among Astronauts', *Aviation, Space, and Environmental Medicine*, vol. 78, no. 4, pp. A9-A13.
- Ping, Y. & Tim, N. 2016, 'Development of Advanced ISS-WPA Catalysts for Organic Oxidation at Reduced Pressure/Temperature', *46th International Conference on Environmental Systems*
- Post, J.W., Veerman, J., Hamelers, H.V.M., Euverink, G.J.W., Metz, S.J., Nymeijer, K. & Buisman, C.J.N. 2007, 'Salinity-gradient power: Evaluation of pressure-retarded osmosis and reverse electrodialysis', *Journal of Membrane Science*, vol. 288, no. 1, pp. 218-30.
- Pronk, W., Biebow, M. & Boller, M. 2006, 'Electrodialysis for Recovering Salts from a Urine Solution Containing Micropollutants', *Environmental Science & Technology*, vol. 40, no. 7, pp. 2414-20.
- Pronk, W., Palmquist, H., Biebow, M. & Boller, M. 2006, 'Nanofiltration for the separation of pharmaceuticals from nutrients in source-separated urine', *Water Research*, vol. 40, no. 7, pp. 1405-12.
- Pruitt, J.M., Carter, L., Bagdigian, R.M. & Kayatin, M.J. 2015, 'Upgrades to the ISS Water Recovery System', paper presented to the 45th International Conference on Environmental Systems, Washington, United States, 12th of May.
- Putnam, D. 1971a, 'Composition and Concentrative proprieties of human urine', *NASA, WASHINGTON, United States*.
- Putnam, D. 1971b, 'Composition and Concentrative proprieties of Human Urine', *NASA, Huntington Beach, CA*.
- Putnam, D. & Thomas, E. 1969, 'Recovery of potable water from human urine', *Aerospace Medicine*, vol. 40, no. 7, pp. 736-9.
- Randall, D.G., Krähenbühl, M., Köpping, I., Larsen, T.A. & Udert, K.M. 2016, 'A novel approach for stabilizing fresh urine by calcium hydroxide addition', *Water Research*, vol. 95, pp. 361-9.
- Randall, D.G. & Naidoo, V. 2018, 'Urine: the liquid gold of wastewater', *Journal of Environmental Chemical Engineering*.
- Ray, H., Saetta, D. & Boyer, T.H. 2018, 'Characterization of urea hydrolysis in fresh human urine and inhibition by chemical addition', *Environmental Science: Water Research & Technology*, vol. 4, no. 1, pp. 87-98.
- Reddy, P.M.K. & Subrahmanyam, C. 2012, 'Green Approach for Wastewater Treatment—Degradation and Mineralization of Aqueous Organic Pollutants by Discharge Plasma', *Industrial & Engineering Chemistry Research*, vol. 51, no. 34, pp. 11097-103.

- Rezania, S., Din, M.F.M., Taib, S.M., Dahalan, F.A., Songip, A.R., Singh, L. & Kamyab, H. 2016, 'The efficient role of aquatic plant (water hyacinth) in treating domestic wastewater in continuous system', *International Journal of Phytoremediation*, vol. 18, no. 7, pp. 679-85.
- Rich Earth Institute 2020, <https://richearthinstitute.org/>, viewed 2020, <<https://richearthinstitute.org/>>.
- Rickman, M., Pellegrino, J. & Davis, R. 2012, 'Fouling phenomena during membrane filtration of microalgae', *Journal of Membrane Science*, vol. 423-424, pp. 33-42.
- Rijnaarts, T., Moreno, J., Saakes, M., de Vos, W.M. & Nijmeijer, K. 2019, 'Role of anion exchange membrane fouling in reverse electrodialysis using natural feed waters', *Colloids and Surfaces A: Physicochemical and Engineering Aspects*, vol. 560, pp. 198-204.
- Roma, E., Philp, K., Buckley, C., Xulu, S. & Scott, D. 2013, 'User perceptions of urine diversion dehydration toilets: Experiences from a cross-sectional study in eThekweni municipality', *Water SA*, vol. 39, no. 2, pp. 305-11.
- Rose, C., Parker, A., Jefferson, B. & Cartmell, E. 2015, 'The Characterization of Feces and Urine: A Review of the Literature to Inform Advanced Treatment Technology', *Critical Reviews in Environmental Science and Technology*, vol. 45, no. 17, pp. 1827-79.
- Sahebi, S., Phuntsho, S., Eun Kim, J., Hong, S. & Kyong Shon, H. 2015, 'Pressure assisted fertiliser drawn osmosis process to enhance final dilution of the fertiliser draw solution beyond osmotic equilibrium', *Journal of Membrane Science*, vol. 481, pp. 63-72.
- Schneider, V., Oganov, V., LeBlanc, A., Rakmonov, A., Taggart, L., Bakulin, A., Huntoon, C., Grigoriev, A. & Varonin, L. 1995, 'Bone and body mass changes during space flight', *Acta Astronautica*, vol. 36, no. 8, pp. 463-6.
- Schwarz, A.O., Rittmann, B.E., Crawford, G.V., Klein, A.M. & Daigger, G.T. 2006, 'Critical Review on the Effects of Mixed Liquor Suspended Solids on Membrane Bioreactor Operation', *Separation Science and Technology*, vol. 41, no. 7, pp. 1489-511.
- Sharma, K.K., Garg, S., Li, Y., Malekizadeh, A. & Schenk, P.M. 2013, 'Critical analysis of current microalgae dewatering techniques', *Biofuels*, vol. 4, no. 4, pp. 397-407.
- Sherwin Gormly & Flynn, M., 'Recycle process concept development for exploration life support: a source of advanced concepts for sustainable small wastewater systems', *National Aeronautics and Space Administration Reports*.
- Sherwin Gormly, Michael Flynn & Howe, S. 2012, 'Space Cargo Transport Bags Through Membrane Water Treatment Elements To Space Architecture

Building Element: A Total Product Sustainability And Life Cycle Design Optimisation Experiment', *Journal of Green Building*, vol. 7, no. 1, pp. 71-84.

Siddiqui, F.A., She, Q., Fane, A.G. & Field, R.W. 2018, 'Exploring the differences between forward osmosis and reverse osmosis fouling', *Journal of Membrane Science*, vol. 565, pp. 241-53.

Silva, T.L.S., Morales-Torres, S., Esteves, C.M.P., Ribeiro, A.R., Nunes, O.C., Figueiredo, J.L. & Silva, A.M.T. 2018, 'Desalination and removal of organic micropollutants and microorganisms by membrane distillation', *Desalination*, vol. 437, pp. 121-32.

Simha, P., Lalander, C., Ramanathan, A., Vijayalakshmi, C., McConville, J.R., Vinnerås, B. & Ganesapillai, M. 2018, 'What do consumers think about recycling human urine as fertiliser? Perceptions and attitudes of a university community in South India', *Water Research*, vol. 143, pp. 527-38.

Simpson-Hebert, M. 2007, 'Low-cost Arborloo offers Ethiopians health and agriculture benefits', *Waterlines*, vol. 26, no. 2, pp. 12-4.

Smith, S.M., Wastney, M.E., O'Brien, K.O., Morukov, B.V., Larina, I.M., Abrams, S.A., Davis-Street, J.E., Oganov, V. & Shackelford, L.C. 2005, 'Bone Markers, Calcium Metabolism, and Calcium Kinetics During Extended-Duration Space Flight on the Mir Space Station', *Journal of Bone and Mineral Research*, vol. 20, no. 2, pp. 208-18.

Song, Y., Dai, Y., Hu, Q., Yu, X. & Qian, F. 2014, 'Effects of three kinds of organic acids on phosphorus recovery by magnesium ammonium phosphate (MAP) crystallization from synthetic swine wastewater', *Chemosphere*, vol. 101, pp. 41-8.

Srisurichan, S., Jiraratananon, R. & Fane, A.G. 2005, 'Humic acid fouling in the membrane distillation process', *Desalination*, vol. 174, no. 1, pp. 63-72.

Stephenson, A.L., Dennis, J.S., Howe, C.J., Scott, S.A. & Smith, A.G. 2010, 'Influence of nitrogen-limitation regime on the production by *Chlorella vulgaris* of lipids for biodiesel feedstocks', *Biofuels*, vol. 1, no. 1, pp. 47-58.

Straub, A.P., Deshmukh, A. & Elimelech, M. 2016, 'Pressure-retarded osmosis for power generation from salinity gradients: is it viable?', *Energy & Environmental Science*, vol. 9, no. 1, pp. 31-48.

Straub, J.E.I., Plumlee, D.K., Wallace, W.T., Alverson, J.T., Benoit, M.J., Gillispie, R.L., Hunter, D., Kuo, M., Rutz, J.A., Hudson, E.K., Loh, L.J. & Gazda, D.B. 2018, 'Chemical Characterization of ISS Potable Water Collected in 2017', paper presented to the 48th International Conference on Environmental Systems, Albuquerque, New Mexico, 8-12 July.



- Strauss, M. 1986, 'Health aspects of nightsoil and sludge use in agriculture and aquaculture. Part II: Pathogen survival (04/85)', *International Reference Centre for Waste Disposal*.
- Sydney Water 2019, 'Water analysis: Potts Hill water supply system.'
- Tang, C., Wang, Z., Petrinić, I., Fane, A.G. & Hélix-Nielsen, C. 2015, 'Biomimetic aquaporin membranes coming of age', *Desalination*, vol. 368, pp. 89-105.
- Tang, C.Y., She, Q., Lay, W.C.L., Wang, R. & Fane, A.G. 2010, 'Coupled effects of internal concentration polarization and fouling on flux behavior of forward osmosis membranes during humic acid filtration', *Journal of Membrane Science*, vol. 354, no. 1-2, pp. 123-33.
- Tang, C.Y., Zhao, Y., Wang, R., Hélix-Nielsen, C. & Fane, A.G. 2013, 'Desalination by biomimetic aquaporin membranes: Review of status and prospects', *Desalination*, vol. 308, pp. 34-40.
- Tang, Q., Jiang, W., Zhang, Y., Wei, W. & Lim, T.M. 2009, 'Degradation of Azo Dye Acid Red 88 by Gas Phase Dielectric Barrier Discharges', *Plasma Chemistry and Plasma Processing*, vol. 29, no. 4, pp. 291-305.
- Tarpeh, W.A., Barazesh, J.M., Cath, T.Y. & Nelson, K.L. 2018, 'Electrochemical Stripping to Recover Nitrogen from Source-Separated Urine', *Environmental Science and Technology*, vol. 52, no. 3, pp. 1453-60.
- Tarpeh, W.A., Udert, K.M. & Nelson, K.L. 2017, 'Comparing ion exchange adsorbents for nitrogen recovery from source-separated urine', *Environmental Science and Technology*, vol. 51, no. 4, pp. 2373-81.
- Tijing, L.D., Woo, Y.C., Choi, J.-S., Lee, S., Kim, S.-H. & Shon, H.K. 2015, 'Fouling and its control in membrane distillation—A review', *Journal of Membrane Science*, vol. 475, pp. 215-44.
- Tiraferri, A., Yip, N.Y., Phillip, W.A., Schiffman, J.D. & Elimelech, M. 2011, 'Relating performance of thin-film composite forward osmosis membranes to support layer formation and structure', *Journal of Membrane Science*, vol. 367, no. 1, pp. 340-52.
- Tomaszewska, M. 1996, 'Preparation and properties of flat-sheet membranes from poly(vinylidene fluoride) for membrane distillation', *Desalination*, vol. 104, no. 1, pp. 1-11.
- Tommerup M., K.K., Vogel J., Flynn M. and Shaw A. 2016, 'Testing Aquaporin Inside Membrane on the International Space Station', *46th International Conference on Environmental Systems*.
- Tommerup, M.B., Kleinschmidt, K., Vogel, J., Flynn, M. & Shaw, H. 2016, 'Testing Aquaporin InsideTM Membrane on the International Space Station', paper

presented to the 46th International Conference on Environmental Systems, Vienna, Austria.

- Tommerup, M.B., Kleinschmidt, K., Vogel, J., Flynn, M. & Shaw, H. 2017, 'Testing Aquaporin Inside™ Membrane on the International Space Station – Part II', paper presented to the 47th International Conference on Environmental Systems, Charleston, USA.
- Tran, N.H., Reinhard, M. & Gin, K.Y.-H. 2018, 'Occurrence and fate of emerging contaminants in municipal wastewater treatment plants from different geographical regions-a review', *Water Research*, vol. 133, pp. 182-207.
- Troccaz, M., Niclass, Y., Anziani, P. & Starkenmann, C. 2013, 'The influence of thermal reaction and microbial transformation on the odour of human urine', *Flavour and Fragrance Journal*, vol. 28, no. 4, pp. 200-11.
- Tuantet, K., Temmink, H., Zeeman, G., Janssen, M., Wijffels, R.H. & Buisman, C.J.N. 2014, 'Nutrient removal and microalgal biomass production on urine in a short light-path photobioreactor', *Water Research*, vol. 55, pp. 162-74.
- Tun, L.L., Jeong, D., Jeong, S., Cho, K., Lee, S. & Bae, H. 2016, 'Dewatering of source-separated human urine for nitrogen recovery by membrane distillation', *Journal of Membrane Science*, vol. 512, pp. 13-20.
- Udert, K., Fux, C., Münster, M., Larsen, T., Siegrist, H. & Gujer, W. 2003, 'Nitrification and autotrophic denitrification of source-separated urine', *Water Science and Technology*, vol. 48, no. 1, pp. 119-30.
- Udert, K.M., Buckley, C.A., Wächter, M., McArdell, C.S., Kohn, T., Strande, L., Zöllig, H., Fumasoli, A., Oberson, A. & Etter, B. 2015, 'Technologies for the treatment of source-separated urine in the eThekweni Municipality', *Water Sa*, vol. 41, no. 2, pp. 212-21.
- Udert, K.M., Larsen, T.A., Biebow, M. & Gujer, W. 2003, 'Urea hydrolysis and precipitation dynamics in a urine-collecting system', *Water Research*, vol. 37, no. 11, pp. 2571-82.
- Udert, K.M., Larsen, T.A. & Gujer, W. 2003, 'Biologically induced precipitation in urine-collecting systems', *Water Science and Technology: Water Supply*, vol. 3, no. 3, pp. 71-8.
- Udert, K.M., Larsen, T.A. & Gujer, W. 2006, 'Fate of major compounds in source-separated urine', *Water Science and Technology*, Conference Paper, vol. 54, pp. 413-20, <<https://www.scopus.com/inward/record.uri?eid=2-s2.0-33846645010&doi=10.2166%2fwst.2006.921&partnerID=40&md5=f6c9f6b73634f4b5a1822daedb3ec414>>.
- Udert, K.M. & Wächter, M. 2012, 'Complete nutrient recovery from source-separated urine by nitrification and distillation', *Water Research*, vol. 46, no. 2, pp. 453-64.

- United Nations 2017, *World Population Prospects: The 2017 Revision, Key Findings and Advance Tables*, Working Paper No. ESA/P/WP/248, <[https://esa.un.org/unpd/wpp/publications/Files/WPP2017\\_KeyFindings.pdf](https://esa.un.org/unpd/wpp/publications/Files/WPP2017_KeyFindings.pdf)>.
- Valladares Linares, R., Li, Z., Yangali-Quintanilla, V., Ghaffour, N., Amy, G., Leiknes, T. & Vrouwenvelder, J.S. 2016, 'Life cycle cost of a hybrid forward osmosis - low pressure reverse osmosis system for seawater desalination and wastewater recovery', *Water Research*, vol. 88, pp. 225-34.
- Van Der Bruggen, B. & Luis, P. 2015, 'Forward osmosis: Understanding the hype', *Reviews in Chemical Engineering*, vol. 31, no. 1, pp. 1-12.
- Van Vuuren, D.P., Bouwman, A.F. & Beusen, A.H.W. 2010, 'Phosphorus demand for the 1970–2100 period: A scenario analysis of resource depletion', *Global Environmental Change*, vol. 20, no. 3, pp. 428-39.
- Veerman, J., Saakes, M., Metz, S.J. & Harmsen, G.J. 2010, 'Electrical Power from Sea and River Water by Reverse Electrodialysis: A First Step from the Laboratory to a Real Power Plant', *Environmental Science & Technology*, vol. 44, no. 23, pp. 9207-12.
- Veerman, J., Saakes, M., Metz, S.J. & Harmsen, G.J. 2011, 'Reverse electrodialysis: A validated process model for design and optimization', *Chemical Engineering Journal*, vol. 166, no. 1, pp. 256-68.
- Verlicchi, P., Al Aukidy, M. & Zambello, E. 2012, 'Occurrence of pharmaceutical compounds in urban wastewater: Removal, mass load and environmental risk after a secondary treatment—A review', *Science of The Total Environment*, vol. 429, pp. 123-55.
- Verlicchi, P. & Zambello, E. 2015, 'Pharmaceuticals and personal care products in untreated and treated sewage sludge: Occurrence and environmental risk in the case of application on soil — A critical review', *Science of The Total Environment*, vol. 538, pp. 750-67.
- Vermaas, D.A., Kunteng, D., Saakes, M. & Nijmeijer, K. 2013, 'Fouling in reverse electrodialysis under natural conditions', *Water Research*, vol. 47, no. 3, pp. 1289-98.
- Viskari, E.-L., Grobler, G., Karimäki, K., Gorbatoeva, A., Vilpas, R. & Lehtoranta, S. 2018, 'Nitrogen Recovery With Source Separation of Human Urine—Preliminary Results of Its Fertiliser Potential and Use in Agriculture', *Frontiers in Sustainable Food Systems*, vol. 2, no. 32.
- Volpin, F., Chekli, L., Phuntsho, S., Cho, J., Ghaffour, N., Vrouwenvelder, J.S. & Kyong Shon, H. 2018, 'Simultaneous phosphorous and nitrogen recovery from source-separated urine: A novel application for fertiliser drawn forward osmosis', *Chemosphere*, vol. 203, pp. 482-9.

- Volpin, F., Gonzales, R.R., Lim, S., Pathak, N., Phuntsho, S. & Shon, H.K. 2018, 'GreenPRO: A novel fertiliser-driven osmotic power generation process for fertigation', *Desalination*, vol. 447, pp. 158-66.
- Volpin, F., Heo, H., Hasan Johir, M.A., Cho, J., Phuntsho, S. & Shon, H.K. 2019, 'Techno-economic feasibility of recovering phosphorus, nitrogen and water from dilute human urine via forward osmosis', *Water Research*, vol. 150, pp. 47-55.
- Volpin, F., Yu, H., Cho, J., Lee, C., Phuntsho, S., Ghaffour, N., Vrouwenvelder, J.S. & Shon, H.K. 2019, 'Human urine as a forward osmosis draw solution for the application of microalgae dewatering', *Journal of Hazardous Materials*, vol. 378, p. 120724.
- Vuna Ltd. 2020, *VUNA Ltd. Company Website*, 2020, <[http://www.vuna.ch/index\\_en.html](http://www.vuna.ch/index_en.html)>.
- Wang, P., Cui, Y., Ge, Q., Fern Tew, T. & Chung, T.-S. 2015, 'Evaluation of hydroacid complex in the forward osmosis–membrane distillation (FO–MD) system for desalination', *Journal of Membrane Science*, vol. 494, pp. 1-7.
- Wang, Z. & Leung, K.M.Y. 2015, 'Effects of unionised ammonia on tropical freshwater organisms: Implications on temperate-to-tropic extrapolation and water quality guidelines', *Environmental Pollution*, vol. 205, pp. 240-9.
- Wett, B., Omari, A., Podmirseg, S.M., Han, M., Akintayo, O., Gómez Brandón, M., Murthy, S., Bott, C., Hell, M., Takács, I., Nyhuis, G. & O'Shaughnessy, M. 2013, 'Going for mainstream deammonification from bench to full scale for maximized resource efficiency', *Water Science and Technology*, vol. 68, no. 2, pp. 283-9.
- WHO and UNICEF 2017, *Joint Monitoring Programme for Water Supply, Sanitation and Hygiene - Annual Report*, WHO/UNICEF.
- Wicaksana, F., Fane, A.G., Tang, C. & Wang, R. 2011, *Nature Meets Technology: Forward Osmosis Membrane Technology.*, Springer, Dordrecht, Biomedical Engineering.
- Wijffels, R.H., Barbosa, M.J. & Eppink, M.H.M. 2010, 'Microalgae for the production of bulk chemicals and biofuels', *Biofuels, Bioproducts and Biorefining*, vol. 4, no. 3, pp. 287-95.
- Wilsenach, J.A. & Loosdrecht, M.C.v. 2006, 'Integration of Processes to Treat Wastewater and Source-Separated Urine', *Journal of Environmental Engineering*, vol. 132, no. 3, pp. 331-41.
- Winker, M. & Saadoun, A. 2011, 'Urine and brownwater separation at GTZ main office building Eschborn, Germany; Case study of sustainable sanitation projects', *Retrieved Jan*, vol. 17, p. 2012.

- Wood, F.C. 1982, 'The changing face of desalination — A consulting engineer's viewpoint', *Desalination*, vol. 42, no. 1, pp. 17-25.
- World Bank Group 2018, 'GEM Commodities, World Bank Group'.
- Xie, M., Luo, W., Guo, H., Nghiem, L.D., Tang, C.Y. & Gray, S.R. 2018, 'Trace organic contaminant rejection by aquaporin forward osmosis membrane: Transport mechanisms and membrane stability', *Water Research*, vol. 132, pp. 90-8.
- Xie, M., Nghiem, L.D., Price, W.E. & Elimelech, M. 2014, 'Toward Resource Recovery from Wastewater: Extraction of Phosphorus from Digested Sludge Using a Hybrid Forward Osmosis-Membrane Distillation Process', *Environmental Science and Technology Letters*, vol. 1, no. 2, pp. 191-5.
- Xu, K., Li, J., Zheng, M., Zhang, C., Xie, T. & Wang, C. 2015, 'The precipitation of magnesium potassium phosphate hexahydrate for P and K recovery from synthetic urine', *Water Research*, vol. 80, pp. 71-9.
- Yang, L., Giannis, A., Chang, V.W.C., Liu, B., Zhang, J. & Wang, J.-Y. 2015, 'Application of hydroponic systems for the treatment of source-separated human urine', *Ecological Engineering*, vol. 81, pp. 182-91.
- Yang, Q., Chung, T.-S. & Santoso, Y.E. 2007, 'Tailoring pore size and pore size distribution of kidney dialysis hollow fiber membranes via dual-bath coagulation approach', *Journal of Membrane Science*, vol. 290, no. 1, pp. 153-63.
- Ye, K., Wang, G., Cao, D. & Wang, G. 2018, 'Recent Advances in the Electro-Oxidation of Urea for Direct Urea Fuel Cell and Urea Electrolysis', vol. 376, no. 6, p. 42.
- Yip, N.Y. & Elimelech, M. 2012, 'Thermodynamic and Energy Efficiency Analysis of Power Generation from Natural Salinity Gradients by Pressure Retarded Osmosis', *Environmental Science & Technology*, vol. 46, no. 9, pp. 5230-9.
- Yip, N.Y. & Elimelech, M. 2014, 'Comparison of Energy Efficiency and Power Density in Pressure Retarded Osmosis and Reverse Electrodialysis', *Environmental Science & Technology*, vol. 48, no. 18, pp. 11002-12.
- Zhang, J., Li, J.-D., Duke, M., Xie, Z. & Gray, S. 2010, 'Performance of asymmetric hollow fibre membranes in membrane distillation under various configurations and vacuum enhancement', *Journal of Membrane Science*, vol. 362, no. 1, pp. 517-28.
- Zhang, J., She, Q., Chang, V.W., Tang, C.Y. & Webster, R.D. 2014a, 'Mining nutrients (N, K, P) from urban source-separated urine by forward osmosis dewatering', *Environ Sci Technol*, vol. 48, no. 6, pp. 3386-94.

- Zhang, J., She, Q., Chang, V.W.C., Tang, C.Y. & Webster, R.D. 2014b, 'Mining nutrients (N, K, P) from urban source-separated urine by forward osmosis dewatering', *Environmental Science and Technology*, vol. 48, no. 6, pp. 3386-94.
- Zhang, R., Sun, P., Boyer, T.H., Zhao, L. & Huang, C.H. 2015, 'Degradation of pharmaceuticals and metabolite in synthetic human urine by UV, UV/H<sub>2</sub>O<sub>2</sub>, and UV/PDS', *Environmental Science and Technology*, vol. 49, no. 5, pp. 3056-66.
- Zhang, S., Lim, C.Y., Chen, C.L., Liu, H. & Wang, J.Y. 2014, 'Urban nutrient recovery from fresh human urine through cultivation of *Chlorella sorokiniana*', *J Environ Manage*, vol. 145, pp. 129-36.
- Zhang, S., Wang, P., Fu, X. & Chung, T.-S. 2014, 'Sustainable water recovery from oily wastewater via forward osmosis-membrane distillation (FO-MD)', *Water Research*, vol. 52, pp. 112-21.
- Zhao, D., Chen, S., Guo, C.X., Zhao, Q. & Lu, X. 2016, 'Multi-functional forward osmosis draw solutes for seawater desalination', *Chinese Journal of Chemical Engineering*, vol. 24, no. 1, pp. 23-30.
- Zhao, D., Wang, P., Zhao, Q., Chen, N. & Lu, X. 2014, 'Thermoresponsive copolymer-based draw solution for seawater desalination in a combined process of forward osmosis and membrane distillation', *Desalination*, vol. 348, pp. 26-32.
- Zhao, P., Gao, B., Yue, Q. & Shon, H.K. 2015, 'The performance of forward osmosis process in treating the surfactant wastewater: The rejection of surfactant, water flux and physical cleaning effectiveness', *Chemical Engineering Journal*, vol. 281, pp. 688-95.
- Zhao, Z.P., Xu, L., Shang, X. & Chen, K. 2013, 'Water regeneration from human urine by vacuum membrane distillation and analysis of membrane fouling characteristics', *Separation and Purification Technology*, vol. 118, pp. 369-76.
- Zhou, Y., Huang, M., Deng, Q. & Cai, T. 2017, 'Combination and performance of forward osmosis and membrane distillation (FO-MD) for treatment of high salinity landfill leachate', *Desalination*, vol. 420, pp. 99-105.
- Zöllig, H., Remmele, A., Fritzsche, C., Morgenroth, E. & Udert, K.M. 2015, 'Formation of Chlorination Byproducts and Their Emission Pathways in Chlorine Mediated Electro-Oxidation of Urine on Active and Nonactive Type Anodes', *Environmental Science and Technology*, vol. 49, no. 18, pp. 11062-9.

